RADIOLOGY AND ONCOLOGY

vol.54 no.2
june 2020

ORR: objektivna stopnja odziva; OS: celokupno preživetje; PFS: preživetje brez napredovanja bolezni

Referenci: 1. Choueiri TK, Escudier B, Powles T, *et al*. Cabozantinib versus everolimus in advanced renal cell carcinoma (METEOR): final results from a randomised, open-label, phase 3 trial. The Lancet Oncology. 2016;17(7):917-27. **2.** Povzetek glavnih značilnosti zdravila Cabometyx.

Skrajšan povzetek glavnih značilnosti zdravila

CABOMETYX 20 mg filmsko obložene tablete
CABOMETYX 40 mg filmsko obložene tablete
CABOMETYX 60 mg filmsko obložene tablete
(kabozantinib)

TERAPEVTSKE INDIKACIJE Zdravljenje napredovalega karcinoma ledvičnih celic (KLC) pri predhodno nezdravljenih odraslih bolnikih s srednje ugodnim ali slabim prognostičnim obetom ter pri odraslih bolnikih po predhodnem zdravljenju, usmerjenem v vaskularni endotelijski rastni faktor (VEGF). V monoterapiji zdravljenje hepatocelularnega karcinoma (HCK) pri odraslih bolnikih, ki so se predhodno že zdravili s sorafenibom. **ODMERJANJE IN NAČIN UPORABE** Pri bolnikih s KLC in HKC je priporočeni odmerek 60 mg enkrat na dan. Zdravljenje je treba nadaljevati tako dolgo, dokler bolnik več nima kliničnih koristi od terapije ali do pojava nesprejemljive toksičnosti. Pri sumu na neželene reakcije na zdravilo bo morda treba zdravljenje začasno prekiniti in/ali zmanjšati odmerek. Če je treba odmerek zmanjšati, se priporoča zmanjšanje na 40 mg na dan in nato na 20 mg na dan. Prekinitev odmerka se priporoča pri obravnavi toksičnosti 3. ali višje stopnje po CTCAE (*common terminology criteria for adverse events*) ali nevzdržni toksičnosti 2. stopnje. Zmanjšanje odmerka se priporoča za dogodke, ki bi lahko čez čas postali resni ali nevzdržni. V primeru pojava neželenih učinkov 1. in 2. stopnje, ki jih bolnik prenaša in jih je možno enostavno obravnavati, prilagoditev odmerjanja običajno ni potrebna. Treba je uvesti podporno oskrbo. V primeru pojava neželenih učinkov 2. stopnje, ki jih bolnik ne prenaša in jih ni mogoče obravnavati z zmanjšanjem odmerka ali podporno oskrbo, je treba zdravljenje prekiniti, dokler neželeni učinki ne izzvenijo do ≤ 1. stopnje, uvesti podporno oskrbo in razmisliti o ponovni uvedbi zdravljenja z zmanjšanim odmerkom. V primeru pojava neželenih učinkov 3. stopnje je treba zdravljenje prekiniti, dokler neželeni učinki ne izzvenijo do ≤ 1. stopnje, uvesti podporno oskrbo in ponovno uvesti zdravljenje z zmanjšanim odmerkom. V primeru pojava neželenih učinkov 4. stopnje je treba zdravljenje prekiniti, uvesti ustrezno zdravniško oskrbo, in če neželeni učinki izzvenijo do ≤ 1. stopnje, ponovno uvesti zdravljenje z zmanjšanim odmerkom. Če neželeni učinki ne izzvenijo, je treba trajno prenehati z uporabo zdravila. Pri bolnikih z blago ali zmerno ledvično okvaro je treba kabozantinib uporabljati previdno. Uporaba se ne priporoča pri bolnikih s hudo ledvično okvaro. Pri bolnikih z blago okvaro jeter odmerka ni treba prilagajati. Pri bolnikih z zmerno okvaro jeter (Child Pugh B) priporočil za odmerjanje ni možno podati. Pri teh bolnikih je priporočljivo skrbno spremljanje celokupne varnosti. Pri bolnikih s hudo okvaro jeter (Child Pugh C) uporaba kabozantiniba ni priporočljiva. Način uporabe: Tablete je treba pogoltniti cele in jih ni dovoljeno drobiti. Bolnikom je treba naročiti, naj vsaj 2 uri pred uporabo zdravila in 1 uro po tem ničesar ne jedo. **KONTRAINDIKACIJE** Preobčutljivost na učinkovino ali katero koli pomožno snov. **POSEBNA OPOZORILA IN PREVIDNOSTNI UKREPI** Večina dogodkov se pojavi zgodaj v teku zdravljenja, zato mora zdravnik bolnika v prvih 8 tednih zdravljenja skrbno spremljati, da oceni, ali je treba odmerek prilagoditi. Dogodki, ki se običajno pojavijo zgodaj, vključujejo hipokalciemijo, hipokaliemijo, trombocitopenijo, hipertenzijo, sindrom palmarno-plantarne eritrodisestezije (PPES), proteinurijo in gastrointestinalne dogodke (bolečine v trebuhu, vnetje sluznice, zaprtje, driska, bruhanje). Pred uvedbo zdravljenja s kabozantinibom je priporočljivo izvesti preiskave delovanja jeter (ALT, AST in bilirubin), vrednosti skrbno spremljati med zdravljenjem in po potrebi prilagoditi odmerek. Bolnike je treba spremljati glede znakov in simptomov jetrne encefalopatije. Bolnike, ki imajo vnetno bolezen črevesja (npr. Crohnovo bolezen, ulcerozni kolitis, peritonitis, divertikulitis ali apendicitis), ki imajo tumorsko infiltracijo prebavil ali so imeli pred posegom na prebavilih zaplete (zlasti v povezavi z zapoznelim ali nepopolnim celjenjem), je treba pred uvedbo zdravljenja skrbno oceniti, nato pa natančno spremljati za pojav simptomov perforacij in fistul, vključno z abscesi in sepso. Trajna ali ponavljajoča se driska med zdravljenjem je lahko dejavnik tveganja za nastanek analne fistule. Uporabo kabozantiniba je treba pri bolnikih, pri katerih se pojavi gastrointestinalna perforacija ali fistula, ki je ni možno ustrezno obravnavati, prekiniti. Driska, navzea/bruhanje, zmanjšanje apetita in vnetje ustne sluznice/bolečina v ustni votlini so nekateri od najpogosteje poročanih neželenih učinkov na prebavila. Nemudoma je treba uvesti ustrezne medicinske ukrepe, vključno s podpornim zdravljenjem z antiemetiki, antidiaroiki ali antacidi, da se prepreči dehidracija, neravnovesje elektrolitov in izguba telesne mase. Če pomembni neželeni učinki na prebavila vztrajajo ali se ponavljajo, je treba presoditi o prekinitvi odmerjanja, zmanjšanju odmerka ali trajni ukinitvi zdravljenja s kabozantinibom. Kabozantinib je treba uporabljati previdno pri bolnikih, pri katerih obstaja tveganje za pojav venske trombembolije, vključno s pljučno embolijo, in arterijske trombembolije ali imajo te dogodke v anamnezi. Z uporabo je treba prenehati pri bolnikih, pri katerih se razvije akutni miokardni infarkt ali drugi klinično pomembni znaki zapletov trombembolije. Kabozantiniba se ne sme dajati bolnikom, ki hudo krvavijo, ali pri katerih obstaja tveganje za hudo krvavitev. Uporaba zaviralcev poti VEGF pri bolnikih s hipertenzijo ali brez nje lahko spodbudi nastanek anevrizem in/ali disekcij arterij. Pred uvedbo kabozantiniba je treba to tveganje skrbno preučiti pri bolnikih z dejavniki tveganja, kot sta hipertenzija ali anamneza anevrizme. Med zdravljenjem s kabozantinibom je treba spremljati vrednosti trombocitov in odmerek prilagoditi glede na resnost trombocitopenije. Zdravljenje s kabozantinibom je treba ustaviti vsaj 28 dni pred načrtovanim kirurškim posegom, vključno z zobozdravstvenim, če je mogoče. Kabozantinib je treba ukiniti pri bolnikih z zapleti s celjenjem rane, zaradi katerih je potrebna zdravniška pomoč. Pred uvedbo kabozantiniba je treba dobro obvladati krvni tlak. Med zdravljenjem je treba vse bolnike spremljati za pojav hipertenzije in jih po potrebi zdraviti s standardnimi antihipertenzivi. V primeru trdovratne hipertenzije, kljub uporabi antihipertenzivov, je treba odmerek kabozantiniba zmanjšati. Z uporabo je treba prenehati, če je hipertenzija resna ali trdovratna kljub zdravljenju z antihipertenzivi in zmanjšanemu odmerku kabozantiniba. V primeru hipertenzijske krize je treba zdravljenje prekiniti. Pri resni PPES je treba razmisliti o prekinitvi zdravljenja. Nadaljevanje zdravljenja naj se začne z nižjim odmerkom, ko se PPES umiri do 1. stopnje. V času zdravljenja je treba redno spremljati beljakovine v urinu. Pri bolnikih, pri katerih se razvije nefrotični sindrom, je treba z uporabo kabozantiniba prenehati. Pri uporabi kabozantiniba so opazili sindrom reverzibilne posteriorne levkoencefalopatije (RPLS), znan tudi kot sindrom posteriorne reverzibilne encefalopatije (PRES). Na ta sindrom je treba pomisliti pri vseh bolnikih s številnimi prisotnimi simptomi, vključno z epileptičnimi napadi, glavobolom, motnjami vida, zmedenostjo ali spremenjenim mentalnim delovanjem. Pri bolnikih z RPLS je treba zdravljenje prekiniti. Kabozantinib je treba uporabljati previdno pri bolnikih s podaljšanjem intervala QT v anamnezi, pri bolnikih, ki jemljejo antiaritmike, in pri bolnikih z relevantno obstoječo boleznijo srca, bradikardijo ali elektrolitskimi motnjami. Uporaba kabozantiniba je bila povezana z večjo pojavnostjo elektrolitskih nepravilnosti (vključno s hipokaliemijo, hiperkaliemijo, hipomagneziemijo, hipokalciemijo in hiponatriemijo), zato je priporočljivo spremljati biokemijske parametre in po potrebi uvesti ustrezno nadomestno zdravljenje v skladu s standardno klinično prakso. Bolniki z redko dedno intoleranco za galaktozo, laponsko obliko zmanjšane aktivnosti laktaze ali malabsorpcijo glukoze/galaktoze ne smejo jemati tega zdravila. Plodnost, nosečnost in dojenje: Ženskam v rodni dobi je treba svetovati, da v času zdravljenja s kabozantinibom ne smejo zanositi. Zanositev morajo preprečiti tudi ženske partnerice moških bolnikov, ki uporabljajo kabozantinib. Med zdravljenjem in še vsaj 4 mesece po končanju terapije morajo tako bolniki in bolnice kot tudi njihovi partnerji uporabljati zanesljiv način kontracepcije. Kabozantiniba se ne sme uporabljati med nosečnostjo, razen če zdravljenje ni nujno potrebno zaradi kliničnega stanja ženske. Matere med zdravljenjem s kabozantinibom in še 4 mesece po končanju terapije ne smejo dojiti. Zdravljenje s kabozantinibom lahko predstavlja tveganje za plodnost pri moških in ženskah. **INTERAKCIJE** Kabozantinib je substrat za CYP3A4. Pri sočasni uporabi močnih zaviralcev CYP3A4 (npr. ritonavirja, itrakonazola, eritromicina, klaritromicina, soka grenivke) je potrebna previdnost. Kronični sočasni uporabi močnih induktorjev CYP3A4 (npr. fenitoina, karbamazepina, rifampicina, fenobarbitala ali pripravkov zeliščnega izvora iz šentjanževke) se je treba izogibati. Razmisliti je treba o sočasni uporabi alternativnih zdravil, ki CYP3A4 ne inducirajo in ne zavirajo ali pa inducirajo in zavirajo le neznatno. Pri sočasni uporabi zaviralcev MRP2 (npr. ciklosporina, efavirenza, emtricitabina) je potrebna previdnost, saj lahko povzročijo povečanje koncentracij kabozantiniba v plazmi. Učinka kabozantiniba na farmakokinetiko kontraceptivnih steroidov niso preučili, vendar pa se priporoča dodatna kontracepcijska metoda (pregradna metoda). Zaradi visoke stopnje vezave kabozantiniba na plazemske beljakovine je možna interakcija z varfarinom v obliki izpodrivanja s plazemskih beljakovin, zato je treba spremljati vrednosti INR. Kabozantinib morda lahko poveča koncentracije sočasno uporabljenih substratov P-gp v plazmi. Osebe je treba opozoriti na uporabo substratov P-gp (npr. feksofenadina, aliskirena, ambrisentana, dabigatran eteksilata, digoksina, kolhicina, maraviroka, posakonazola, ranolazina, saksagliptina, sitagliptina, talinolola, tolvaptana) sočasno s kabozantinibom.

NEŽELENI UČINKI Za popolno informacijo o neželenih učinkih, prosimo, preberite celoten povzetek glavnih značilnosti zdravila Cabometyx. Najpogostejši resni neželeni učinki zdravila v populaciji bolnikov s KLC so bili driska, hipertenzija, dehidracija, hiponatriemija, navzea, zmanjšanje apetita, embolija, utrujenost, hipomagneziemija in PPES. Najpogostejši neželeni učinki katere koli stopnje (ki so se pojavili pri vsaj 25 % bolnikov) v populaciji bolnikov s KLC so bili driska, hipertenzija, utrujenost, zvišanje vrednosti AST, zvišanje vrednosti ALT, navzea, zmanjšanje apetita, PPES, paragevzija, zmanjšanje števila trombocitov, stomatitis, anemija, bruhanje, zmanjšanje telesne mase, dispepsija in konstipacija. Najpogostejši resni neželeni učinki zdravila v populaciji bolnikov s HCK so bili jetrna encefalopatija, PPES, astenija in driska. Najpogostejši neželeni učinki katere koli stopnje (ki so se pojavili pri vsaj 25 % bolnikov) v populaciji bolnikov s HCK so bili driska, PPES, utrujenost, zmanjšanje apetita, hipertenzija in navzea. *Zelo pogosti (≥ 1/10):* anemija, hipotiroidizem, zmanjšan apetit, hipomagneziemija, hipokaliemija, paragevzija, glavobol, omotica, hipertenzija, krvavitev, disfonija, dispneja, kašelj, driska, navzea, bruhanje, stomatitis, konstipacija, bolečine v trebuhu, dispepsija, bolečina v zgornjem predelu trebuha, PPES, izpuščaj, bolečine v okončinah, utrujenost, vnetje sluznice, astenija, periferni edem, zmanjšanje telesne mase, zvišanje vrednosti ALT v serumu, zvišanje vrednosti AST. *Pogosti (≥ 1/100, < 1/10):* absces, trombocitopenija, nevtropenija, dehidracija, hipoalbuminemija, hipofosfatemija, hiponatriemija, hipokalciemija, hiperkaliemija, hiperbilirubinemija, hiperglikemija, hipoglikemija, periferna senzorična nevropatija, tinitus, venska tromboza, arterijska tromboza, pljučna embolija, gastrointestinalna perforacija, fistula, gastroezofagealna refluksna bolezen, hemoroidi, bolečina v ustni votlini, suha usta, jetrna encefalopatija, pruritus, alopecija, suha koža, akneiformni dermatitis, sprememba barve las oz. dlak, mišični krči, artralgija, proteinurija, zvišanje vrednosti ALP v krvi, GGT, kreatinina v krvi, amilaze, lipaze, holesterola v krvi, zmanjšanje števila belih krvnih celic. *Občasni (≥ 1/1.000, < 1/100):* limfopenija, konvulzije, pankreatitis, glosodinija, holestatični hepatitis, osteonekroza čeljusti, zvišanje vrednosti trigliceridov v krvi, zapleti z ranami. *Neznana pogostnost (ni mogoče oceniti iz razpoložljivih podatkov):* možganska kap, miokardni infarkt, anevrizme in disekcije arterij. **Vrsta ovojnine in vsebina:** Plastenka vsebuje 30 filmsko obloženih tablet. **Režim izdaje:** Rp/Spec **Imetnik dovoljenja za promet z zdravilom:** Ipsen Pharma, 65 quai Georges Gorse, 92100 Boulogne-Billancourt, Francija
Pred predpisovanjem, prosimo, preberite celoten povzetek glavnih značilnosti zdravila!
CAB-301019

▼ Za to zdravilo se izvaja dodatno spremljanje varnosti. Tako bodo hitreje na voljo nove informacije o njegovi varnosti. Zdravstvene delavce naprošamo, da poročajo o katerem koli domnevnem neželenem učinku zdravila.

IPSEN
Innovation for patient care

SAMO ZA STROKOVNO JAVNOST
CAB1219-05, december 2019

PharmaSwiss
Choose More Life

PharmaSwiss d.o.o., Brodišče 32, 1236 Trzin
telefon: +386 1 236 47 00, faks: +386 1 236 47 05

RADIOLOGY AND ONCOLOGY

June 2020
Vol. 54 No. 2
Pages 135-252
ISSN 1318-2099
UDC 616-006
CODEN: RONCEM

Publisher

Association of Radiology and Oncology

Aims and Scope

Radiology and Oncology is a multidisciplinary journal devoted to the publishing original and high quality scientific papers and review articles, pertinent to diagnostic and interventional radiology, computerized tomography, magnetic resonance, ultrasound, nuclear medicine, radiotherapy, clinical and experimental oncology, radiobiology, medical physics and radiation protection. Therefore, the scope of the journal is to cover beside radiology the diagnostic and therapeutic aspects in oncology, which distinguishes it from other journals in the field.

Editorial office

Radiology and Oncology
Zaloška cesta 2
P. O. Box 2217
SI-1000 Ljubljana
Slovenia
Phone: +386 1 5879 369
Phone/Fax: +386 1 5879 434
E-mail: gsersa@onko-i.si

Reader for English
Vida Kološa

Secretary
Mira Klemenčič
Zvezdana Vukmirović

Design
Monika Fink-Serša, Samo Rovan, Ivana Ljubanović

Layout
Matjaž Lužar

Printed by
Tiskarna Ozimek, Slovenia

Published quarterly in 400 copies

Beneficiary name: DRUŠTVO RADIOLOGIJE IN ONKOLOGIJE
Zaloška cesta 2
1000 Ljubljana
Slovenia

Beneficiary bank account number: SI56 02010-0090006751
IBAN: SI56 0201 0009 0006 751
Our bank name: Nova Ljubljanska banka, d.d.,
Ljubljana, Trg republike 2,
1520 Ljubljana; Slovenia

SWIFT: LJBASI2X

Subscription fee for institutions EUR 100, individuals EUR 50

The publication of this journal is subsidized by the Slovenian Research Agency.

Indexed and abstracted by:

- *Baidu Scholar*
- *Case*
- *Chemical Abstracts Service (CAS) - CAplus*
- *Chemical Abstracts Service (CAS) - SciFinder*
- *CNKI Scholar (China National Knowledge Infrastructure)*
- *CNPIEC - cnpLINKer*
- *Dimensions*
- *DOAJ (Directory of Open Access Journals)*
- *EBSCO (relevant databases)*
- *EBSCO Discovery Service*
- *Embase*
- *Genamics JournalSeek*
- *Google Scholar*
- *Japan Science and Technology Agency (JST)*
- *J-Gate*
- *Journal Citation Reports/Science Edition*
- *JournalGuide*
- *JournalTOCs*
- *KESLI-NDSL (Korean National Discovery for Science Leaders)*
- *Medline*
- *Meta*
- *Microsoft Academic*
- *Naviga (Softweco)*
- *Primo Central (ExLibris)*
- *ProQuest (relevant databases)*
- *Publons*
- *PubMed*
- *PubMed Central*
- *PubsHub*
- *QOAM (Quality Open Access Market)*
- *ReadCube*
- *Reaxys*
- *SCImago (SJR)*
- *SCOPUS*
- *Sherpa/RoMEO*
- *Summon (Serials Solutions/ProQuest)*
- *TDNet*
- *Ulrich's Periodicals Directory/ulrichsweb*
- *WanFang Data*
- *Web of Science - Current Contents/Clinical Medicine*
- *Web of Science - Science Citation Index Expanded*
- *WorldCat (OCLC)*

This journal is printed on acid- free paper

On the web: ISSN 1581-3207
https://content.sciendo.com/raon
http://www.radioloncol.com

contents

review

Current and innovative approaches in the treatment of non-muscle invasive bladder cancer: the role of transurethral resection of bladder tumor and organoids

Milena Taskovska[1,2], Mateja Erdani Kreft[3], Tomaz Smrkolj[1,2]

[1] Department of Urology, University Medical Centre Ljubljana, Ljubljana, Slovenia
[2] Department of Surgery, Faculty of Medicine, University of Ljubljana, Ljubljana, Slovenia
[3] Institute for Cell Biology, Faculty of Medicine, University of Ljubljana, Ljubljana, Slovenia

Radiol Oncol 2020; 54(2): 135-143.

Received 19 January 2020
Accepted 30 January 2020

Correspondence to: for organoids – Prof. Mateja Erdani-Kreft, Ph.D., Institute for Cell Biology, Faculty of Medicine, University of Ljubljana, Vrazov trg 2, SI-1000 Ljubljana, Slovenia. E-mail: mateja.erdani@mf.uni-lj.si

Correspondence to: for monopolar/bipolar TURB – Assoc. Prof. Tomaž Smrkolj, M.D., Ph.D., Department of Urology, University Medical Centre Ljubljana, Zaloška 7, 1000 Ljubljana, Slovenia or Department of Surgery, Faculty of Medicine, University of Ljubljana, Zaloška 7, SI-1000 Ljubljana, Slovenia. Email: tomaz.smrkolj@kclj.si

Disclosure: No potential conflicts of interest were disclosed.

Background. Bladder cancer is the 7th most common cancer in men. About 75% of all bladder cancer are non-muscle invasive (NMIBC). The golden standard for definite diagnosis and first-line treatment of NMIBC is transurethral resection of bladder tumour (TURB). Historically, the monopolar current was used first, today bipolar current is preferred by most urologists. Following TURB, depending on the tumour grade, additional intravesical chemo- or/and immunotherapy is indicated, in order to prevent recurrence and need for surgical resection. Development of new technologies, molecular and cell biology, enabled scientists to develop organoids – systems of human cells that are cultivated in the laboratory and have characteristics of the tissue from which they were harvested. In the field of urologic cancers, the organoids are used mainly for studying the course of different diseases, however, in the field of bladder cancer the data are scarce.

Conclusions. Different currents - monopolar and bipolar, have different effect on urothelium, that is important for oncological results and pathohistological interpretation. Specimens of bladder cancer can be used for preparation of organoids that are further used for studying carcinogenesis. Bladder organoids are step towards personalised medicine, especially for testing effectiveness of chemo-/immunotherapeutics.

Key words: bladder cancer; transurethral resection of bladder tumour; monopolar/bipolar current; organoids, mitomycin C; BCG

Introduction

Bladder cancer is 7th most common cancer in men. In the European Union (EU) age-standardised incidence rate is 19.1 for men and 4.0 in women.[1] In Europe, bladder cancer incidence is 27.1 and mortality 8.9.[2] The highest incidence rate in the EU is reported in Belgium and lowest in Finland. On the global level, incidence and mortality rates vary due to different methodologies and diagnostic practices.[1,2] Approximately three-quarters of all bladder cancer are non-muscle invasive (NMIBC) – the disease is confined to the mucosa (stage Ta, CIS) and submucosa (stage T1) (Table 1, Figure 1), in patients younger than 40 years this proportion is even higher.[1,3-5] According to the data from Cancer registry of the Republic of Slovenia, bladder cancer is the 8th most common cancer in men and the 13th most common when both genders are considered. Age standardised incidence rate is

11.74 in men and 2.97 in women. Age-standardised mortality rate is 5.46 in men and 1.52 in women.[6] Although many European countries experience incidence rise, the projected growth rate of bladder cancer incidence rates by 2030 in Slovenia is extremely high, i.e. 92% for men and 256% for women.

Standard treatment of NMIBC is transurethral resection of bladder tumour (TURB). Depending on the histopathological tumour characteristics, additional treatment with intravesical chemotherapeutics or immunotherapeutics is indicated. The aim of intravesical therapy is to decrease the rate of recurrence and need for surgical intervention.[1]

Organoids are 3D models which consist of cells derived from specific tissue or organ and are grown in the laboratory with the aim to study different cell biological mechanisms, homeostasis, development of disease and effect of different medications. Organoids have characteristics of the cells from which are derived, although differences could appear because of the effect of microenvironment.[7] There are some new data about organoids used to study oncogenesis and different treatments in urological cancers (prostate, kidney, bladder).[8]

Aim of this review is to present different modalities of TURB for treatment of NMIBC, and the role of bladder/urothelium organoids for studying oncogenesis, therapeutic modalities and personalised medicine in NMIBC.

Transurethral resection of bladder tumour (TURB)

TURB is a golden standard in diagnosis, treatment, and staging of NMIBC as well as in diagnosis of muscle invasive bladder cancer (MIBC).[1,9] The first published report involving the application of electric current for endoscopic resection of papillary bladder tumours through cystoscope originates in 1910s. The initial case was performed using water as medium. Since then, TURB has become standard in evaluation and treatment of patients with bladder cancer.[9] Guidelines of three urologic associations (European Association of Urology, EAU; American Urology Association, AUA; and Canadian Urology Association, CUA) emphasize the importance of TURB for diagnosis, staging and treatment of NMIBC (1, 9, 10, 11).[1,9,10,11]

TABLE 1. 2017 TNM classification of urinary bladder cancer [5]

T - primary tumour
TX Primary tumour cannot be assessed
T0 No evidence of primary tumour
Ta Non-invasive papillary carcinoma
Tis Carcinoma in situ: 'flat tumour'
T1 Tumour invades subepithelial connective tissue
T2 Tumour invades muscle
T2a Tumour invades superficial muscle (inner half)
T2b Tumour invades deep muscle (outer half)
T3 Tumour invades perivesical tissue
T3a Microscopically
T3b Macroscopically (extravesical mass)
T4 Tumour invades any of the following: prostate stroma, seminal vesicles, uterus, vagina, pelvic wall, abdominal wall
T4a Tumour invades prostate stroma, seminal vesicles, uterus or vagina
T4b Tumour invades pelvic wall or abdominal wall
N - regional lymph nodes
NX Regional lymph nodes cannot be assessed
N0 No regional lymph node metastasis
N1 Metastasis in a single lymph node in the true pelvis (hypogastric, obturator, external iliac, or presacral)
N2 Metastasis in multiple regional lymph nodes in the true pelvis (hypogastric, obturator, external iliac, or presacral)
N3 Metastasis in common iliac lymph node(s)
M - distant metastasis
M0 No distant metastasis
M1a Non-regional lymph nodes
M1b Other distant metastases

TURB is a relatively safe procedure with few complications, in some countries is performed in an outpatient setting. The most common complications are haematuria and urinary tract infection. One of the most important aims of TURB is to resect the whole tumour (depending on the size and invasion in muscle layer) and resect muscle layer in order to obtain the correct pathological stage.[1,10,11] Since its introduction in the 1910s, technology has developed and so has equipment and technique of TURB.[9] In 1900 Joseph Rivere discovered that a spark arcing from an electrode coagulates skin and he used it for treatment of skin lesions. In the following decades, this technique was used to treat skin lesions, lesions in the oral cavity, bladder, coagulation of vascular tumours and haemorrhoids. In 1920s Clark was one of the first who observed the tissues exposed to current under a microscope and found that they shrink from dehydration. Bovie constructed the first diathermy unit that was used for cutting, coagulation, and dissection and was first used on October 1st 1926 in Boston. Since then, this instrument is used in everyday surgical practice (12).[12]

The clinical effect of electrocautery is a consequence of heat. When oscillating current is applied to the tissue, the rapid movement of electrons through the cytoplasm causes an increase of intracellular temperature. The effect on the tissue depends upon the amount of thermal energy delivered and the time rate of delivery. Temperature below 45°C causes reversible thermal damages, when increased it causes denaturation and loss of protein structure, above 90°C liquid evaporates, resulting in vaporization if heated rapidly or desiccation if heated slowly. Temperatures over 200°C cause carbonization.[12]

Electric energy could be monopolar or bipolar. Monopolar energy delivery requires the current to pass from the generator to the active electrode through the patient and out of the body through a dispersive electrode pad which is connected to the generator in order to complete the circuit. On the other hand, bipolar delivery does not require a dispersive return electrode because both active and return electrodes are integrated into energy delivery forceps with target tissue between them (Figure 2).[12]

Monopolar electrocautery for TURB

In urology, TURB was introduced in the 1910s by Beer using monopolar current for fulguration (Figure 2).[13,14] Monopolar electrocautery requires high energy and voltage to allow current transmission from the loop to the tissue. In monopolar electrocautery glycine is used as a medium that is associated with limitations, such as short resection time due to the risk of development of TURB syndrome. The heat generated while cutting the tissue causes damage to the surrounding cells. Because of the thermal artefacts, pathologic assessment of the specimen is sometimes difficult.[13] There are studies which compared monopolar and bipolar elec-

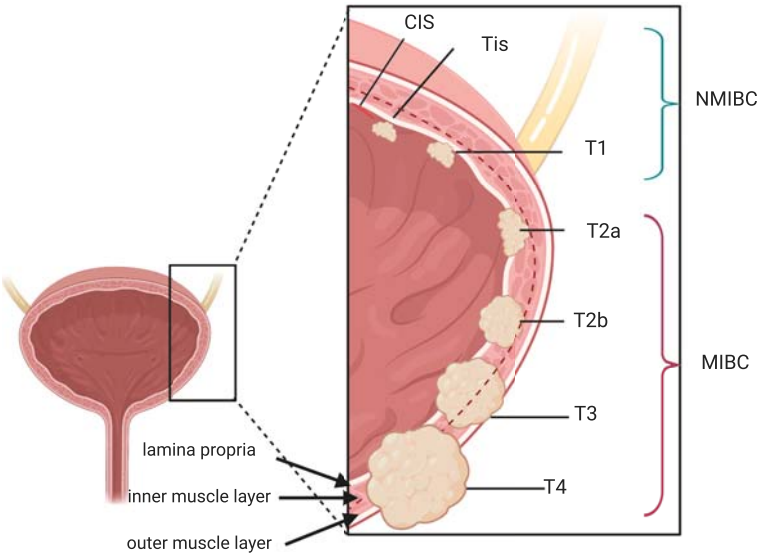

FIGURE 1. Classification of bladder cancer.

MIBC = Muscle invasive bladder cancer; NMIBC = Non muscle invasive bladder cancer

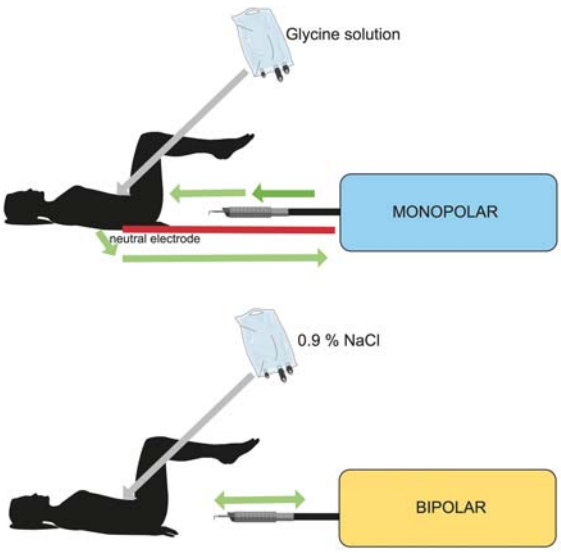

FIGURE 2. Monopolar vs. bipolar transurethral resection of bladder tumor.

TABLE 2. Comparison of monopolar and bipolar current for TURB[1,9-14]

Variable	Monopolar	Bipolar
Dispersive electrode pad	yes	no
Energy	high	low
Voltage	high	low
Working medium	glycine	saline
Temperature at thermal effect (°C)	400	40–70
Time of resection	limited	extended (not strictly limited)
TUR syndrome	common	rare
Obturator jerk	common	rare
Quality of haemostasis and coagulum	poor	good

trocautery for TURB and concluded that there is very little or no difference in thickness of thermal artefacts.[14] One study has shown mean depth of thermal artefacts of 0.237 mm when using bipolar electrocautery and 0.26 mm when using monopolar electrocautery.[9] Monopolar electrocautery is not inferior to bipolar electrocautery regarding intra and postoperative bleeding, and perforation of bladder wall (Table 2).[14]

Bipolar electrocautery for TURB

Bipolar electrocautery has been introduced about 30 years ago and a few years after its introduction has gained popularity over monopolar electrocautery.[12] Bipolar electrocautery was first used for transurethral resection of the prostate (TURP) for benign prostate enlargement and obstruction. It was quickly adopted for TURB because of advantages: (1) isotonic medium could be used (such as saline), (2) electric circuit is completed using only resection loop and sheath of the device itself, so the patient is not included in the circuit, (3) risk for TUR syndrome is low, (4) time for resection is extended, which is of essential importance in case of large bladder tumours, (5) incidence of obturator jerk is lower, (6) there are fewer bladder perforations. It is also related to fewer postoperative complications such as clot retention and contracture of the bladder neck (Table 2).[9]

One of the main differences between monopolar electrocautery and bipolar electrocautery systems is the coagulation mechanism. In bipolar electrocautery system voltage is low and energy dissipates as heat in the tissue leading to the formation of coagulum and haemostasis.[13]

In monopolar electrocautery, electrical injury directed into the tissues and electrical resistance creates temperature as high as 400°C which causes tissue desiccation and collateral tissue damage. Radiofrequency energy of bipolar electrocautery systems converts the conductive medium into a plasma field with highly ionised particles that disrupt the organic bonds between tissues and allows thermal effect to occur at lower temperatures (between 40 and 70°C). Pathologists sometimes classify thermal damage into three categories: (1) cautery artefact less than 1/3 of the specimen, (2) cautery artefact of 1/3 to 2/3 of the specimen and (3) over 2/3 of the specimen.[13] Although different electrocautery systems are used for more than 30 years we have no data on the effect of different electrocautery systems on cellular level.

Adjuvant treatment of NMIBC

Intravesical chemotherapy

TURB is used as definitive therapy in TaT1 tumours. The adjuvant treatment of NMIBC is indicated when dealing with high grade NMIBC. Immediate single intravesical instillation of chemotherapy is used to destroy circulating tumour cells after TURB and has an ablative effect on residual tumour cells at the resection site and on small overlooked tumours. Immediate single intravesical instillation should be performed within the first 24 hours after TURB to maximise its effect. Meta-analyses were performed which have shown that after immediate single intravesical instillation the recurrence rate is lower. Recent reviews and meta-analysis have shown that immediate single intravesical instillation also reduces 5-year recurrence rate.[1,15]

The most commonly used chemotherapeutics for immediate single intravesical instillation are mitomycin C (MMC), epirubicin and pirarubicin.[1] In Slovenia, we use MMC for immediate single intravesical instillation. In literature, there is data that further repeat instillations of chemotherapy also have an impact on the recurrence rate. The length and frequency of chemotherapy instillation are still controversial. According to data available, the length of this treatment should not exceed one year.[1,16]

There is evidence that intravesical chemotherapy combined with microwave-induced hyperthermia in high-risk patients has enhanced efficacy – it has improved recurrence-free survival at 24 months. There are also undergoing trials regarding use of different methods of hyperthermic intravesical chemotherapy and electromotive drug administration but data about their efficacy is still lacking.[1,17] In Slovenia, we are not using combinations with microwave, hyperthermia or electromotive drug

administration, since the use of these combinations is not confirmed by randomised controlled trials.

Intravesical bacillus Calmette-Guerin (BCG) immunotherapy

There is evidence in the literature that BCG after TURB is superior to TURB alone or in combination with chemotherapy for preventing recurrence of NMIBC. BCG maintenance therapy reduces the recurrence rate for 32% in comparison to MMC, but increases risk for 28% in patients who did not receive maintenance therapy with BCG.[1,18] The main disadvantage of BCG intravesical immunotherapy is in its side effects. According to data in the literature, serious side effects are encountered in less than 5% of treated patients. Side effects are a consequence of systemic absorption of BCG.[1,19] Caution is needed in immunocompromised patients, although some studies have not shown that immunocompromised patients are more prone to experience side effects.[1] For BCG instillation is used 6-week schedule introduced by Morales.[1,20] Many studies were conducted but none has shown advantages or disadvantages of this schedule compared to others.[1,21] Meta-analysis has shown that at least one year of maintenance BCG is required to obtain superiority of BCG over MMC for prevention of recurrence or progression. Regarding BCG dose, studies have shown that one-third dose is required to be effective for intermediate-risk tumors, full dose is needed for high-risk tumors.[1,22]

According to the EAU guidelines on NMIBC, BCG intravesical immunotherapy is recommended to patients with intermediate and high-risk tumors, three year maintenance therapy is more effective in patients with high-risk tumors to prevent recurrence.[1]

There are cases when BCG intravesical chemotherapy fails: (1) muscle invasive bladder cancer (MIBC) detected during follow-up, (2) BCG-refractory tumor - (a) if high-grade NMIBC is detected at three months, (b) CIS is present at three and six months and (c) high grade tumor is detected after BCG therapy. Therefore, radical cystectomy is indicated.[1]

Personalized treatment - precision medicine in the treatment of bladder cancer

The efficacy of cancer management is challenging and depends upon genomic, molecular and immunologic characteristics of cancer. New discoveries in these fields are making cancer treatment more targeted and efficient. Concerning bladder cancer, mutations in genes of DNA repair pathway (e.g. *ERCC2, FANCC, ATM, RB1* and etc.) can predict response to neoadjuvant platinum-based systemic chemotherapies. Therapies that influence the immune system such as immune checkpoint inhibitors (PDA, PDL1, CTLA4) are approved for use in treatment of bladder cancer and represent renaissance in medical oncological treatment of this disease.[23]

Cancer treatment based on the response of bladder cancer organoid could contribute to more personalized approach in the treatment of this disease.

Role of organoids in studying bladder cancer

Organoids

In order to understand the role of cancer-specific genetic alterations in tumorigenesis, maintenance of tumor and sensibility age-standardized response to different therapeutics, development of *in vitro* and *in vivo* model systems that accurately reflect genetic diversity and lineage specificity of cancer was required.[7,8] For this purpose, cell lines are used. Their disadvantages is that they are mainly long term 2D cultures, and there is a lack of clinical data regarding the organ of origin. To overcome these disadvantages *in vivo* models are used.[8] The advantage of i*n vivo* models is that they are able to recapitulate histological and therapeutic response but there are species-specific differences and inaccurate recapitulation of *in vivo* human tumour biology that are main disadvantage.[7,8] In combination with organoids derived from normal cells, tumour cell organoids can be used to study transformation from normal to malignant, when exposed to different carcinogens.[8]

Sato *et al*. in 2009 discovered that single leucine-rich repeat containing G-protein coupled receptor 5-positive intestinal stem cell is able to generate a continuously expanding, self-organizing, physiological epithelial structure that was similar to normal gut tissue. It was named organoid culture.[24] Liu *et al*. demonstrated that combination of ROCK inhibitor and feeder fibroblast culture conditions enables the infinite growth of multiple primary human epithelial cell types. Based on this, organoids from normal and tumour cells might be able to proliferate indefinitely *in vitro*, with no need to transduct exogenous viral or cellular genes

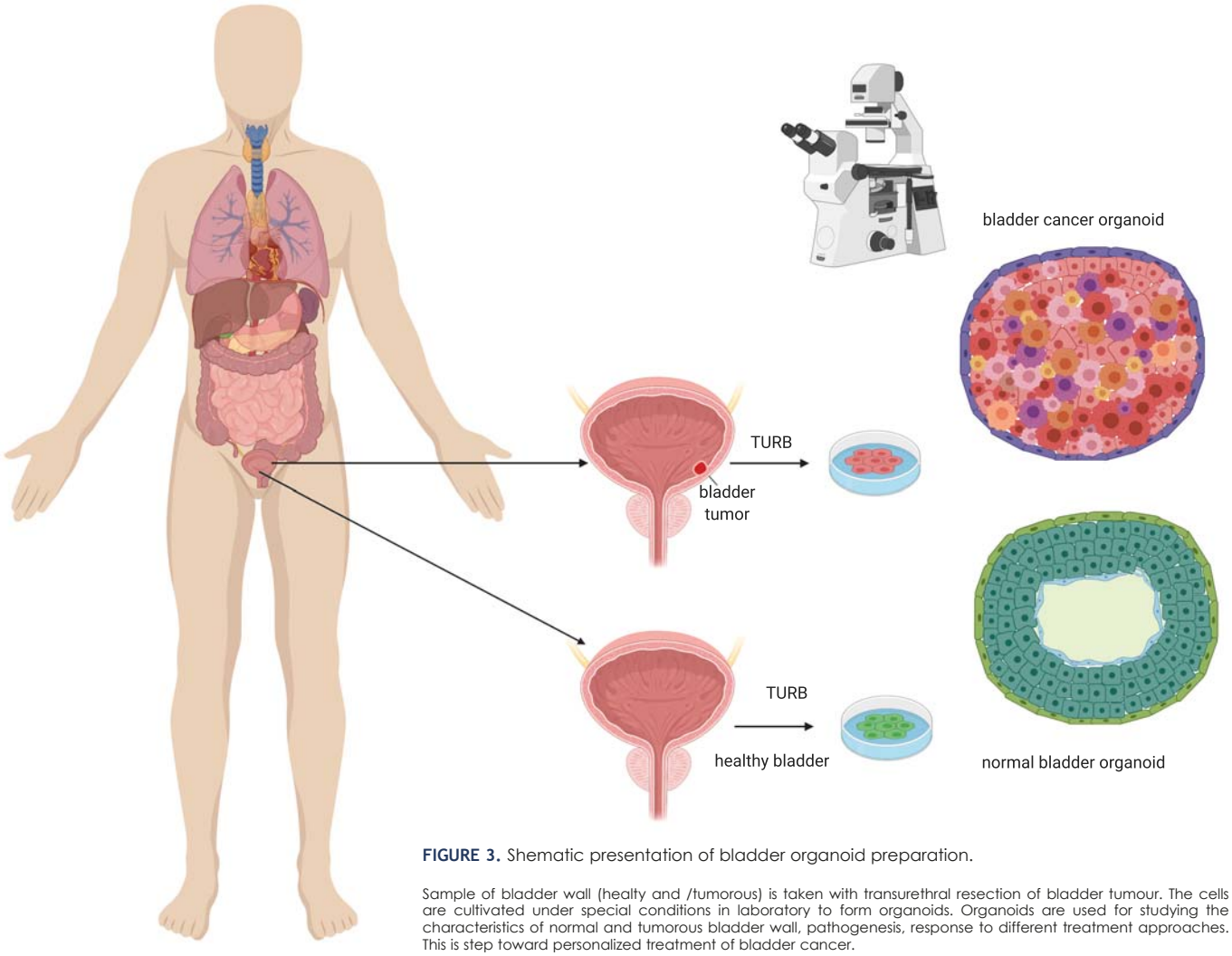

FIGURE 3. Shematic presentation of bladder organoid preparation.

Sample of bladder wall (healty and /tumorous) is taken with transurethral resection of bladder tumour. The cells are cultivated under special conditions in laboratory to form organoids. Organoids are used for studying the characteristics of normal and tumorous bladder wall, pathogenesis, response to different treatment approaches. This is step toward personalized treatment of bladder cancer.

(Figure 3).[8,25,26] Organoids are nowadays used for research of different cancers.[7,8] In the field of urology there are studies/reports on kidney, prostate and bladder organoids.[8,27,28]

3D organoids could be derived from cell lines, primary tissues, induced pluripotent stem cells, embryonic stem cells and embryonic whole organs such as organ explants that consist of many tissue types. Organoid is composed of multiple cell types and contains multicellular organ structures, which mimic the tissue of origin and functions in a similar manner. Organoids can be generated in different manners.[7,8]

Cell lines

In 3D culture conditions, some immortalized cell lines are able to form polarized 3D structures.[8] Smith *et al*. cultured human bladder cells that were used to investigate how terminally differentiated human urothelial cells interact with uropathogenic *E.coli*. They cultured 5637 cells under microgravity conditions within a rotating wall vessel bioreactor. Under these conditions, cells remain in suspension and form organoids that reflect characteristics of *in vivo* tissue-specific determination. Human bladder cells in this model had developed into a model that expresses specific markers and structures, characteristic of differentiated human urothelium.[8,29]

Lee *et al*. have shown that patient-derived bladder tumour organoids have most characteristics of parental tumour, although in a culture they may change their marker phenotype. Organoids could be used for studying the biology of the tumour and the effect of different therapies on tumour of individual patient.[7] In the future, these models could be used for personalized treatment of the patient according to tumour characteristics.[7]

Primary adult stem cells

Primary adult stem cells could also be used for organoids.[8] Matulay *et al*. collected bladder tumour specimens during cystoscopy, enzymatically digested them into single cells and cell clusters and then cultured them in organoid-prompting, embedded-cell culture conditions. They used these bladder organoids to analyse genetic mutations in bladder cancer.[8,30]

Pluripotent stem cells

Pluripotent stem cells have the ability to form all cellular components of an organ (epithelial, stromal and endothelial cells). Organoid could be generated from embryonic or induced pluripotent stem cells (iPSC). Using organoid 3D system, scientists are able to induce pluripotent stem cells to develop into organoids of the desired organ. Until 2014 there were two protocols to induce human embryonic stem cells or human iPSC into urothelium.[8] Osborn *et al*. have developed *in vitro* culture system that was matrix-free and cell-contact-free, and was able to induce human embryonic stem cells or human iPSC to differentiate into definitive endoderm and then urothelium using directed differentiation in urothelium specific medium.[8,31] Kang *et al*. have developed a protocol that used a chemically defined culture system to induce human iPSC to differentiate into endoderm and bladder urothelial cells.[8,32]

Application of organoids in diagnosis and management of bladder cancer

Organoids could be used to predict the response to treatment and guide the medicine regimen. For colorectal cancer, 3D organoid based drug sensitivity screen was developed. It identifies molecular signatures associated with altered drug responses. A similar strategy could be used with bladder cancer organoids.[33,34] Resistance to chemotherapy is promoted by cancer stem cells. Models with origin from cancer stem cells may be helpful for identifying effective prognostic biomarkers and for individual treatment.[8] In case of prostate cancer, there are already organoids being used to test different drugs, even further, there are models developed to screen for prostate cancer instead of cored biopsy, so-called liquid biopsy.[8,30,36]

Matulay *et al*. have established urothelial cancer organoids from patient-derived tissue samples. Using DNA sequencing analysis, they have shown that organoid lines have similar mutational profiles to those of tumour sample and can provide a platform for personalized drug-response assays in urothelial cancers.[8,30]

There are few studies aim of which was to identify bladder cancer stem cells, but the results are inconclusive.[8] In one study, researchers have described Sonic hedgehog (Shh) expressing and cytokeratin-5 (Ck5) expressing basal urothelial cells from ShhCreER/WT; R26mTmG/WT mice in organoid culture. Those were multipotent stem cells capable of self-renewal and regeneration into all cell types within urothelium in response to chemical injury or bacterial infection. Individual Shh-expressing cells formed cyst-like organoids after 5–7 weeks of 3D culture. CK5 was expressed in the outer layer. They also formed a luminal space in which CK5 and Shh were not expressed. Individual cells of these organoids were capable of self-renewal and differentiation, however, the origin and formation of bladder cancer stem cells remain unknown.[8,37]

Mullenders *et al*. collected samples of tumours of MIBC and NMIBC patients who underwent radical cystectomy and TURB, and normal macroscopically looking urothelium and established a sample of 50 human bladder organoids. Besides histological and functional investigations, they also used organoids for testing the efficacy of different intravesical chemotherapeutics. They applied different concentrations of anticancer drugs for time period of 5 days and found different responses in different organoids.[38]

Neal *et al*. purposed an *in vitro* model of different cancers for studying immunotherapy. One of them was also bladder cancer and responsiveness to immunotherapy with checkpoint inhibitors.[34]

Limitations of organoids

Organoids have a potentially important role in urological research, clinical decision-making, and treatment of urological cancers. Limitations of organoids are that the spatial orientation of tissues is random, also in many cases, the cellular components that are present in *in vivo* systems such as stromal, vascular endothelial and immune cells are missing.[8]

Conclusions

Bladder cancer presents public health problem because incidence and mortality are constant despite

the development of technology, molecular and cell biology, pharmacology and improvement of surgical technique. TURB is the golden standard for diagnosis, staging, and treatment of NMIBC. Both monopolar and bipolar current are equally effective, bipolar current having fewer complications. Development of molecular and cell biology leads to the construction of organoids which are a step towards personalized medicine. We expect that they will enable us to treat our patients based on the data acquired from organoids, regarding oncogenesis, responsiveness to different therapeutic modalities and possibilities for reconstruction.

References

1. European Association of Urology. *Guidelines. Non-invasive muscle bladder cancer*. [cited 2019 Dec 15]. Available at: https://uroweb.org/guideline/non-muscle-invasive-bladder-cancer/
2. European Commission. ECIS - European Cancer Information System. Incidence and mortality of bladder cancer in Europe. [cited 2018 Sep 15]. Available at: https://ecis.jrc.ec.europa.eu/explorer.php?$1-All$2-All$4-1,2$3-38$6-0,14$5-2008,2008$7-7,8$0-0$CEstByCountry$X0_8-3$CEstRelative$X1_8-3$X1_9-AE28
3. Compérat E, Larré S, Roupret M, Neuzillet Y, Pignot G, Quintens H, et al. Clinicopathological characteristics of urothelial bladder cancer in patients less than 40 years old. *Virchows Arch* 2015; **466:** 589-94. doi: 10.1007/s00428-015-1739-2.
4. Burger M, Catto JW, Dalbagni G, Grossman HB, Herr H, Karakiewicz P, et al. Epidemiology and risk factors of urothelial bladder cancer. *Eur Urol* 2013; **63:** 234-41. doi: 10.1016/j.eururo.2012.07.033
5. UICC International Union Against Cancer. Urinary bladder. In: Sobin LH, Gospodarowicz MK, Wittekind Ch, editors. *TNM classification of malignant tumours*, 7th edition. Chichester: Wiley-Blackwell, 2009. p. 262-5.
6. Slora. Slovenia and cancer. Basic epidemiologic data on cancer. Urinary bladder (C67). [cited 2018 Mar 03]. Available at: http://www.slora.si/documents/11561/20219/bladder.pdf?version=1.2
7. Lee SH, Hu W, Matulay JT, Silva MV, Owczarek TB, Kim K, et al. Tumor evolution and drug response in patient-derived organoid models of bladder cancer. *Cell* 2018; **173:** 515-28.e17. doi: 10.1016/j.cell.2018.03.017
8. Wang S, Gao D, Chen Y. The potential of organoids in urological cancer research. *Nat Rev Urol* 2017; **14:** 401-14. doi: 10.1038/nrurol.2017.65
9. Zainfeld D, Daneshmand S. Transurethral resection of bladder tumors: improving quality through new techniques and technologies. *Curr Urol Rep* 2017; **18:** 34. doi: 10.1007/s11934-017-0680-0
10. American Urological Association. Treatment of non-metastatic muscle-invasive bladder cancer: AUA/ASCO/ASTRO/SUO Guideline (2017). [2019 Dec 15]. Available at: https://www.auanet.org/guidelines/bladder-cancer-non-metastatic-muscle-invasive
11. Kassouf W, Traboulsi SL, Kulkarni GS, Breau RH, Zlotta A, Fairey A, et al. CUA guidelines on the management of non-muscle invasive bladder cancer. *Can Urol Assoc J* 2015; **9**: E690-704. doi: 10.5489/cuaj.3320
12. Massarweh NN, Cosgriff N, Slakey DP. Electrosurgery: history, principles, and current and future uses. *J Am Coll Surg* 2006; **202:** 520-30. doi: 10.1016/j.jamcollsurg.2005.11.017
13. Osman Y, Harraz AM. A review comparing experience and results with bipolar versus monopolar resection for treatment of bladder tumors. *Curr Urol Rep* 2016; **17:** 21. doi: 10.1007/s11934-016-0579-1
14. Mashni J, Godoy G, Haarer C, Dalbagni G, Reuter VE, Al-Ahmadie H, et al. Prospective evaluation of plasma kinetic bipolar resection of bladder cancer: comparison to monopolar resection and pathologic findings. *Int Urol Nephrol* 2014; **46:** 1699-705. doi: 10.1007/s11255-014-0719-9
15. Sylvester RJ, Oosterlinck W, Holmang S, Sydes MR, Birtle A, Gudjonsson S, et al. Systematic review and individual patient data meta-analysis of randomized trials comparing a single immediate instillation of chemotherapy after transurethral resection with transurethral resection alone in patients with stage pTa-pT1 urothelial carcinoma of the bladder: which patients benefit from the instillation? *Eur Urol* 2016; **69:** 231-44. doi: 10.1016/j.eururo.2015.05.050
16. Sylvester RJ, Oosterlinck W, Witjes JA. The schedule and duration of intravesical chemotherapy in patients with non-muscle-invasive bladder cancer: a systematic review of the published results of randomized clinical trials. *Eur Urol* 2008; **53:** 709-19. doi: 10.1016/j.eururo.2008.01.015
17. Arends TJ, Nativ O, Maffezzini M, de Cobelli O, Canepa G, Verweij F, et al. Results of a randomised controlled trial comparing intravesical chemohyperthermia with mitomycin C versus bacillus Calmette-Guerin for adjuvant treatment of patients with intermediate- and high-risk non-muscle-invasive bladder cancer. *Eur Urol* 2016; **69:** 1046-52. doi: 10.1016/j.eururo.2016.01.006
18. Malmstrom PU, Sylvester RJ, Crawford DE, Friedrich M, Krege S, Rintala E, et al. An individual patient data meta-analysis of the long-term outcome of randomised studies comparing intravesical mitomycin C versus bacillus Calmette-Guerin for non-muscle-invasive bladder cancer. *Eur Urol* 2009; **56:** 247-56. doi: 10.1016/j.eururo.2009.04.038
19. van der Meijden AP, Sylvester RJ, Oosterlinck W, Hoeltl W, Bono AV; EORTC Genito-Urinary Tract Cancer Group. Maintenance Bacillus Calmette-Guerin for Ta T1 bladder tumors is not associated with increased toxicity: results from a European Organisation for Research and Treatment of Cancer Genito-Urinary Group Phase III Trial. *Eur Urol* 2003; **44:** 429-34. doi: 10.1016/s0302-2838(03)00357-9
20. Morales A, Eidinger D, Bruce AW. Intracavitary bacillus Calmette-Guerin in the treatment of superficial bladder tumors. *J Urol* 1976; **116:** 180-3. doi: 10.1016/s0022-5347(17)58737-6
21. Sylvester, RJ, van der Meijden AP, Lamm DL. Intravesical bacillus Calmette-Guerin reduces the risk of progression in patients with superficial bladder cancer: a meta-analysis of the published results of randomized clinical trials. *J Urol* 2002; **168:** 1964-70. doi: 10.1097/01.ju.0000034450.80198.1c
22. Ojea A, Nogueira JL, Solsona E, Flores N, Gómez JM, Molina JR, et al. A multicentre, randomised prospective trial comparing three intravesical adjuvant therapies for intermediate-risk superficial bladder cancer: low-dose bacillus Calmette-Guerin (27 mg) versus very low-dose bacillus Calmette-Guerin (13.5 mg) versus mitomycin C. *Eur Urol* 2007; **52:** 1398-406. doi: 10.1016/j.eururo.2007.04.062
23. Flsenstein KM, Theodorescu D. Precision medicine for urothelial bladder cancer: update on tumour genomics and immunotherapy. *Nat Rev Urol* 2018; **15:** 92-111. doi: 10.1038/nrurol.2017.179
24. Sato T, Vries RG, Snippert HJ, van de Wetering M, Barker N, Stange DE, et al. Single Lgr5 stem cells build crypt-villus structures in vitro without a mesenchymal niche. *Nature* 2009; **459:** 262-5. doi: 10.1038/nature07935
25. Liu X, Ory V, Chapman S, Yuan H, Albanese C, Kallakury B, et al. ROCK inhibitor and feeder cells induce the conditional reprogramming of epithelial cells. *Am J Pathol* 2012; **180:** 599-607. doi: 10.1016/j.ajpath.2011.10.036
26. Chapman S, Liu X, Meyers C, Schlegel R, McBride AA. Human keratinocytes are efficiently immortalized by a Rho kinase inhibitor. *J Clin Invest* 2010; **120:** 2619-26. doi: 10.1172/JCI42297
27. Santos CP, Lapi E, Martínez de Villarreal J, Alvaro-Espinosa L, Fernandez-Barral A, Barbáchano A, et al. Urothelial organoids originating from Cd49fhigh mouse stem cells display Notch-dependent differentiation capacity. *Nat Commun* 2019; **10:** 4407. doi: 10.1038/s41467-019-12307-1.
28. Vasytin I, Zerihun L, Ivan C, Atala A. Bladder organoids and spheroids: potential tools for normal and diseased tissue modelling. *Anticancer Res* 2019; **39:** 1105-18. doi: 10.21873/anticanres.13219
29. Smith YC, Grande KK, Rasmussen SB, O'Brien AD. Novel three-dimensional organoid model for evaluation of the interaction of uropathogenic Escherichia coli with terminally differentiated human urothelial cells. *Infect Immun* 2006; **74:** 750-7. doi: 10.1128/IAI.74.1.750-757.2006
30. Matulay JT, Barlow LJ, Silva MV, Chua CW, Benson MC, McKiernan JM, et al. Genetic mutations in patient-derived bladder tumor organoids mimic parental tumor samples [abstract PD38-07]. *J Urol* 2016; **195(Suppl):** e926. doi: 10.1016/j.juro.2016.02.1487

31. Osborn SL, Thangappan R, Luria A, Lee JH, Nolta J, Kurzrock EA, et al. Induction of human embryonic and induced pluripotent stem cells into urothelium. *Stem Cells Transl Med* 2014; **3:** 610-9. doi: 10.5966/sctm.2013-0131

32. Kang M, Kim HH, Han YM. Generation of bladder urothelium from human pluripotent stem cells under chemically defined serum- and feeder-free system. *Int J Mol Sci* 2014; **15:** 7139-57. doi: 10.3390/ijms15057139

33. Banerjee S, Southgate J. Bladder organoids a step towards personalised cancer therapy? *Transl Androl Urol* 2019; **8:** S300-2. doi: 10.21037/tau.2019.06.10

34. Neal JT, Li X, Zhu J, Giangarra V, Grzeskowiak CL, Ju J, et al. Organoid modeling of the tumor immune microenvironment. *Cell* 2018; **175:** 1972-88. doi: 10.1016/j.cell.2018.11.021

35. Scher HI, Heller G, Molina A, Attard G, Danila DC, Jia X, et al. Circulating tumor cell biomarker panel as an individual-level surrogate for survival in metastatic castration-resistant prostate cancer. *J Clin Oncol* 2015; **33:** 1348-55. doi: 10.1200/JCO.2014.55.3487

36. Lozar T, Gersak K, Cemazar M, Grasic Kuhar C, Jesenko T. The biology and clinical potential of circulating tumor cells. *Radiol Oncol* 2019; **53:** 131-47. doi: 10.2478/raon-2019-0024

37. Shin K, Lee J, Guo N, Kim J, Lim A, Qu L, et al. Hedgehog/Wnt feedback supports regenerative proliferation of epithelial stem cells in bladder. *Nature* 2011; **472:** 110-4. doi: 10.1038/nature09851

38. Mullenders J, de Jongh E, Brousali A, Roosen M, Blom JPA, Begthel, et al. Mouse and human urothelial cancer organoids: a tool for bladder cancer research. *Proc Natl Acad Sci U S A* 2019; **116:** 4567-74. doi: 10.1073/pnas.1803595116.

review

Mechanical recanalization for acute bilateral cerebral artery occlusion – literature overview with a case

Miran Jeromel[1,2], Zoran V. Milosevic[1], Janja Pretnar Oblak[3]

[1] Department of Diagnostic and Interventional Neuroradiology, University Medical Centre Ljubljana, Ljubljana, Slovenia
[2] Department of Diagnostic and Interventional Radiology, General Hospital Slovenj Gradec, Slovenj Gradec, Slovenia
[3] Department for Vascular Neurology and Intensive Neurological Therapy, University Medical Centre Ljubljana, Ljubljana, Slovenia

Radiol Oncol 2020; 54(2): 144-148.

Received 19 January 2020
Accepted 5 March 2020

Correspondence to: Miran Jeromel, M.D., Ph.D., Department of Diagnostic and Interventional Radiology, General Hospital Slovenj Gradec, Gosposvetska cesta 1, SI-2380 Slovenj Gradec, Slovenia. E-mail: miran.jeromel@gmail.com

Disclosure: No potential conflicts of interest were disclosed.

Background. Acute bilateral internal carotid artery (ICA) and/or middle cerebral artery (MCA) occlusion is extremely rare and associated with poor clinical outcomes. There are only a few reports in the literature about mechanical thrombectomy being performed for acute bilateral occlusions. The treatment strategies and prognoses (clinical outcomes) are therefore unclear.

Methods. A systematic review of the literature was performed through several electronic databases with the following search terms: acute bilateral stroke, mechanical recanalization and thrombectomy.

Results. In the literature, we identified five reports of six patients with bilateral ICA and/or MCA occlusion treated with mechanical recanalization. Additionally, we report our experience with a subsequent contralateral large brain artery occlusion during intravenous thrombolytic therapy, where the outcome after mechanical thrombectomy was not dependent on the time from stroke onset but rather on the capacity of collateral circulation exclusively.

Conclusions. Acute bilateral cerebral (ICA and/or MCA) occlusion leads to sudden severe neurological deficits (comas) with unpredicted prognoses, even when mechanical recanalization is available. As the collateral capacity seems to be more important than the absolute time to flow restoration in determining the outcomes, simultaneous thrombectomy by itself probably does not lead to improved functional outcomes.

Key words: acute bilateral stroke; mechanical recanalization; thrombectomy

Introduction

Acute embolic bilateral internal carotid artery (ICA) and/or middle cerebral artery (MCA) occlusion leads to sudden comas with poor prognoses.[1-9] The reported incidence of this condition in stroke patients treated with intravenous or intra-arterial therapy is 0.34%.[8] There are few reports on the endovascular treatment (mechanical recanalization – thrombectomy) of this rare condition. The treatment strategies and prognoses (clinical outcomes) are therefore unclear.

The aim of the present article was to discuss our experience with the treatment of this severe condition through a few published reports. To the best of our knowledge, we report the first case of subsequent contralateral large brain artery occlusion during intravenous thrombolytic therapy, where the outcome after mechanical thrombectomy was not dependent on the time from stroke onset but

rather on the capacity of collateral circulation exclusively.

Methods

A systematic review of the literature was performed through several electronic databases:

PubMed (US National Library of Medicine, http://www.ncbi.nlm.nih.gov/pubmed), Google Scholar (https://scholar.google.com/), Scopus (Elsevier, http://www.scopus.com/), DeGruyer (https://www.degruyer.com) and Cochrane Library (http://www.cocranelibrary.com). The following search terms were used: acute bilateral stroke, mechanical recanalization and thrombectomy.

Results

Altogether, five reports of six patients with bilateral ICA and/or MCA occlusion that met the inclusion criteria were identified (Table 1). Four patients were females (age range 64–78 years), one was male (72 years), and one was a middle-aged patient of an undetermined sex. All patients were treated with mechanical recanalization (thrombectomy) using different endovascular techniques (stent retriever, aspiration or a combination of both). Flow in the occluded artery was completely or partially restored in all cases. The clinical outcome ranged from complete recovery (without neurological deficits) to a coma (a fatal outcome).

We present a case of a 77-year-old female patient with a medical history of hypertension, diabetes mellitus type 2, hyperlipidaemia and atrial fibrillation who was admitted to the general hospital with an acute onset of left-sided hemiplegia and dysarthria (National Institutes of Health Stroke Scale [NIHSS]: 4, Modified Rankin Scale [mRS]: 3). The patient was last seen without deficits 80 minutes prior to admission. The initial computed tomography (CT) scan revealed no ischaemic brain damage, and CT angiography showed right M1 MCA occlusion (Figure 1). Intravenous thrombolysis (IVT) was administered after 173 minutes and discontinued due to the sudden loss of conscience, the deviation of the head toward the left side and tonic-clonic spasms of the left extremities. The control CT scan performed under general anaesthesia

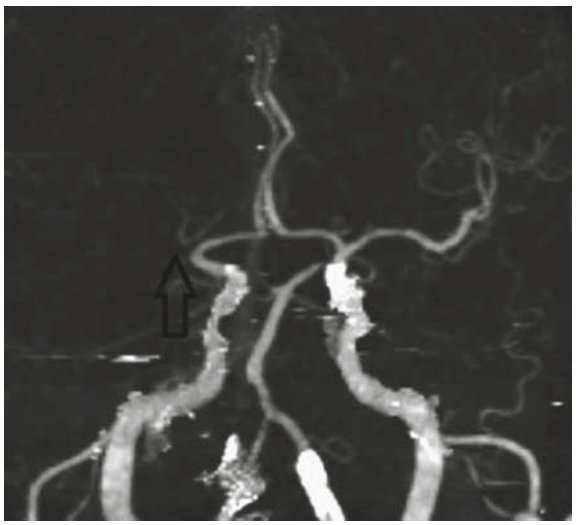

FIGURE 1. Initial imaging workup upon arrival at the general hospital. CT angiography (CTA) shows right M1 occlusion (arrow).

TABLE 1. Comparing 6 reported cases of mechanical thrombectomy in acute bilateral ICA and/or MCA occlusions

Author, (Year), reference	Clinical presentation	Sex/age (years)	Site of occlusion		Mechanical thrombectomy (technique)	Clinical outcome
			ICA	MCA		
Dietrich *et al.* (2014)[5]	left hemiparesis, progressing to coma	M/72	-	+ (M1)	aspiration+stent- retriever	minor deficit
Pop *et al.* (2014)[6]	impaired consciousness	F/78	+	+ (M2)	stent-retriever	no deficit
Pop *et al.* (2014)[6]	right sided weakness	F/66	+	+ (M1)	stent-retriever	severe deficit
Braksick *et al.* (2018)[7]	coma	F/76	-	+ (M1)	- (no data)	coma
Larrew *et al.* (2019) [8]	coma	- (no data) / middle age	+	+ -	aspiration	fatal
Storey *et al.* 2019)[9]	hemiparesis / hemiplegia	F/64	+	+ (M1,M2)	aspiration+stent-retriever	minor deficit

F = female; ICA = internal carotid artery; M = male; MCA = middle cerebral artery

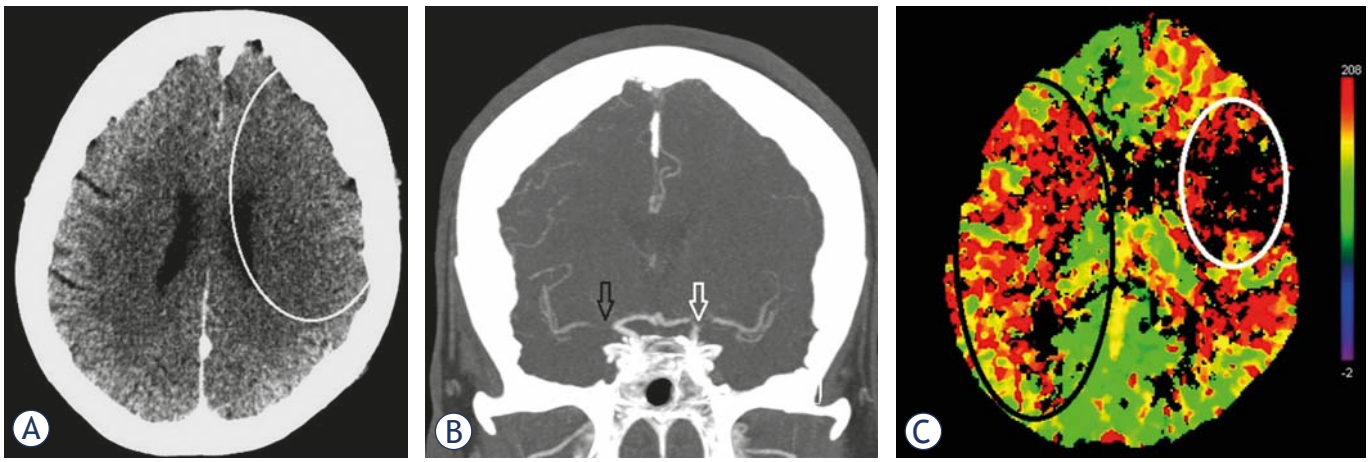

FIGURE 2. (A) Control images taken in the general hospital after clinical deterioration during intravenous thrombolysis and before the transfer to the tertiary institution. There were still no signs of ischaemic brain damage in the right cerebral hemisphere but there were subtle signs of stroke in the left middle cerebral artery (MCA) territory (white line delineates loss of cortical grey matter – white matter differentiation in the frontoparietal lobe with sulcal effacement). **(B)** Control images taken in the general hospital after clinical deterioration during intravenous thrombolysis and before the transfer. CT angiography (CTA) showed persistent right M1 occlusion (black arrow) but also left carotid "T" occlusion (white arrow). **(C)** Control images taken in the general hospital after clinical deterioration during intravenous thrombolysis and before the transfer. CT perfusion imaging (CTP) showed a penumbra in the right MCA territory (black circle) and irreversible brain damage in the left MCA territory (white circle).

showed no haemorrhagic complications. Since it was assumed that the patient had a symptomatic epileptic seizure, IVT was continued. The sedated patient was immediately transported to a tertiary institution, where a multimodal CT protocol (native CT scan, CT angiography [CTA] and CT perfusion imaging [CTP]) was performed, and the results revealed no signs of ischaemic brain damage in the symptomatic right cerebral hemisphere despite the presence of M1 occlusion and subtle (newly appeared) signs of irreversible brain damage in the contralateral MCA territory due to left ICA ("T") occlusion. It was obvious that an additional embolic occlusion occurred during the IVT treatment. Although the time of occlusion was long, the CTP imaging results showed a penumbra in the right MCA territory and not in the contralateral left MCA territory, where irreversible brain damage occurred within 3 hours (Figure 2).

Conventional (digital subtraction) angiography confirmed right MCA occlusion with good collateral flow provided by the right anterior cerebral artery (ACA). However, the situation on the left side had changed. Namely, a complete recanalization of the carotid "T" occlusion was seen angiographically as a consequence of thrombolysis and distal migration of the thrombembolus (now presenting with proximal M2 segment occlusion of the major MCA branch). However, no collateral flow was observed despite complete left ACA patency (Figure 3). Endovascular mechanical recanalization with aspiration was successfully performed on the right side (Figure 4A). The same procedure was not performed on the left side because there was irreversible brain damage in the whole occluded arterial territory and a high risk of haemorrhagic complications. The postprocedural thrombolysis in cerebral infarction (TICI) scores were 3 (right MCA) and 2b (left MCA).

The control CT and magnetic resonance imaging (MRI) scans performed on the next and subsequent days revealed no ischaemic damage on the right side and acute ischaemic stroke in the corresponding left MCA territory (Figure 4B). The patient was discharged with an improved clinical condition. However, severe neurological deficits (global dysphasia, dysarthria, spastic hemiplegia of the right limbs) were a consequence of permanent brain damage on the left side (NIHSS 5, mRS 5).

Discussion

To the best of our knowledge, there are only six reports about mechanical thrombectomy being performed for acute bilateral ICA and/or MCA occlusions.[5-9] A 2014 report by Dietrich *et al.* describes two M1 MCA thrombectomy procedures being performed in sequence. Aspiration was attempted without success, so multiple passes with

stent retrievers were performed for successful recanalization.[5] Another report from the same year (2014) by Pop *et al*. demonstrates two cases for which ICA-MCA (M1, M2) bilateral thrombectomy procedures with stent retrievers were successful.[6] A recent report by Larrew *et al*. (2019) describes a novel successful method for bilateral ICA occlusion, simultaneous recanalization, which utilizes two interventionalists and technicians simultaneously for aspiration thrombectomy.[8] In the latest report by Storey *et al*. (2019), sequential M1-M2 MCA mechanical thrombectomy was successfully performed using a combination of the stent retriever and aspiration techniques.[9] A case of stroke similar to that described in our study was reported by Braksick *et al*. (2018), where M1 MCA occlusion also occurred during the thrombolytic treatment of contralateral M1 MCA occlusion. Despite attempts at clot retrieval, flow was not completely restored, and the patient remained comatose.[7]

As so few related cases have been reported, it is unclear whether the outcomes can be improved by the optimization of the assessment and endovascular approach.[10] A comparison of our case with the abovementioned cases shows that the initial clinical presentations are similar, as they are cases of rapid deterioration with a loss of conscience. A prompt, adequate workup and treatment (a successful combination of standard care and mechanical recanalization) have led to clinical improvements and minimize morbidity and mortality.[9] However, the clinical outcomes reported in the literature are still diverse.[5-9] It is unclear whether simultaneous thrombectomy, as described by Larrew *et al*.[8], can improve the outcome by means of faster recanalization. The answer can possibly be found in our case study. Namely, an important conclusion from our case study is that the collateral capacity was more important than the time from stroke onset to successful flow restoration. It is well known that good collateral circulation in acute stroke patients is associated with better clinical and functional outcomes.[11] The results of the DAWN trial show that thrombectomy plus standard care compared to standard care alone, even 6 to 24 hours after acute ischaemic stroke, yields better functional improvements in people with mismatch between clinical deficit and infarction.[12] It is becoming obvious that the presence of the collateral flow, which defines the minimal blood flow in the penumbra, is equally important as the time in stroke patients being assessed for IVT.[13] The clinical outcome in our patient with bilateral stroke during the same thrombolytic time window therefore confirms the importance of collaterals. Namely, the region within the brain with good collateral circulation showed a complete recovery after mechanical recanalization at 7 hours after stroke onset, while the other (contralateral) region without collateral circulation exhibited a poor outcome no more than 3 hours after stroke onset. Our case shows that even in the same individual, the presence of collateral circulation varies across regions. Namely, the affected brain territory, even with comparable anatomic vascular architecture (patent ACA with possible collateral inflow) as the contralateral territory, exhibited shorter time from onset of occlusion to recanalization (with distal thrombus migration) but did not exhibit collaterals, leading to an immediate and irreversible inju-

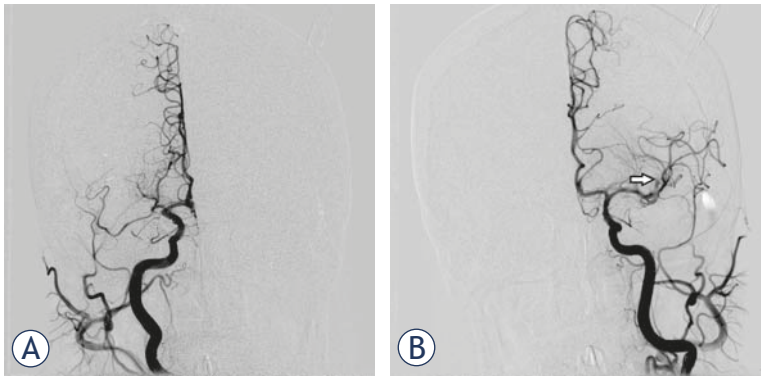

FIGURE 3. (A) Digital subtraction angiography (DSA) at the beginning of mechanical recanalization. Right internal carotid contrast injection confirming right M1 occlusion. **(B)** DSA at the beginning of mechanical recanalization. Left side contrast injection showing complete spontaneous recanalization of the carotid "T" occlusion with thrombembolar distal migration (occlusion of the proximal M2 segment of the major MCA branch) (arrow).

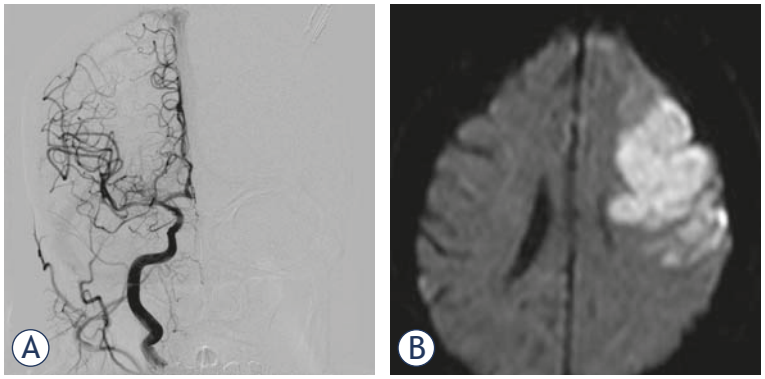

FIGURE 4. (A) Digital subtraction angiography (DSA) after mechanical recanalization. Right M1 mechanical recanalization (aspiration device) led to complete flow restoration. **(B)** MR diffusion weighted imaging (DWI) scan taken 6 days after mechanical recanalization: complete salvage of the affected right middle cerebral artery (MCA) brain parenchyma (recanalization at 7 hours after stroke onset). In contrast, subsequent persistent left M2 occlusion without collateral flow resulted in significant stroke within 3 hours after stroke onset.

ry. To the best of our knowledge, we presented the first case of subsequent contralateral large cerebral artery (MCA-ICA/MCA) occlusion during IVT, where the outcome after standard care and mechanical thrombectomy was not dependent on the time from stroke onset but rather on the capacity of collateral circulation exclusively.

Simultaneous thrombectomy, as described by Larrew *et al.*[8], offers an efficient and feasible means to reduce the time to recanalization. However, our case study confirms the fact that the outcome is still very much dependent on the capacity of collateral circulation. The main drawback of simultaneous thrombectomy (compared to subsequent thrombectomy) is that it requires two neurointerventionalists and technicians (nurses). The procedure is technically challenging, and the team must be methodical and organized and communicate effectively to allow effective, efficient, simultaneous and safe progression on both sides.[10] It is likely that simultaneous thrombectomy would not have any impact on the outcome in our case study of a patient with poor collaterals. Interestingly, the TICI scores for the patient in our study were the same as those reported for patients treated with simultaneous thrombectomy in previous study (TICI 3 for one side and TICI 2b for contralateral side). The presence of collateral capacity, the location of the residual occlusion (MCA vs ACA-MCA), and a concomitant disease (better cardiac function) were key determinants of better outcomes in the patient in our study.

Understanding the importance of collaterals and preprocedural imaging with techniques that enable collateral flow assessment is becoming extremely important. Multiphase CT angiography (CTA), which enables the evaluation of collateral circulation within a single contrast injection, is a simple example.[14] It is already accepted that for good outcomes, the onset-to-reperfusion time window should be adjusted according to the collateral status.[15] In the future, perhaps a pretreatment imaging assessment of the thrombus itself will make stroke treatment planning easier.[16] However, it seems that even in the era of mechanical recanalization, bilateral stroke is a severe condition with unpredicted outcomes.

Conclusions

Acute bilateral cerebral (ICA and/or MCA) occlusion leads to sudden severe neurological deficits (comas) with unpredicted prognoses, even in the era of mechanical recanalization.

As a the collateral capacity seems to be more important than the absolute time to flow restoration in determining the outcomes, simultaneous thrombectomy by itself probably does not lead to improved functional outcomes.

Because there are only a few reported cases, additional experience is needed to fully understand the outcomes of sequential and simultaneous thrombectomy.

References

1. Kwon SU, Lee SH, Kim JS. Sudden coma from acute bilateral internal carotid artery territory infarction. *Neurology* 2002; **58:** 1846-9. doi: 10.1212/wnl.58.12.1846
2. Hu WT, Wijdicks EF. Sudden coma due to acute bilateral M1 occlusion. *Mayo Clin Proc* 2007; **10:** 1155. doi: 10.4065/82.10.1155
3. Zubkov AY, Klassen BT, Burnett MS, Rabinstein AA. Bilateral internal carotid artery occlusions resulting in near total acute brain infraction. *Neurocrit Care* 2007; **7:** 247-9. doi: 10.1007/s12028-007-0076-y
4. Nawashiro H, Wada K, Kita H. Decerebrate posture following bilateral middle cerebral artery occlusion. *Intern Med* 2011; **50:** 2063. doi: 10.2169/internalmedicine.50.5843
5. Dietrich U, Graf T, Schäbitzb WR. Sudden coma from acute bilateral M1 occlusion: successful treatment with mechanical thrombectomy. *Case Rep Neurol* 2014; **6:** 144-8. doi: 10.1159/000362160
6. Pop R, Manisor M, Wolff V, Habashy M, Rouyer O, Kehrli P, et al. Endovascular treatment in two cases of bilateral ischemic stroke. *Cardiovasc Intervent Radiol* 2014; **37:** 829-34. doi: 10.1007/s00270-013-0746-4
7. Braksick SA, Robinson CP, Wijdicks EFM. Bilateral middle cerebral artery occlusion in rapid succession during thrombolysis. *Neurohospitalist* 2018; **8:** 102-3. doi: 10.1177/1941874417712159
8. Larrew T, Hubbard Z, Almallouhi E, Banerjee C, Moss M, Spiotta AM. Simultaneous bilateral carotid thrombectomies: a technical note. *Oper Neurosurg* 2019; **pii:** opz230. doi: 10.1093/ons/opz230
9. Storey C, Lebovitz J, Sweid A, Tjoumakaris S, Gooch R, Rosenwasser RH, Jabbour P. Bilateral mechanical thrombectomies for simultaneous MCA occlusions. *World Neurosurg* 2019; **132:** 165-8. doi: 10.1016/j.wneu.2019.08.236
10. Srivatsan A, Kan P. Commentary: simultaneous bilateral carotid thrombectomies: a technical note. *Oper Neurosurg* 2019. **pii:** opz273. doi: 10.1093/ons/opz273.
11. Bang OY, Goyal M, Liebeskind DS. Collateral circulation in ischemic stroke: assessment tools and therapeutic strategies. *Stroke* 2015; **46:** 3302-9. doi: 10.1161/STROKEAHA.115.010508
12. Nogueira RG, Jadhav AP, Haussen DC, Bonafe A, Budzik RF, Bhuva P, et al. Thrombectomy 6 to 24 hours after stroke with a mismatch between deficit and infarct. *N Engl J Med* 2018; **378:** 11-21. doi: 10.1056/NEJMoa1706442
13. Bivard A, Spratt N, Miteff F, Levi C, Parsons MW. Tissue is more important than time in stroke patients being assessed for thrombolysis. *Front Neurol* 2018; **9:** 41. doi: 10.3389/fneur.2018.00041
14. Garcia-Tornel A, Carvalho V, Boned S, Flores A, Rodríguez-Luna D, Pagola J, et al. Improving the evaluation of collateral circulation by multiphase computed tomography angiography in acute stroke patients treated with endovascular reperfusion therapies. *Interv Neurol* 2016; **5:** 209-17. doi: 10.1159/000448525
15. Kim BM, Beak JH, Heo JH, Nam HS, Kim YD, Yoo J, et al. Collateral status affects the onset-to-reperfusion time window for good outcome. *J Neurol Neurosurg Psychiatry* 2018; **89:** 903-9. doi: 10.1136/jnnp-2017-317627
16. Vidmar J, Bajd F, Milosevic ZV, Kocijancic IJ, Jeromel M, Sersa I. Retrieved cerebral thrombi studied by T2 and ADC mapping: preliminary results. *Radiol Oncol* 2019; **53:** 427-33. doi: 10.2478/raon-2019-0056

research article

Major and ancillary features according to LI-RADS in the assessment of combined hepatocellular-cholangiocarcinoma

Vincenza Granata[1], Roberta Fusco[1], Sergio Venanzio Setola[1], Fabio Sandomenico[1], Maria Luisa Barretta[1], Andrea Belli[2], Raffaele Palaia[2], Fabiana Tatangelo[3], Roberta Grassi[4], Francesco Izzo[2], Antonella Petrillo[1]

[1] Radiology Division, "Istituto Nazionale Tumori IRCCS Fondazione Pascale – IRCCS di Napoli", Naples, Italy
[2] Hepatobiliary Surgical Oncology Division, "Istituto Nazionale Tumori IRCCS Fondazione Pascale – IRCCS di Napoli", Naples, Italy
[3] Pathology Diagnostic Division, "Istituto Nazionale Tumori IRCCS Fondazione Pascale – IRCCS di Napoli", Naples, Italy
[4] Division of Radiology, University of Campania Luigi Vanvitelli, Naples, Italy

Radiol Oncol 2020; 54(2): 149-158.

Received 6 February 2020
Accepted 22 April 2020

Correspondence to: Roberta Fusco, M.D., Department of Radiology, Istituto Nazionale Tumori Fondazione G. Pascale, Naples, I-80131, Italy. E-mail: r.fusco@istitutotumori.na.it

Disclosure: No potential conflicts of interest were disclosed.

Background. The aim of the study was to investigate the performance of the Liver Imaging Reporting and Data System (LI-RADS) v2018 for combined hepatocellular-cholangiocarcinoma (cHCC-CCA) identifying the features that allow an accurate characterization.

Patients and methods. Sixty-two patients (median age, 63 years; range, 38–80 years), with pre-surgical biopsy diagnosis of hepatocellular carcinoma (HCC) that underwent hepatic resection, comprised our retrospective study. All patients were subject to multidetector computed tomography (MDCT); 23 patients underwent to magnetic resonance (MR) study. The radiologist reported the presence of the HCC by using LIRADS v2018 assessing major and ancillary features.

Results. Final histological diagnosis was HCC for 51 patients and cHCC-CCA for 11 patients. The median nodule size was 46.0 mm (range 10–190 mm). For cHCC-CCA the median size was 33.5 mm (range 20–80 mm), for true HCC the median size was 47.5 mm (range 10–190 mm). According to LIRADS categories: 54 (87.1%) nodules as defined as LR-5, 1 (1.6%) as LR-3, and 7 (11.3%) as LR-M. Thirty-nine nodules (63%) showed hyper-enhancement in arterial phase; among them 4 were cHCC-CCA (36.4% of cHCC-CCA) and 35 (68.6%) true HCC. Forty-three nodules (69.3%) showed wash-out appearance; 6 cHCC-CCAs (54.5% of cHCC-CCA) and 37 true HCC (72.5%) had this feature. Only two cHCC-CCA patients (18.2% of cHCC-CCA) showed capsule appearance. Five cHCC-CCA (71.4% of cHCC-CCA) showed hyperintensity on T2-W sequences while two (28.6%) showed inhomogeneous signal in T2-W. All cHCC-CCA showed restricted diffusion. Seven cHCC-CCA patients showed a progressive contrast enhancement and satellite nodules.

Conclusions. The presence of satellite nodules, hyperintense signal on T2-W, restricted diffusion, the absence of capsule appearance in nodule that shows peripheral and progressive contrast enhancement are suggestive features of cHCC-CCA.

Key words: hepatocellular carcinoma; combined hepatocellular-cholangiocarcinoma; multidetector computed tomography; magnetic resonance imaging.

Introduction

Combined hepatocellular-cholangiocarcinoma (cHCC-CCA) is considered a rare entity of primary liver tumour consisting of mixed elements of hepatocellular carcinoma (HCC) and cholangiocarcinoma (CCA) or cancer cells with hepatic progenitor/stem cell traits.[1,2] The incidence of cHCC-CCA

ranging from 1.0%–4.7% of all primary hepatic tumours.[3,4] Described risk factors are male gender, cirrhosis, hepatitis infection (hepatitis B virus [HBV] and hepatitis C virus [HCV]), family history of liver cancer, heavy alcohol consumption and diabetes mellitus.[5-10] Therefore, that cHCC-CCA is associated with overlapping clinical features of both HCC and CCA.[3] An exact pre-surgical diagnosis is very complicated and, it is due to its heterogeneous imaging characteristics with overlapping features of HCC and CCA. The predominant histologic elements within the tumour determine the predominant radiographic features.[3] Therefore, in this scenario the hallmark radiological findings of HCC show an overlapping with those of CCA.[3] Since cHCC-CCAs are predominant in patients at high risk of HCC, and the possibility that this tumour can mimic HCC in imaging appearance, this is problematic considering the current dependence on the non-invasive diagnosis of HCC.[11-17] Specifically, given that surgical resection is the current standard of care for cHCC-CCAs and controversies surround the appropriateness of other therapies, such us ablative therapies, imaging misdiagnosis of cHCC-CCA can lead to non standard treatments for cHCC-CCA.[18] The current imaging-based criteria to characterize a HCC lesion have several limitations, including the lack of established consensus regarding the exact definitions of imaging features, binary categorization (either definite or not definite HCC), and failure to address non-HCC malignancies and vascular invasion.[13] Therefore, The American College of Radiology sustained the spread of Liver Imaging Reporting and Data System (LI-RADS) to homogenizing the interpreting, reporting and data collection of HCC imaging. LI-RADS is a scheme for interpreting and reporting of imaging features on multidetector computed tomography (MDCT) and magnetic resonance (MR) studies in patients at risk for HCC. In the current (v2018) LI- RADS[19], the diagnosis of HCC is based on the presence of major imaging features. These are features used to categorize LI-RADS-category 3 (LR-3), LI-RADS- category 4 (LR-4), and LI-RADS-category 5 (LR-5) and include arterial-phase hyperenhancement, tumour diameter, washout appearance, capsule appearance, and thresh-old growth. Ancillary features favoring HCC diagnosis include the hepatobiliary phase hypointensity (after administration of liver-specific MR contrast agent), transitional phase hypointensity, mild to moderate T2 hyperintensity, restricted diffusion, distinctive rim, corona enhancement, mosaic architecture, nodule-in-nodule architecture, intra-lesional fat, lesional iron or fat sparing, blood products, and diameter increase less than the threshold growth. The presence of ancillary features favoring malignancy may be used to up- grade by one category, but not beyond LR-4 (e.g. from LR-3 to LR-4). Absence of ancillary features must not be used to downgrade an LR category.[19]

The purpose of this study is to investigate the performance of the LI-RADS v2018 for cHCC-CCA identifying which features allow an exact characterization respected to HCC.

Patients and methods

Study population

The institutional review board approved this retrospective study, and the requirement for patient informed consent was waived. We searched the surgical database at our institution from January 2013 to September 2018 and selected 74 patients with pre surgical biopsy and radiological diagnosis of HCC, who underwent hepatic resection. The inclusion criteria for the study population were as follows: *(a)* patients who had pathologically-proven HCC; *(b)* patients who had undergone MR imaging and liver MDCT with less than a 1-month interval between imaging modalities; *(c)* patients who had less than a 1-month interval between imaging and pathologic diagnosis; and *(d)* availability of diagnostic quality pictures of the cut sections of the resected specimens in patients who underwent surgical resection for matching of imaging and pathology findings. The exclusion criteria were as follows: *(a)* conflict between the imaging-based diagnosis and the pathologically confirmed diagnosis, *(b)* no available MR or MDCT images.

In total, 73 patients with HCC confirmed at pathology fulfilled the inclusion criteria during the study period. Among them, 11 patients were excluded for the following reasons: *(a)* 4 patients no had available MR or MDCT images and *(b)* 7 patients because the final diagnosis were not HCC. Finally, 62 patients (14 women, 48 men; median age, 63 years; range, 38–80 years), with pre-surgical biopsy and radiological diagnosis of HCC comprised our study population. Characteristics of the 62 patients are summarized in Table 1.

Lesion confirmation: reference standard

All original pathological samples were reviewed by one experienced hepatic pathologist (F.T.). Lesions were confirmed histopathologically as he-

patic tumours comprising unequivocal elements of both HCC and CC according to the tumour classification of the World Health Organization. The CC component was defined as glandular differentiation with mucin production, while the HCC component was defined as trabecular, solid sheet, or pseudoacinar arrangements with interspersed sinusoids. All pathological samples displayed an intimate intermingling of trabecular hepatocellular and true glandular elements (type C). The bidirectional differentiation was further supported by immunohistochemical stain. For each specimen, biliary differentiation was confirmed with mucin positivity or with immunohistochemical stains characteristic of bile duct differentiation (cytokeratin 7, cytokeratin 19), whereas hepatocellular differentiation was confirmed with immunohistochemical stains characteristic of hepatocyte differentiation (Hepatocyte-Paraffin-1).

TABLE 1. Characteristics of the 62 selected patients

Description	Numbers (%)/ range
Gender	Men 48 (77.4%)
	Women 14 (22.6%)
Age	63 y; range. 38–80 y
Number of hepatic nodules	
Single nodule	62 (100%)
Multiple nodules	/
Nodule size (mm)	median size 46.0 mm; range 10-190 mm
Risk factor for HCC	
Chronic hepatitis B; HBV-related liver cirrhosis	37 (59.7%)
Chronic hepatitis C; HCV-related liver cirrhosis	23 (37.1)
Alcoholic liver cirrhosis	2 (3.2%)
Child–Pugh Classification	
A	62 (100%)
B	

HBV = hepatitis B virus; HCC = hepatocellular carcinoma; hepatitis C virus

MDCT and MR examinations

All patients underwent to MDCT and 23 to MR.

MDCT protocol

MDCT was performed with a 64-detector row scanner (Optima 660, GE Healthcare, United States). MDCT scanning parameters were 120 kVp, 100–470 mAs (NI 16.36), 2.5 mm slice thickness and table speed 0.984/1 mm/rotation. Scans were carried out including a region encompassing the liver from diaphragm to iliac crests. Liver protocol examinations were composed of quadruple phases, including the unenhanced, arterial, portal venous, and equilibrium phases. CT images were obtained after injection of 120 mL of a nonionic contrast medium (iomeprol, Iomeron 400, Bracco, Milan, Italy) at a rate of 3.0–4.0 mL/sec by using an automatic power injector (Empower CTA, E-Z-EM Inc., New York, United States). Image acquisition in the arterial phase was initiated 19 seconds after attenuation in the descending aorta reached 100 HU, as measured with the bolus tracking method; in the portal venous phase, images were acquired 33 seconds after the arterial phase; in the equilibrium phase, images were acquired 180 seconds after administration of contrast media.

MR imaging protocol

MR imaging was performed by using a 1.5 T scanner (Magnetom Symphony, with Total Imaging Matrix Package, Siemens, Erlangen, Germany) with an 8-element body coil and a phased array coil. Our routine liver MR imaging protocol consisted of a breath-hold fat-saturated and not fat-saturated T2-weighted turbo spin-echo sequence, an in- and opposed-phase T1-weighted gradient-echo sequence, dynamic imaging with a fat-saturated T1-weighted gradient-echo sequence, and diffusion-weighted imaging. Diffusion weighted imaging (DWI) was obtained with planar echo-pulse sequence (*b* values 0, 50, 100, 200, 400, 600, and 800 s/mm^2). A non-specific agent the Gd-BT-DO3A (Gadovist, Bayer Schering Pharma, Germany) was employed. All patients received 0.1 ml/kg of Gd-BT-DO3A by means of a power injector (Spectris Solaris® EP MR, MEDRAD Inc., Indianola, IA, USA), at an infusion rate of 2 ml/s followed by a 30-mL saline flush. Arterial phase images were acquired 7 seconds after contrast material arrival at the thoracic aorta by using an MR fluoroscopic monitoring system. Thereafter, portal venous phase and equilibrium phase were obtained 60 seconds and 3 minutes after contrast material administration, respectively. Detailed information regarding the MR imaging parameters are summarized in Table 2.

Image analysis

For each patient, MDCT and MR images were independently and blindly evaluated in random or-

der within and between three radiologists (V.G., S.V.S., A.P.; 10, 15, and 20 years of experience in abdominal imaging). A consensus evaluation was performed when there was disagreement between the readers. The readers were blinded to previous radiological examination, pathologic results and history of previous treatment but were aware that the patients had cirrhosis and thus were at higher risk for HCC. To reduce recall bias, all three readers maintained an interval of more than 2 weeks between interpretation sessions of MR and MDCT images.

Each radiologist was asked to identify the presence of lesion, that was considered to be detectable if the nodule had attenuation or signal intensity that differed from that of the surrounding liver parenchyma. Thereafter, they reported the presence of the HCC by using LIRADS v2018 assessing major and ancillary features[19]; also the radiologists reported any radiological accessory findings if detected.

Readers assessed and recorded the following parameters: greatest nodule diameter, attenuation at unenhanced CT, signal intensity on T1- and T2-weighted images, vascular hyperenhancement pattern during arterial phase (wash-in), wash-out appearance during portal phase, vascular enhancement during equilibrium or late phases.[13]

Region of interests (ROIs) have been manually drawn by an expert radiologist on T1-w and T2-w images and on DW images at the highest b value (including hyperintense voxels at b value 800 s/mm^2) considering the same slices position. The contours of lesions were validated by another expert radiologist of 25 years of experience.

The signal intensity of the lesions in T1-w and T2-w images was categorized subjectively as isointense, hypointense, and hyperintense compared to surrounding liver parenchyma. We assessed the signal on DWI sequences and measured the apparent diffusion coefficient (ADC) of each lesion. The diffusion weighted signal decay was analyzed using the mono-exponential model, according to the equation, the apparent diffusion coefficient ADC = (ln [S0/ Sb])/b, where Sb is the signal intensity with diffusion weighting b and S0 is the non-diffusion-weighted signal intensity. This analysis was ROI-based using median value of single voxel signals for each b value. Median diffusion parameters of ROI were used as representative values for each lesion. No motion correction algorithm was used but ROIs were drawn taking care to exclude areas in which movement artifacts or blurring caused voxel misalignments.

We analysed the enhancement pattern during arterial, portal, equilibrium or late phase and described it as homogeneous, heterogeneous, or progressive. We described the capsule appearance, defined as a peripheral rim of smooth hyperenhancement in the portal or delayed phase, as complete or partial. In addition, we recorded the number and segmental location of the nodule for all detected lesions and the presences of satellite nodules.

Statistical analyses

Each continuous variable was expressed in terms of median value ± range while each variable categorical was summarized by frequencies and percentages. Fisher's exact test was performed to assess statistically significant difference between percentage values. Mann Whitney non parametric test were used to compare a continuous variable between 2 groups. A p value < 0.05 was considered statistically significant.

All statistical analysis was performed with SPSS for Windows (Version 23.0; SPSS Inc, Chicago, Ill).

Results

We assessed 62 patients that underwent surgical treatment with preoperative diagnosis of HCC. According to the surgical procedure, 10 patients underwent to lobectomy, 3 meso-hepatectomy, 23 bi-segmentectomy and 27 segmentectomy (8 for VII, 1 for I, 2 for II, 2 for III, 6 for IV, 6 for V and 2 for VI hepatic segment).

Pathological features

After pathological evaluation the final diagnosis was HCC for 51 patients and cHCC-CCA for 11 patients (17.7%).

Twelve patients were classified as G3 (19.4%) and 50 G2 (80.6%) according to the grading system of Edmondson-Steiner.[21]

Among cHCC-CCA 8 patients were classified as G2 (72.7%) and 3 as G3 (27.3%). In 8 out of 11 (72.7%) cHCC-CCA microvascular infiltration was reported.

In two cHCC-CCA patients were reported nodal metastases.

Imaging features

All lesions were detected and analyzed by readers. The consensus in the assessment of the nodules

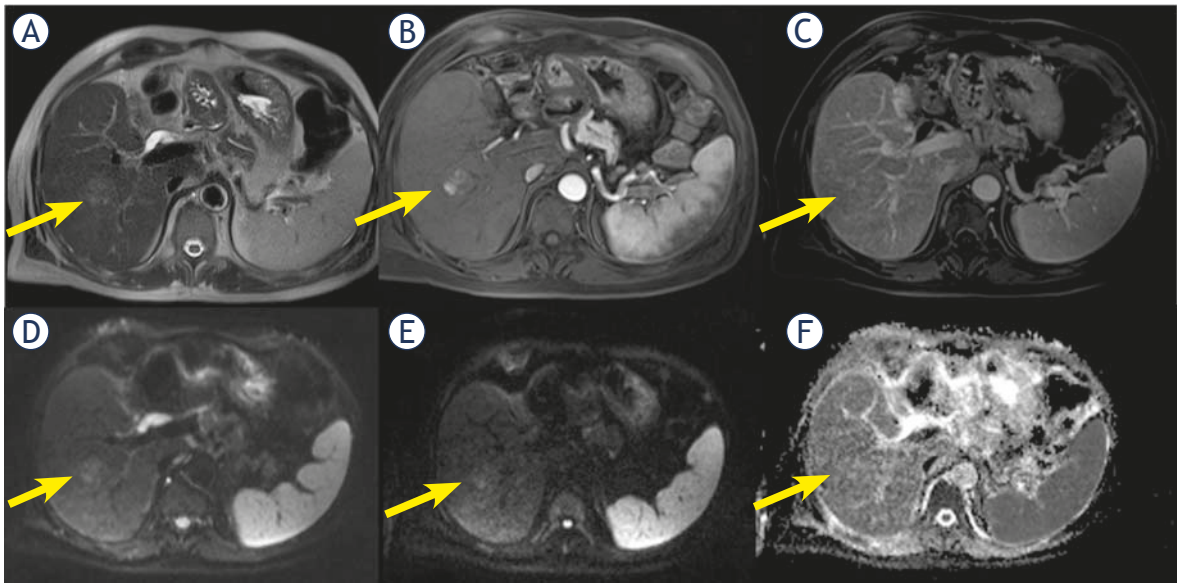

FIGURE 1. Man 56 y with combined hepatocellular-cholangiocarcinoma (cHCC-CCA) on VI hepatic segment. MRI study. The nodule is iso-hyperintense (arrow) in T2-W sequence **(A)**, with inhomogeneous hypervascular appearance (arrow) during arterial phase of contrast study **(B)**, without wash-out or capsule appearance (arrow) during portal phase of contrast study **(C)**. The nodule shows restricted (arrow) diffusion **(D**, **E** and **F)** in diffusion weighted imaging (DWI) sequences.

was 100%. The median nodule size was 46.0 mm (range 10–190 mm). For cHCC-CCA the median size was 33.5 mm (range 20–80 mm), for true HCC the median size was 47.5 mm (range 10–190 mm).

The consensus between pre-surgical radiological report and second evaluation was 100% for each LIRADS categories: LR-5 for 54 (87.1%) nodules, LR-3 for 1 (1.6%) lesion, and LR-M for 7 (11.3%) nodules.

Thirty-nine nodules (63%) showed hyperenhancement in arterial phase; among them 4 were cHCC-CCA (36.4% of cHCC-CCA) and 35 (68.6%) true HCC.

Twenty nodules (32.2%) showed an inhomogeneous hyperenhancement in arterial phase; 7 of them were cHCC-CCA (63.6% of cHCC-CCA) (Figure 1). We found this feature in 13 (25.5%) true HCC.

Forty-three nodules (69.3%) showed wash-out appearance; 6 cHCC-CCAs (54.5% of cHCC-CCA) and 37 true HCC (72.5%) had this feature.

We found inhomogeneous wash-out in 13 (20.9%) nodules; 4 nodules with inhomogeneous wash-out were cHCC-CCA (35.4% of cHCC-CCA). A one cHCC-CCA (9.1% of cHCC-CCA) patient did not show this feature. Nine true HCC (17.6%) showed inhomogeneous wash-out.

Thirty-three (53.2%) nodules showed capsule appearance, 28 (45.2%) did not show this feature and in one patient we found a peripheral halo sign.

Only two cHCC-CCA patients (18.2% of cHCC-CCA) showed capsule appearance while 9 cHCC-CCAs (81.8% of cHCC-CCA) did not have this feature (Figure 2).

Thirty-one (60.8%) true HCC showed capsule appearance and 19 (37.2%) true HCC did not show this feature.

Only 23 patients underwent MR study, among them 7 out of cHCC-CCA. We found T2 hyperintensity of signal in 20 nodules (86.9%), two lesions (8.6%) were isointense and one (4.3%) hypointense.

Five cHCC-CCA (714 % of cHCC-CCA) showed hyperintensity on T2-W sequences while two (28.6%) showed inhomogeneous signal in T2-W (Figure 3).

Fifteen true HCC (93.7%) had hyperintense signal on T2-W and one true HCC (6.2%) inhomogeneous signal on T2-W.

We found restricted diffusion in 23 (100%) nodules with median ADC of 975.6 x 10^{-3}mm^2/s.

All cHCC-CCA showed restricted diffusion with median ADC of 880.7 x 10^{-3} mm^2/s.

All true HCC showed restricted diffusion with median ADC of 1210.0 x 10^{-3} mm^2/s.

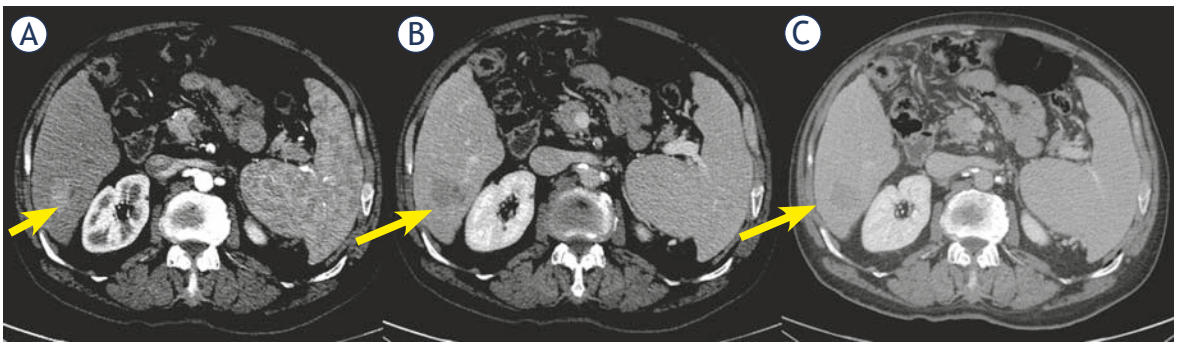

FIGURE 2. Woman 68 y with combined hepatocellular-cholangiocarcinoma (cHCC-CCA) on VI hepatic segment. Multidetector computed tomography (MDCT) study. The nodule shows hypervascular appearance (arrow) during arterial phase of contrast study **(A)**, with wash-out appearance (arrow) and without capsule appearance (arrow) during portal and late phase of contrast study **(B** and **C)**.

Progressive contrast enhancement: nine (14.5%) patients showed a progressive contrast enhancement; among them 7 were cHCC-CCA (63.6% of cHCC-CCA) (Figure 4) and 2 (3.9% of HCC) true HCC.

In ten patients (16.1%) we found satellite nodules (neighboring micrometastases), among them 7 were cHCC-CCA (63.6% of cHCC-CCA) (Figure 5) and 3 (5.9% of HCC) were true HCC.

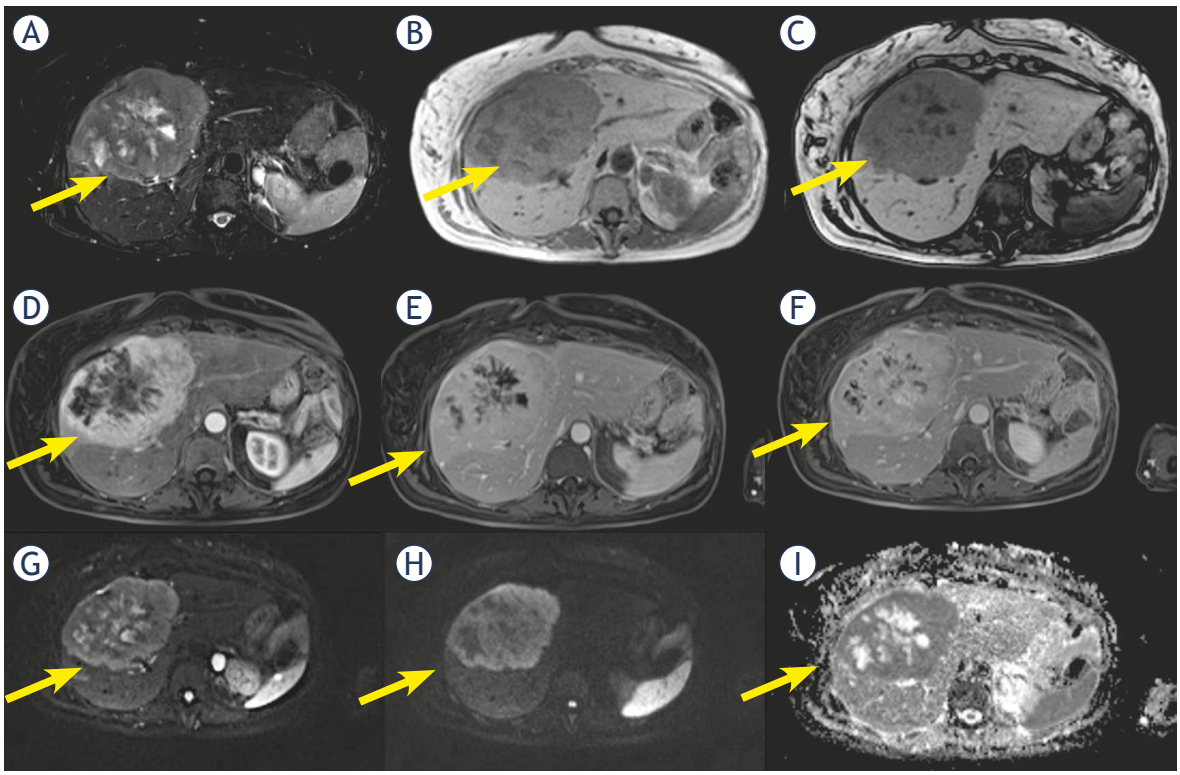

FIGURE 3. Woman 58 y with combined hepatocellular-cholangiocarcinoma (cHCC-CCA) on IV-V-VIII hepatic segment. MRI study. Pre surgical radiological diagnosis was cholangiocarcinoma (CCA). The lesion shows inhomogeneous hyperintense signal (arrow) in T2-W sequence **(A)** with central more hyperintense area. In T1-W in-out phase sequence **(B** and **C)** the lesion is inhomogeneous hypointense (arrow). During contrast study **(D:** arterial phase, **E:** portal phase; **F:** late phase) the lesion shows progressive contrast enhancement (arrow). In diffusion weighted imaging (DWI) **(G, H** and **I)** it shows restricted diffusion (arrow).

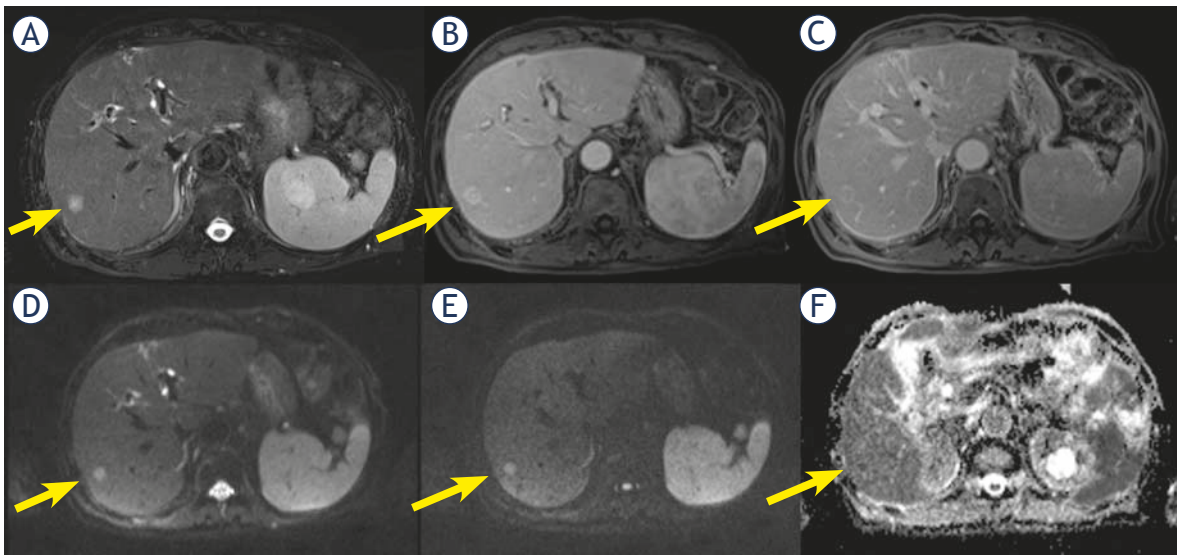

FIGURE 4. Man 71 y with combined hepatocellular-cholangiocarcinoma (cHCC-CCA) on VI hepatic segment. MRI study. The nodule shows hyperintense signal (arrow) in T2-W sequence **(A)** and target like pattern of enhancement (arrow) during arterial **(B)** and portal **(C)** phase of contrast study. Restricted diffusion (arrow) in diffusion weighted imaging (DWI) **(D**, **E** and **F)** sequence.

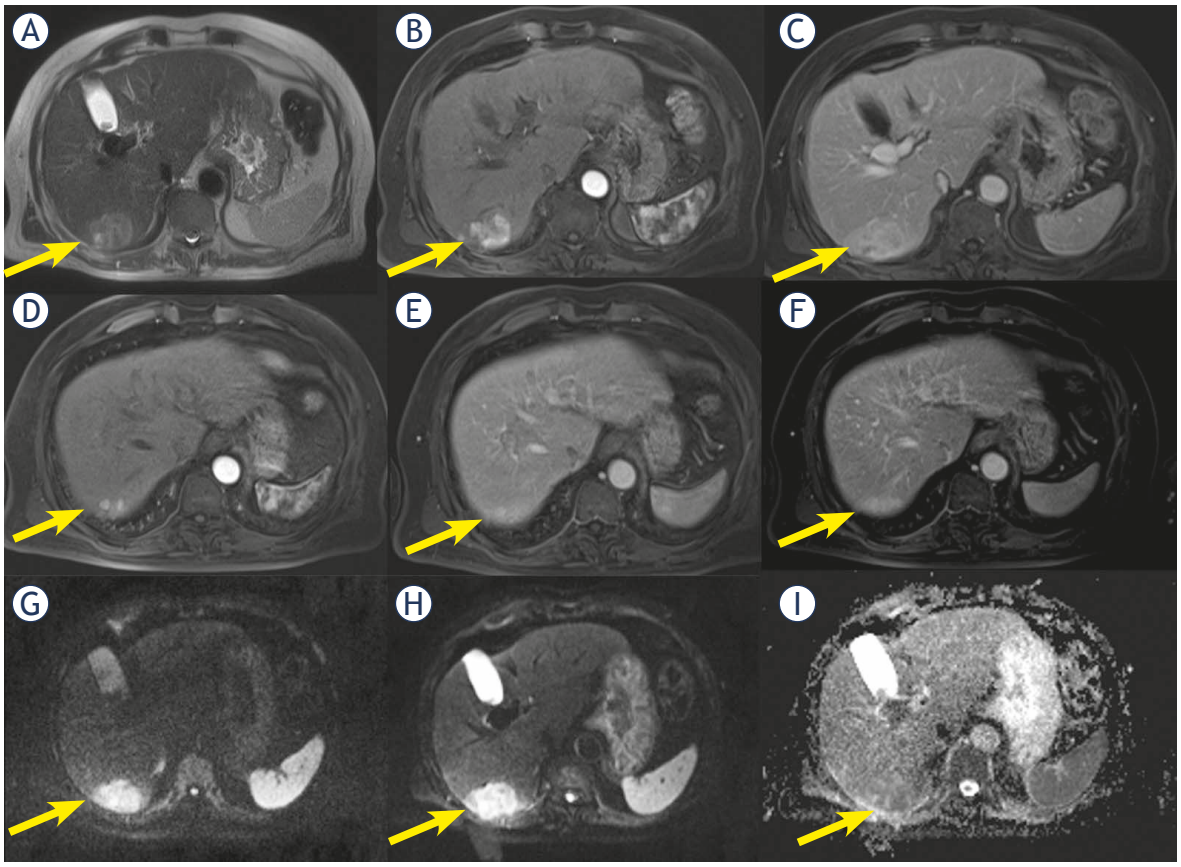

FIGURE 5. Man 69 y with combined hepatocellular-cholangiocarcinoma (cHCC-CCA) on VI hepatic segment. MRI study. The nodule shows inhomogeneous hyperintense signal (arrow) in T2-W sequence **(A)** and progressive pattern of enhancement (arrow) during arterial **(B)** and portal **(C)** phase of contrast study. In **(D**, **E** and **F)** arrow shows a nodule satellite. Restricted diffusion (arrow) in diffusion weighted imaging (DWI) **(G**, **H** and **I)** sequence.

TABLE 2. Imaging features in study population

	True HCC (n 51)	cHCC-CCA (n 11)	P value*
Arterial hyperenhancement			
Yes	35 (68.6%)	4 (36. 4%)	
No	3 (5.8%)	0 (0%)	**0.04**
Inhomogeneous	13 (25.5%)	7 (63.6%)	
Wash-out appearance			
Yes	37 (72.5%)	6 (54.5%)	
No	5 (17.6%)	1 (9.1%)	0.38
Inhomogeneous	9 (17.6%)	4 (35.4%)	
Capsule appearance			
Yes	31 (60.8%)	2 (18.2%)	
No	19 (37.2%)	9 (81.8%)	**0.03**
Inhomogeneous	1 (1.9%) alo-sign		
MR features	16	7	
T2-W hyperintensity			
Yes	15 (93.7%)	5 (71.4%)	0.14
Inhomogeneous	1 (6.2%)	2 (28.6%)	
Diffusion restricted			
Yes	15 (100%)	7 (100%)	-
No			
Median ADC	1210 x 10^{-3}mm^2/s	880.7 x 10^{-3}mm^2/s	**0.03**
Progressive contrast enhancement	2 (3.9%)	7 (63.6%)	**<<0.001**
Satellite nodules	3 (5.9%)	7 (63.6%)	**<<0.001**

* Fisher's exact test

ADC = apparent diffusion coefficient; HCC = hepatocellular carcinoma; cHCC-CCA = combined hepatocellular-cholangiocarcinoma; MR = magnetic resonance

Statistical analysis

The hyperenhancement in arterial phase (p value = 0.04), the absence of the pseudocapsule (p value = 0.03), progressive contrast enhancement (p value < 0.001) and satellite nodules (neighboring micrometastases, p value < 0.001) showed percentages statistically different respect to the presence of combined HCC and cholangiocarcinoma at Fisher's exact test (see Table 2).

A statistically significant difference (p value = 0.03 at Mann Whitney test) was detected between ADC median value of the two groups pure HCC and cHCC-CCA group.

Discussion

In this study, we assessed 62 patients with liver single nodule that underwent surgical treatment with preoperative biopsy diagnosis of HCC and presurgical radiological diagnosis of HCC in 54 lesion and LR-M in 7 lesions.

All 7 lesions classified as LR-M were cHCC-CCA; 4 cHCC-CCA patients were wrongly identified as HCC patients. In this subgroup the median size lesion was 21 mm, while the subgroup LR-M showed a median size of 54 mm. In this scenario we think that radiological features are also related to median lesion diameter.

When we assessed the major features, we found that arterial hyperenhancement, portal wash-out and capsule appearance were more frequent for true HCC group (68.6%, 72.5%, and 60.8%, respectively) than cHCC-CCA group (36.4%, 54.5%, and 18.2%, respectively). Our results are different from what is reported by Jeon *et al*.[18] In fact, these researches reported that a substantial proportion of cHCC-CCAs was categorized as LR-5 or LR-4 showing higher frequencies of major HCC features: arterial hyperenhancement was present in 96.2% of cHCC-CCA, washout appearance in 80.8% of cHCC-CCA and enhancing capsule in 34.6% of cHCC-CCA.[18] Arterial phase hyperenhancement is considered a crucial precondition to define HCC[19], and it is considered the most important feature for imaging diagnosis. This feature reflects the neoangiogenesis, which is associated with the stepwise process of carcinogenesis and becomes the dominant blood supply in overt HCC lesions.[13] However, it is non-specific condition and may be detected in benign pathologies. Also in our previous study we demonstrated that arterial phase hyperenhancement is a prerequisite but not sufficient for LR-5 classification.[12] The post-contrast feature, "rim arterial phase hyperenhancement" is a subtype of LR-M in which arterial phase enhancement is most pronounced in observation periphery and it is defined as a''target appearance''. ''Target appearance'' or ''targetoid mass'' includes other features as peripheral "Washout", in which apparent washout is most pronounced in observation periphery, and delayed central enhancement, in which we find a central area of progressive post-arterial phase enhancement. In our study we found that cHCC-CCAs showed in 63.6% of lesions inhomogeneous arterial contrast enhancement, with a peripheral rim during arterial phase of contrast study and a progressive contrast enhancement (63.6% of lesions). Our findings

are comparable with the results of Lee *et al*.[21] that found that in cHCC-CCA group the more frequent radiological findings were suggestive of LR-M.[21] In fact. Also Potretzke *et al*. found that 93.4% of cHCC-CCA showed at least one ancillary feature favouring non-HCC malignancy.[22] Conversely, Sammon *et al*.[23] reported that arterial enhancement was seen in 90.9% (n. 30) of the cHCC-CCA group, although the most common enhancement patterns in the cHCC-CCA group were peripheral persistent and heterogeneous hyperenhancement with washout. In our study, the wash-out appearance was seen in 54.5% (n. 6) of patients, so we think it is not a feature that allow identifying that patients as a cHCC-CCA. Conversely, the absence of capsule appearance is more frequent (81.8%) in cHCC-CCA group than in true HCC group (37.2%). Therefore, according to our results, the absence of capsule appearance in nodule that shows peripheral and progressive contrast enhancement should guide the radiologist in differential diagnosis, since these features are more specific for cHCC-CCA. Also Fowler *et al*. confirmed that peripheral arterial enhancement was the most common pattern observed in their study population. The target like or reverse target like pattern of enhancement, was a common feature of cHCC-CCA; this pattern was rarely seen with HCC in their population.[24]

In our study, only 23 patients were subject to pre-surgical MR study, among them only 7 cHCC-CCA patients. According to our protocol study for lesion characterization, we employed a non-hepatospecific contrast medium, so no one of our patients was subject to EOB-MR. In our previous study we showed that when we analyzed the degree of arterial phase hyperenhancement, we found that the degree was higher with Gd-BT-DO3A than GD-EOB-DTPA, with significant statistically difference. In addition, the image quality degradation was lower with Gd-BT- DO3A than with GD-EOB-DTPA. There was significant statistically difference between the quality on arterial phase with Gd-BT-DO3A and the quality on arterial phase with GD-EOB-DTPA.[12]

Regarding the signal observed on T2-W sequences we found that 15/16 (93.7%) of true HCC showed hyperintense signal on T2-W and 5/7 (71.4%) of cHCC-CCA had this feature. T2-W hyperintensity was a highly specific marker of nodule malignancy, although poorly sensitive.[13] Kim *et al*.[25] evaluated the most predictive finding among hyperintensity on T2-W, DWI, washout, capsular enhancement, and hypointensity on gadoxetic acid-enhanced hepatobiliary phase images in the detailed characterization of arterial phase enhancing nodules 1 cm in diameter and smaller. They showed that for hypervascular lesions 1 cm in diameter or smaller, T2-weighted images have the highest sensitivity among tests with an odds ratio statistically separable from 1 for differentiating HCC from benign hypervascular lesions 1 cm or smaller.[25] Our results confirmed that hypeintensity on T2-W is suggestive of malignancy, in fact 20/23 nodules (86.9%) showed this feature, however it is not allow characterizing cHCC-CCA as a separate lesion to HCC.

In our study, all cHCC-CCA patients showed restricted diffusion with a median ADC value of 880.7 x 10^{-3}mm^2/s so as all true HCC showed restricted diffusion with median ADC of 1210.0 x 10^{-3} mm^2/s. DWI has been applied to liver imaging as an excellent tool for detection and characterization of focal liver lesions, increasing clinical confidence and decreasing false positives.[11] DWI could be used as a helpful diagnostic tool for HCC in patients with chronic liver disease, since DWI can accurately detect HCC in patients with chronic liver disease regardless of the lesion size.[11,12] A potential reason for the better accuracy of DWI is that this does not rely on morphologic features only. Malignant tissues tend to be hypercellular with an accumulation of macromolecular proteins leaving a small extracellular space resulting in a decrease of the ADC value. The major limits of DWI are the different parameters used in DWI sequences that may affect the results of ADC calculation.[11,12] In our study, ADC value could allow to distinguish cHCC-CCA as a separate group from true HCC patients.

An interesting radiological finding that we found was the presence in cHCC-CCA group of satellite nodules, expression of micrometastases, as confirmed by pathologist. In fact, we found this finding in 63.6% (n. 7) cHCC-CCA patients and only in 5.9% (n. 3) true HCC. At the best of our knowledge, no previous study reported this result. We think that it is linked to more aggressiveness of this type of lesion, data confirmed also by the presence of nodal metastases in two cHCC-CCA patients.

There are several limitations to our study. First, the sample size was small because of the rarity of cHCC-CCA and it is a single-center experience. Second that this is a retrospective study and the readers were aware, the cohort comprised of cHCC-CC and HCC. Third, the study is defective of radiology-pathology correlation. Our future prospective is to assess radiology-pathology correlation to better show how the relative composition of these mixed tumours translates into their imaging appearance.

Conclusions

A proper diagnosis of cHCC-CCA is mandatory given that surgical resection is the current standard of care for cHCC-CCAs and controversies surround the appropriateness of other therapies. An exact pre-surgical diagnosis is very complicated due to its heterogeneous imaging characteristics with overlapping features of HCC and CCA. However according to our results in patients at risk for HCC, when the lesion shows satellite nodules, hyperintense signal on T2-W, restricted diffusion and especially the absence of capsule appearance in nodule that shows peripheral and progressive contrast enhancement, the radiologist should consider the diagnosis of cHCC-CCA.

Acknowledgements

The authors are grateful to Alessandra Trocino, librarian at the National Cancer Institute of Naples, Italy. Moreover, for the collaboration, authors are grateful to Assunta Zazzaro and Dr Ivano Rossi, TSRM at Radiology Division, "Istituto Nazionale Tumori IRCCS Fondazione Pascale – IRCCS di Napoli", Naples, I-80131, Italy.

References

1. Garancini M, Goffredo P, Pagni F, Romano F, Roman S, Sosa JA, et al. Combined hepatocellular-cholangiocarcinoma: a population-level analysis of an uncommon primary liver tumor. *Liver Transpl* 2014; **20:** 952-9. doi: 10.1002/lt.23897
2. Joo I, Kim H, Lee JM. Cancer stem cells in primary liver cancers: pathological concepts and imaging findings. *Korean J Radiol* 2015; **16:** 50-68. doi: 10.3348/kjr.2015.16.1.50
3. Gera S, Ettel M, Acosta-Gonzalez G, Xu R. Clinical features, histology, and histogenesis of combined hepatocellular-cholangiocarcinoma. *World J Hepatol* 2017; **9:** 300-9. doi: 10.4254/ wjh. v9. i6.300
4. Akiba J, Nakashima O, Hattori S, Tanikawa K, Takenaka M, Nakayama M, et al. Clinicopathologic analysis of combined hepatocellular-cholangiocarcinoma according to the latest WHO classification. *Am J Surg Pathol* 2013; **37:** 496-505. doi: 10.1097/PAS.0b013e31827332b0
5. Portolani N, Baiocchi GL, Coniglio A, Piardi T, Grazioli L, Benetti A, et al. Intrahepatic cholangiocarcinoma and combined hepatocellular-cholangiocarcinoma: a Western experience. *Ann Surg Oncol* 2008; **15:** 1880-90. doi: 10.1245/s10434-008-9933-y
6. Yeh MM. Pathology of combined hepatocellular-cholangiocarcinoma. *J Gastroenterol Hepatol* 2010; **25:** 1485-92. doi: 10.1111/j.1440-1746.2010.06430.x
7. Yoon YI, Hwang S, Lee YJ, Kim KH, Ahn CS, Moon DB, et al. Postresection outcomes of combined hepatocellular carcinoma-cholangiocarcinoma, hepatocellular carcinoma and intrahepatic cholangiocarcinoma. *J Gastrointest Surg* 2016; **20:** 411-20. doi: 10.1007/s11605-015-3045-3
8. Allen RA, Lisa JR. Combined liver cell and bile duct carcinoma. *Am J Pathol* 1949; **25:** 647-55. PMID: 18152860
9. Okuda K. Natural history of hepatocellular carcinoma including fibrolamellar and hepato-cholangiocarcinoma variants. *J Gastroenterol Hepatol* 2002; **17:** 401-5. doi: 10.1046/j.1440-1746.2002.02734.x
10. Zhou YM, Zhang XF, Wu LP, Sui CJ, Yang JM. Risk factors for combined hepatocellular-cholangiocarcinoma: a hospital-based case-control study. *World J Gastroenterol* 2014; **20:** 12615-20. doi: 10.3748/wjg.v20.i35.12615
11. Granata V, Fusco R, Filice S, Catalano O, Piccirillo M, Palaia R, et al. The current role and future prospectives of functional parameters by diffusion weighted imaging in the assessment of histologic grade of HCC. *Infect Agent Cancer* 2018; **13:** 23. doi: 10.1186/s13027-018-0194-5
12. Granata V, Fusco R, Avallone A, Filice F, Tatangelo F, Piccirillo M, et al. Critical analysis of the major and ancillary imaging features of LI-RADS on 127 proven HCCs evaluated with functional and morphological MRI: lights and shadows. *Oncotarget* 2017; **8:** 51224-37. doi: 10.18632/oncotarget.17227
13. Granata V, Fusco R, Avallone A, Catalano O, Filice F, Leongito M, et al. Major and ancillary magnetic resonance features of LI-RADS to assess HCC: an overview and update. *Infect Agent Cancer* 2017; **12:** 23. doi: 10.1186/s13027-017-0132-y
14. Granata V, Fusco R, Catalano O, Guarino B, Granata F, Tatangelo F, et al. Intravoxel incoherent motion (IVIM) in diffusion-weighted imaging (DWI) for hepatocellular carcinoma: correlation with histologic grade. *Oncotarget* 2016; **7:** 79357-64. doi: 10.18632/oncotarget.12689
15. Granata V, de Lutio di Castelguidone E, Fusco R, Catalano O, Piccirillo M, Palaia R, et al. Irreversible electroporation of hepatocellular carcinoma: preliminary report on the diagnostic accuracy of magnetic resonance, computer tomography, and contrast-enhanced ultrasound in evaluation of the ablated area. *Radiol Med* 2016; **121:** 122-31. doi: 10.1007/s11547-015-0582-5.
16. Zhang XY, Luo Y, Wen TF, Jiang L, Li C, Zhong XF, et al. Contrast-enhanced ultrasound: improving the preoperative staging of hepatocellular carcinoma and guiding individual treatment. *World J Gastroenterol* 2014; **20:** 12628-36. doi: 10.3748/wjg.v20.i35.12628
17. Ayuso C, Rimola J, García-Criado A. Imaging of HCC. *Abdom Imaging* 2012; **37:** 215-30. doi: 10.1007/s00261-011-9794-x
18. Jeon SK, Joo I, Lee DH, Lee SM, Kang HJ, Lee KB, et al. Combined hepatocellular cholangiocarcinoma: LI-RADS v2017 categorisation for differential diagnosis and prognostication on gadoxetic acid-enhanced MR imaging. *Eur Radiol* 2019; **29:** 373-82. doi: 10.1007/s00330-018-5605-x
19. The American College of Radiology. Liver Reporting & Data System (LI-RADS). [cited 2020 Jan 15]. Available at: https://www.acr.org/Clinical-Resources/Reporting-and-Data-Systems/LI-RADS
20. Edmondson HA, Steiner PE. Primary carcinoma of the liver: a study of 100 cases among 48,900 necropsies. *Cancer* 1954; **7:** 462-503. doi: 10.1002/1097-0142(195405)7:3<462::aid-cncr2820070308>3.0.co;2-e
21. Lee HS, Kim MJ, An C. How to utilize LR-M features of the LI-RADS to improve the diagnosis of combined hepatocellular-cholangiocarcinoma on gadoxetate-enhanced MRI? *Eur Radiol* 2019; **29:** 2408-16. doi: 10.1007/s00330-018-5893-1
22. Potretzke TA, Tan BR, Doyle MB, Brunt EM, Heiken JP, Fowler KJ. Imaging features of biphenotypic primary liver carcinoma (hepatocholangiocarcinoma) and the potential to mimic hepato- cellular carcinoma: LI-RADS analysis of CT and MRI features in 61 cases. *AJR Am J Roentgenol* 2016; **207:** 25-31. doi: 10.2214/AJR.15.14997
23. Sammon J, Fischer S, Menezes R, Hosseini-Nik H, Lewis S, Taouli B, et al. MRI features of combined hepatocellular-cholangiocarcinoma versus mass forming intrahepatic cholangiocarcinoma. *Cancer Imaging* 2018; **18:** 8. doi: 10.1186/s40644-018-0142-z
24. Fowler KJ, Sheybani A, Parker RA 3rd, Doherty S, M Brunt E, Chapman WC, et al. Combined hepatocellular and cholangiocarcinoma (biphenotypic) tumors: imaging features and diagnostic accuracy of contrast-enhanced CT and MRI. *AJR Am J Roentgenol* 2013; **201:** 332-9. doi: 10.2214/AJR.12.9488
25. Kim JE, Kim SH, Lee SJ, Rhim H. Hypervascular hepatocellular carcinoma 1 cm or smaller in patients with chronic liver disease: characterization with gadoxetic acid-enhanced MRI that includes diffusion-weighted imaging. *AJR Am J Roentgenol* 2011; **196:** W758-65. doi: 10.2214/AJR.10.4394

research article

Relation of the chondromalatia patellae to proximal tibial anatomical parameters, assessed with MRI

Mohammadreza Tabary[1], Azadehsadat Esfahani[2], Mehdi Nouraie[3], Mohammad Reza Babaei[4], Ali Reza Khoshdel[5], Farnaz Araghi[6], Mostafa Shahrezaee[1,7]

[1] Department of Science and Research Branch, AJA University of Medical Sciences, Tehran, Iran
[2] School of Medicine, Tehran University of Medical Sciences, Tehran, Iran
[3] Division of Pulmonary, Allergy and Critical Care Medicine, Department of Medicine, University of Pittsburgh, Pittsburgh, PA, USA
[4] Department of Interventional Radiology, Firouzgar Hospital, Iran University of Medical Sciences, Tehran, Iran
[5] Modern Epidemiology Research Center, AJA University of Medical Sciences, Tehran, Iran
[6] School of Medicine, Shahid Beheshti University of Medical Sciences, Tehran, Iran
[7] Department of Orthopedics, AJA University of Medical Sciences, Tehran, Iran

Radiol Oncol 2020; 54(2): 159-167.

Received 13 February 2020
Accepted 18 March 2020

Correspondence to: Mostafa Shahrezaee, M.D., Professor of Orthopedics, Department of Science and Research Branch, AJA University of Medical Sciences, Etemadzadeh St., Tehran, Iran. E-mail: moshahrezayee@yahoo.com

Disclosure: No potential conflicts of interest were disclosed.

Background. Magnetic resonance imaging (MRI) is a non-invasive highly sensitive tool for diagnosing chondromalacia patellae in the early stages. Many studies have evaluated patellar and trochlear morphology with different radiologic indices. We aimed to assess the discriminative power of tibial, patellar, and femoral indices in MRI for chondromalacia patellae.

Patients and methods. 100 cases of chondromalacia, as well as 100 age-matched controls among the patients who underwent knee MRI between February 2017 and March 2019, were included. The standard protocol of knee MRI was applied and the diagnosis of chondromalacia was made on MRI findings. Chondromalacia subjects were also classified as grade 1 to 4 according to the Modified Outerbridge's MRI grading system. We measured 25 MRI parameters in the knee and adjacent structures to determine the relation between chondromalacia patellae and anatomical MRI parameters.

Results. Tibial slope, trochlear depth, lateral trochlear inclination, and lateral patellar tilt angle had significant correlation with chondromalacia. Any increase in lateral trochlear inclination and lateral patellar tilt angle could increase the probability of the disease (Odds ratio [OR] 1.15, 1.13; 95% CI: 1.03–1.30; 1.02–1.26, respectively), while any increase in medial tibial slope and trochlear depth could decrease the probability of chondromalacia (OR 0.85, 0.06; 95% CI: 0.73–0.98, 0.02–0.17, respectively). We also designed a model for the severity of disease by using the patellar height index (relative odds ratio: 75.9).

Conclusions. The result of this study showed the novelty role of tibial anatomy in developing chondromalacia and its mechanism. We also concluded that patellar height might be an important factor in defining disease severity.

Key words: magnetic resonance imaging; chondromalacia patellae; anatomical indices

Introduction

Chondromalacia patellae is a common reason for patellofemoral pain syndrome. It is defined as the disruption of patellar cartilage due to repeated stress to the articular surface.[1] These patients may experience frequent recurrence and chronic pain, which limits daily life activities.[2] Radiographs

were traditionally used to diagnose chondromalacia; however, this modality was unable to visualize patellar alignment and congruency angles[3], and the complete anatomy was not visualized using X-ray.

Magnetic resonance imaging (MRI), a non-invasive tool to detect chondromalacia patellae with a high soft tissue contrast, can detect chondromalacia in the lower stages with a sensitivity of 66%. Moreover, this sensitivity rises to 85–100% for the higher stages.[4] Many key findings can be detected in the early stage of chondral loss including signal irregularities, fissures, and chondral thinning; thus, leading to earlier diagnosis.[5]

Multiple mechanisms can cause chondromalacia, including vascular insufficiency, trauma, and structural abnormalities.[6] In line with the mechanism of structural abnormalities, many studies have evaluated patellar and femoral trochlear morphology with different radiologic indices. Femoral intertrochlear notch angle, femoral trochlear depth, femoral sulcus angle, femoral trochlear angle, patellar tilt angle, and patellar height indices were among these factors. Many patellar height indices, measured as patellar tendon to patellar length ratio, seemed to correlate with cartilage defects.[7] Furthermore, the correlation between tibial structural abnormalities and patellar cartilage stress, but not cartilage defects, was evaluated previously.[8] On the other hand, some studies focused on the correlation between soft tissue structure and chondromalacia, particularly subcutaneous fat and adjacent muscles.[8, 9]

Radiologic findings of the knee joint differ between low-grade (grade 1, 2) and high-grade (grade 3,4) chondromalacia. For instance, the sulcus angle and trochlear depth were shown to be significantly different between mild and severe cartilage defects.[10]

The role of tibial anatomy is not well-known in developing chondromalacia. Some studies evaluated the role of tibial anatomy in dynamic models, but not in human subjects.[11]

To our knowledge, there is no published diagnostic model of radiological findings for chondromalacia that includes all important findings including tibial anatomical parameters. We aimed to develop a model and assess the discriminative power of tibial, patellar, and femoral indices for chondromalacia and emphasize the role of tibial anatomy for the first time. We also hypothesize that patellar height is a substantial factor, affecting the development of the disease.

Patients and methods

Patients and population

We reviewed all the radiology records of the patients who underwent knee MRI in our institute between February 2017 and March 2019. We reviewed almost 2000 MRI images of the patients who referred to our institution. After reviewing all the images, we included 200 cases of chondromalacia patellae without any other accompanied diseases in MRI images. The diagnosis of chondromalacia was made on MRI findings including irregularity of the cartilage and the loss of cartilage thickness in at least two consecutive slices. The exclusion criteria were as follows: age more than 65 or less than 18, history of trauma to the knee and adjacent structures in the last 6 months, history of knee surgery, osteoarthritis grade 3 and 4, presence of a fracture or space-occupying lesion in MRI, and patellar subluxation. Patients were contacted and referred to our clinic for clinical evaluation. Patients with other clinical signs not related to chondromalacia were also excluded. After applying exclusion criteria and considering clinical signs, we included 100 cases of chondromalacia patellae. Chondromalacia cases were also classified as grade 1 to 4 according to the Modified Outerbridge's MRI grading system.[12] In case of the presence of more than a single grade lesion, the higher grade was selected.

After reviewing MRI images, we selected 200 controls without any significant changes in bony, ligamentous, chondral, tendinous, and muscular structures around the knee. Selection bias was minimized by using case-matched controls regarding age, gender, and BMI. The patellar cartilage was evaluated intact in the control group. After clinical evaluation, we excluded 100 controls with positive clinical finding in the knee. We finally included 100 healthy matched controls in the final analysis. A radiologist experienced in musculoskeletal imaging (A.E.) performed all the measurements. The same radiologist repeated the MRI measurement after 4 weeks in a random sample of the whole population to test the intra-rater reliability. The reader was blinded to participant's names, sex, age. The ethical approval for this study was obtained from local ethics committee and written consent was obtained from the patients.

MRI evaluation

A 1.5 Tesla Achieva (Philips, Best, Netherlands) MRI device with an extremity superficial coil was used to perform the scans. All the measurements

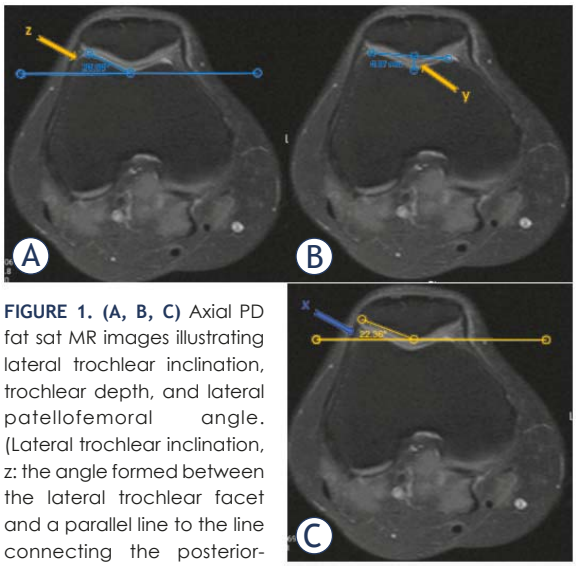

FIGURE 1. (A, B, C) Axial PD fat sat MR images illustrating lateral trochlear inclination, trochlear depth, and lateral patellofemoral angle. (Lateral trochlear inclination, z: the angle formed between the lateral trochlear facet and a parallel line to the line connecting the posterior-most cortical surfaces of the femoral condyles; Trochlear depth, y: the distance between the deepest point of trochlear sulcus and the line connecting the anterior points of the medial and lateral condyles; Lateral patellar tilt angle, x: the angle between the line parallel to the patellar lateral facet and the line connecting the most posterior parts of femoral condyles)

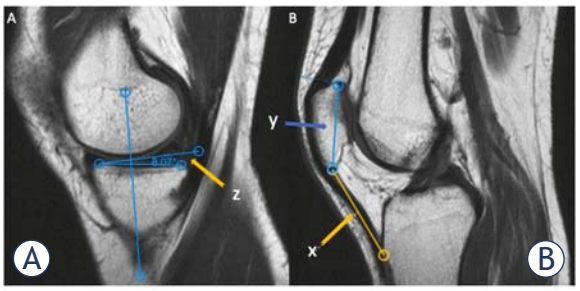

FIGURE 2. (A, B) Sagittal T1-Weighted MR images illustrating medial tibial slope and Insall-Salvati index. (Medial tibial slope, z: the angle formed between the line running along the tibial slope of the medial tibial condyle and the perpendicular line to the tibial axis; Insall-Salvati index: the ratio of x to y; x, the length of patellar tendon and y, the greatest diagonal length of patella)

and processing were performed in the Picture Archiving Communication System (Marco PACS, Version 10). The standard protocol of knee MRI was applied (neutral knee position) with a slice thickness of 3 mm. T1 and T2 (sagittal), Proton density (PD) fat saturation (axial, coronal, and sagittal) sequences were recorded. We measured 25 MRI parameters in the knee and adjacent structures. The definition and the procedure of all measurements were described elsewhere and are summarized in Figure 1,2,3 (Figure 1 & Figure 2 illustrates the significant MRI measurements in the final model). Intercondylar notch angle (INA), medial tibial slope (MTS), lateral tibial slope (LTS), anterior tibial slope (ATS), coronal tibial slope (CTS), intercondylar depth (ID), condylar width (CW), intercondylar width (IW), medial condylar width (MCW), lateral condylar width (LCW), notch width index (NWI), and patellar tendon tibial shaft (PTTS) angle were evaluated in previous studies in cruciate ligament injuries[13-15], but not in chondromalacia subjects. Subchondral and cartilaginous Wiberg-angle (SWA and CWA) were evaluated in trochlear dysplasia[16], but not in chondromalacia patients. Tilting deformity was evaluated in healthy subject by using patellar-patellar tendon (P-PT) angle[17]; however, it was not evaluated in chondromalacia cases. Lateral patellar tilt angle (LPTA), sulcus angle (SA), trochlear depth (TD), lateral trochlear inclination (LTI), medial trochlear inclination (MTI), patellar facet angle (PFA) and trochlear angle (TA) were studied in chondromalacia cases; however, the controls were not matched to the cases regarding gender and BMI.[18] Also, they were analyzed in a single variable model using *student t-test* method and not in a multi-variable model. Tibial tuberosity-trochlear groove (TTTG) distance was described in patellofemoral pain syndrome[19], but not assessed specifically in chondromalacia cases. Patellar height index was also described in previous studies[20]; however, we evaluated the predictive power of Insall-Salvati index (ISI) for the severity (grading) of the disease.

Statistical analysis

MRI measurements were presented in the case and control group by median (interquartile range). Odds ratio (95% CI) for each measurement was calculated including the clustering of observations within subjects. We applied multiple alternative variable selection approaches, including backward and forward stepwise approach to develop the most parsimonious predictive model with the highest calibration. Final model was selected based on Akaike Information Criterion. Then we applied bootstrapping (with 50 replications) to assess the internal validity of the model. The final Odds ratio (95%CI) was reported from bootstrapping results. In the final model, we calculated the Area Under Curve using bootstrapping internal validation. Same analysis approach was replicated to compare two group of cases with low disease severity (grade 1, 2) vs. high severity (grade 3,4). Intra-class correlation coefficient was used to assess intra-rater reli-

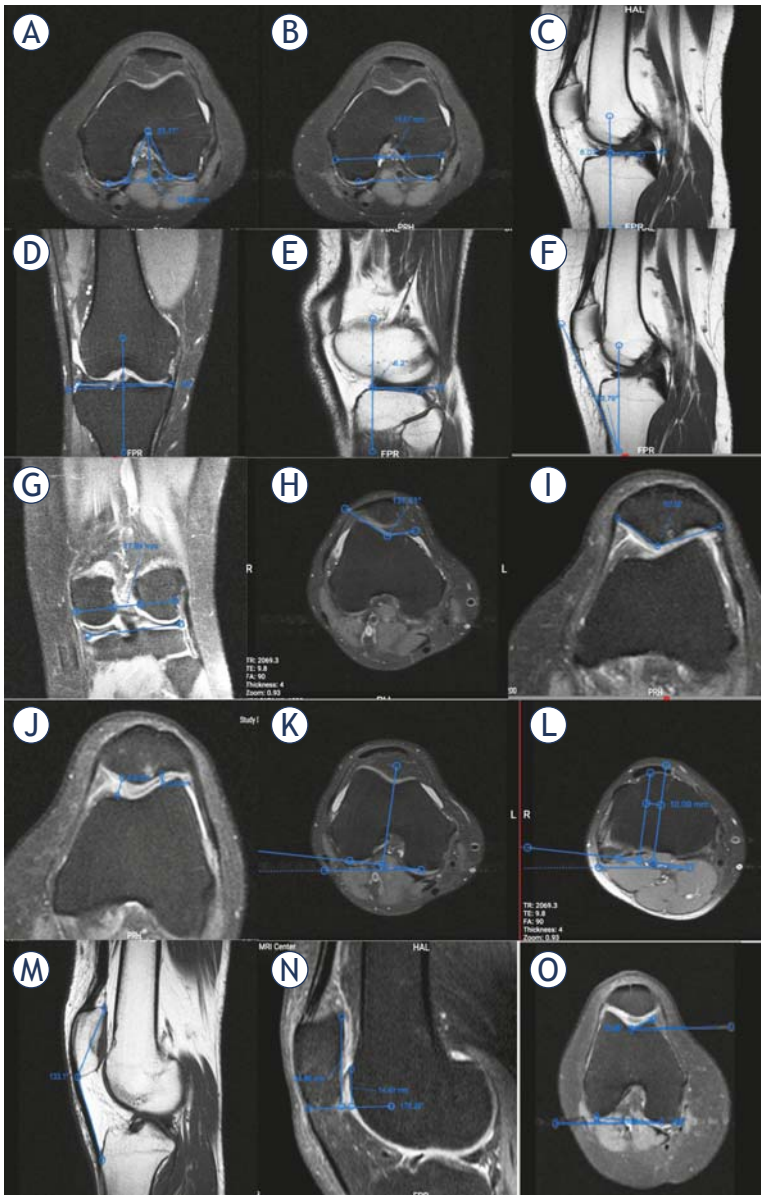

FIGURE 3. Measurements of nonsignificant MRI parameters in the final model. **(A)** Axial MRI plane of the knee showing Intercondylar notch angle (INA) and Intercondylar depth (ID): The posterior bicondylar line is drawn. ID is the distance between top of the notch to the bi-epicondylar line. Intercondylar notch angle is defined as the angle formed by the 2 lines going from the top of the notch to the most inferior aspect of the notch at the medial and lateral condyles; **(B)** Axial MRI plane of the knee showing Intercondylar Width (IW), Medial condyle width (MCW), and Lateral condyle width (LCW): IW is the distance between the medial and lateral femoral condyle walls at the anterior third of the intercondylar depth (the middle line), the other two distances in this axial cut represent LCW, and MCW; **(C)** Sagittal MRI plane of the knee showing anterior tibial slope (ATS): At first the tibial axis is drawn by joining to midpoints between the anterior and posterior cortex of the tibial diaphysis with at least 5cm distance from each other. The anterior tibial slope is then defined as the angle between a perpendicular line (inferior line) to the longitudinal axis and a line passing through the anterior cruciate ligament tibial footprint (superior line); **(D)** Sagittal MRI plane of the knee showing coronal tibial slope (CTS): The coronal tibial slope is defined as the angle between a line joining the highest points on the medial and lateral aspects of the tibial plateau (inferior horizontal line) and a perpendicular line (superior horizontal white line) to the longitudinal axis as mentioned above; **(E)** Sagittal MRI plane of the knee showing lateral tibial slope (LTS): the angle formed between the line running along the tibial slope of the medial tibial condyle and the perpendicular line to the tibial axis; **(F)** Sagittal MRI plane of the knee showing patellar tibial tendon shaft angle (PTTS angle): PTTS angle is measured as the angle between Proximal tibial anatomical axis described above and patellar tendon axis in the mid-sagittal section; **(G)** Coronal MRI plane of the knee showing notch width index (NWI): first Bicondylar width parallel to the joint line at the level of popliteal groove is measured (1). Then notch width is measured at the level of popliteal groove, using the line joining the innermost margins of the femoral condyles at the borders of the intercondylar notch (2). The NWI is ratio of 2/1; **(H)** Axial MRI plane of the knee showing sulcus angle (SA): The angle formed between the medial and lateral trochlear facets; **(I)** Axial MRI plane of the knee showing patellar facet angle (PFA): the angle between two line connecting the central ridge to the middle of patellar facets; **(J)** Axial MRI plane of the knee showing patellofemoral index (PFI): the ratio of medial to lateral interspaces; **(K, L)** Axial MRI plane of the knee showing tibial tuberosity trochlear groove distance (TTTG): posterior line was drawn at posterior border of femoral condyles. A vertical line is drawn at trochlear groove and the other parallel line is drawn along the tibial tuberosity that transferred to this level. Distance between the two lines is measured as TT-TG; **(M)** Sagittal MRI plane of the knee showing Patella-patellar tendon angle (P-PT angle): The P–PT angle was defined as the angle between the upper patellar pole and the lower patellar pole, and the tibial tuberosity; **(N)** Sagittal MRI plane of the knee showing Patellotrochlear index (PTI): it is defined as the length of patellar cartilage overlapping the trochlear cartilage divided by length of patellar cartilage; **(O)** Axial MRI plane of the knee showing medial trochlear inclination (MTI): the angle formed between the medial trochlear facet and a parallel line to the line connecting the posterior-most cortical surfaces of the femoral condyles.

ability. All analyses were performed in Stata 15.0 (StataCorp, College Station, TX).

Results

Patients' characteristics

Firstly we evaluated the records of 2000 knee MRIs. Overall, 400 patients were eligible to enter the study, while after applying inclusion and exclusion criteria and clinical examination, 100 cases of chondromalacia were eligible for the final analysis. We evaluated MRI findings of 200 participants, including 100 cases (50 male) with chondromalacia aged between 21 to 64, and 100 healthy controls (51

TABLE 1. MRI measurements of the control patients versus chondromalacia cases

MRI Measurements	Median (IQR)		Odds ratio	95% CI†	P-value
	Control	Case			
INA (degree)	52.0 (48.0–57.0)	53.0 (48.0–56.0)	1.00	0.96–1.05	0.863
IW (mm)	21.5 (20.1–23.4)	20.3 (19.0–21.7)	0.77	**0.67–0.88**	**< 0.001**
ID (mm)	28.2 (26.7–29.8)	25.9 (26.7–29.8)	0.76	**0.68–0.85**	**< 0.001**
MCW (mm)	26.5 (24.9–28.5)	24.8 (23.2–26.7)	0.79	**0.70–0.88**	**< 0.001**
LCW (mm)	27.2 (25.5–28.8)	24.4 (23.3–26.1)	0.77	**0.69–0.86**	**< 0.001**
ATS (degree)	8.0 (5.5–11.5)	8.0 (6.0–10.5)	1.01	0.94–1.09	0.727
CTS (degree)	3.5 (2.0–5.0)	4.0 (2.5–5.2)	1.13	0.96–1.32	0.144
MTS (degree)	7.5 (5.2–9.5)	7.0 (4.5–9.5)	0.95	0.87–1.04	0.252
LTS (degree)	5.5 (3.5–7.5)	5.5 (3.5–7.5)	0.96	0.88–1.05	0.448
PTTS angle (degree)	27.0 (23.0–30.0)	27.0 (24.0–30.0)	1.01	0.95–1.08	0.46
NWI	0.29 (0.27–0.31)	0.29 (0.27–0.31)	0.18	0.00–6399.00	0.749
TD (mm)	5.30 (4.82–5.87)	4.04 (3.51–4.60)	0.14	**0.08–0.24**	**< 0.001**
SA (degree)	140.0 (134.0–145.0)	142.0 (137.0–150.0)	1.04	**1.01–1.08**	**0.009**
LTI (degree)	20.0 (18.0–23.0)	20.0 (17.5–24.0)	0.99	0.93–1.05	0.683
MTI (degree)	18.0 (15.0–21.0)	16.0 (13.5–20)	0.93	**0.89–0.99**	**0.020**
LPTA (degree)	13.0 (10.0–16.0)	14.0 (10.5–17.0)	1.03	0.97–1.08	0.294
PFA (degree)	138.0 (133.0–142.0)	136.0 (132.5–141.0)	0.97	0.93–1.01	0.160
PFI	1.14 (1.01–1.35)	1.32 (1.07–1.59)	3.02	**1.37–6.65**	**0.006**
TTTG (mm)	12.5 (10.2–15.2)	12.3 (10.5–16.1)	1.01	0.95–1.09	0.603
SCF (mm)	20.5 (17.3–25.3)	26.7 (21.7–34.8)	1.14	**1.09–1.19**	**< 0.001**
CWI	0.52 (0.50–0.54)	0.52 (0.50–0.54)	0.76	0.00–3481.00	0.949
SWI	0.57 (0.54–0.59)	0.56 (0.54–0.58)	0.01	0.00–34.80	0.270
P-PT angle (degree)	140.5 (137.0–144.0)	140.0 (137.5–143.5)	0.99	0.93–1.05	0.802
ISI	0.98 (0.89–1.07)	1.00 (0.89–1.14)	4.62	0.60–35.20	0.139
PTI	0.31 (0.26–0.36)	0.30 (0.25–0.35)	0.04	0.00–2.21	0.115

† IQR represents 25th–75th interquartile range, 95% CI represents 95% confidence interval for odds ratio

ATS = Anterior tibial slope; CTS = Coronal tibial slope; CWI = Cartilaginous Wiberg index; ID = Intercondylar depth; INA = Intercondylar notch angle; ISI = Insall-Salvati index; IW = Intercondylar width; LCW = Lateral condyle width; LPTA = Lateral patellar tilt angle; LTI = Lateral trochlear inclination; LTS = Lateral tibial slope; MCW = Medial condyle width; MTI = Medial trochlear inclination; MTS = Medial tibial slope; NWI = Notch width index; P-PT angle = Patella-patellar tendon angle; PTTS angle = Patellar tibial tendon shaft angle; PFA = Patellar facet angle; PFI = Patellofemoral index; PTI = Patellotrochlear index; SA = Sulcus angle; SCF = Subcutaneous fat pad; SWI = Subchondral Wiberg index; TD = Trochlear depth; TTTG = Tibial tuberosity trochlear groove distance

male) aged between 20 and 57. The mean age of the chondromalacia subjects and cases were 32.7 ± 9.3 and 30.2 ± 7.2, respectively (P-value = 0.21)

Radiographic measurements

We measured 25 radiographic parameters. Table 1 summarizes the radiographic features in patients and controls. Intercondylar width, intercondylar depth, medial condyle width, lateral condyle width, trochlear depth, and medial trochlear inclination pad were significantly lower in chondromalacia cases (P-value = < 0.001, < 0.001, 0.020), while sulcus angle, patellofemoral index, and subcutaneous fat were significantly higher in cases compared to controls (P-value = 0.009, 0.006, < 0.001).

Predictive model for chondromalacia

We developed a predictive model for chondromalacia. This model included medial tibial slope, trochlear depth, lateral trochlear inclination, and lateral patellar tilt angle and age. This model predicted the disease with an excellent AUC (area under curve) of 0.92 (95% CI: 0.85–0.94). Any increase in lateral trochlear inclination and lateral patellar

TABLE 2. Predictive model for chondromalacia including MRI measurements

MRI measurements	Odds ratio	95% CI	P-value	Intra-rater reliability	Contribution of any increase in this parameter to chondromalacia
LTI	1.15	1.03–1.30	0.014	0.992	Increases disease probability
LPTA	1.13	1.02–1.26	0.018	0.996	Increases disease probability
MTS	0.85	0.73–0.98	0.026	0.997	Decreases disease probability
TD	0.06	0.02–0.17	0.000	0.995	Decreases disease probability
Age	1.10	1.02–1.20	0.015	-	Increases disease probability

LTI = Lateral trochlear inclination; LPTA = Lateral patellar tilt angle; MTS = Medial tibial slope; TD = Trochlear depth

The Area under curve (AUC) for this model is estimated as 0.92 (bootstrap bias-corrected 95% CI: 0.85–0.94). Any increase in lateral trochlear inclination and lateral patellar tilt angle could increase the probability of the disease (positive correlation), while any increase in medial tibial slope and trochlear depth could decrease the probability of the disease (negative correlation)

TABLE 3. Predictive model for chondromalacia severity including MRI measurements

MRI measurements	Odds ratio	95%CI	P-value	Intra-rater reliability	Contribution of any increase in this parameter to chondromalacia severity
ISI	75.89	2.17–2652.69	0.017	0.997	Increases disease grade
Age	1.14	1.07–1.21	0.000	-	Increase disease grade

ISI = Insall-Salvati index

The Area under curve (AUC) for this model is estimated as 0.82 (bootstrap bias-corrected 95% CI: 0.64–0.86). Grade 1 and 2 are considered as non-severe, while grade 3 and 4 are assumed as severe. Increase in patellar height and age will increase disease grade (positive correlation with disease severity)

tilt angle could increase the probability of the disease (positive correlation with chondromalacia) (Odds ratio 1.15, 1.13; 95% CI: 1.03–1.30; 1.02–1.26, respectively).

However, any increase in medial tibial slope and trochlear depth could decrease the probability of chondromalacia (negative correlation with chondromalacia) (Odds ratio 0.85, 0.06; 95% CI: 0.73–0.98, 0.02–0.17, respectively), (Table 2). Increasing age could also increase the probability of the disease (positive correlation with chondromalacia) (Odds ratio 1.10; 95%CI: 1.02–1.20).

INA, IW, ID, MCW, LCW, ATS, CTS, LTS, PTTS angle, NWI, SA, MTI, PFA, PFI, TTTG, SCF, CWI, SWI, P-PT angle, PTI, and ISI were not significant (no correlation with chondromalacia) in the multivariable analysis regarding the presence of chondromalacia (P-value = 0.20, 0.24, 0.15, 0.19, 0.56, 0.30, 0.09, 0.39, 0.43, 0.32, 0.21, 0.55, 0.07, 0.15, 0.11, 0.11, 0.19, 0.66, 0.09, 0.27, 0.29; respectively).

Predictive model for the severity of the disease

Patients were classified as grade 1 lesion (38 patients), grade 2 lesion (28 patients), grade 3 lesion (14 patients), and grade 4 lesion (20 patients). We combined grade 1 and 2 *vs.* grade 3 and 4 to develop a predictive model for severity of disease in patients with chondromalacia.

We designed a two-variable model for predicting the severity of the disease using age and Insall-Salvati index concurrently. Insall-Salvati index and age were two factors that could predict disease severity (Odds ratio = 75.89, 1.14; 95% CI: 2.17–2652.69, 1.07–1.21, respectively) with an AUC of 0.82 (95% CI: 0.64–0.86) (Table 3). Any increase in Insall-Salvati index (*i.e.* any increase in patellar height) and age could increase the severity of the disease (resulted in higher grades of chondromalacia). It means that if patellar height increases, patients will experience more severe disease (higher grades).

Discussion

Prediction models are becoming more popular in medicine. Previous studies focused their attention on the correlation between trochlear morphology and chondromalacia patellae, in a single variable analysis model. We developed a model to predict chondromalacia. We included medial tibial slope, lateral trochlear inclination, lateral patellar tilt an-

gle, trochlear depth, and age in the final predictive model for chondromalacia. We found that any increase in lateral trochlear inclination and lateral patellar tilt angle could increase the probability of the disease, while any increase in medial tibial slope and trochlear depth could decrease the probability of the disease. We also found that if patellar height increases, patients would experience more severe disease (higher grades).

Lateral patellar tilt angle (LPTA) was suggested as one of the predictive factors in the final model. LPTA was shown to be increased in chondromalacia subjects. Abnormal position of the patella in the femoral trochlear groove may play a role in the progression of chondromalacia patellae.[21,22] Studies have shown that lateral patellar displacement is associated with cartilage loss.[23] This can be justified by the fact that lateral tilting happens as a result of lateral compressive forces which acts on the lateral facet and increases shear forces in the central ridge area. These forces will increase chondrocyte activity, until the functional requests exceed chondrocyte potential and results in chondrocyte degeneration.[24] Moreover, previous studies have found that LPTA correlates with the sulcus angle in different knee flexion angles.[25] Sulcus angle has been reported to be greater in lateral maltrackers compared to non-lateral maltrackers[26], and it also correlates with cartilage lesions.[27] A wider sulcus is responsible for the increased pressure on patellofemoral articular surface and will predispose the patient to cartilage loss.[27] This correlation between the sulcus angle and LPTA may justify our result. However, LPTA has been reported to correlate significantly with chondral lesions in the lateral compartment of the patellofemoral joint (odds ratio < 1) and non-significantly with chondral lesions in the medial compartment of the patellofemoral joint (odds ratio > 1) in previous studies.[27] In this study, we did not define the side of cartilage defect. As chondromalacia impacts the medial side more frequently[28], we may speculate that this relationship in our study should be judged according to the side of involvement.

In addition, LTI was positively correlated with chondromalacia according to our results. Kuroda *et al.* showed that elevation of lateral trochlea facet (increased LTI) could increase average patellofemoral contact pressure (40% increased with 10 mm lateral trochlear elevation). This may also induce the degradation of the cartilage.[29]

The most important finding of the present study is that the tibial slope may play an important role in the progression of chondromalacia. We found that with the medial tibial slope increasing, the risk of chondromalacia decreases. Studies suggest that an increase in the tibial slope leads to a decrease in patellofemoral contact force.[30] Posterior positioning of femoral components and increase in quadriceps lever arm are responsible for this association.[31-33] We deduce that the tibial slope correlates with chondromalacia patellae; however, the effect of tibial slope on medial and lateral patellar facets may be different. Furthermore, correcting the tibial slope with a greater angle has been shown to reduce anterior tibial strains, which are imposed on the patella.[34] Moreover, studies in patients with osteoarthritis suggested that increasing the tibial slope in unicompartmental knee arthroplasty of medial patellar facet will reduce the tension on the medial side.[11] This may also show the clinical importance of tibial slope on decreasing patellofemoral stress.

Our study suggests that trochlear depth would be sufficient for measuring the association of trochlear dysplasia with chondromalacia. Sulcus angle and trochlear depth are the two important factors associated with trochlear dysplasia in previous studies[35], and the congruency of the patella and femoral trochlea has been underscored in the development of cartilage lesions.[10] Patellofemoral tracking is also considered an important factor in patellofemoral pain syndrome.[36] Trochlear depth has been reported to be an important determinant of patellofemoral stability[37], thus, it may be an important factor in the process of tracking. Tuna *et al.* reported sulcus angle and trochlear depth to be significantly different in patients with and without the disease.[18] They reported greater mean of sulcus angle and lower mean of trochlear depth in chondromalacia subjects. Our findings are consistent with the latter study. We found that with the trochlear depth decreasing, the risk of chondromalacia increases to a great extent. This may be explained by the fact that when the trochlear surface becomes shallower, the surface area for articulation at the patellofemoral joint increases. Although it may provide a better distribution of joint load[37], the increased friction may result in cartilage defects. Further studies are needed to evaluate this proposed kinematics in active knee movements. This finding may underscore the clinical importance of trochlear depth. Takahashi *et al.* also showed better adaptation of the implants featuring deep trochlea to the native patella (low-contact stress implant and NexGen implant).[38]

We also proposed a predictive model of disease severity. In our study, ISI and age could predict

higher disease severity. To our knowledge, this is the first predictive model for the severity of chondromalacia with an excellent AUC. A model was proposed in the previous study by Lu *et al*. for chondromalacia but not severity by using Insall-Salvati index (ISI). This model was based on the patella alta and baja and could diagnose chondromalacia with an AUC of 0.596.[7]

In both predictive models proposed by our findings, age was remained as an important factor. A study in the United States population showed that the contribution of chondromalacia to the patellofemoral pain syndrome increases by age up to 59 years.[39] We also excluded patients older than 65 years and the results may not be applicable to older age groups.

There are some limitations to our study. This was a single center study, we used MRI to detect chondral lesion and early lesions might be considered as normal. MRI evaluations were performed during rest. Muscle contractions may alter these findings as described by previous studies.[42] We did not evaluate the exact site of the cartilage lesions. Moreover, medial and lateral facet chondromalacia might have different natures. Previous studies reported the predominance of chondromalacia in the medial patellar facet.[22] We did not define the side of chondromalacia in our subjects, so more pieces of evidence are needed to define the exact correlation of tibial slope with both medial- and lateral-facet chondromalacia.

The advantage of this study in knowledge is that when more diverse anatomical factors are analyzed regarding the presence of chondromalacia, tibial anatomical factors play a role in the progression of the disease. This study may clarify the mechanism of chondromalacia and emphasize the role of tibial slopes in the mechanism of cartilage loss. Previous studies focused on femoral trochlear dysplasia, and did not include tibial anatomical parameters in their analysis. The result of this study meight also affect the treatment of chondromalacia, as new treatment plans for healing cartilage and bone defects are being introduced and focus on altering tibial anatomy including tubercle osteotomy.[40,41] The result of this study shew the role of tibial anatomy in developing chondromalacia. In addition, the clinical importance of this study was the fact that tibial slope should be precisely set in knee surgeries; however, more studies are needed to determine the best cut-off for tibial slope.

References

1. Endo Y, Stein BE, Potter HG. Radiologic assessment of patellofemoral pain in the athlete. *Sports Health* 2011; **3:** 195-210. doi: 10.1177/1941738110397875
2. Crossley KM, Stefanik JJ, Selfe J, Collins NJ, Davis IS, Powers CM, et al. Patellofemoral pain consensus statement from the 4th International Patellofemoral Pain Research Retreat, Manchester. Part 1: Terminology, definitions, clinical examination, natural history, patellofemoral osteoarthritis and patient-reported outcome measures. *Br J Sports Med* 2016; **50:** 839-43. doi: 10.1136/bjsports-2016-096384
3. Davies AP, Costa ML, Shepstone L, Glasgow MM, Donell S. The sulcus angle and malalignment of the extensor mechanism of the knee. *J Bone Joint Surg Br* 2000; **82:** 1162-6. doi: 10.1302/0301-620x.82b8.10833
4. Aysin IK, Askin A, Mete BD, Guvendi E, Aysin M, Kocyigit H. Investigation of the relationship between anterior knee pain and chondromalacia patellae and patellofemoral malalignment. *Eurasian J Med* 2018; **50:** 28-33. doi: 10.5152/eurasianjmed.2018.17277
5. LLopis E, Padron M. Anterior knee pain. *Eur J Radiol* 2007; **62:** 27-43. doi: 10.1016/j.ejrad.2007.01.015
6. Neusel E, Graf J. The influence of subchondral vascularisation on chondromalacia patellae. *Arch Orthop Trauma Surg* 1996; **115:** 313-5. doi: 10.1007/bf00420322
7. Lu W, Yang J, Chen S, Zhu Y, Zhu C. Abnormal patella height based on insall-salvati ratio and its correlation with patellar cartilage lesions: an extremity-dedicated low-field magnetic resonance imaging analysis of 1703 Chinese cases. *Scand J Surg* 2016; **105:** 197-203. doi: 10.1177/1457496915607409
8. Liao TC, Yin L, Powers CM. The influence of isolated femur and tibia rotations on patella cartilage stress: a sensitivity analysis. *Clin Biomech* 2018; **54:** 125-31. doi: 10.1016/j.clinbiomech.2018.03.003
9. Kok HK, Donnellan J, Ryan D, Torreggiani WC. Correlation between subcutaneous knee fat thickness and chondromalacia patellae on magnetic resonance imaging of the knee. *Can Assoc Radiol J* 2013; **64:** 182-6. doi: 10.1016/j.carj.2012.04.003
10. Ali SA, Helmer R, Terk MR. Analysis of the patellofemoral region on MRI: association of abnormal trochlear morphology with severe cartilage defects. *AJR Am J Roentgenol* 2010; **194:** 721-7. doi: 10.2214/AJR.09.3008
11. Weber P, Woiczinski M, Steinbruck A, Schmidutz F, Niethammer T, Schroder C, et al. Increase in the tibial slope in unicondylar knee replacement: analysis of the effect on the kinematics and ligaments in a weight-bearing finite element model. *Biomed Res Int* 2018; **2018:** 8743604. doi: 10.1155/2018/8743604
12. Hayes CW, Conway WF. Evaluation of articular cartilage: radiographic and cross-sectional imaging techniques. *Radiographics* 1992; **12:** 409-28. doi: 10.1148/radiographics.12.3.1609135
13. Huang M, Li Y, Guo N, Liao C, Yu B. Relationship between intercondylar notch angle and anterior cruciate ligament injury: a magnetic resonance imaging analysis. *J Int Med Res* 2019; **47:** 1602-9. doi: 10.1177/0300060518824447
14. Alentorn-Geli E, Pelfort X, Mingo F, Lizano-Diez X, Leal-Blanquet J, Torres-Claramunt R, et al. An evaluation of the association between radiographic intercondylar notch narrowing and anterior cruciate ligament injury in men: the notch angle is a better parameter than notch width. *Arthroscopy* 2015; **31:** 2004-13. doi: 10.1016/j.arthro.2015.04.088
15. K S, Chamala T, Kumar A. Comparison of anatomical risk factors for noncontact anterior cruciate ligament injury using magnetic resonance imaging. *J Clin Orthop Trauma* 2019; **10:** 143-8. doi: 10.1016/j.jcot.2017.08.002
16. Fucentese SF, von Roll A, Koch PP, Epari DR, Fuchs B, Schottle PB. The patella morphology in trochlear dysplasia--a comparative MRI study. *Knee* 2006; **13:** 145-50. doi: 10.1016/j.knee.2005.12.005
17. Aksahin E, Aktekin CN, Kocadal O, Duran S, Gunay C, Kaya D, et al. Sagittal plane tilting deformity of the patellofemoral joint: a new concept in patients with chondromalacia patella. *Knee Surg Sports Traumatol Arthrosc* 2017; **25:** 3038-45. doi: 10.1007/s00167-016-4083-4
18. Tuna BK, Semiz-Oysu A, Pekar B, Bukte Y, Hayirlioglu A. The association of patellofemoral joint morphology with chondromalacia patella: a quantitative MRI analysis. *Clin Imaging* 2014; **38:** 495-8. doi: 10.1016/j.clinimag.2014.01.012

19. Tahmasebi MN, Aghaghazvini L, Mirkarimi SS, Zehtab MJ, Sheidaie Z, Sharafatvaziri A. The influence of tibial tuberosity-trochlear groove distance on development of patellofemoral pain syndrome. *Arch Bone Jt Surg* 2019; **7:** 46-51.

20. Ozel D. The relationship between early-onset chondromalacia and the position of the patella. *Acta Radiol* 2020; **61:** 370-5. doi: 10.1177/0284185119861901

21. Hunter DJ, Zhang YQ, Niu JB, Felson DT, Kwoh K, Newman A, et al. Patella malalignment, pain and patellofemoral progression: the Health ABC Study. *Osteoarthritis Cartilage* 2007; **15:** 1120-7. doi: 10.1016/j.joca.2007.03.020

22. Fulkerson JP. *Disorders of the patellofemoral joint*. Fourth edition. Baltimor: Lippincott Williams & Wilkins; 2004.

23. Yang B, Tan H, Yang L, Dai G, Guo B. Correlating anatomy and congruence of the patellofemoral joint with cartilage lesions. *Orthopedics* 2009; **32:** 20. doi: 10.3928/01477447-20090101-27

24. Mazzola C, Mantovani D. Patellofemoral malalignment and chondral damage: current concepts. *Joints* 2013; **1:** 27-33. PMID: 25606514

25. Hoshmand LT, Helmes E, Kazarian S, Tekatch G. Evaluation of two relaxation training programs under medication and no-medication conditions. *J Clin Psychol* 1985; **41:** 22-9. doi: 10.1002/1097-4679(198501)41:1<22::aid-jclp2270410105>3.0.co;2-e

26. Harbaugh CM, Wilson NA, Sheehan FT. Correlating femoral shape with patellar kinematics in patients with patellofemoral pain. *J Orthop Res* 2010; **28:** 865-72. doi: 10.1002/jor.21101.

27. Kalichman L, Zhang Y, Niu J, Goggins J, Gale D, Felson DT, et al. The association between patellar alignment and patellofemoral joint osteoarthritis features--an MRI study. *Rheumatology* 2007; **46:** 1303-8. doi: 10.1093/rheumatology/kem095

28. Fulkerson JP, Buuck DA. *Disorders of the patellofemoral joint*. Philadelphia: Lippincott Williams & Wilkins; 2004.

29. Batailler C, Neyret P. Trochlear dysplasia: imaging and treatment options. *EFORT Open Rev* 2018; **3:** 240-7. doi: 10.1302/2058-5241.3.170058

30. Okamoto S, Mizu-uchi H, Okazaki K, Hamai S, Nakahara H, Iwamoto Y. Effect of tibial posterior slope on knee kinematics, quadriceps force, and patellofemoral contact force after posterior-stabilized total knee arthroplasty. *J Arthroplasty* 2015; **30:** 1439-43. doi: 10.1016/j.arth.2015.02.042

31. Ostermeier S, Hurschler C, Windhagen H, Stukenborg-Colsman C. In vitro investigation of the influence of tibial slope on quadriceps extension force after total knee arthroplasty. *Knee Surg Sports Traumatol Arthrosc* 2006; **14:** 934-9. doi: 10.1007/s00167-006-0078-x

32. Wachowski MM, Walde TA, Balcarek P, Schuttrumpf JP, Frosch S, Stauffenberg C, et al. Total knee replacement with natural rollback. *Ann Anat* 2012; **194:** 195-9. doi: 10.1016/j.aanat.2011.01.013

33. Browne C, Hermida JC, Bergula A, Colwell CW, Jr., D'Lima DD. Patellofemoral forces after total knee arthroplasty: effect of extensor moment arm. *Knee* 2005; **12:** 81-8. doi: 10.1016/j.knee.2004.05.006

34. Bai B, Baez J, Testa N, Kummer FJ. Effect of posterior cut angle on tibial component loading. *J Arthroplasty* 2000; **15:** 916-20. doi: 10.1054/arth.2000.9058

35. Pennock AT, Chang A, Doan J, Bomar JD, Edmonds EW. 3D knee trochlear morphology assessment by magnetic resonance imaging in patients with normal and dysplastic trochleae. *J Pediatr Orthop* 2020; **40:** 114-9. doi: 10.1097/BPO.0000000000001188

36. Powers CM. Patellar kinematics, part II: the influence of the depth of the trochlear groove in subjects with and without patellofemoral pain. *Phys Ther* 2000; **80:** 965-78. PMID: 11002432

37. Teichtahl AJ, Parkins K, Hanna F, Wluka AE, Urquhart DM, English DR, et al. The relationship between the angle of the trochlear groove and patella cartilage and bone morphology--a cross-sectional study of healthy adults. *Osteoarthritis Cartilage* 2007; **15:** 1158-62. doi: 10.1016/j.joca.2007.03.010

38. Takahashi A, Sano H, Ohnuma M, Kashiwaba M, Chiba D, Kamimura M, et al. Patellar morphology and femoral component geometry influence patellofemoral contact stress in total knee arthroplasty without patellar resurfacing. *Knee Surg Sports Traumatol Arthrosc* 2012; **20:** 1787-95. doi: 10.1007/s00167-011-1768-6

39. Glaviano NR, Kew M, Hart JM, Saliba S. Demographic and epidemiological trends in patellofemoral pain. *Int J Sports Phys Ther* 2015; **10:** 281-90. PMID: 26075143

40. Safikhani MM, Zamanian A, Ghorbani F, Asefnejad A, Shahrezaee M. Bi-layered electrospun nanofibrous polyurethane-gelatin scaffold with targeted heparin release profiles for tissue engineering applications. *J Polym Eng* 2017; **37:** 933-41. doi: 10.1515/polyeng-2016-0291

41. Jack C, Rajaratnam S, Khan H, Keast-Butler O, Butler-Manuel P, Heatley F. The modified tibial tubercle osteotomy for anterior knee pain due to chondromalacia patellae in adults: A five-year prospective study. *Bone Joint Res* 2012; **1:** 167-73. doi: 10.1302/2046-3758.18.2000083.

42. Felicio LR, Saad MC, Liporaci RF, Baffa Ado P, Dos Santos AC, Bevilaqua-Grossi D. Evaluating patellar kinematics through magnetic resonance imaging during open- and closed-kinetic-chain exercises. *J Sport Rehabil* 2010; **19:** 1-11. doi: 10.1123/jsr.19.1.1

research article

Pulsed low dose-rate irradiation response in isogenic HNSCC cell lines with different radiosensitivity

Vesna Todorovic[1], Ajda Prevc[1], Martina Niksic Zakelj[1], Monika Savarin[1], Simon Bucek[2], Blaz Groselj[3], Primoz Strojan[3,4], Maja Cemazar[1,5], Gregor Sersa[1,6]

[1] Institute of Oncology Ljubljana, Department of Experimental Oncology, Ljubljana, Slovenia
[2] Institute of Oncology Ljubljana, Department of Cytopathology, Ljubljana, Slovenia
[3] Institute of Oncology Ljubljana, Department of Radiation Oncology, Ljubljana, Slovenia
[4] University of Ljubljana, Faculty of Medicine, Ljubljana, Slovenia
[5] University of Primorska, Faculty of Health Sciences, Izola, Slovenia
[6] University of Ljubljana, Faculty of Health Sciences, Ljubljana, Slovenia

Radiol Oncol 2020; 54(2): 168-179.

Received 10 February 2020
Accepted 1 March 2020

Correspondence to: Prof. Gregor Sersa, Ph.D., Institute of Oncology Ljubljana, Zaloška 2, SI-1000 Ljubljana, Slovenia. E-mail: gsersa@onko-i.si

Disclosure: No potential conflicts of interest were disclosed.

Background. Management of locoregionally recurrent head and neck squamous cell carcinomas (HNSCC) is challenging due to potential radioresistance. Pulsed low-dose rate (PLDR) irradiation exploits phenomena of increased radiosensitivity, low-dose hyperradiosensitivity (LDHRS), and inverse dose-rate effect. The purpose of this study was to evaluate LDHRS and the effect of PLDR irradiation in isogenic HNSCC cells with different radiosensitivity.

Materials and methods. Cell survival after different irradiation regimens in isogenic parental FaDu and radioresistant FaDu-RR cells was determined by clonogenic assay; post irradiation cell cycle distribution was studied by flow cytometry; the expression of DNA damage signalling genes was assesed by reverse transcription-quantitative PCR.

Results. Radioresistant Fadu-RR cells displayed LDHRS and were more sensitive to PLDR irradiation than parental FaDu cells. In both cell lines, cell cycle was arrested in G_2/M phase 5 hours after irradiation. It was restored 24 hours after irradiation in parental, but not in the radioresistant cells, which were arrested in G_1-phase. DNA damage signalling genes were under-expressed in radioresistant compared to parental cells. Irradiation increased DNA damage signalling gene expression in radioresistant cells, while in parental cells only few genes were under-expressed.

Conclusions. We demonstrated LDHRS in isogenic radioresistant cells, but not in the parental cells. Survival of LDHRS-positive radioresistant cells after PLDR was significantly reduced. This reduction in cell survival is associated with variations in DNA damage signalling gene expression observed in response to PLDR most likely through different regulation of cell cycle checkpoints.

Key words: DNA damage; isogenic cell lines; low dose irradiation; pulsed low dose-rate irradiation; radiosensitivity

Introduction

Low dose hyperradiosensitivity (LDHRS) is a phenomenon of increased radiosensitivity to single doses below 0.5 Gy.[1] LDHRS has been demonstrated in various normal and tumour cell lines, tumour spheroids and human tumours.[2–7] LDHRS was not observed in the intrinsically radiosensitive cell lines, whereas radioresistant cell lines demonstrated the most marked LDHRS.[3,8] LDHRS precedes the occurrence of increased radioresistance (IRR) to cell killing by radiation over the dose range of 0.5 – 1 Gy.[1] Transition from LDHRS to IRR is cell type-dependent and has been typically observed in the dose range of 0.2 Gy to 0.6 Gy.[1,2,9,10]

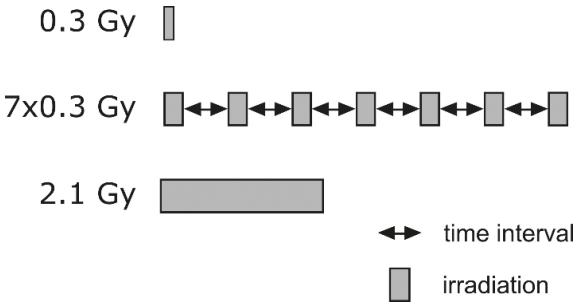

FIGURE 1. Schematic diagram of irradiation schedule.

Another phenomenon of increased radiosensitivity, especially in some LDHRS-positive tumor cells, is the inverse dose-rate effect. In contrary to normal tissue sparing due to repair of sublethal DNA damage during low dose-rate irradiation, increased radiosensitivity of tumour cells was observed when the dose-rate was decreased.[11] The inverse dose-rate effect can be observed at dose-rates below 1 Gy/h in cells showing LDHRS.[11,12]

The LDHRS and the inverse dose-rate effect were exploited in pulsed low-dose rate (PLDR) radiotherapy as a treatment strategy combining multiple low doses (hyperfractionation) in a pulsed delivery to reduce the effective dose-rate.[13] Its effectiveness was evaluated first in the radioresistant gliomas.[14] The delivery of low dose fractions in a pulsed fashion significantly reduced surviving fraction of glioma cell lines *in vitro*[13], greatly inhibited tumour growth of orthotopic xenografts, preserved vascular density, caused less neuronal cell death *in vivo*[15,16], and allowed retreatment of recurrent glioma tumors.[14] A similar low-dose fractionated regime significantly increased tumour growth delay in metastatic melanoma, leiomyosarcoma, breast cancer, and non-Hodgkin lymphoma.[6] In the last decade, PLDR irradiation has been used clinically for re-irradiation of recurrent tumours in the previously irradiated areas.[14,17]

Both glioblastoma and head and neck squamous cell carcinoma (HNSCC) are known for tumour recurrences within the previously irradiated area.[18–20] Based on the promising glioblastoma results using PLDR radiotherapy, this approach could be beneficial also to improve HNSCC management, namely to decrease regrowth of recurrent tumours and to reduce normal tissue toxicity. Management of HNSCC remains challenging due to complex anatomy of the region, the need for preserving function of the involved organs, locoregional recurrence of radioresistant tumours, and normal tissue toxicity.[19] In HNSCC cell lines with different radiosensitivity, so far no apparent

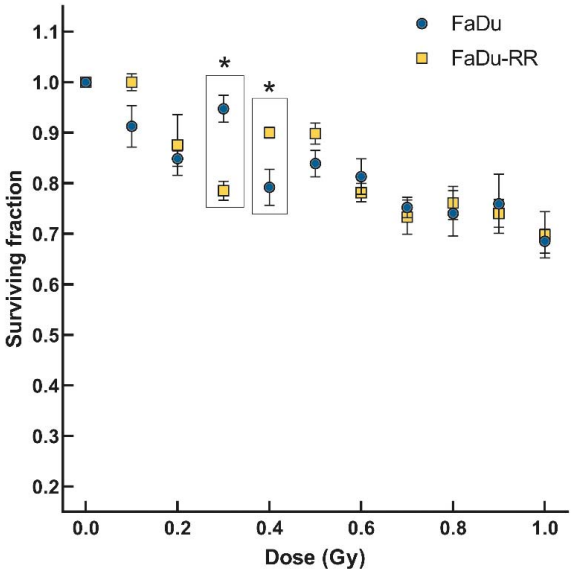

FIGURE 2. Surviving fraction of parental FaDu and radioresistant FaDu-RR cells after exposure to low doses of ionizing radiation. Symbols are mean ± standard error of the mean from four independent experiments. * - significantly different from FaDu cells.

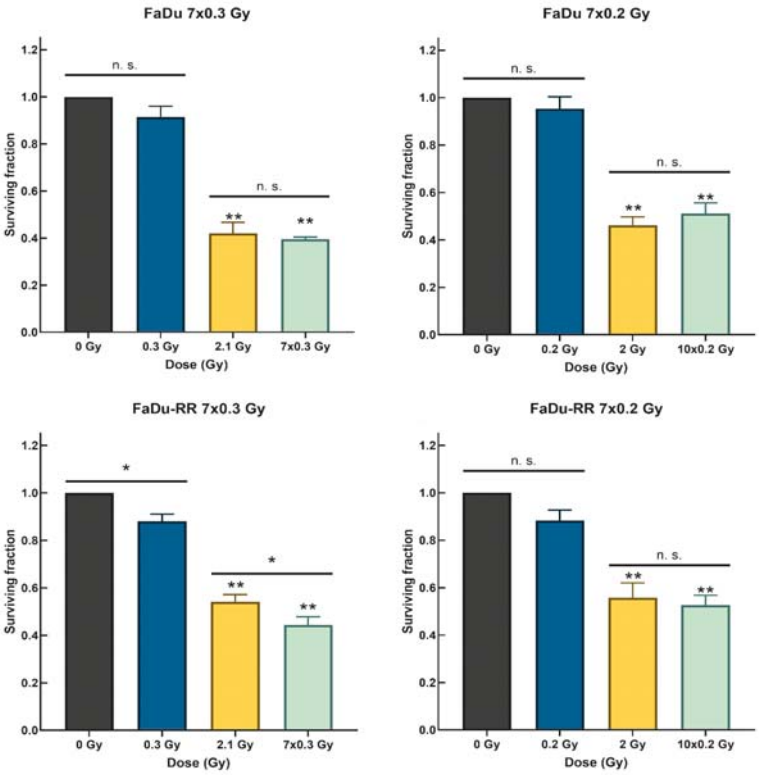

FIGURE 3. Surviving fraction of parental FaDu and radioresistant FaDu-RR after exposure to different PLDR irradiation regimes. **(A)** Surviving fraction of parental FaDu cells after 7x0.3 Gy PLDR and **(B)** after 10x0.2 Gy PLDR irradiation. **(C)** Surviving fraction of radioresistant FaDu-RR cells after 7x0.3 Gy PLDR and **(D)** after 10x0.2 Gy PLDR irradiation. Bars present mean ± SEM from four independent experiments. ** = significantly different from 0 Gy and low dose IR (0.3 Gy or 0.2 Gy); * = significant difference between the groups; n. s. = non-significant difference.

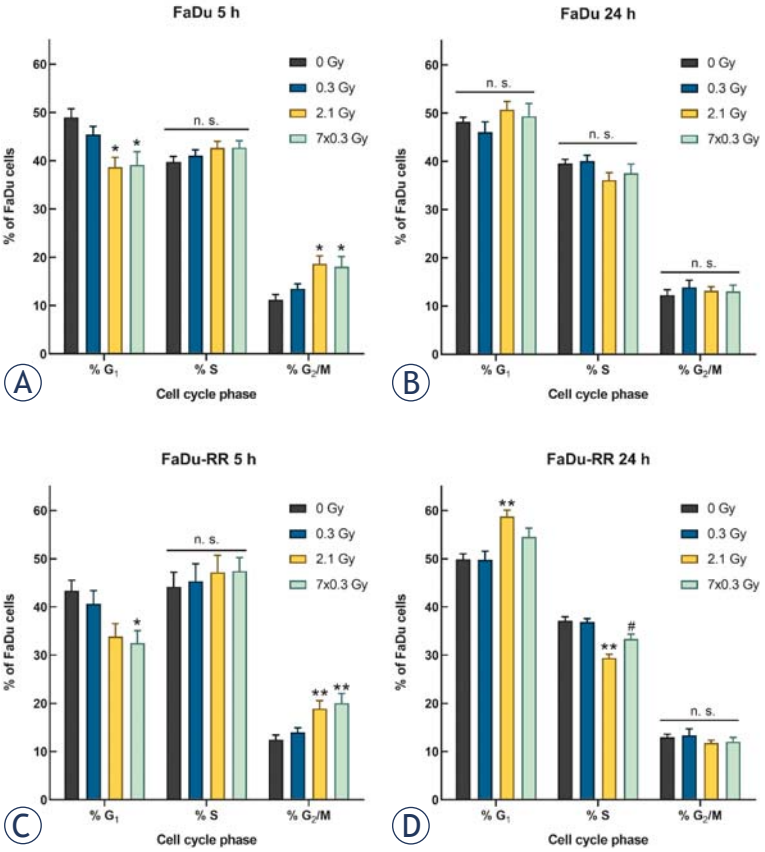

FIGURE 4. Cell cycle distribution in parental FaDu and radioresistant FaDu-RR cells after exposure to different PLDR irradiation regimes. **(A)** Cell cycle distribution in FaDu cells 5 h and **(B)** 24 h after irradiation. **(C)** Cell cycle distribution in FaDu-RR cells 5 h and **(D)** 24 h after irradiation. Bars present mean ± SEM from four independent experiments. * = significantly different from 0 Gy; ** = significantly different from 0 Gy and 0.3 Gy; # = significantly different from 0 Gy, 0.3 Gy and 2.1 Gy; n. s. = non-significant difference.

difference was observed between conventional and low dose irradiation, however, LDHRS status of these HNSCC cell lines was unknown.[21] Therefore, proper selection of LDHRS-positive cell lines and tumours is crucial to evaluate the effect of PLDR radiotherapy and/or ultrahyperfractionated irradiation in HNSCC.

The exact mechanisms causing the LDHRS are not clear yet. Most prominently LDHRS appears in G_2-phase cells, where the threshold amount of DNA damage needs to occur to overcome LDHRS and induce IRR.[22,23] DNA damage signalling network is involved in cell cycle checkpoint activation and plays an important role in cellular radiosensitivity.[24,25] Isogenic cell lines with different LDHRS status are an attractive model to study the mechanisms involved in the LDHRS response. Due to the same genetic background, observed difference in the response to PLDR irradiation can be attributed to the activation of different cellular mechanisms.

The purpose of this study was first: to evaluate the LDHRS status of two isogenic HNSCC cell lines with different radiosensitivity, followed by the evaluation of cell survival after PLDR irradiation in the isogenic cell lines. Second, with the aim to explore the underlying mechanisms of radiosensitivity of radioresistant cells to PLDR irradiation, we determined cell cycle progression and DNA damage signalling gene expression in response to low dose, conventional and PLDR irradiation.

Materials and methods

Cell lines

Human pharyngeal HNSCC cell line FaDu (ATCC, HTB-43) and 2.6-fold more radioresistant FaDu-RR cells, were established in our laboratory from the parental FaDu cells after repeated exposure to ionizing radiation as previously described.[26] Both cell lines were grown in Advanced Dulbecco's Modified Eagle Medium (DMEM, Gibco, Thermo Fisher, MA, USA) supplemented with 5% fetal bovine serum (FBS, Gibco, Thermo Fisher), 10 mM L-glutamine (GlutaMAX, Gibco), penicillin (100 U/mL) (Grünenthal, Germany) and gentamicin (50 mg/mL) (Krka, Slovenia). Cells were routinely subcultured twice a week and incubated in a humidified atmosphere at 37°C and 5% CO_2.

Low dose irradiation

Irradiation was delivered using a Gulmay MP1-CP225 X-ray unit (Gulmay Medical Ltd, UK) with a filter consisting of Cu thickness of 0.55 mm and Al thickness of 1.8 mm at 200 kV and 1.0 mA to achieve the low dose rate 0.185 Gy/min. The low dose rate was used to allow precise delivery of single low dose (0.1 Gy was delivered in 0.5 min). To determine the radiosensitivity of parental FaDu and radioresistant FaDu-RR cells, cells were exposed to single doses of 0.1 – 1 Gy in steps of 0.1 Gy and plated for clonogenic assay as described below.

Pulsed low dose-rate irradiation

Cells were exposed to three different irradiation schedules (Figure 1). The control, non-irradiated cells, were handled as irradiated samples but were not exposed to any irradiation. The irradiated cells were exposed to either a single dose of 0.3 Gy, a series of seven 0.3 Gy pulses (7x0.3 Gy) or a single dose of 2.1 Gy. A series of 0.3 Gy pulses was sep-

ules, they were plated for clonogenic assay as described below.

Clonogenic assay

For all irradiation doses, 350 cells/dish were plated onto 60-mm tissue culture dish and irradiated with a specific single dose or specific irradiation schedule using Gulmay MP1-CP225 X-ray unit, as described above. After 10 days, the resulting colonies were stained with crystal violet and counted. Surviving fraction was calculated as a ratio of the plating efficiencies for irradiated and control non-irradiated cells. The experiments were repeated 3 to 4 times in triplicates.

Cell cycle

Cell cycle distribution of parental FaDu and radioresistant FaDu-RR cells after irradiation was determined by flow cytometry as previously described.[26] Briefly, the samples were prepared following the standard procedure using fluorochrome DAPI (4',6-diamidino-2-phenylindole-dihydrochloride). The samples were acquired using a flow cytometer Partec PAS II (Partec GmbH, Germany) and at least 30,000 cells per sample were collected during sample acquisition. Results were analyzed with MultiCycle AV DNA analysis software (Phoenics Flow Systems, Inc., CA, USA) and percent of cells in G_1, S and G_2/M phases of the cell cycle were calculated. The experiment was repeated 4 times.

DNA damage signalling gene expression

An array of 84 pathway-specific and 5 reference genes (Human DNA Damage Signalling Pathway RT^2 ProfilerTM PCR Array, PAHS-029Z, Qiagen, Germany) was used to study the DNA damage response in parental FaDu and radioresistant FaDu-RR cells after the low dose and PLDR irradiation. Genomic DNA control, reverse transcription control, and positive PCR controls were included in the array. Samples for gene expression analysis were prepared as previously described.[26] Briefly, 5 hours after different irradiation protocols, total RNA was isolated from the cells using RNeasy Plus Mini Kit (Qiagen), and RNA concentration and sample purity ($A_{260/280}$) were determined spectrophotometrically. For cDNA synthesis, 2 μg total RNA was used using the RT^2 First Strand Kit (Qiagen). Reverse transcription-quantitative PCR was carried out on QuantStudio 3 Real-time PCR

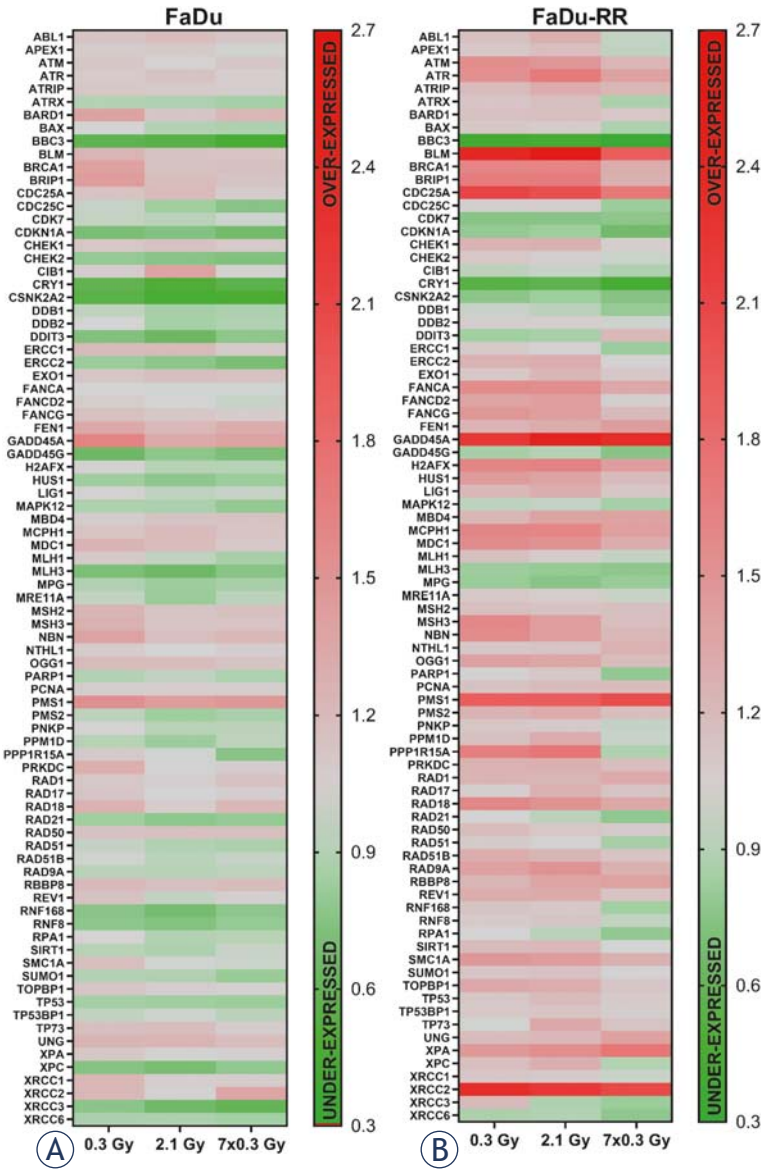

FIGURE 5. Heat maps of DNA damage signalling gene expression in parental FaDu **(A)** and radioresistant FaDu-RR cells **(B)** in 0.3 Gy, 2.1 Gy and 7x0.3 Gy irradiated cells relative to the gene expression in control non-irradiated cells. The magnitude of the fold change in gene expression of each gene from three independent experiments is represented by the colour. Green indicates under-expressed genes, and red indicates over-expressed genes.

arated by 4.5 min intervals to create an apparent dose rate of 0.055 Gy/min. Additionally, a series of 0.2 Gy pulses was separated by 3 min intervals, to create an apparent dose rate of 0.053 Gy/min, and was compared to the effect of single 2 Gy dose. A 4.5-minute and 3 min interval between the doses for each of the above PLDR irradiation protocols, was chosen to create a similar apparent dose-rate as proposed by Tome *et al*.[13] To determine radiosensitivity of the cells to these irradiation sched-

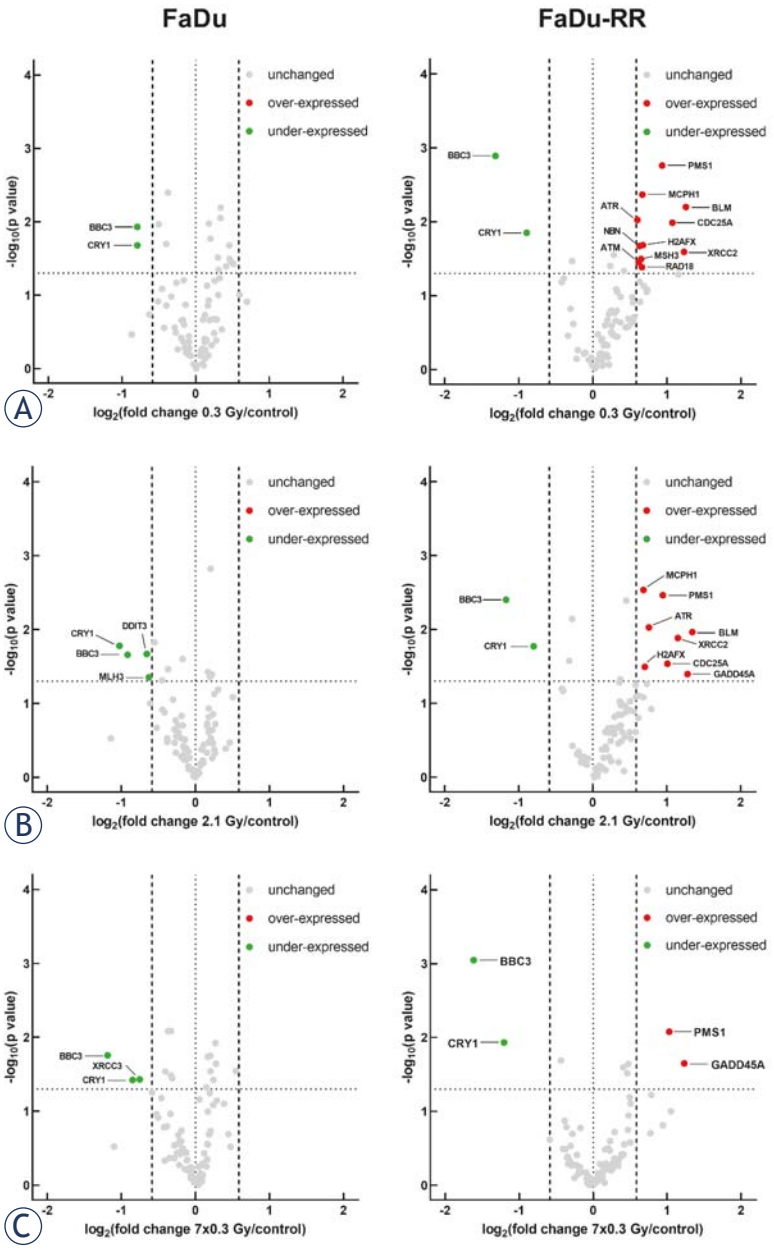

FIGURE 6. DNA damage signalling gene expression in parental FaDu and radioresistant FaDu-RR cells in response to different irradiation protocols. **(A)** Gene expression of FaDu cells in response to 0.3 Gy, 2.1 Gy, and 7x0.3 Gy irradiation relative to the control non-irradiated FaDu cells. **(B)** Gene expression in FaDu-RR cells in response to 0.3 Gy, 2.1 Gy, and 7x0.3 Gy irradiation relative to the control non-irradiated FaDu-RR cells. Volcano plots show the fold change in gene expression and statistical significance (p value). The horizontal line shows the statistical significance threshold (p value < 0.05). Two vertical dashed lines show the threshold of over-expressed (right) and under-expressed genes (left), while the solid vertical line shows no change in gene expression. Symbols represent the mean gene expression of each tested gene in irradiated cells relative to control non-irradiated cells from three independent experiments.

System (Applied Biosystems, USA) using RT² qPCR Sybr Green ROX Mastermix (Qiagen) and cycling conditions as described previously.[26]

GeneGlobe Data Analysis Center (Qiagen) was used to analyze the results. Data were normalized to the gene expression of the reference gene with the most stable expression (*HPRT1*). Fold change in gene expression was calculated using the ΔΔCT method.[27] We used 1.5 fold-change in gene expression as a threshold and p values less than 0.05 to identify significantly different gene expression.

Statistics

GraphPad Prism 8.1.2 (GraphPad Software, Inc., CA, USA) was used for graphs and statistical analysis. Normal distribution of data was tested using the Shapiro-Wilk test. For normally distributed data, data are shown as the mean ± standard error of the mean (SEM). Differences between parental and radioresistant cells were identified by unpaired two-tailed t-test. One Way ANOVA with Tukey test for posthoc multiple comparisons were used to identify the difference between groups. Differences were considered significant for p values less than 0.05.

For statistical analysis of DNA damage signalling gene expression data, Student's t-test (two-tail distribution and equal variances between the two samples) was used on the replicate $2^{-\Delta\Delta CT}$ values for each gene in each irradiation protocol compared to the control non-irradiated cells from 3 independent experiments.

Results

Low dose irradiation

We observed similar radiosensitivity to single low doses of ionizing radiation in parental FaDu and radioresistant FaDu-RR cells, except at 0.3 Gy and 0.4 Gy doses (Figure 2). Surviving fraction of radioresistant FaDu-RR at 0.3 Gy was significantly lower (p=0.006) than the surviving fraction of parental FaDu cells, exposed to the same irradiation dose. From 0.3 Gy up to 0.5 Gy, an increase in the surviving fraction of radioresistant FaDu-RR cells was observed compared to parental FaDu cells, the difference was significant at 0.4 Gy (p=0.048), but not at 0.5 Gy (p=0.160).

Pulsed low-dose rate irradiation

Based on our experimental results, the radioresistant FaDu-RR cells showed the highest radiosensitivity at 0.3 Gy, therefore we used this dose to deliver PLDR irradiation. In both parental FaDu

and radioresistant FaDu-RR, the surviving fraction of cells irradiated with either a single dose of 2.1 Gy or a PLDR dose of 7x0.3 Gy was significantly reduced in comparison to control non-irradiated cells or cells irradiated with a single dose of 0.3 Gy ($p<0.0001$). However, no difference in surviving fraction was observed between parental FaDu cells irradiated with a single dose of 2.1 Gy or PLDR irradiation of 7x0.3 Gy ($p=0.607$) (Figure 3A). On the contrary, surviving fraction of radioresistant FaDu-RR cells irradiated with PLDR dose of 7x0.3 Gy was significantly reduced ($p=0.028$) in comparison to cells irradiated with a single dose of 2.1 Gy (Figure 3C). Similarly, a significant reduction of surviving fraction after irradiation with 0.3 Gy was observed in radioresistant FaDu-RR cells ($p=0.020$), but not in parental FaDu cells ($p=0.178$) compared with the control non-irradiated cells. Modifying PLDR irradiation to 10x0.2 Gy abolished the difference in cell survival between PLDR and single-dose irradiation in radioresistant FaDu-RR cells ($p=0.951$) (Figure 3B and 3D).

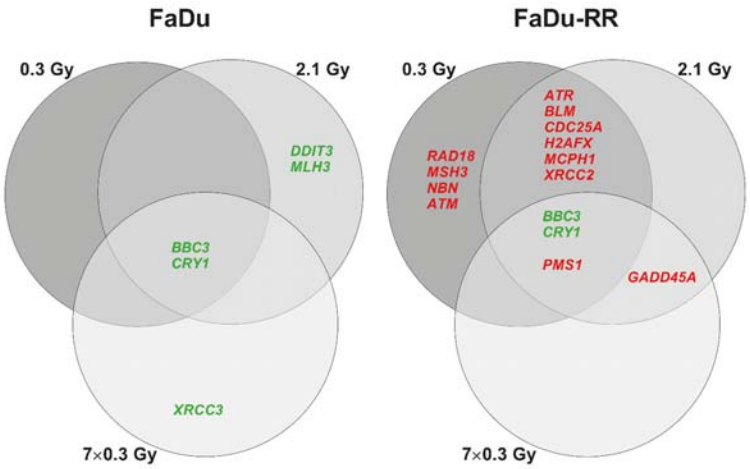

FIGURE 7. Venn diagrams of DNA damage signalling gene expression in parental FaDu and radioresistant FaDu-RR cells showing overlapping and differential gene expression. Only genes significantly over-expressed or under-expressed relative to control non-irradiated cells are shown. Genes in bold red are over-expressed, genes in bold green are under-expressed.

Cell cycle

Differences in cell cycle distribution in parental FaDu and radioresistant FaDu-RR were evaluated at 5- and 24-hour time point after different irradiation protocols (Figure 4). Asynchronous populations of non-irradiated FaDu and FaDu-RR cells did not differ in the cell cycle distribution. In response to different irradiation schemes, perturbations of cell cycle were observed in both FaDu and FaDu-RR cells. Namely, 5 hours after irradiation with a single dose of 2.1 Gy and a PLDR dose of 7x0.3 Gy, the percent of G_1-phase FaDu cells was significantly reduced ($p=0.021$ and $p=0.027$, respectively), while the percent of G_2/M-phase FaDu cells was significantly increased ($p=0.023$ and $p=0.035$, respectively) in comparison to control, non-irradiated FaDu cells. Contrary to FaDu cells, the percent of G_1-phase radioresistant FaDu-RR cells was significantly reduced only after PLDR irradiation ($p=0.047$), while the percent of G_2/M-phase cells was increased after both, a single dose of 2.1 Gy and a PLDR dose of 7x0.3 Gy ($p=0.037$ and $p=0.014$, respectively). No difference was observed in S-phase in FaDu nor FaDu-RR cells in all treatment groups. Cell cycle phase distribution was restored 24 hours after different irradiation protocols in FaDu cells, but not in FaDu-RR cells where an increase in G_1-phase and a decrease in S-phase cells was observed after 2.1 Gy irradiation regimen ($p=0.007$ and $p=0.0001$). A similar increase in G_1-phase and decrease in S-phase cells was observed also in PLDR-irradiated FaDu-RR cells, however not as prominent as after a single dose of 2.1 Gy. No difference in G_2/M-phase of FaDu-RR cells was observed in any group.

DNA damage signalling gene expression

Different DNA damage signalling gene expression pattern was observed in response to different irradiation protocols relative to the control non-irradiated cells. In parental FaDu cells, more DNA damage signalling genes were under-expressed (Figure 5A), while in the radioresistant FaDu-RR cells, DNA damage signalling genes were predominantly over-expressed in response to irradiation (Figure 5B). In parental FaDu cells, significant under-expression of 2, 4, and 3 genes was observed in response to 0.3 Gy, 2.1 Gy, and 7x0.3 Gy irradiation, respectively (Figure 6A). In radioresistant FaDu-RR cells, significant under-expression of 2 genes and over-expression of 11, 8, and 2 genes was observed in response to 0.3 Gy, 2.1 Gy, and 7x0.3 Gy irradiation, respectively (Figure 6B). Specifically, *BBC3* and *CRY1* genes were under-expressed in both parental FaDu and radioresistant FaDu-RR cells in response to all irradiation schedules (Figure 7). *PMS1* was over-expressed in radioresistant FaDu-RR cells in response to all three irradiation schedules, while *ATR*, *BLM*, *CDC25A*, *H2AFX*, *MCPH1*, and *XRCC2* were over-expressed in 0.3 Gy and 2.1 Gy irradiated FaDu-RR cells.

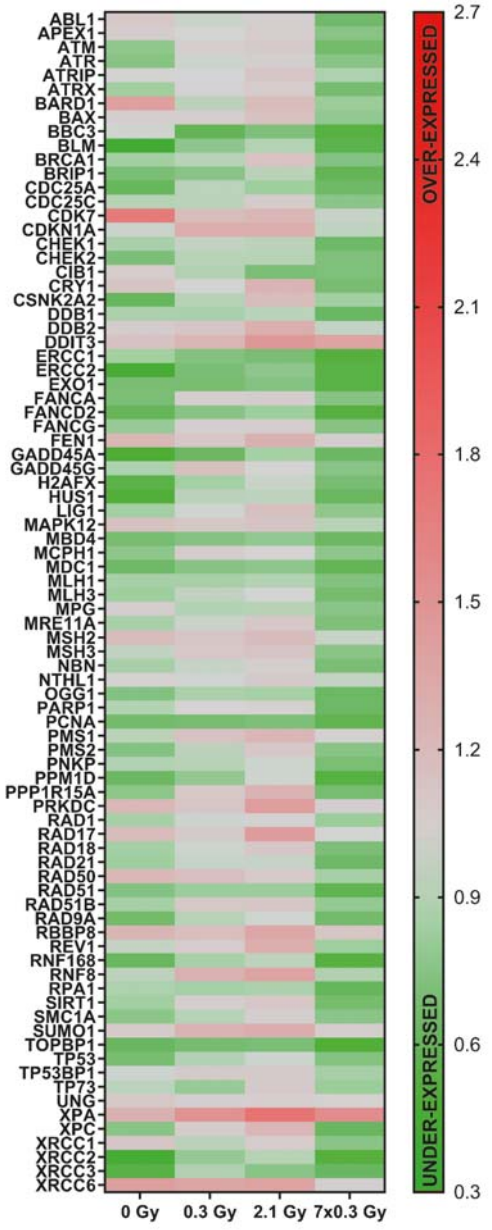

FIGURE 8. Heat maps of DNA damage signalling gene expression in radioresistant FaDu-RR cells relative to the gene expression in parental FaDu cells. The magnitude of the fold change in gene expression of each gene from three independent experiments is represented by colour. Green indicates under-expressed genes, and red indicates over-expressed genes.

GADD45A was over-expressed in 2.1 Gy and 7x0.3 Gy irradiated FaDu-RR cells, while *ATM*, *MSH3*, *NBN*, and *RAD18* were over-expressed in 0.3 Gy irradiated FaDu-RR cells only.

Direct comparison of the DNA damage gene expression in radioresistant FaDu-RR relative to parental FaDu cells identified differences in gene expression profile in non-irradiated cells and 7x0.3 Gy irradiated cells, but not 0.3 Gy and 2.1 Gy irradiated cells (Figure 8). Specifically, 71% of the tested DNA damage signalling genes in the control non-irradiated FaDu-RR cells were under-expressed, of which 7 genes (*BLM*, *ERCC2*, *H2AFX*, *HUS1*, *RNF168*, *TOPBP1*, *XRCC3*) were significantly under-expressed (Figure 9A). No significant difference in gene expression was observed in 0.3 Gy (Figure 9B) and 2.1 Gy (Figure 9C) irradiated FaDu-RR cells relative to FaDu cells. In 7x0.3 Gy irradiated FaDu-RR cells, 6 genes (*ERCC1*, *EXO1*, *MBD4*, *PCNA*, *PPM1D*, *TOPBP1*) were under-expressed and 1 gene (*XPA*) was over-expressed relative to parental FaDu cells irradiated with the same irradiation scheme (Figure 9D). TOPBP1 was the only gene under-expressed in both non-irradiated and PLDR-irradiated radioresistant FaDu cells relative to parental FaDu cells (Figure 10).

Discussion

Understanding molecular mechanisms of cellular response to low dose irradiation is important in order to evaluate risks and benefits of such exposure.[28] In radioresistant tumors this could provide the basis for a more tailored and effective radiotherapy. Re-irradiation of recurrent tumours in the previously irradiated areas is a feasible approach that improves survival, but is limited due to normal tissue toxicity.[19] However, altered fractionation regimen could improve the therapeutic outcome of re-irradiated tumours and reduce normal tissue toxicities.[14,15,29,30]

In this study, we confirmed the presence of LDHRS in the experimentally established radioresistant FaDu-RR cells *in vitro*, but not in its parental FaDu cells. Furthermore, radioresistant FaDu-RR cells were more sensitive to PLDR irradiation than parental FaDu cells, likely due to the observed perturbations of the cell cycle and changes in the expression of DNA damage signalling genes observed in these cells.

The use of PLDR irradiation in local recurrent HNSCC has been recently tested in a clinical trial in order to evaluate safety and treatment efficacy.[31–33] PLDR irradiation was initially proposed for the treatment of recurrent radioresistant gliomas.[13,16] It exploits two phenomena, LDHRS, and the inverse dose-rate effect. First, the low dose fractions used in this approach fall within the LDHRS region, generally observed in the more radioresistant tu-

mour cells.[3,8] Second, the short intervals between low dose pulses create an apparently reduced dose-rate, which contributes to the normal tissue sparing and results in increased radiosensitivity of tumour cells.[11] PLDR irradiation can be delivered over multiple days to increase the total irradiation dose, and improve the antitumor effects compared to conventional fractionation.[4]

LDHRS has to be confirmed prior to PLDR irradiation. Tailoring the PLDR parameters, such as the low dose and time intervals between the low doses, can further increase radiosensitivity.[34] Low dose pulses should be applied within the LDHRS range of specific cell type, however, this might not be straightforward. The transition dose from LDHRS to IRR is cell type-specific and has been observed in the range of 0.2 Gy to 0.6 Gy for different tumour cells.[1,2,9,10] In the clinics, this transition dose might differ between tumours as well as within the tumour due to tumour cell heterogeneity; identification of specific LDHRS markers is needed to select patients, which could benefit from PLDR irradiation. Deciphering mechanisms contributing to the LDHRS could provide a better starting point to determine the efficient low irradiation doses used for PLDR clinically. In our study, dose reduction from 0.3 Gy to 0.2 Gy abolished the difference in cell survival between PLDR and single-dose irradiation in parental FaDu and radioresistant FaDu-RR cells.

To describe the survival curve of LDHRS-positive cell lines, the linear-quadratic model fails in the low dose region and has to be adjusted to account for the increased radiosensitivity and IRR bellow 1 Gy. To take account for these specific processes, the induced repair model was proposed by Joiner et al.[35] In addition to the induced repair model, alternative models have been proposed[5,36,37], such as the variable induced repair, which is more complex, but does not account for the dose rate effect.[5] As a proof of LDHRS, different approaches can be considered. Namely, the condition $\alpha_S > \alpha_R$, confidence limits of α_S and α_R not overlapping, and D_C value significantly greater than zero can be used to deduce the presence of LDHRS.[4,5] Due to the variability in the measurements made by conventional clonogenic assay, which is typical at such high survival levels[35], the experimental data fit the induced repair model in a variable extent. Because LDHRS is prevalent in radioresistant tumour cell lines[3,8], we first evaluated the LDHRS status in the isogenic FaDu and radioresistant FaDu-RR cells, which was confirmed in the latter but not in the parental cell line. The observed transition from LDHRS to IRR in the 0.3 to 0.4 Gy dose range is similar to observations in other reports.[1,2,9,10] In this preliminary experiment, we focused on the low dose response and did not evaluate cell survival in response to doses above 1 Gy due to technical limitations of our X-ray unit. Fitting these experimental data to the induced repair model is not balanced due to the lack of high dose response, and the parameters describing LDHRS (α_S, α_R, and D_C) cannot be estimated with confidence intervals, which is a drawback of this study. In addition, the model-derived D_C and the experimental dose with the lowest survival are not always the same. Mathematically, D_C is defined as the dose required for 63% induction of radioresistance,[35] therefore variations are expected

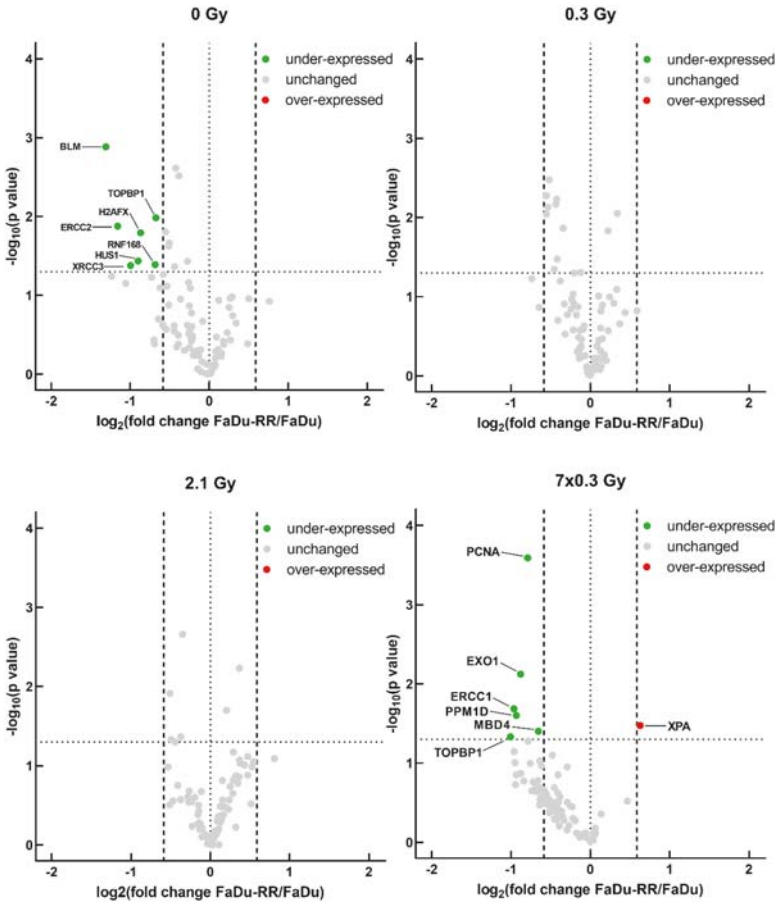

FIGURE 9. DNA damage signalling gene expression in radioresistant FaDu-RR cells relative to parental FaDu. **(A)** Gene expression in control non-irradiated cells. **(B)** Gene expression in 0.3 Gy irradiated cells. **(C)** Gene expression in 2.1 Gy irradiated cells. **(D)** Gene expression in 7x0.3 Gy irradiated cells. Volcano plots show the fold change in gene expression in radioresistant FaDu-RR relative to parental FaDu cells and statistical significance (p value). The horizontal line shows the statistical significance threshold (p value < 0.05). Two vertical dashed lines show the threshold of over-expressed (right) and under-expressed genes (left), while the solid vertical line shows no change in gene expression. Symbols represent the mean gene expression of each tested gene in radioresistant FaDu-RR cells relative to parental FaDu cells from three independent experiments.

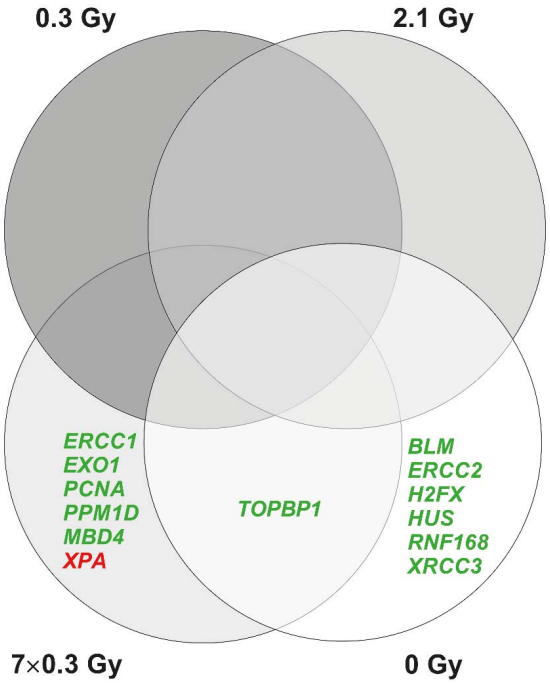

FIGURE 10. Venn diagrams of DNA damage signalling gene expression in radioresistant FaDu-RR cells showing overlapping and different gene expression after different irradiation protocols relative to parental FaDu cells. Only genes significantly over-expressed or under-expressed relative to parental FaDu cells are shown. Gene in bold red is over-expressed, genes in bold green are under-expressed.

between model-derived and experimentally observed transition points from increased radiosensitivity to increased radioresistance.[4]

LDHRS can be efficient, if the proposed pulsed irradiation scheme delivers pulses of smaller dose than the transition dose from LDHRS to IRR.[13] In our study, the PLDR irradiation scheme therefore consisted of a series of 0.3 Gy pulses. While surviving fraction of parental FaDu cells did not differ between single-dose and PLDR irradiation, a significantly lower survival was observed in PLDR-irradiated radioresistant FaDu-RR cells in comparison to single-dose irradiation. Similarly, several *in vivo* studies showed PLDR irradiation tumour volume reduction, resulting in a longer tumour growth delay in comparison to continuous irradiation.[14,15]

Ample scientific evidence supports an important role of cell cycle checkpoints and DNA damage signalling networks in the mechanisms of LDHRS.[2] Cellular repair processes are induced above a certain threshold dose as described by the induced repair model.[9] Below this threshold dose, cells can show increased radiosensitivity, while above this dose cell survival is increased due to induced signalling and repair. In the IRR range, DNA double-strand break (DSB) repair is reportedly more efficient than in the LDHRS dose range.[38] Evaluation of LDHRS in isogenic cell lines has not been studied extensively and therefore the isogenic cell lines with different LDHRS statuses are an attractive model to study the mechanisms of LDHRS in more detail. Novel insights into the unknown mechanisms of LDHRS could thus be gained.

DNA repair is tightly coordinated with the cell cycle checkpoints.[9] In our study, low dose irradiation did not affect cell cycle in isogenic cells, while irradiation with a higher single dose and PLDR irradiation resulted in cell cycle perturbations. Following G_2/M arrest 5 hours after single and PLDR irradiation in both FaDu and FaDu-RR cells, the cell cycle was restored 24 hours after irradiation in FaDu, but not in FaDu-RR cells. This indicates a differential regulation of the cell cycle in radioresistant FaDu-RR cells in comparison to parental cells. Differences in cell cycle checkpoints in LDHRS-positive and LDHRS-negative cells have been observed previously. Most notably, in LDHRS-positive cells G_2/M checkpoint was activated at irradiation doses higher than transition dose.[39] Because LDHRS is associated with the G_2-phase enriched populations[40], it is likely that the observed LDHRS is due to inactive G_2/M checkpoint in response to irradiation below the threshold dose.[39]

This data indicate on important role of DNA damage signalling mechanisms in LDHRS. Activation of G_2/M checkpoint in cells with damaged DNA prevents entry into mitosis and provides an opportunity for DNA repair during the cell cycle delay. Increased radiosensitivity, observed in the LDHRS-positive cells, could be associated with inactive DNA damage-induced cell cycle checkpoints. Functional DNA damage signalling and repair mechanisms constitute DNA damage recognition, recruitment of specific signalling and repair proteins to the damage site and effective repair. LDHRS is not associated with reduced recognition of DSB breaks as seen by the same extent of phosphorylated H2AX.[10,41] Persistent gammaH2AX foci after low dose irradiation despite the functional DNA repair mechanisms support different DSB repair kinetics.[39,41] The unchanged level of phosphorylated ATM in response to low dose irradiation indicates an inactive ATM signalling cascade.[38]

In the present study we focused on the expression of DNA damage signalling and repair genes in

isogenic cell lines with different LDHRS status. The gene panel included DNA repair, apoptosis and cell cycle-associated genes. In LDHRS-negative parental FaDu cells, under-expression of DNA damage signalling genes was observed, while over-expression of DNA damage signalling genes was observed in LDHRS-positive radioresistant cells in response to irradiation. Specifically, DNA damage sensor genes (*ATM*, *ATR*, and *H2AFX*), cell cycle checkpoint regulator genes (*CDC25A*, *BLM*, *GADD45A*, *MCPH1*) and genes involved in homologous recombination (*BLM*, *XRCC2*) were over-expressed in response to 0.3 Gy and 2.1 Gy irradiation. On the other hand, after PLDR irradiation the expression of DNA damage sensor genes and homologous recombination genes was not increased, indicating inactive DNA repair mechanisms and decreased cell survival after PLDR. The reduction in cell survival can be associated also with aberrant regulation of cell cycle checkpoints. The observed G_1 cell cycle arrest after 2.1 Gy and PLDR irradiation is likely mediated by over-expression of GADD45A in radioresistant FaDu-RR cells.[42] Inactivation of GADD45A was also associated with chemosensitization and radiosensitization.[43,44]

Exact mechanisms of PLDR irradiation contributing to reduced cell survival of radioresistant cells are not clear yet. The role of GADD45A in the observed G_1 cell cycle arrest should be further confirmed by RNA interference. Differential DNA damage signalling gene expression analysis demonstrated an early radiation-induced expression of various genes involved in the recognition of DNA damage, DNA repair and cell cycle regulation in radioresistant cells. However, after PLDR irradiation only 2 genes were over-expressed indicating inactive DNA damage response. To support the results of this preliminary study, the response to PLDR irradiation should be evaluated in other radioresistant and LDHRS-positive tumour cell lines. Furthermore, since PLDR irradiation is a promising approach for re-irradiation of previously irradiated tissues, *in vivo* analysis of the effects of PLDR irradiation would greatly contribute to the promotion of PLDR irradiation scheme in the clinical setting. However, *in vivo* studies using human HNSCC tumours are limited by the use of immunocompromised animals to enable engraftment of human xenografts. In addition, the antitumor effects of PLDR irradiation might differ from the effects of PLDR irradiation observed in the clinical settings, because immunostimulatory effects of low dose irradiation would be limited in immunocompromised animals.[45] Also, the role of tumour microenvironment should be taken into account, as cell-cell and cell-microenvironment interactions importantly contribute to the radiosensitivity of cells.[46]

Modifications of irradiation schemes to improve the therapeutic index in the clinical management is an emerging approach for the treatment of HPV-positive oropharyngeal tumors.[47–50] Considering the prevalence of LDHRS in radioresistant cells and tumours, PLDR irradiation could be more effective in radioresistant tumours than conventional radiotherapy. Modifications of irradiation schemes to reduce the effective dose rate and increase daily treatment time, such as PLDR irradiation, allow safer retreatment of previously irradiated areas, including recurrent radioresistant tumours of different origin.[6,16,17] In this respect, by using PLDR irradiation, a normal tissue damage could be minimised, and tumour control elevated.[51] Benefits of PLDR irradiation, such as less normal tissue damage, were confirmed in *in vivo* studies of human orthotopic xenografts in nude mice.[14,15]

A limit of the PLDR irradiation is the prolonged radiation delivery of one fraction composed of several pulses, which would lead to a larger burden of medical facilities. Although enhanced cytotoxic effects were observed with shorter intervals of several minutes between low dose fractions, it is possible to introduce variations in time intervals between consecutive doses, dose per fraction and dose rate.[34] Reduced cell survival can be observed also when low doses are separated by intervals of several hours, and additional benefit can be observed when combining this approach with chemotherapy.[52–55]

In this study, we demonstrated LDHRS in isogenic radioresistant cells, but not in the parental cells. Cell survival of LDHRS-positive radioresistant cells after PLDR was significantly reduced in comparison to parental cells. This reduction in cell survival of LDHRS-positive radioresistant cells was associated with variations in DNA damage signalling gene expression observed in response to PLDR. Variations in the DNA damage signalling response could be further exploited for the development of combined treatment approaches to radiosensitizing recurrent and radioresistant HNSCC to improve the therapeutic index.

Acknowledgements

Authors would like to acknowledge Ilija Vojvodic for his help with setting up X-ray unit for low

dose irradiations. This work was supported by the Slovenian Research Agency (program no. P3-0003 and P3-0307).

References

1. Joiner MC, Marples B, Lambin P, Short SC, Turesson I. Low-dose hypersensitivity: Current status and possible mechanisms. *Int J Radiat Oncol Biol Phys* 2001; **49:** 379-89. doi: 10.1016/S0360-3016(00)01471-1
2. Dai X, Tao D, Wu H, Cheng J. Low dose hyper-radiosensitivity in human lung cancer cell line A549 and its possible mechanisms. *J Huazhong Univ Sci Technolog Med Sci* 2009; **29:** 101-6. doi: 10.1007/s11596-009-0122-4
3. Martin LM, Marples B, Lynch TH, Hollywood D, Marignol L. Exposure to low dose ionising radiation: Molecular and clinical consequences. *Cancer Lett* 2014; **349:** 98-106. doi: 10.1016/j.canlet.2013.12.015
4. Schoenherr D, Krueger SA, Martin L, Marignol L, Wilson GD, Marples B. Determining if low dose hyper-radiosensitivity (HRS) can be exploited to provide a therapeutic advantage: A cell line study in four glioblastoma multiforme (GBM) cell lines. *Int J Radiat Biol* 2013; **89:** 1009-16. doi: 10.3109/09553002.2013.825061
5. Guirado D, Aranda M, Ortiz M, Mesa J a, Zamora LI, Amaya E, et al. Low-dose radiation hyper-radiosensitivity in multicellular tumour spheroids. *Br J Radiol* 2012; **85:** 1398-406. doi: 10.1259/bjr/33201506
6. Harney J, Short SC, Shah N, Joiner M, Saunders MI. Low dose hyper-radiosensitivity in metastatic tumors. *Int J Radiat Oncol Biol Phys* 2004; **59:** 1190-5. doi: 10.1016/j.ijrobp.2003.12.029
7. Wouters BG, Sy AM, Skarsgard LD. Low-dose hypersensitivity and increased radioresistance in a panel of human tumor cell lines with different radiosensitivity. *Radiat Res* 1996; **146:** 399-413. doi: 10.2307/3579302
8. Joiner MC, Lambin P, Malaise EP, Robson T, Arrand JE, Skov K a., et al. Hypersensitivity to very-low single radiation doses: Its relationship to the adaptive response and induced radioresistance. *Mutat Res* 1996; **358:** 171-83. doi: 10.1016/S0027-5107(96)00118-2
9. Marples B, Collis SJ. Low-dose hyper-radiosensitivity: past, present, and future. *Int J Radiat Oncol Biol Phys* 2008; **70:** 1310-8. doi: 10.1016/j.ijrobp.2007.11.071
10. Wykes SM, Piasentin E, Joiner MC, Wilson GD, Marples B. Low-dose hyper-radiosensitivity is not caused by a failure to recognize DNA double-strand breaks. *Radiat Res* 2006; **165:** 516-24. doi: 10.1667/RR3553.1
11. Mitchell CR, Folkard M, Joiner MC. Effects of exposure to low-dose-rate 60 Co gamma rays on human tumor cells in vitro. *Radiat Res* 2006; **158:** 311-8. doi: 10.1667/0033-7587(2002)158[0311:eoetld]2.0.co;2
12. Matsuya Y, McMahon SJ, Tsutsumi K, Sasaki K, Okuyama G, Yoshii Y, et al. Investigation of dose-rate effects and cell-cycle distribution under protracted exposure to ionizing radiation for various dose-rates. *Sci Rep* 2018; **8:** 1-14. doi: 10.1038/s41598-018-26556-5
13. Tomé W a., Howard SP. On the possible increase in local tumour control probability for gliomas exhibiting low dose hyper-radiosensitivity using a pulsed schedule. *Br J Radiol* 2007; **80:** 32-7. doi: 10.1259/bjr/15764945
14. Dilworth JT, Krueger S a., Dabjan M, Grills IS, Torma J, Wilson GD, et al. Pulsed low-dose irradiation of orthotopic glioblastoma multiforme (GBM) in a pre-clinical model: Effects on vascularization and tumor control. *Radiother Oncol* 2013; **108:** 149-54. doi: 10.1016/j.radonc.2013.05.022
15. Park SS, Chunta JL, Robertson JM, Martinez AA, Oliver Wong CY, Amin M, et al. MicroPET/CT imaging of an orthotopic model of human glioblastoma multiforme and evaluation of pulsed low-dose irradiation. *Int J Radiat Oncol Biol Phys* 2011; **80:** 885-92. doi: 10.1016/j.ijrobp.2011.01.045
16. Adkison JB, Tomé W, Seo S, Richards GM, Robins HI, Rassmussen K, et al. Reirradiation of large-volume recurrent glioma with pulsed reduced-dose-rate radiotherapy. *Int J Radiat Oncol Biol Phys* 2011; **79:** 835-41. doi: 10.1016/j.ijrobp.2009.11.058
17. Richards GM, Tomé WA, Robins HI, Stewart JA, Welsh JS, Mahler PA, et al. Pulsed reduced dose-rate radiotherapy: A novel locoregional retreatment strategy for breast cancer recurrence in the previously irradiated chest wall, axilla, or supraclavicular region. *Breast Cancer Res Treat* 2009; **114:** 307-13. doi: 10.1007/s10549-008-9995-3
18. Chan JL, Lee SW, Fraass BA, Normolle DP, Greenberg HS, Junck LR, et al. Survival and failure patterns of high-grade gliomas after three-dimensional conformal radiotherapy. *J Clin Oncol* 2002; **20:** 1635-42. doi: 10.1016/s0169-5002(97)90162-8
19. Strojan P, Corry J, Eisbruch A, Vermorken JB, Mendenhall WM, Lee AWM, et al. Recurrent and second primary squamous cell carcinoma of the head and neck: when and how to reirradiate. *Head Neck* 2015; **37:** 134-50. doi: 10.1002/hed.23542
20. Blanchard P, Baujat B, Holostenco V, Bourredjem A, Baey C, Bourhis J, et al. Meta-analysis of chemotherapy in head and neck cancer (MACH-NC): A comprehensive analysis by tumour site. *Radiother Oncol* 2011; **100:** 33-40. doi: 10.1016/j.radonc.2011.05.036
21. Boehringer-Wyss N, Clarkson SG, Allal AS. No benefits of ultrafractionation in two head-and-neck cancer cell lines with different inherent radiosensitivity. *Int J Radiat Oncol Biol Phys* 2002; **52:** 1099-103. doi: 10.1016/S0360-3016(01)02793-6
22. Marples B. Is low-dose hyper-radiosensitivity a measure of G2-phase cell radiosensitivity? *Cancer Metastasis Rev* 2004; **23:** 197-207. doi: 10.1023/B:CANC.0000031761.61361.2a
23. Leonard BE. Thresholds and transitions for activation of cellular radioprotective mechanisms - Correlations between HRS/IRR and the "inverse" dose-rate effect. *Int J Radiat Biol* 2007; **83:** 479-89. doi: 10.1080/09553000701370902
24. Matt S, Hofmann TG. The DNA damage-induced cell death response: a roadmap to kill cancer cells. *Cell Mol Life Sci* 2016; **73:** 2829-50. doi: 10.1007/s00018-016-2130-4
25. Pavlopoulou A, Bagos PG, Koutsandrea V, Georgakilas AG. Molecular determinants of radiosensitivity in normal and tumor tissue: A bioinformatic approach. *Cancer Lett* 2017; **403:** 37-47. doi: 10.1016/j.canlet.2017.05.023
26. Todorovic V, Prevc A, Zakelj MN, Savarin M, Brozic A, Groselj B, et al. Mechanisms of different response to ionizing irradiation in isogenic head and neck cancer cell lines. *Radiat Oncol* 2019; **14:** 1-20. doi: 10.1186/s13014-019-1418-6
27. Livak KJ, Schmittgen TD. Analysis of relative gene expression data using real-time quantitative PCR and the 2(-Delta Delta C(T)) Method. *Methods* 2001; **25:** 402-8. doi: 10.1006/meth.2001.1262
28. Piotrowski I, Kulcenty K, Suchorska WM, Skrobała A, Skórska M, Kruszyna-Mochalska M, et al. Carcinogenesis induced by low-dose radiation. *Radiol Oncol* 2017; **51:** 369-77. doi: 10.1515/raon-2017-0044
29. Lacas B, Bourhis J, Overgaard J, Zhang Q, Grégoire V, Nankivell M, et al. Role of radiotherapy fractionation in head and neck cancers (MARCH): an updated meta-analysis. *Lancet Oncol* 2017; **18:** 1221-37. doi: 10.1016/S1470-2045(17)30458-8
30. Shuryak I, Hall EJ, Brenner DJ. Optimized hypofractionation can markedly improve tumor control and decrease late effects for head and neck cancer. *Int J Radiat Oncol Biol Phys* 2019; **104:** 272-8. doi: 10.1016/j.ijrobp.2019.02.025
31. Li J, Zhao Z, Du G, Dai T, Zhen X, Cai H, et al. Safety and efficacy of pulsed low-dose rate radiotherapy for local recurrent esophageal squamous cell carcinoma after radiotherapy. *Medicine (Baltimore)* 2019; **98:** 1-5. doi: 10.1097/md.0000000000016176
32. Burr AR, Robins HI, Bayliss RA, Howard SP. Pulsed reduced dose rate for reirradiation of recurrent breast cancer. *Pract Radiat Oncol* 2020; **10:** e61-70.; doi: 10.1016/j.prro.2019.09.004
33. Lee CT, Dong Y, Li T, Freedman S, Anaokar J, Galloway TJ, et al. Local control and toxicity of external beam reirradiation with a pulsed low-dose-rate technique. *Int J Radiat Oncol Biol Phys* 2018; **100:** 959-64. doi: 10.1016/j.ijrobp.2017.12.012
34. Terashima S, Hosokawa Y, Tsuruga E, Mariya Y, Nakamura T. Impact of time interval and dose rate on cell survival following low-dose fractionated exposures. *J Radiat Res* 2017; **58:** 782-90. doi: 10.1093/jrr/rrx025
35. Marples B, Joiner MC. The response of chinese hamster V79 cells to low radiation doses: evidence of enhanced sensitivity of the whole cell population. *Radiat Res* 1993; **133:** 41-51. doi: 10.2307/3578255
36. Madas BG, Drozsdik EJ. Computational modeling of low dose hyper-radiosensitivity and induced radioresistance applying the principle of minimum mutation load. *Radiat Prot Dosimetry* 2019; **183:** 147-50. doi: 10.1093/rpd/ncy227

37. Contreras C, Carrero G, de Vries G. A mathematical model for the effect of low-dose radiation on the G2/M transition. *Bull Math Biol* 2019; **81:** 3998-4021. doi: 10.1007/s11538-019-00645-6

38. Enns L, Rasouli-Nia A, Hendzel M, Marples B, Weinfeld M. Association of ATM activation and DNA repair with induced radioresistance after low-dose irradiation. *Radiat Prot Dosimetry* 2015; **166:** 131-6. doi: 10.1093/rpd/ncv203

39. Krueger S a., Wilson GD, Piasentin E, Joiner MC, Marples B. The effects of G2-phase enrichment and checkpoint abrogation on low-dose hyper-radiosensitivity. *Int J Radiat Oncol Biol Phys* 2010; **77:** 1509-17. doi: 10.1016/j.ijrobp.2010.01.028

40. Krueger S a., Collis SJ, Joiner MC, Wilson GD, Marples B. Transition in survival from low-dose hyper-radiosensitivity to increased radioresistance is independent of activation of ATM SER1981 activity. *Int J Radiat Oncol Biol Phys* 2007; **69:** 1262-71. doi: 10.1016/j.ijrobp.2007.08.012

41. Osipov AN, Pustovalova M, Grekhova A, Eremin P, Vorobyova N, Pulin A, et al. Low doses of X-rays induce prolonged and ATM-independent persistence of γH2AX foci in human gingival mesenchymal stem cells. *Oncotarget* 2015; **6:** 27275-87. doi: 10.18632/oncotarget.4739

42. Kleinsimon S, Longmuss E, Rolff J, Jäger S, Eggert A, Delebinski C, et al. GADD45A and CDKN1A are involved in apoptosis and cell cycle modulatory effects of viscumTT with further inactivation of the STAT3 pathway. *Sci Rep* 2018; **8:** 1-14. doi: 10.1038/s41598-018-24075-x

43. Yang C, Hill R, Lu X, Van Dyke T, Yin C, Hollander MC, et al. Inactivation of gadd45a sensitizes epithelial cancer cells to ionizing radiation in vivo resulting in prolonged survival. *Cancer Res* 2008; **68:** 3579-83. doi: 10.1158/0008-5472.can-07-5533

44. Liu J, Jiang G, Mao P, Zhang J, Zhang L, Liu L, et al. Down-regulation of GADD45A enhances chemosensitivity in melanoma. *Sci Rep* 2018; **8:** 4111. doi: 10.1038/s41598-018-22484-6

45. Janiak MK, Wincenciak M, Cheda A, Nowosielska EM, Calabrese EJ. Cancer immunotherapy: how low-level ionizing radiation can play a key role. *Cancer Immunol Immunother* 2017; **66:** 819-32. doi: 10.1007/s00262-017-1993-z

46. Chandna S, Dwarakanath BS, Khaitan D, Mathew TL, Jain V. Low-dose radiation hypersensitivity in human tumor cell lines: effects of cell-cell contact and nutritional deprivation. *Radiat Res* 2002; **157:** 516-25. doi: 10.1667/0033-7587(2002)157[0516:ldrhih]2.0.co;2

47. Prevc A, Niksic Zakelj M, Kranjc S, Cemazar M, Scancar J, Kosjek T, et al. Electrochemotherapy with cisplatin or bleomycin in head and neck squamous cell carcinoma: Improved effectiveness of cisplatin in HPV-positive tumors. *Bioelectrochemistry* 2018; **123:** 248-54. doi: 10.1016/j.bioelechem.2018.06.004

48. Wu C-C, Horowitz DP, Deutsch I, Rahmati R, Schecter JM, Saqi A, et al. De-escalation of radiation dose for human papillomavirus-positive oropharyngeal head and neck squamous cell carcinoma: A case report and preclinical and clinical literature review. *Oncol Lett* 2016; **11:** 141-9. doi: 10.3892/ol.2015.3836

49. Wierzbicka M, Szyfter K, Milecki P, Składowski K, Ramlau R. The rationale for HPV-related oropharyngeal cancer de-escalation treatment strategies. *Contemp Oncol* 2015; **19:** 313-22. doi: 10.5114/wo.2015.54389

50. Kimple RJ, Harari PM. Is radiation dose reduction the right answer for HPV-positive head and neck cancer? *Oral Oncol* 2014; **50:** 560-4. doi: 10.1016/j.oraloncology.2013.09.015

51. Meyer JE, Finnberg NK, Chen L, Cvetkovic D, Wang B, Zhou L, et al. Tissue TGF-β expression following conventional radiotherapy and pulsed low-dose-rate radiation. *Cell Cycle* 2017; **16:** 1171-4. doi: 10.1080/15384101.2017.1317418

52. Short SC, Kelly J, Mayes CR, Woodcock M, Joiner MC. Low-dose hypersensitivity after fractionated low-dose irradiation in vitro. *Int J Radiat Biol* 2001; **77:** 655-64. doi: 10.1080/09553000110041326

53. Gupta S, Koru-Sengul T, Arnold SM, Devi GR, Mohiuddin M, Ahmed MM. Low-dose fractionated radiation potentiates the effects of cisplatin independent of the hyper-radiation sensitivity in human lung cancer cells. *Mol Cancer Ther* 2011; **10:** 292-302. doi: 10.1158/1535-7163.MCT-10-0630

54. Chendil D, Oakes R, Alcock RA, Patel N, Mayhew C, Mohiuddin M, et al. Low dose fractionated radiation enhances the radiosensitization effect of paclitaxel in colorectal tumor cells with mutant p53. *Cancer* 2000; **89:** 1893-900. doi: 10.1002/1097-0142(20001101)89:9<1893::AID-CNCR4>3.3.CO;2-2

55. Spring PM, Arnold SM, Shajahan S, Brown B, Dey S, Lele SM, et al. Low dose fractionated radiation potentiates the effects of taxotere in nude mice xenografts of squamous cell carcinoma of head and neck. *Cell Cycle* 2004; **3:** 477-83. doi: 10.4161/cc.3.4.786

research article

The prevalence of occult ovarian cancer in the series of 155 consequently operated high risk asymptomatic patients – Slovenian population based study

Andreja Gornjec[1], Sebastijan Merlo[1], Srdjan Novakovic[2], Vida Stegel[2], Barbara Gazic[3], Andraz Perhavec[4], Ana Blatnik[5], Mateja Krajc[5]

[1] Department for Gynaecological Oncology, Institute of Oncology Ljubljana, Ljubljana, Slovenia
[2] Molecular Diagnostics Department, Institute of Oncology Ljubljana, Ljubljana, Slovenia
[3] Pathology Department, Institute of Oncology Ljubljana, Ljubljana, Slovenia
[4] Department for Surgical Oncology, Institute of Oncology Ljubljana, Ljubljana, Slovenia
[5] Cancer Genetics Clinic, Institute of Oncology Ljubljana, Ljubljana, Slovenia

Radiol Oncol 2020; 54(2): 180-186.

Received 11 December 2019
Accepted 22 March 2020

Correspondence to: Assist. Prof. Mateja Krajc, M.D., Ph.D., Cancer Genetics Clinic, Institute of Oncology Ljubljana, Zaloška cesta 2, SI-1000 Ljubljana, Slovenia. E-mail: mkrajc@onko-i.si

Disclosure: No potential conflicts of interest were disclosed.

Background. We assessed the prevalence, localization, type and outcome of occult cancer at risk-reducing salpingo-oophorectomy or salpingectomy (RRSO) in asymptomatic carriers of pathogenic or likely pathogenic *BRCA1/2* variants and high-risk *BRCA1/2* negative women.

Patients and methods. A retrospective analysis of all consecutive gynaecologic preventive surgeries from January 2009 to December 2015 was performed. Participants underwent genetic counselling and *BRCA1/2* testing before the procedure. Data on clinical parameters, adjuvant treatment and follow-up were collected and analysed.

Results. One hundred and fifty-five RRSO were performed in 110 *BRCA1*, 35 *BRCA2* carriers of pathogenic or likely pathogenic variants and 10 high-risk *BRCA1/2* negative women, at the mean age of 48.3 years. Nine occult cancers (9/155, 5.8%) were identified; eight in *BRCA1* positive women and one in high-risk *BRCA1/2* negative woman. We identified four non-invasive serous intraepithelial tubal carcinomas (3 in *BRCA1* carriers and 1 in a high-risk *BRCA1/2* negative woman) and five invasive tubo-ovarian high grade serous cancers (all detected in *BRCA1* carriers). Only one out of nine patients (11.1%) with occult cancer had a slightly elevated CA-125 value preoperatively.

Conclusions. A 5.8% prevalence of occult invasive and noninvasive tubo-ovarian serous cancer after RRSO was found in high risk asymptomatic and screen negative women. We conclude that RRSO should be performed in *BRCA1/2* carriers and in high-risk *BRCA1/2* negative women. Age of preventive gynaecologic surgery should be carefully planned, taking into account the completion of childbearing age and type of mutation. The results favour the tubal hypothesis of tubal origin of high grade serous ovarian and peritoneal cancer. Cytology result of peritoneal cavity washing was important for the decision making process in determining treatment. Cytology examination should be performed in all cases of RRSO. CA-125 assay did not prove to be an effective screening tool for early cancer detection in our patients.

Key words: risk-reducing salpingo-oophorectomy (RRSO); occult serous cancer; serous tubal intraepithelial cancer (STIC); *BRCA1/2* pathogenic or likely pathogenic variant

Introduction

Worldwide, ovarian cancer is the seventh most common cancer and the eighth cause of death from cancer in women.[1] According to the Slovenian cancer registry, the median age at the time of diagnosis for ovarian cancer patients is 62 years.[2] Epithelial ovarian cancer (EOC), being the commonest, is thought to be hereditary in at least 10% of cases, mostly due to *BRCA1* or *BRCA2* germline pathogenic or likely pathogenic variants. Ovarian cancer risk in *BRCA* carriers ranges from 36%–53% in *BRCA1* and 11%–25% in *BRCA2* carriers by the age of 80 years, compared to 1–2% in the general population.[3] In addition, it presents at a younger age than in patients without a genetic predisposition. Genetic counselling, testing and appropriate screening and preventive strategies can highly reduce the risk.[3-6]

In more than 70%, EOC is diagnosed in advanced stages (III/IV). This is mainly due to vague and non-specific symptoms, and because of an ineffective ovarian cancer screening. *BRCA* carriers are therefore recommended to undergo salpingo-oophorectomy or salpingectomy as a risk-reducing strategy for ovarian cancer.[3,7,8] A new paradigm of high grade pelvic serous cancer carcinogenesis puts fallopian tubes as an anatomic origin of the primary lesion. Salpingectomy with delayed oophorectomy might therefore be offered to *BRCA* carriers younger than 40 (after given informed consent in a research setting) who have completed their reproduction.[9,10]

So far, no precancerous lesions, like intraepithelial carcinoma, have ever been found in the ovaries. Precancerous lesions were found only in fallopian tubes. The first report of precancerous lesions in fallopian tubes after risk-reducing salpingo-oophorectomy (RRSO) was as a non-invasive serous tubal intraepithelial carcinoma (STIC).[11,12] Occult ovarian and tubal cancers where also found in specimens of *BRCA* carriers after RRSO. Occult cancers have been reported to occur between 2% and 17% and STICs between 3% and 12%, respectively.[13-22] The occult cancer detection is probably influenced by the age at RRSO, gynaecological screening prior to RRSO, extent of the surgical removal of specimens and the accuracy of tubal pathohistological assessment. It is known that the protocol for sectioning and extensively examining the fimbriated end of the Fallopian tube (SEE-FIM) enables a more exact histopathological examination of the distal tube with its fimbrial part.[23]

Ovarian cancer risk reduction after RRSO is reported to be between 80%–96%. The risk of primary peritoneal cancer after RRSO is between 1%–4%.[24,25] Recurrence rate of ovarian cancer after the diagnosis of an occult invasive carcinoma at RRSO is relatively high (16%–47%), despite predominantly early stage, and small volume disease.[17,25] On the other hand, the STICs rarely recur as carcinoma (5.8%–9%), and therefore chemotherapy may not be needed.[24,26] Recommendations about the optimal treatment of STICs lesions remain unclear. Opinions for treatment of STIC lean toward staging procedures and observations, if no other lesions are found.

Our study aimed to assess the prevalence, localization, type and outcome of occult cancer at RRSO in asymptomatic carriers of pathogenic or likely pathogenic *BRCA1/2* variants and high-risk *BRCA1/2* negative women.

Patients and methods

All consecutively operated women (asymptomatic carriers of pathogenic or likely pathogenic *BRCA1/2* variants and high-risk *BRCA1/2* negative) who underwent RRSO or salpingectomy from January 2009 to December 2015 at the Institute of Oncology Ljubljana, Slovenia, were included in our study.

From 1999 genetic counselling and testing is offered at the Institute for women with positive family history of ovarian and breast cancer. Women with confirmed *BRCA* pathogenic or likely pathogenic variants and *BRCA* negative women with high ovarian cancer risk (at least two first or second-degree relatives with ovarian cancer) are assessed in a multidisciplinary setting by an onco–genetic team. In accordance with the guidelines high risk women are advised to perform risk reducing procedures (RRSO).[7,8,27] Until 2014, RRSO was offered only after women turned 40 years of age. From 2014 tubectomy with delayed oophorectomy is offered in a research setting to women younger than 40 years who have completed their reproduction.

Clinical data were retrospectively collected from women with occult ovarian/tube/peritoneal cancer or non-invasive high-grade serous intraepithelial tube carcinoma diagnosed at the time of RRSO. Collected data included age at RRSO, mutation status, type of mutation, preoperative cancer antigen 125 (CA-125) level, histopathology result, staging, treatment (surgery and adjuvant chemotherapy),

recurrence rate, prior history or development of breast cancer after RRSO, disease status and vital status. Asymptomatic women with negative ovarian cancer screening test (normal CA-125 and gynaecological ultrasound) 6 months prior to RRSO were included. Patients with ovarian or tubal cancer diagnosis prior to RRSO and those whose RRSO was a part of breast cancer treatment were excluded from the analysis.

All RRSOs had the same surgical and pathological protocol. During surgery, before the salpingo-oophorectomy took place, peritoneal washing was performed and the material was sent for cytological examination. If there was no free fluid in the *cavum Douglasi*, we eluted the pelvis with 10 mL of physiologic solution and the material was sent for cytological examination. At our institution SEEFIM protocol is used for RRSO specimens.[23] When occult cancer and STIC are diagnosed, staging procedure is offered. After staging procedure is performed, cancers are managed according to the national guidelines.[7] In women with STIC, when no other lesion is found at staging procedure, only observation with regular follow up is offered. When malignant cells are found at cytological examination of peritoneal cavity washing with no other lesion at staging procedure, chemotherapy with carboplatin and paclitaxel is offered.

The start of follow-up after RRSO was defined as the date of RRSO, where no other treatment was required. After cancer treatment with chemotherapy, the start of follow-up was defined as the date of the last given chemotherapy. The end of follow-up was defined as the last outpatient visit at our institution.

The study was approved by the Ethical Committee of the Institute of Oncology Ljubljana (Number ERID–EK/15).

Statistics

Statistical analysis was performed using SPSS 22.0 for Windows. Descriptive statistics was used to describe the basic features of the data in the study. Differences between the groups were investigated with Student-t test. P-values <0.05 were considered to be statistically significant.

Results

In the period of our study (January 2009 – December 2015), 155 women underwent RRSO due to high ovarian cancer risk.

Characteristic of patients and RRSO procedures

In our cohort, there were 110/155 (71.0%) *BRCA1* mutation carriers, 35/155 (22.6%) *BRCA2* mutation carriers and 10/155 (6.5%) high-risk *BRCA* negative patients. A variant of uncertain significance (VUS) was detected in 4/10 high risk *BRCA* negative women.

Mean age at RRSO among our patients was 48.3 (29–72); 47.6 (29–72) for *BRCA1* carriers and 49.1 (38–66) for *BRCA2* carriers, the difference did not differ significantly (p = 0.4). In high-risk *BRCA* negative women mean age at RRSO was 52.2 (36–64) years. Median age at RRSO was also assessed for further comparison with other studies and accounted 47 years.

Before RRSO was performed, 110/155 (71.0%) women had already been diagnosed with breast cancer, 4/155 (2.6%) women had the first breast cancer diagnosis before and the second breast cancer diagnosis after RRSO and 1/155 (0.6%) woman was diagnosed with breast cancer after RRSO.

Among women where RRSO was performed, the mean age at breast cancer diagnosis was 54.0 (33–64) among women with STIC and 49.3 (38–61) among women with invasive cancer. The mean age of breast cancer diagnosis in *BRCA1* carriers was 42.0 (27–62) in *BRCA2* carriers 43.7 (26–57), which was not significantly different. In *BRCA* negative women it was 42.7 (26–64) years.

Of all the RRSO procedures (N = 155), there were 141 (91.0%) bilateral laparoscopic salpingo–oophorectomies, 5 (3.2%) unilateral laparoscopic salpingo-oophorectomies and 7 (4.5%) laparoscopic salpingectomies. One patient (0.6%) had a bilateral and one had (0.6%) a unilateral laparoscopic salpingo-oophorectomy.

Pathological findings at RRSO

Non-invasive or invasive serous high-grade cancer was diagnosed in 9 out of 155 (5.8%) operated women (Table 1). There were five (3.2%) occult ovarian cancers and 4 (2.6%) STICs. All cancers were detected among *BRCA1* positive women as described in Table 1. Among STICs there were three *BRCA1* carriers and one without a known mutation, but from the high risk group.

Among patients with occult invasive cancers, two were 39 years of age, all the other were older, mean age being 50.4 years. Mean age of patients with STICs was 57.8 years. The difference was not

TABLE 1. Clinical characteristics of occult findings after RRSO

Patient Number	Age at RRSO (years)	Occult finding	*BRCA* gene involved	Type of pathogenic variant	FIGO STAGE	Cytology	Treatment	Vital status
1	53	STIC	*BRCA1*	deletion exons 4–9	STIC	NEG	Surgery	NED
2	69	STIC	*BRCA1*	c.3018_3021delTTCA	STIC	NEG	Surgery	NED
3	64	STIC	negative/high risk		STIC	NEG	Surgery	NED
4	45	STIC	BRCA1	deletion exons 4–9	(Staging procedure NEG) I C	PC	Surgery+ACT	NED
5	56	HGSC	*BRCA1*	c.181T>G	III B	PC	Surgery+ACT	DOOD
6	39	HGSC	*BRCA1*	c.5266dup.C	III B	PC	Surgery+ACT	OT
7	57	HGSC	*BRCA1*	c.5266dup.C	I C	PC	Surgery+ACT	NED
8	39	HGSC	*BRCA1*	c.1687C>T	III A	PC	Surgery+ACT	NED
9	61	HGSC	*BRCA1*	deletion exons 4–9	III A	PC	Surgery+ACT	OT

ACT = adjuvant chemotherapy; DOOD = died of other disease; FIGO = International Federation of Gynecology and Obstetrics; HGSC = high grade serous cancer; NED = no evidence of disease; NEG = negative; OT = on treatment; PC = peritoneal carcinomatosis; RRSO = risk reducing oophorectomy; STIC = serous intraepithelial tubal cancer

statistically significant. There were no occult cancers diagnosed among *BRCA2* carriers.

Stages of cancer

Three of four women with STIC underwent surgical staging procedure (Table 1). In three cases with STIC, staging procedure did not find any additional neoplastic cells and observation with no adjuvant treatment was recommended. In one case, the malignant cells were detected in the peritoneal cavity by cytological examination only. Stage was assessed to be I C. This patient received adjuvant chemotherapy with paclitaxel and carboplatin.

Among patients with occult cancers, one was assessed as stage I C, two as stage III A and two as stage III B. All received the adjuvant treatment with six courses of paclitaxel and carboplatin (Table 1).

Localisation of findings

Two STICs were found at the fimbrial part of fallopian tube and in the other two STICs, fallopian tube only was reported as a localisation. In invasive cancer patients, cancer cells were found in (i) two cases at the fimbrial part of the Fallopian tube and in one ovary, (ii) in one case the disease was present in both ovaries and in both Fallopian tubes, (iii) in one case cancer cells were present on the surface of both ovaries with normal Fallopian tubes and, (iv) in one case cancer cells were present on the surface of one ovary and in the Fallopian tube. Pathohistological findings included one patient with focally atypical epithelium of the fallopian tube with the addition of transitional cell metaplasia, one patient with adenomatoid hyperplasia with bilateral proliferation of Sertoli cells in both hiluses of ovaries that represented embryonal remnants and one patient with transitional cell metaplasia.

CA-125 and cytology results

All except one patient with STIC had a negative cytology result; on the other hand, all occult cancers had positive cytological findings.

Before the RRSO CA-125 measurement was performed in 83.9% of women. It was negative in all occult cancers and STICs except in one occult cancer, where it was slightly elevated, being 48 kU/L (normal value being ≤ 35 kU/L). When considering CA-125 specificity in premenopausal years and normal vaginal ultrasound, patient was considered screen negative.

Follow-up time of women with occult invasive and non-invasive cancer

In our study the follow-up period was 23 to 73 months. Until December 2018 one woman with occult cancer died of gastric cancer which was diagnosed after adjuvant treatment for ovarian cancer. Two out of nine (22.2%) are being treated for their third recurrence of disease, the rest (6/9, 66.7%) are alive with no signs of disease. Mean follow-up of patients with occult invasive and non-invasive ovarian cancer was 29 months (15–51). After RRSO, no woman developed peritoneal cancer.

Discussion

We are presenting a population based study which aimed to address the prevalence, localization, type and outcome of occult cancer at RRSO in asymptomatic carriers of pathogenic or likely pathogenic BRCA1/2 variants and high-risk BRCA1/2 negative women.

Our main outcome was the detection of pathologic serous changes in tubes and ovaries in 5.8% of all operated women.

At RRSO we found occult serous cancer in 5.5% of *BRCA* carriers, with 3.4% (5/145) having high-grade cancers and 2.1% (3/145) STICs; all were found in *BRCA1* positive women. The prevalence of occult cancers in *BRCA1* positive women in our study was 7.3% (8/110). According to the available literature, the prevalence of occult cancer found after RRSO varies from 2% to 17%.[13-22,28] In our study, the prevalence of occult cancer in *BRCA1/2* positive women was 5.5%, which is similar to what Conner *et al*. have found.[29] We detected fewer occult cancers than Powell *et al*. who reported a rate of 7.9% and more than Reitsma *et al*. (2.2%) and Finch *et al.* (4.2%).[14,16,24] It would be expected that studies that reported lower prevalence of occult cancers also had a lower median age at RRSO. Reitsma *et al*. reported the median age at RRSO to be 44 years of age, which is less than in our study where the median age at RRSO was 47.[14] Since only asymptomatic women and screen negative women were included, the age at RRSO seems to be the most important factor which determines the higher prevalence of pathologic findings. When considering *BRCA1/2* carriers, all pathological changes in our study were detected among the *BRCA1* positive patients. In contrast, there were no pathological changes in 35 *BRCA2* positive women. The speculative reason for this might be lower ovarian cancer penetrance and the later age of onset in *BRCA2* carriers in comparison with *BRCA1* carriers and therefore critical number of cases for one case to be found was probably not achieved until the end of this evaluation.

Among high-risk *BRCA* negative women, the prevalence of occult serous disease was 10% (1/10). Limited data is available for the comparison of prevalence of occult cancers after RRSO in *BRCA* negative women. Only Reitsma's study from Netherlands found one (1/57) case of STIC and one (1/57) case of atypical hyperplasia in RRSO specimens of *BRCA*-negative women with VUS.[14] Our finding suggests the benefit and the importance of preventive surgeries in these women as well, though the number of our patients was very small.

An interesting and counterintuitive finding is the comparison of mean age among invasive and noninvasive cancers found at RRSO. Surprisingly, women diagnosed with STIC were older than women diagnosed with cancer. Mean age was 57.8 (45–69) and 50.4 (39–61) years, respectively. The difference was not statistically significant, most probably due to relatively small sample size. Furthermore, there was also insignificant trend of noninvasive cancer patients having breast cancer at an older age than those with invasive cancer. Similar findings were mentioned also in study from Powell *et al*.[16]

The localization of occult serous pelvic disease was coherent with the literature. Occult cancers were found in the tubal epithelium in 60% (3/5) and only in 40% (2/5) in the ovaries. In two cases the ovary was infiltrated only on the surface epithelium, in all other cases the cortex and stroma were also infiltrated. Intraepithelial serous lesions were found only in the tubal epithelium. In 50% (2/4) of cases, STICs were found at the fimbrial part of tubes. In other two cases exact localization was not defined and is being revised.[17]

International Federation of Gynaecology and Obstetrics (FIGO) stage distribution among occult cancers diagnosed after RRSO was undoubtedly different and much more favourable than among population that presents with symptoms. There were 55.6% (4/9) of cancers staged I, II or *in situ*. There were no cancers staged higher than III B, two were III B and two were III A. The long term outcome is therefore expectedly better among patients diagnosed with ovarian/fallopian/peritoneal cancer after RRSO.

Cytological examination of peritoneal cavity washing was found to be very important. When all pathologic findings are negative, positive cytology finding is the only one that may determine further treatment. Women with positive cytology with all other specimens being negative are advised systemic chemotherapy based on cytology findings.[26]

Screening for ovarian cancer in the general population with CA-125 (and possibly transvaginal ultrasound) is generally not recommended due to its low sensitivity and specificity. It is, however, seen as a reasonable temporary alternative for women at high risk, who wish to delay RRSO.[30] In our study, only one patient with an occult cancer had serum CA-125 levels above the cut-off value. CA-125 assay did not prove to be an effective screening tool for early cancer detection in our patients.

Genotype-phenotype correlations in BRCA carriers are not well defined and it is therefore difficult

to estimate the exact risk of ovarian cancer associated with specific pathogenic variants.[31] The mutational spectrum in patients with occult carcinoma in our study is in line with what is otherwise known about Slovenian *BRCA* carriers. Three of the detected variants are very common in Slovenian *BRCA1* carriers, i.e. c.181T>G p.(Cys61Ser), c.1687C>T p.(Gln563*) and c.5266dupC p.(Gln1756Profs*74).[32] In contrast, the deletion of exons 4–9 is only seen in 3.4% of our *BRCA* positive families but appears to be associated with a particularly high ovarian cancer risk. In this study, three out of eight (37.5%) *BRCA* positive patients with occult cancer carried this variant, which further supports the hypothesis that deletion 4–9 is highly penetrant with regards to ovarian cancer.

The main limitation of our study is already mentioned relatively small sample size that limits statistical evaluation. On the other hand, we were able to obtain an accurate clinical data for the sample studied. All studied women were tested and operated in our centre, where genetic testing and preventive follow up is performed on a national level.

Conclusions

In conclusion, a 5.8% prevalence of occult invasive and noninvasive serous cancer after RRSO was found in high risk asymptomatic and screen negative *BRCA1/2* carriers. Most of occult invasive and noninvasive serous cancers were detected in *BRCA1* positive patients, yet the RRSO should also be considered as a preventive method for *BRCA* negative high risk women. Age at preventive gynaecologic surgery should be carefully considered, taking into account the completion of childbearing age, and ideally, performed soon after 35, at least in *BRCA1* patients. Cytology examination of peritoneal cavity washing should be performed in all cases of RRSO. And finally, our results favour the hypothesis of tubal origin of high-grade serous ovarian and peritoneal cancer.

References

1. Ferlay J, Colombet M, Soerjomataram I, Mathers C, Parkin DM, Piñeros M, et al. Estimating the global cancer incidence and mortality in 2018: GLOBOCAN sources and methods. *Int J Cancer* 2019; **144:**1941-53. doi: 10.1002/ijc.31937
2. Zadnik V, Primic Zakelj M, Lokar K, Jarm K, Ivanus U, Zagar T. Cancer burden in Slovenia with the time trends analysis. *Radiol Oncol* 2017; **51:** 47-55. doi: 10.1515/raon-2017-0008
3. Kuchenbaecker KB, Hopper JL, Barnes DR, Phillips KA, Mooij TM, Roos-Blom MJ, et al. Risks of breast, ovarian, and contralateral breast cancer for BRCA1 and BRCA2 mutation carriers. *JAMA* 2017; **317:** 2402-16. doi: 10.1001/jama.2017.7112
4. Mavaddat N, Peock S, Frost D, Ellis S, Platte R, Fineberg E, et al. Cancer risks for BRCA1 and BRCA2 mutation carriers: results from prospective analysis of EMBRACE. *J Natl Cancer Inst* 2013; **105:** 812-22. doi: 10.1093/jnci/djt095
5. Antoniou A, Pharoah PDP, Narod S, Risch HA, Eyfjord JE, Hopper JL, et al. Average risks of breast and ovarian cancer associated with BRCA1 or BRCA2 mutations detected in case series unselected for family history: a combined analysis of 22 studies. *Am J Hum Genet* 2003; **72:** 1117-30. doi: 10.1086/375033
6. Kotsopoulos J, Gronwald J, Karlan B, Rosen B, Huzarski T, Moller P, at al. Age-specific ovarian cancer risks among women with a BRCA1 or BRCA2 mutation. *Gynecol Oncol* 2018; **150:** 85-91. doi: 10.1016/j.ygyno.2018.05.011
7. *Guidelines for assessment of ovarian cancer patients*. [Slovenian]. Ljubljana: Institute of Oncology Ljubljana; 2016. [cites 2019 Nov 13]. Available from: https://www.onko-i.si/dejavnosti/zdravstvena-dejavnost/priporocila-in-klinicne-poti/priporocila
8. *Guidelines for diagnosis and treatment of breast cancer.* [cites 2019 Nov 14]. Ljubljana: Institute of Oncology Ljubljana; 2018. Available from: https://www.onko-i.si/fileadmin/onko/datoteke/Smernice/Smernice_diagnostike_in_zdravljenja_raka_dojk_2018.pdf
9. Levanon K, Crum C, Drapkin R. New insights into the pathogenesis of serous ovarian cancer and its clinical impact. *J Clin Oncol* 2008; **26:** 5284-93. doi: 10.1200/JCO.2008.18.1107
10. Nebgen DR, Hurteau J, Holman LL, Bradford A, Munsell MF, Soletsky BR, et al. Bilateral salpingectomy with delayed oophorectomy for ovarian cancer risk reduction: a pilot study in women with BRCA1/2 mutations. *Gynecol Oncol* 2018; **150:** 79-84. doi: 10.1016/j.ygyno.2018.04.564
11. Leeper K, Garcia R, Swisher E, Goff B, Greer B, Paley P. Pathologic findings in prophylactic oophorectomy specimens in high-risk women. *Gynecol Oncol* 2002; **87:** 52-6. doi: 10.1006/gyno.2002.6779
12. Callahan MJ, Crum CP, Medeiros F, Kindelberger DW, Elvin JA, Garber JE, et al. Primary fallopian tube malignancies in BRCA-positive women undergoing surgery for ovarian cancer risk reduction. *J Clin Oncol* 2007; **25:** 3985-90. doi: 10.1200/JCO.2007.12.2622
13. Evans DG, Clayton R, Donnai P, Shenton A, Lalloo F. Risk-reducing surgery for ovarian cancer: outcomes and 300 surgeries suggest a low peritoneal primary risk. *Eur J Hum Genet* 2009; **17:** 1381-5. doi: 10.1038/ejhg.2009.60
14. Reitsma W, De Bock GH, Oosterwijk JC, Bart J, Hollema H, Mourits MJE. Support of the "fallopian tube hypothesis" in a prospective series of risk-reducing salpingo-oophorectomy specimens. *Eur J Cancer* 2013; **49:** 132-41. doi: 10.1016/j.ejca.2012.07.021
15. Manchanda R, Abdelraheim A, Johnson M, Rosenthal AN, Benjamin E, Brunell C, et al. Outcome of risk-reducing salpingo-oophorectomy in BRCA carriers and women of unknown mutation status. *BJOG An Int J Obstet Gynaecol* 2011; **118:** 814-24. doi: 10.1111/j.1471-0528.2011.02920
16. Powell CB, Swisher EM, Cass I, McLennan J, Norquist B, Garcia RL, et al. Long term follow up of BRCA1 and BRCA2 mutation carriers with unsuspected neoplasia identified at risk reducing salpingo-oophorectomy. *Gynecol Oncol* 2013; **129:** 364-71. doi.: org/10.1016/j.ygyno.2013.01.029
17. Sherman ME, Piedmonte M, Mai PL, Ioffe OB, Ronnett BM, Van Le L, et al. Pathologic findings at risk-reducing salpingo-oophorectomy: Primary results from Gynecologic Oncology Group trial GOG-0199. *J Clin Oncol* 2014; **32:** 3275-83. doi: 10.1200/JCO.2013.54.1987
18. Thompson C, McCormick C, Kamran W, O'Riain C, Norris L, Gallagher D, et al. Risk reduction surgery (RRS) for tubo-ovarian cancer in an Irish gynaecological practice: an analysis of indications and outcomes. *Ir J Med Sci* 2018; **187:** 789-94. doi: 10.1007/s11845-017-1717-6
19. Ricciardi E, Tomao F, Aletti G, Bazzurini L, Bocciolone L, Boveri S, et al. Risk-reducing salpingo-oophorectomy in women at higher risk of ovarian and breast cancer: a single institution prospective series. *Anticancer Res* 2017; **37:** 5241-48. doi: 10.21873/anticanres.11948
20. Blok F, Dasgupta S, Dinjens WNM, Roes EM, van Beekhuizen HJ, Ewing-Graham PC. Retrospective study of a 16 year cohort of BRCA1 and BRCA2 carriers presenting for RRSO: Prevalence of invasive and in-situ carcinoma, with follow-up. *Gynecol Oncol* 2019; **153:** 326-34. doi: 10.1016/j.ygyno.2019.03.003

21. Zakhour M, Danovitch Y, Lester J, Rimel BJ, Walsh CS, Li AJ, Karlan BY, Cass I. Occult and subsequent cancer incidence following risk-reducing surgery in BRCA mutation carriers. *Gynecol Oncol* 2016; **143:** 231-35. doi: 10.1016/j.ygyno.2016.08.336

22. Giannos A, Stavrou S, Douskos A, Drakakis P, Loutradis D. A salpingeal carcinoma revealed after prophylactic salpingoophorectomy in an asymptomatic BRCA1 carrier with breast malignancy. *Int J Surg Case Rep* 2018; **52:** 107-10. doi: 10.1016/j.ijscr.2018.10.014

23. Clarke BA, Crum CP, Nucci, MR, Oliva MR. Protocol for the examination of specimens from patients with carcinoma of the fallopian tube. Based on AJCC/UICC TNM, 7th edition, and FIGO 2006 Annual Report. [cites 2019 Nov 15]. Available from: http://webapps.cap.org/apps/docs/committees/cancer/cancer_protocols/2013/FallopianTube_13protocol_3101.pdf

24. Finch APM, Lubinski J, Møller P, Singer CF, Karlan B, Senter L, et al. Impact of oophorectomy on cancer incidence and mortality in women with a BRCA1 or BRCA2 mutation. *J Clin Oncol* 2014; **32:** 1547-53. doi: 10.1200/JCO.2013.53.2820

25. Domchek SM, Friebel TM, Singer CF, Evans DG, Henry T, Isaacs C, et al. Europe PMC funders group association of risk-reducing surgery in BRCA1 or BRCA2 mutation carriers with cancer risk and mortality. *JAMA* 2010; **304:** 967-75. doi: 10.1001/jama.2010.1237

26. Patrono MG, Corzo C, Iniesta M, Ramirez PT. Management of preinvasive lesions. *Clin Obstet Gynecol* 2017; **60:** 771-9. doi: 10.1097/GRF.0000000000000316

27. Genetic/Familial High-Risk Assessment: Breast and Ovarian, version 3.2019, NCCN Guidelines, January 18, 2019. [cites 2019 Nov 15]. Available from: https://www.nccn.org/professionals/physician_gls/default.aspx#detection

28. Lavie O, Moskoviz MG, Auslender R, Gemer O, Bitterman A, Younes G, et al. Clinical and pathological characteristics of incidental diagnostic early occult malignancy after risk-reducing salpingo-oophorectomy in BRCA mutation carriers. *Int J Gynecol Cancer* 2016; **26:** 233-9. doi: 10.1097/IGC.0000000000000624

29. Conner JR, Meserve E, Pizer E, Garber J, Roh M, Urban N, et al. Outcome of unexpected adnexal neoplasia discovered during risk reduction salpingo-oophorectomy in women with germ-line BRCA1 or BRCA2 mutations. *Gynecol Oncol* 2014; **132:** 280-6. doi: 10.1016/j.ygyno.2013.12.009

30. Drescher CW, Anderson GL. The yet unrealized promise of ovarian cancer screening. *JAMA Oncol* 2018; **4:** 456-7. doi: 10.1001/jamaoncol.2018.0028

31. Rebbeck TR, Mitra N, Wan F, Sinilnikova OM, Healey S, McGuffog L, et al. Association of type and location of BRCA1 and BRCA2 mutations with risk of breast and ovarian cancer. *JAMA* 2015; **313:** 1347-61. doi: 10.1001/jama.2014.5985

32. Stegel V, Krajc M, Zgajnar J, Teugels E, De Grève J, Hočevar M, et al. The occurrence of germline BRCA1 and BRCA2 sequence alterations in Slovenian population. *BMC Med Genet* 2011; **12:** 9. doi: 10.1186/1471-2350-12-9

research article

Dietary iodine intake, therapy with radioiodine, and anaplastic thyroid carcinoma

Nikola Besic[1],Barbara Gazic[2]

[1] Department of Surgical Oncology, Institute of Oncology Ljubljana, Slovenia
[2] Department of Pathology, Institute of Oncology Ljubljana, Slovenia

Radiol Oncol 2020; 54(2): 187-193.

Received 16 November 2019
Accepted 30 March 2020

Correspondence to: Prof. Nikola Bešić, M.D., Ph.D., Department of Surgical Oncology, Institute of Oncology Ljubljana, Zaloška 2, 1000 Ljubljana, Slovenia. E-mail: nbesic@onko-i.si

Disclosure: No potential conflicts of interest were disclosed.

Background. Anaplastic thyroid cancer (ATC) is one of the most aggressive tumors. The aim of the study was to determine the correlation between a higher dietary intake of iodine, frequency of ATC and the characteristics of ATC, and to find out how often patients with ATC had a history of radioiodine (RAI) therapy.

Patients and methods. This retrospective study included 220 patients (152 females, 68 males; mean age 68 years) with ATC who were treated in our country from 1972 to 2017. The salt was iodinated with 10 mg of potassium iodide/kg before 1999, and with 25 mg of potassium iodide/kg thereafter. The patients were assorted into 15-year periods: 1972–1986, 1987–2001, and 2002–2017.

Results. The incidence of ATC decreased after a higher iodination of salt ($p = 0.04$). Patients are nowadays older ($p = 0.013$) and have less frequent lymph node metastases ($p = 0.012$). The frequency of distant metastases did not change over time. The median survival of patients in the first, second, and third periods was 3, 4, and 3 months, respectively ($p < 0.05$). The history of RAI therapy was present in 7.7% of patients.

Conclusions. The number of patients with a history of RAI therapy did not change statistically over time. The incidence of ATC in Slovenia decreased probably because of higher salt iodination.

Key words: anaplastic thyroid carcinoma; iodination of salt; treatment, survival

Introduction

Anaplastic thyroid cancer (ATC) is one of the most aggressive tumors known in humans.[1] It is a locally widely invasive disease which progresses despite treatment and finally results in metastatic disease in the majority of patients.[2] Fortunately, ATC is a rare disease and the estimated annual incidence is about two per million of the population.[3,4] In the USA and Japan, ATC represents less than 2% of thyroid carcinomas.[5,6] On the other hand, the incidence of ATC has been stable in the last decades.[1,7]

In the literature, there are only limited data about the history of radioiodine (RAI) therapy in patients with ATC. The aim of the study was to find out how often patients had a history of RAI therapy. In one of our recent studies we compared the incidence of ATC during the periods when the intake of potassium iodide in salt was 10 and 25 mg/kg in the Republic of Slovenia.[8] It was observed that the incidence of ATC decreased with a higher iodination of salt in Slovenia.[8] Another aim of the study was to determine the correlation between a higher dietary intake of iodine, frequency of ATC and the characteristics of ATC.

Patients and methods

The data on the patients with ATC treated at the Institute of Oncology in Ljubljana in the years 1972–2017 were collected retrospectively. During this period, there were 220 patients (152 females, 68 males; median age 69 years; mean age 68 years) with ATC. The Cancer Registry of Republic of Slovenia is one of the oldest population-based

cancer registries in Europe.[9] It was founded in 1950 at the Institute of Oncology in Ljubljana as a special service for collecting and processing data on cancer incidence and cancer patients' survival. Notification of cancer has been compulsory in Slovenia since the foundation of the Registry and prescribed by law.[9] The main sources of data are notifications of cancer, gathered from all hospitals and diagnostic centers in Slovenia.[9] Furthermore, all the patients with thyroid cancer are treated at the Institute of Oncology in Ljubljana, so our data represent a population based study.

For each patient, the data on sex, age, history of treatment with radioiodine, clinical and tumor characteristics, and duration of survival were collected. Distant metastases were diagnosed by clinical examination and additional diagnostic procedures, including lung and/or bone X-ray, radionuclide investigations, ultrasonography, computed tomography, and/or nuclear magnetic resonance imaging. Data about the treatment of our patients have already been reported.[10,11]

The Protocol Review Board and Ethics Committee of the Institute of Oncology on 12th December 2018 (ERID-KSOPKR/43, OIRIKE 00448) reviewed and approved the study, which was conducted in accordance with the ethical standards prescribed in the Declaration of Helsinki. For retrospective studies, informed consent is not necessary according to the national regulations. The need for consent was waived by the Institutional Review Board and Ethics Committee of the Institute of Oncology Ljubljana.

All cases were reviewed by pathologists and cytopathologists at our comprehensive cancer center, experienced in thyroid pathology. Histological specimens were retrieved by surgical removal of the thyroid tumor, surgical biopsy, or autopsy, whereas cytological samples were obtained by fine-needle aspiration biopsy of the primary tumor or its metastases. The diagnosis of ATC was confirmed by both histology and cytology in 75 patients, by cytology alone in 97 patients, and by histology alone in 48 patients.

In Slovenia, salt was iodinated with 10 mg of potassium iodide/kg and 25 mg of potassium iodide/kg during the periods 1972–1998 and 1999–2017, respectively.[12,13] All salt that was on the market in Slovenia during the first and the second 15-year periods had the required content of iodine. Slovenia has been considered to be an area with an adequate iodine supply since 1999.[12,13] Since 2004, when Slovenia became a member of the European Union, salt with a lower content of iodine and Himalayan salt with no iodine added at all have also been available in health food stores. Furthermore, in the last decade, the use of prefabricated or frozen food became more popular in Slovenia. Fortunately, almost all households in Slovenia use salt with 25 mg of potassium iodide/kg, which is evident from epidemiological studies in schoolchildren.[12,14]

For the purposes of the present study, patients were assorted into one of three 15-year periods according to the year of diagnosis of ATC: 1972–1986, 1987–2001, and 2002–2017. The frequency of ATC during these three periods and the characteristics of the patients during these periods were compared.

The characteristics of the patients and tumors and the history of RAI therapy according to 15-year periods were statistically analyzed using contingency tables and analysis of variance. SPSS 16.0 for Windows (SPSS, Chicago, IL) was also used in Kaplan–Meier univariate analysis for the assessment of patients' survival.

Results

The incidence of ATC in Slovenia has decreased. ATC was diagnosed in the periods 1972–1987, 1988–2003, and 2004-2017 in 95, 87, and 38 patients, respectively ($p = 0.04$). The mean incidence of ATC in the periods 1972–1986, 1987–2001, and 2002–2017 was 6.3 (range 2–12), 5.8 (range 3-10), and 2.5 (range 1–10) patients per year, respectively.

The characteristics of patients and their outcomes according to 15-year periods are presented in Table 1. Patients with ATC are older now than they used to be ($p = 0.013$). During the periods 1972–1986, 1987–2001, and 2002–2017, the patients' mean age was 66 (SD ±11.8) years, 69 (SD ±8.4) years, and 72 (SD ±11.8) years. The mean tumor diameter in the three time periods was 9.1 cm, 9.9 cm, and 8.5 cm respectively. The difference was not statistically significant ($p = 0.26$). However, a tumor diameter larger than 10 cm was more frequent in patients during the 1972–2001 periods than thereafter ($p < 0.05$). Lymph node metastases were less commonly diagnosed in the last period ($p = 0.012$). However, the frequency of distant metastases did not change over time ($p = 0.65$). The median survival of patients during the first, second, and third 15-year periods was 3 months, 4 months, and 3 months, respectively ($p < 0.05$).

Cumulative yearly doses of ^{131}I applied in medicine from 1994 to 2017 in Slovenia are presented in Figure 1. Altogether, 17/220 (7.7%) of patients had a

TABLE 1. Clinical characteristics of patients and 15-year periods

Clinical characteristic	Subgroup	All patients N = 220 Number	Patients 1972–1986 N=95 Number	Patients 1987–2001 N = 87 Number	Patients 2002-2017 N = 38 Number	p-value
Gender	Male	68	27	29	12	0.77
	Female	152	68	58	26	
Age	70 years or less	124	59	49	16	0.11
	71 years or more	96	36	38	22	
History of radioiodine therapy	No	203	89	83	31	0.023
	Yes	17	6	4	7	
Previous thyroid enlargement (> 1 year)	No or no data	110	46	49	26	0.036
	Yes	110	49	38	12	
General condition	Good	92	47	33	12	0.13
	Moderate	58	25	20	13	
	Poor	70	23	34	13	
Tumor growth	≥ 3 months	173	70	72	31	0.29
	< 3 months	47	25	15	7	
Local tumor extension	Extrathyroid	199	87	78	34	0.88
	Intrathyroid	21	8	9	4	
Tumor size	< 5 cm	35	20	12	3	0.043
	5–10 cm	105	40	39	26	
	≥ 10 cm	80	35	36	9	
Tumor volume (width² x length)/2	< 50 ml	16	7	5	4	0.68
	50–99 ml	37	19	14	4	
	100–149 ml	22	6	12	4	
	150–199 ml	18	9	7	2	
	200 ml or more	127	54	49	24	
Lymph nodes metastases	No	127	45	54	28	0.012
	Yes	93	50	33	10	
Distant metastases	No	113	46	48	19	0.65
	Yes	107	49	39	19	
Presentation of anaplastic carcinoma	Incidental	8	4	4	0	0.50
	Evident	212	91	83	38	
TNM stage	IVA	17	5	9	3	0.73
	IVB	96	41	39	16	
	IVC	107	49	39	19	
Thyroid surgery	Without surgery	130	48	52	30	0.029
	Biopsy	23	13	10	0	
	Subtotal thyroidectomy	13	10	3	0	
	Extracapsular lobectomy with isthmusectomy	17	9	7	1	
	Total or near-total thyroidectomy	37	15	15	7	
Residual tumor after surgery	Biopsy or no surgery	153	61	62	30	0.55
	R0	32	18	10	4	
	R1	18	9	6	3	
	R2	17	7	9	1	
Lymph node dissection	No	211	90	83	38	0.36
	Yes	9	5	4	0	
External beam irradiation	No	37	22	11	4	0.087
	Yes	183	73	76	36	
External beam irradiation	Without or ≤ 20 Gy	54	33	15	6	0.001
	> 20 Gy and 45 Gy	74	41	26	7	
	> 45 Gy	92	21	46	25	
Chemotherapy	No	81	38	24	19	0.04
	Yes	139	57	63	19	
Death because of anaplastic carcinoma	No (alive, other causes, lost from follow-up)	13	3	7	13	0.32
	Yes	207	92	80	25	

TABLE 2. Clinical characteristics of the patients and the history of radioiodine therapy

Clinical characteristic	Subgroup	All patients N = 220	Without history of RAI therapy N = 203	With history of RAI therapy N = 17	p-value
Gender	Male	68	66	2	0.10
	Female	152	137	15	
Age	70 years or less	124	114	10	1.00
	71 years or more	96	89	7	
Year of diagnosis	1972–1986	95	89	6	0.023
	1987–2001	87	83	4	
	2002–2017	38	31	7	
Previous thyroid enlargement (> 1 year)	No or no data	110	108	2	0.001
	Yes	110	95	15	
General condition	Good	92	85	7	0.063
	Moderate	58	57	1	
	Poor	70	61	9	
Tumor growth	≥ 3 months	173	157	16	0.13
	< 3 months	47	16	1	
Local tumor extension	Extrathyroid	199	183	16	1.00
	Intrathyroid	21	20	1	
Tumor size	< 5 cm	35	34	1	0.50
	5–10 cm	105	96	9	
	≥ 10 cm	80	73	7	
Tumor volume (width^2 x length)/2	< 50 ml	16	16	0	0.19
	50–99 ml	37	36	1	
	100–149 ml	22	20	2	
	150–199 ml	18	18	0	
	200 ml or more	127	113	14	
Lymph nodes metastases	No	127	117	10	1.00
	Yes	93	86	7	
Distant metastases	No	113	105	8	0.83
	Yes	107	98	9	
Presentation of anaplastic carcinoma	Incidental	8	8	0	0.51
	Evident	212	195	17	
TNM stage	IVA	17	16	1	0.91
	IVB	96	89	7	
	IVC	107	98	9	
Thyroid surgery	Without surgery	130	117	13	0.56
	Biopsy	23	22	1	
	Subtotal thyroidectomy	13	12	1	
	Extracapsular lobectomy with isthmusectomy	17	17	0	
	Total or near-total thyroidectomy	37	35	2	
Residual tumor after surgery	Biopsy or no surgery	153	139	14	0.32
	R0	32	32	0	
	R1	18	17	1	
	R2	17	15	2	
Lymph node dissection	No	211	194	17	1.00
	Yes	9	9	0	
External beam irradiation	No	37	30	7	0.005
	Yes	183	173	10	
Dose of radiotherapy	Without or ≤ 20 Gy	54	47	7	0.244
	> 20 Gy and ≤ 45 Gy	74	70	4	
	> 45 Gy	92	86	6	
Chemotherapy	No	81	75	6	1.00
	Yes	139	128	11	
Death because of ATC	No (alive, other causes, lost from follow up)	13	12	1	1.00
	Yes	207	191	16	

ATC = anaplastic thyroid cancer; RAI = radioiodine

history of radioiodine therapy from 4 months to 40 years before the diagnosis of ATC. The number of patients with ATC who had a history of RAI therapy did not change statistically over time, while the incidence of patients with ATC decreased over time ($p = 0.023$). Data about patients with regard to the history of RAI therapy are presented in Table 2. Previous enlargement of thyroid gland was more common in patients with a history of RAI therapy in comparison to those who received no RAI ($p < 0.001$). There was no difference in survival of patients with and without a history of RAI therapy ($p = 0.49$).

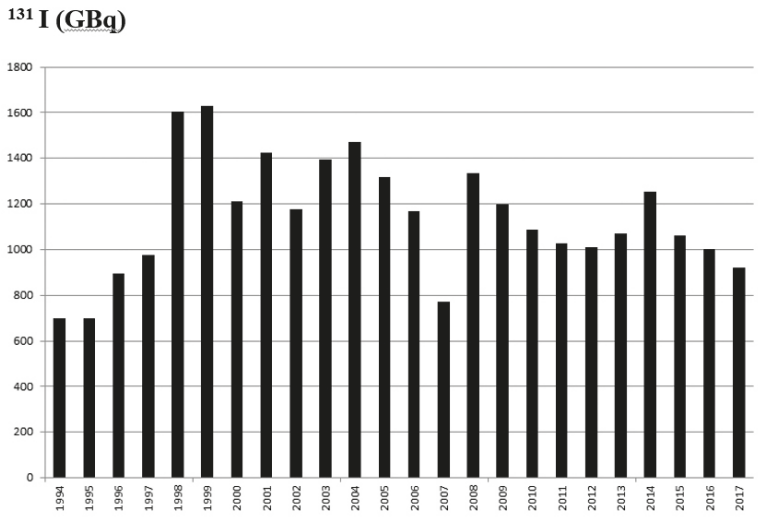

FIGURE 1. Cumulative yearly doses of ^{131}I applied in medicine from 1994 to 2017 in Slovenia.

Discussion

Salt was iodinated in Slovenia with 10 mg of potassium iodide/kg and 25 mg of potassium iodide/kg during the periods 1972–1998 and 1999–2017, respectively.[12,13] As expected and reported in other countries[15], ten years after the beginning of higher salt iodination in Slovenia, the incidence of diffuse goiter in adolescents and adults decreased.[12-14,16] Furthermore, from 1999 to 2009, the incidence of thyroid autonomy in Slovenia decreased from 32.7/100.000 to a 27 % lower value.[12] During the same time period, the baseline incidence of Graves' disease (27.8/100.000) did not change significantly.[12] On the other hand, the incidence of Hashimoto's thyroiditis (73.2/100.000 in 1999) gradually increased to levels more than twice as high as before.[12] During the same time period, the incidence of thyroid carcinoma increased from 5.1/100.000 to 7.25/100.000,[17] but the incidence of anaplastic carcinoma decreased after higher iodination of salt in Slovenia.[9] A similar observation about the incidence of ATC after higher salt iodination was reported in other endemic goiter regions, namely the Tyrol region in Austria and Argentina.[18,19]

In contrast to differentiated thyroid cancer, which often has a subtle clinical presentation and may be difficult to detect, ATC is correctly diagnosed in nearly all cases in countries with adequate health care because of rapid tumor growth and the clinical presentation.[9,20] Risk factors for ATC are: a history of goiter or a prior co-existing differentiated thyroid cancer[21-23], insufficient iodine in the diet[9,18,24,25], low level of education[21], type B blood group[21], and presence of TERT mutation in coexisting thyroid papillary carcinoma[26]. We think that the drop in ATC incidence in Slovenia was mainly caused by higher salt iodination. A lower rate of goiter in Slovenia, which was also due to higher iodination of salt, is another risk factor that contributed to a lower incidence of ATC in our country.[12,13] Other risk factors for ATC, namely the educational level of the population, the socioeconomic status of the general population, or the rate of persons with type B blood group, did not change over time in Slovenia.

RAI treatment for benign thyroid disease is considered to be a safe procedure.[27,28] A meta-analysis showed no increase in the overall cancer risk after RAI treatment for hyperthyroidism. However, there was a trend towards increased risk of thyroid, stomach, and kidney cancer.[27,28] In 1990, Venkatesh *et al*.[29] reported in a series of 121 cases with ATC that seven (6%) patients had received prior RAI treatment. Even 7.7% of patients from our present study also had a history of RAI therapy. A history of RAI therapy in patients with ATC is more frequent than the proportion of persons treated with RAI therapy in the Slovenian population. The use of ^{131}I increased in Slovenia in the 1990s and was at 1630.9 GBq in 1999. Thereafter, the use of ^{131}I has slowly been decreasing as seen in Figure 1. In 2011, a total of 531 diagnostic procedures with ^{131}I or ^{123}I for thyroid imaging with an accumulative effective dose of 2.29 manSv were done in Slovenia.[30] ^{131}I and ^{123}I were used in 48% and 52% of diagnostic procedures, which contributed to 69% and 31% of the collective effective dose for diagnostic procedures, respectively.[30] On the other hand, the therapy with ^{131}I was done in 512 patients with a benign disease and 151 patients with a carcinoma in 2014. The main difference between RAI therapy in benign thyroid disease and thyroid carcinoma is the dose

of RAI. In benign disease and thyroid carcinoma, 10–15 mCi (370–555 MBq)[28] and 50–200 mCi (1.8–7.4 GBq)[31] of RAI is used, respectively.

In 1982, Kapp *et al*.[32] reported that in two patients with a differentiated carcinoma, ATC occurred after irradiation. In one of them, the transformation to ATC occurred five years after 39.6 Gy of external beam irradiation, while in the other patient, ATC was diagnosed one year after 149 mCi of RAI. A component of differentiated thyroid carcinoma is usually identified in the primary ATC on histology examination.[22] But, the transformation of differentiated thyroid cancer to ATC may be found also in metastatic lymph nodes.[33] It was detected in two of five patients during initial surgery of primary tumor and regional lymph node dissection, while in three of five cases, the interval between treatment of differentiated carcinoma and occurrence of ATC was 46, 74, and 266 months after initial surgery. None of them had a history of RAI therapy, while one patient received external beam irradiation because of recurrent papillary carcinoma before the occurrence of ATC.[33]

In our patients, RAI therapy was applied from 4 months to 40 years before the diagnosis of ATC. For some patients with a very short interval between RAI therapy and the diagnosis of ATC, we could suspect that they already had a differentiated carcinoma and possibly a very small ATC which was not detected. Namely, in patients with Graves' disease without clinically evident nodes, a thyroid ultrasound investigation is not recommended according to the ATA Guidelines for diagnosis and management of hyperthyroidism and other causes of thyrotoxicosis.[28] Furthermore, the use of thyroid scintigraphy to preselect only the cold nodules for cytology is advocated by some authors.[34] However, there are at least eight case reports in the literature about patients with a follicular variant of papillary thyroid carcinoma as autonomous functioning thyroid nodule.[35] On the other hand, ATC was also reported in a long-standing multinodular goiter or a Hürthle cell tumor following RAI therapy.[36-38]

This study has some limitations. Because it is a retrospective analysis over a very long time period, we do not have reliable data about the reasons for RAI therapy in our patients. Furthermore, diagnostic radiological methods have changed dramatically over last decades. Modern precise imaging investigations have an impact on the detection of very small regional and/or distant metastases. The detection of small distant metastases possibly influences therapeutic decisions, which might explain why a lesser proportion of patients were treated with radical surgery during the last 15-year period in comparison to prior periods.

In the literature, data on how the patients' and tumors' characteristics in ATC have changed over time are very limited.[39] We observed that, nowadays, patients are older and have less frequent regional metastases in comparison to previous periods. However, the mean tumor diameter has not changed significantly over time, and ATC was inoperable because of infiltration to the surrounding structures at the time of diagnosis in the majority of our patients. Unfortunately, the frequency of distant metastases has not changed over time. Thus, in Slovenia, the survival of patients with ATC remains short. By contrast, in South Korea where an opportunistic screening is performed in the general population for thyroid carcinoma, the proportion of cases with a differentiated thyroid carcinoma and only anaplastic foci has increased over time, while that of evident ATC has decreased from 1985 to 2013.[39] As a consequence, the survival rate is significantly higher than it used to be. Obviously, in patients with a very early ATC, lymphatic invasion was the most significant postoperative prognosticator, so the choice of ATC treatment has to be modified based on resectability and the lymphatic invasion of cancer.[39]

Conclusions

A history of RAI therapy was present in 7.7% of patients with ATC, and the number of patients with a history of RAI therapy did not change over time. The incidence of ATC in Slovenia probably decreased because of higher salt iodination. Patients are nowadays older and have less frequent lymph node metastases than in the past. The frequency of distant metastases did not change over time. The median survival of patients remains short.

Acknowledgements

This research was funded by the Ministry of Education, Science and Sport of the Republic of Slovenia, grant number P3-0289.

References

1. Nikiforov YE, Seethala RR. Anaplastic (undifferentiated) carcinoma. In: Nikiforov YE, Biddinger PW, Thompson LDR, editors. *Diagnostic pathology and molecular genetics of the thyroid*, 2nd edition. Philadelphia: Lippincott Williams and Wilkins; 2012. p. 263-84.

2. Besic N, Gazic B. Sites of metastases of anaplastic thyroid carcinoma: autopsy findings in 45 cases from a single institution. *Thyroid* 2013; **23**: 709-73. doi: 10.1089/thy.2012.0252

3. Untch BR, Olson JA Jr.. Anaplastic thyroid carcinoma, thyroid lymphoma, and metastasis to thyroid. *Surg Oncol Clin N Am* 2006; **15**: 661-79. doi: 10.1016/j.soc.2006.05.006

4. Ain KB. Anaplastic thyroid carcinoma: a therapeutic challenge. *Semin Surg Oncol* 1999; **16**: 64-9. doi: 10.1002/(sici)1098-2388(199901/02)16:1<64::aid-ssu10>3.0.co;2-u

5. Ain KB. Anaplastic thyroid carcinoma: behavior, biology, and therapeutic approaches. *Thyroid* 1998; **8**: 715-26. doi: 10.1089/thy.1998.8.715

6. Sugitani I, Kasai N, Fujimoto Y, Yanagisawa A. Prognostic factors and therapeutic strategy for anaplastic carcinoma of the thyroid. *World J Surg* 2011; **25**: 617-622. doi: 10.1007/s002680020166

7. Hvilsom GB, Londero SC, Hahn CH, Schytte S, Pedersen HB, Christiansen P, et al. Anaplastic thyroid carcinoma in Denmark 1996-2012: a national prospective study of 219 patients. *Cancer Epidemiol* 2018; **53**: 65-71. doi: 10.1016/j.canep.2018.01.011

8. Besic N, Hocevar M, Zgajnar J. Lower incidence of anaplastic carcinoma after higher iodination of salt in Slovenia. *Thyroid* 2010; **20**: 623-6. doi: 10.1089/thy.2009.0404

9. Institute of Oncology Ljubljana. *Epidemiology and Cancer Registry.* Ljubljana: Institute of Oncology Ljubljana. [cited 2019 Aug 28]. Available at: https://www.onko-i.si/eng/sectors/epidemiology-and-cancer-registry.

10. Besic N, Auersperg M, Us-Krasovec M, Golouh, R, Frkovic-Grazio S, Vodnik A. Effect of primary treatment on survival in anaplastic thyroid carcinoma. *Eur J Surg Oncol* 2001; **27**: 260-4. doi: 10.1053/ejso.2000.1098

11. Besic N, Hocevar M, Zgajnar J, Pogacnik A, Grazio-Frkovic S, Auersperg M. Prognostic factors in anaplastic carcinoma of the thyroid-a multivariate survival analysis of 188 patients. *Langenbecks Arch Surg* 2005; **390**: 203-8. doi: 10.1007/s00423-004-0524-5

12. Zaletel K, Gaberscek S, Pirnat E. Ten-year follow-up of thyroid epidemiology in Slovenia after increase in salt iodization. *Croat Med J* 2011; **52**: 615-21. doi: 10.3325/cmj.2011.52.615

13. Gaberscek S, Zaletel K. Epidemiological trends of iodine-related thyroid disorders: an example from Slovenia. *Arh Hig Rada Toksikol* 2016; **67**: 93-8. doi: 10.1515/aiht-2016-67-2725

14. Kotnik P, Sirca Campa A, Zupancic M, Stimec M, Smole K, Mis NF, et al. Goiter prevalence and urinary iodine concentration in Slovenian adolescents. *Thyroid* 2006; **16**: 769-73. doi: 10.1089/thy.2006.16.769

15. Zimmermann MB, Boelaert K. Iodine deficiency and thyroid disorders. *Lancet Diabetes Endocrinol* 2015; **3**: 286-95. doi: 10.1016/S2213-8587(14)70225-6

16. Bajuk V, Zaletel K, Pirnat E, Hojker S, Gaberšček S. Effects of adequate iodine supply on the incidence of iodine-induced thyroid disorders in Slovenia. *Thyroid* 2017; **27**: 558-66. doi: 10.1089/thy.2016.0186

17. Zadnik V, Primic Zakelj M. *SLORA: Slovenia and cancer.* Ljubljana: Epidemiology and Cancer Registry. Institute of Oncology Ljubljana. [cited 2018 Oct 14]. Available at: www.slora.si

18. Bacher-Stier C, Riccabona G, Tötsch M, Kemmler G, Oberaigner W, Moncayo R. Incidence and clinical characteristics of thyroid carcinoma after iodine prophylaxis in an endemic goiter country. *Thyroid* 1997; **7**: 733-41. doi: 10.1089/thy.1997.7.733

19. Harach HR, Galindez M, Campero M, Ceballos GA. Undifferentiated (anaplastic) thyroid carcinoma and iodine intake in Salta, Argentina. *Endocr Pathol* 2013; **24**: 125-31. doi: 10.1007/s12022-013-9248-9

20. Zimmermann MB, Galetti V. Iodine intake as a risk factor for thyroid cancer: a comprehensive review of animal and human studies. *Thyroid Res* 2015; **8**: 8. doi: 10.1186/s13044-015-0020-8

21. Zivaljevic V, Slijepcevic N, Paunovic I, Diklic A, Kalezic N, Marinkovic J, et al. Risk factors for anaplastic thyroid cancer. *Int J Endocrinol* 2014; **2014:** 815070. doi: 10.1155/2014/815070

22. Smallridge RC, Copland JA. Anaplastic thyroid carcinoma: pathogenesis and emerging therapies. *Clin Oncol (R Coll Radiol)* 2010; **22**: 486-97. doi: 10.1016/j.clon.2010.03.013

23. McIver B, Hay ID, Giuffrida DF, Dvorak CE, Grant CS, Thompson GB, et al. Anaplastic thyroid carcinoma: a 50-year experience at a single institution. *Surgery* 2001; **130**: 1028-34. doi: 10.1067/msy.2001.118266

24. Belfiore A, La Rosa G, Padova G, Sava L, Ippolito O, Vigneri R. The frequency of cold thyroid nodules and thyroid malignancies in patients from an iodine-deficient area. *Cancer* 1987; **60**: 3096-102. doi: 10.1002/1097-0142(19871215)60:12<3096::aid-cncr2820601240>3.0.co;2-v

25. Bakiri F, Djemli FK, Mokrane LA, Djidel FK. The relative roles of endemic goiter and socioeconomic development status in the prognosis of thyroid carcinoma. *Cancer* 1998; **82**: 1146-53. doi: 10.1002/(sici)1097-0142(19980315)82:6<1146::aid-cncr20>3.0.co;2-5

26. Oishi N, Kondo T, Ebina A, Sato Y, Akaishi J, Hino R, et al. Molecular alterations of coexisting thyroid papillary carcinoma and anaplastic carcinoma: identification of TERT mutation as an independent risk factor for transformation. *Mod Pathol* 2017; **11**: 1527-37. doi: 10.1038/modpathol.2017.75

27. Hieu TT, Russell AW, Cuneo R, Clark J, Kron T, Hall P, et al. Cancer risk after medical exposure to radioactive iodine in benign thyroid diseases: a metaanalysis. *Endocr Relat Cancer* 2012; **19**: 645-55. doi: 10.1530/ERC-12-0176

28. Ross DS, Burch HB, Cooper DS, Greenlee MC, Laurberg P, Maia AL, et al. 2016 American Thyroid Association guidelines for diagnosis and management of hyperthyroidism and other causes of thyrotoxicosis. *Thyroid* 2016; **26**: 1343-421. doi: 10.1089/thy.2016.0229

29. Venkatesh YS, Ordonez NG, Schultz PN, Hickey RC, Goepfert H, Samaan NA. Anaplastic carcinoma of the thyroid. A clinicopathologic study of 121 cases. *Cancer* 1990; **66**: 321-30. doi: 10.1002/1097-0142(19900715)66:2<321::aid-cncr2820660221>3.0.co;2-a

30. Skrk D, Zontar D. Estimated collective effective dose to the population from nuclear medicine examinations in Slovenia. *Radiol Oncol* 2013; **47**: 304-10. doi: 10.2478/raon-2013-0048

31. Haugen BR, Alexander EK, Bible KC, Doherty GM, Mandel SJ, Nikiforov YE, et al. 2015 American Thyroid Association management guidelines for adult patients with thyroid nodules and differentiated thyroid cancer: the American Thyroid Association guidelines task force on thyroid nodules and differentiated thyroid cancer. *Thyroid* 2016; **26**: 1-133. doi: 10.1089/thy.2015.0020

32. Kapp DS, LiVolsi VA, Sanders MM. Anaplastic carcinoma following well-differentiated thyroid cancer: etiological considerations. *Yale J Biol Med* 1982; **55**: 521-8. PMID: 7183024

33. Ito Y, Higashiyama T, Hirokawa M, Fukushima M, Inoue H, Yabuta T, et al. Prognosis of patients with papillary carcinoma showing anaplastic transformation in regional lymph nodes that were curatively resected. *Endocr J* 2008; **55**: 985-9. doi: 10.1507/endocrj.k08e-148

34. Verburg FA, Aktolun C, Chiti A, Frangos S, Giovanella L, Hoffmann M, et al. Why the European Association of Nuclear Medicine has declined to endorse the 2015 American Thyroid Association management guidelines for adult patients with thyroid nodules and differentiated thyroid cancer. *Eur J Nucl Med Mol Imaging* 2016; **43**: 1001-5. doi: 10.1007/s00259-016-3327-3

35. Shahbaz A, Fransawy Alkomos M, Mahendhar R, Nabi U, Riaz M, Sachmechi I. Follicular variant of papillary thyroid carcinoma presented as autonomous functioning thyroid nodule: a case report and review of literature. *Cureus* 2018; **7**: e3014. doi: 10.7759/cureus.3014

36. Maatouk J, Barklow TA, Zakaria W, Al-Abbadi MA. Anaplastic thyroid carcinoma arising in long-standing multinodular goiter following radioactive iodine therapy: report of a case diagnosed by fine needle aspiration. *Acta Cytol* 2009; **53**: 581-3. doi: 10.1159/000325388

37. Villa ML, Mukherjee JJ, Tran NQ, Cheah WK, Howe HS, Lee KO. Anaplastic thyroid carcinoma with destructive thyrotoxicosis in a patient with preexisting multinodular goiter. *Thyroid* 2004; **14**: 227-30. doi: 10.1089/105072504773297902

38. Mai DD, Mai KT, Shamji FM. Fine needle aspiration biopsy of anaplastic thyroid carcinoma developing from a Hürthle cell tumor: a case report. *Acta Cytol* 2001; **45**: 761-4. doi: 10.1159/000328300

39. Lee DY, Won JK, Lee SH, Park DJ, Jung KC, Sung MW, et al. Changes of clinicopathologic characteristics and survival outcomes of anaplastic and poorly differentiated thyroid carcinoma. *Thyroid* 2016; **26**: 404-13. doi: 10.1089/thy.2015.0316

research article

Significance of nuclear factor - kappa beta activation on prostate needle biopsy samples in the evaluation of Gleason score 6 prostatic carcinoma indolence

Marko Zupancic[1], Boris Pospihalj[2], Snezana Cerovic[3], Barbara Gazic[4], Primoz Drev[4], Marko Hocevar[5], Andraz Perhavec[5]

[1] Department of Urology, General Hospital Slovenj Gradec, Slovenj Gradec, Slovenia
[2] Department of Pathology, General Hospital Slovenj Gradec, Slovenj Gradec, Slovenia
[3] Institute of Pathology and Forensic Medicine, Military Medical Academy Belgrade, Belgrade, Serbia
[4] Department of Pathology, Institute of Oncology Ljubljana, Ljubljana, Slovenia
[5] Department of Surgical Oncology, Institute of Oncology Ljubljana, Ljubljana, Slovenia

Radiol Oncol 2020; 54(2): 194-200.

Received 3 January 2020
Accepted 24 March 2020

Correspondence to: Marko Zupančič, M.D., M.Sc., Department of Urology, General Hospital Slovenj Gradec, Gosposvetska cesta 1, SI-2380 Slovenj Gradec, Slovenia. E-mail: marko.zupancic@sb-sg.si

Disclosure: No potential conflicts of interest were disclosed.

Background. The goal of our study was to find out whether the immunohistochemical expression of nuclear factor-kappa beta (NF-κB) p65 in biopsy samples with Gleason score 3 + 3 = 6 (GS 6) can be a negative predictive factor for Prostate cancer (PCa) indolence.

Patients and methods. Study was conducted on a retrospective cohort of 123 PCa patients with initial total PSA ≤ 10 ng/ml, number of needle biopsy specimens ≥ 8, GS 6 on biopsy and T1/T2 estimated clinical stage who underwent laparoscopic radical prostatectomy and whose archived formalin-fixed and paraffin-embedded (FFPE) prostate needle biopsy specimens were used for additional immunohistochemistry staining for detection of NF-κB p65. Both cytoplasmic and nuclear NF-κB p65 expression in biopsy cores with PCa were correlated with postoperative pathological stage, positive surgical margins, GS and biochemical progression of disease.

Results. After follow-up of 66 months, biochemical progression (PSA ≥ 0.2 ng/ml) occurred in 6 (5.1%) patients, 3 (50%) with GS 6 and 3 (50%) with GS 7 after radical prostatectomy. Both cytoplasmic and nuclear NF-κB p65 expressions were not significantly associated with pathological stage, positive surgical margin and postoperative GS. Patients with positive cytoplasmic NF-kB reaction had significantly more frequent biochemical progression than those with negative cytoplasmic NF-kB reaction with PSA 0.2 ng/ml as cutoff point (p = 0.015) and a trend towards more biochemical progression with PSA ≥ 0.05 ng/ml as cutoff point (p = 0.068).

Conclusions. Cytoplasmic expression of NF-κB is associated with more biochemical progression and might be an independent prognostic factor for recurrence-free survival (RFS), but further studies including larger patient cohorts are needed to confirm these initial results.

Key words: nuclear factor-kappa beta; prostatic cancer; Gleason 6; needle biopsy sample

Introduction

Prostate cancer (PCa) is the most common cancer in men in developed European countries, particularly those with a high proportion of elderly population, with incidence rate up to 189 per 100.000.[1] In last two decades the disease has emerged as the most frequent cancer amongst men following rapid increases in the detection of a substantial number of early-stage PCa, particularly due to the increased

number of PSA testing. Recognizing that the expected men's life is obviously increasing, PCa also means increasing financial burden for individual countries.[2] Majority of men newly diagnosed with PCa will be candidates for primary curative therapy, either with radical prostatectomy or radiation, but many PCa, however, are low-grade, even indolent and the number of newly diagnosed PCa far outnumbers the number of lethal cases. Indolent PCa may exist for a long period without causing any symptoms or death, so the prediction of low risk and indolent PCa is needed to avoid overtreatment by unnecessary invasive therapies, and select men for active surveillance (AS).[3-5]

The nuclear factor-kappa beta (NF-κB) family of transcription factors plays a crucial role in inflammation as well as in the development and progression of cancer. Extensive evidence indicates that the NF-κB pathway is implicated in controlling the expression of genes involved in cell survival, proliferation, angiogenesis, and invasion.[6] Many studies indicate that activation of NF-κB signaling in PCa cells correlates with PCa progression, including chemoresistance, advanced stage, biochemical progression, and metastatic spread.[7-11] NF-κB is critical for human health, and aberrant NF-κB activation contributes to development of various autoimmune, inflammatory and malignant disorders including rheumatoid arthritis, atherosclerosis, inflammatory bowel diseases, multiple sclerosis and malignant tumors.[12] Despite the growing evidence for a role of NF-κB in prostate tumorigenesis and resistance to therapy, the mechanisms underlying the activation of NF-κB in PCa remain only partially understood.

The main goal of our study was to find out whether the immunohistochemical expression of NF-κB p65 in biopsy samples with Gleason score 3 + 3 = 6 (GS 6) is inversely correlated with prostatic carcinoma indolence.

Patients and methods

Patients

Our study was based on a retrospective cohort of 178 consecutive PCa patients whose archived formalin-fixed and paraffin-embedded (FFPE) prostate needle biopsy specimens were used for additional immunohistochemistry staining. All consecutive patients underwent the extraperitoneal laparoscopic radical prostatectomy (ELRP) or "nerve-sparing" extraperitoneal laparoscopic radical prostatectomy (N-S ELRP) without lymph node dissection between 2006 and 2012 as a first treatment of PCa. All patients were followed-up for at least five years after surgery at Department of Urology in General Hospital Slovenj Gradec. Hospital patient's files were used for clinical data.

The inclusion criteria were total PSA ≤ 10 ng/ml, number of biopsy specimen ≥ 8, histopathological result of prostate cancer GS 6 on biopsy and T1/T2 estimated clinical stage, based on clinical examination only. The exclusion criterion was the presence of chronical diseases in which the activation of NF-kB is common. After the screening review of the clinical data and histopathological revision of prostate needle biopsy specimens, done by two unrelated pathologists with extensive experience in PCa, 15 patients were excluded from the study, as they did not meet the criterion of GS. During the additional microtome cutting of archived FFPE prostate needle biopsy specimens for immunohistochemistry due to the lack of the tissue, another 40 patients were excluded. The final analysis in this study was performed on 123 patients. Based on a PSA levels, two biochemical progression were defined, at PSA cutoff point ≥ 0.05 ng/ml and ≥ 0.2 ng/ml, 6 months or more after radical prostatectomy. Recurrence-free survival (RFS) was defined as the period between the surgery and biochemical progression (i.e. first increase of PSA above one or both PSA cutoff points). 5 patients were excluded due to the initiation of hormonal treatment immediately after surgery, so regarding the biochemical progression 118 patients were analyzed

For control group archived FFPE prostate needle biopsy specimens from 60 patients with PCa GS 7, 30 with 3 + 4 and 30 with 4 + 3, were used.

Study was approved by the Slovene National Medical Ethics Committee No 109/14.

Tissue preparation and immunohistochemical staining

IHC staining for detection of NF-κβ p65 was performed on 2-4 μm FFPE tissue sections, dried at 56^{0}C for 2 hours, using fully automated IHC system Ventana Benchmark XT (manufacturer Ventana ROCHE inc.). Epitope was retrieved on board employing heat-mediated epitope retrieval using high pH Cell Conditioning Solution 1 (cat No 950-124, manufacturer Ventana ROCHE inc.) for 88 minutes at 100^{0}C. Epitope was detected using commercially available mouse monoclonal antibody NF-κβ p65 (clone F-6; cat No sc-8008; manufacturer Santa Cruz Biotechnology inc.) directed against amino acids 1-286 of NF-κβ p65 of human origin. Primary

TABLE 1. Patient characteristics

General, N = 123		
Mean Age, *year, (range)*	63.6 (50–75)	
Mean init. PSA, *ng/ml, (range)*	5.32 (1,32–9,51)	
Mean Prostate V, *ml, (range)*	38.3 (14–97)	
Mean Biopsy cores, *n, (range)*	9.6 (8–10)	
Total Biopsy *cores, n*	1.180	
Clinical stage		
T1, *n, (%)*	113 (91.9)	
T2, *n, (%)*	10 (8.1)	
Biopsy GS 3+3=6, *n, (%)*	123 (100)	
Surgery		
ELRP, *n, (%)*	87 (70.7)	
N-S ELRP, *n, (%)*	36 (29.3)	
Pathological result after RP		
N = 123	**N of total P**	**% of total P**
pT classification		
T2	96	78.0
T3a	23	18.7
T3b	4	3.3
Surgical margins		
Positive	13	10.6
Negative	110	89.4
Gleason score		
3+3=6	79	64.2
3+4=7	37	30.1
4+3=7	7	5.7
Biochemical progression after RP		
N = 118	**N (%)**	**GS 6**	**GS 7**
BP		N(%)	N(%)
PSA 0,05–0.19 ng/ml	14 (11.8)	8(57.1)	6(42.9)
PSA ≥ 0,2 ng/ml	6 (5.1)	3(50)	3(50)

BP = biochemical progression; ELRP = laparoscopic radical prostatectomy; GS = Gleason score; N-S ELRP = "nerve-sparing" extraperitoneal laparoscopic radical prostatectomy; PSA = Prostate-specific antigen; RP = radical prostatectomy; V = volume

antibody was diluted 1:200 using DAKO REAL™ antibody diluent (cat No S2022; manufacturer DAKO Agilent technologies inc.) and incubated on board for 60 minutes at 37⁰C. Primary antibody was visualized using 3–step multimer detection system OptiView DAB IHC Detection Kit (cat No 760-700; manufacturer Ventana ROCHE inc.) according to manufacturer's instructions.

The staining was analysed by pathologist with extensive experience in PCa who was not familiar with patient's clinical data. For nuclear staining, positive result was reported when at least 5% nuclei of cancer cells showed unequivocal brown coloration.[13] To consider reaction as positive, nuclear brown coloration should exceed the effect of cytoplasmic overlapping. The intensity of cytoplasmic staining was assessed as negative, weak, moderate and strong, and for statistical analysis grouped as negative (negative, weak) and positive (moderate, strong).[14]

Statistical analyses

Clinical, laboratory and pathological characteristics were summarized using frequency and percentage for categorical variables, and mean and range for continuous variables. RFS was calculated from the time of primary tumour excision, and was censored at the last contact date if there were no events. Association of NF-kB expression status with pathological findings was tested using Chi-square test. Survival curves were calculated by Kaplan-Meier's method and tested for statistical significance using log-rank test. Multivariate Cox regression model was used to test whether NF-kB expression status is an independent predictor of RFS; other covariates included in the model are known prognostic factors in prostate cancer: final Gleason score, surgical margin status and pathologic stage. The differences were considered statistically significant if the p values were less than 0.05. Software package SPSS 22.0 for Windows was used.

Results

Table 1 shows patients characteristics and biochemical progression in patients after radical prostatectomy. Postoperative pathological stage 3 was noticed in 27 (22%) and positive surgical margins were detected in 13 patients (10.6%). biochemical progression (PSA ≥ 0.05 ng/ml) occurred in 20 (16.9%) patients (11 with GS 6 after radical prostatectomy and 9 with GS 7). Among 118 patients, clinically significant postoperative PSA ≥ 0.2 ng/ml was detected in six patients (5.1%), with GS 6 in 3 and GS 7 in 3. Positive cytoplasmic NF-κB staining was detected in 173 (56.9%) and positive nuclear

TABLE 2. Association of nuclear factor-kappa beta (NF-κB) p65 expression status in cytoplasm with pathological findings

N = 123	N	NF-κB p65 expression		P
		negative	positive	
pT status				
pT2	96	48	48	
pT3	27	12	15	0.667*
Surg. m.				
Negative	110	53	7	
Positive	13	7	6	0.774**
GS				
3 + 3 = 6	79	39	40	
3 + 4 = 7	37	17	20	
4 + 3 = 7	7	5	2	0.465***

* pT2 versus pT3, **negative versus positive surgical margin, ***3 + 3 = 6 *versus* 3 + 4 = 7 *versus* 4 + 3 = 7

GS = Gleason score; Surg. M. = surgical margin

TABLE 3. Cytoplasmic nuclera factor-kappa beta (NF-κB) p65 expression status in biopsy group postoperative Gleason score (GS) 6 and control biopsy group postoperative GS 7

	N	NF-κB p65 expression		P
		negative	positive	
3 + 3 = 6	123	60	63	
3 + 4 = 7	30	3	27	<0.001*
4 + 3 = 7	30	0	30	<0.001**

* 3 + 3 = 6 *versus* 3 + 4 = 7, **3 + 3 = 6 *versus* 4 + 3 = 7

NF-κB staining in 57 (18.7%) of the 304 analyzed biopsy cores with GS 6.

Cytoplasmic NF-κB staining

Cytoplasmic NF-κB p65 expression was not correlated with pathological stage, positive surgical margin and postoperative GS (Table 2). Cytoplasmic

TABLE 4. Multivariate analysis of cytoplasmic nuclear factor-kappa beta (NF-κB) p65 expression and other clinicopathologic variables associated with recurrence-free survival (RFS)

	Hazard ratio (95% CI)	P
Cytoplasmic NF-κB p65 expression (negative *vs.* positive)	2.367 (0.908–6.170)	0.078
Postoperative Gleason score (6 *vs.* 7)	1.105 (0.406–3.008)	0.845
Surgical margin (negative *vs.* positive)	4.845 (1.646–14.260)	0.004
Pathologic stage (T2 *vs.* T3)	1.041 (0.339–3.194)	0.944

NF-κB p65 expression was significantly more common in biochemical progression with PSA cut off point ≥ 0.2 ng/ml (P = 0.015) and there was a trend towards biochemical progression with PSA cut off point ≥ 0.05 ng/ml (P = 0.068) (Figure 1). Cytoplasmic NF-κB p65 expression was positive in 57/60 control group patients with GS 7 (Table 3).

In multivariate analysis only positive surgical margin was significantly associated with worse RFS with a PSA cut off point ≥ 0.05 ng/ml, while postoperative Gleason score 7 and pathologic stage of the disease were not significantly associated with RFS (Table 4). Positive cytoplasmic NF-κB p65 expression negatively affects RFS with borderline statistical significance (p = 0.078). When PSA cut off point was set to ≥ 0.2 ng/ml, none of the prognostic factors was significantly associated with RFS in multivariate analysis.

Nuclear NF-κB staining

Nuclear NF-κB p65 expression was not associated with pathological stage, positive surgical margins and postoperative GS (Table 5), neither with biochemical progression (Figure 2) and did not differ from control group patients with GS 7 (Table 6).

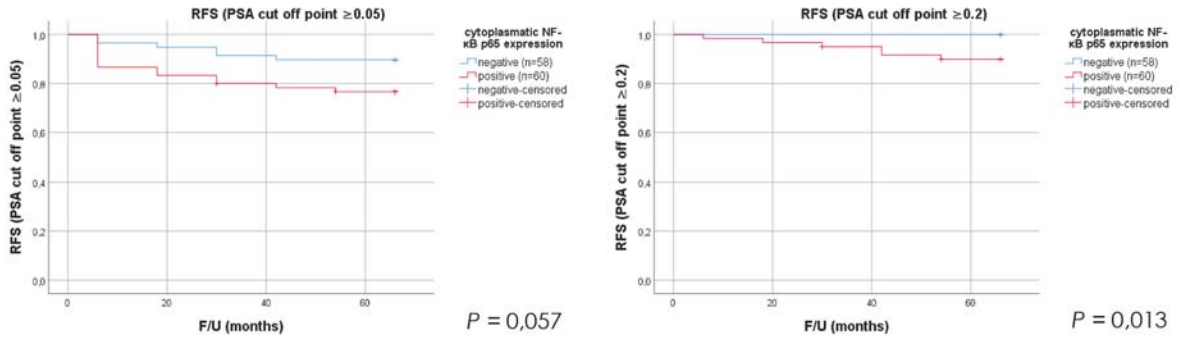

FIGURE 1. Recurrence-free survival (RFS) in patients with positive and negative nuclear factor-kappa beta (NF-κB) p65 expression status in cytoplasm (N = 118).

TABLE 5. Association of nuclear factor-kappa beta (NF-κB) p65 expression status in nucleus with pathological findings

N = 123	N	NF-κB p65 expression		P
		negative	positive	
pT status				
pT2	96	81	15	
pT3	27	22	5	0.769*
Surg. m.				
Negative	110	92	18	
Positive	13	11	2	1**
GS				
3 + 3 = 6	79	66	13	
3 + 4 = 7	37	31	6	
4 + 3 = 7	7	6	1	0.989***

* pT2 versus pT3, **negative versus positive surgical margin, *** 3 + 3 = 6 *versus* 3 + 4 = 7 *versus* 4 + 3 = 7

GS = Gleason score; Surg. M. = surgical margin

TABLE 6. Nuclear factor-kappa beta (NF-κB) p65 expression status in biopsy group GS 6 and control biopsy group GS 7

	N	NF-κB p65 expression		P
		negative	positive	
3+3=6	123	103	20	
3+4=7	30	24	6	0.596*
4+3=7	30	17	13	0.003**

* 3+3=6 versus 3+4=7, **3+3=6 versus 4+3=7

TABLE 7. Multivariate analysis of nuclear factor-kappa beta (NF-κB) p65 expression and other clinicopathologic variables associated with recurrence-free survival (RFS; recurrence defined as PSA ≥ 0.05)

	Hazard ratio (95% CI)	P
NF-κB p65 expression (negative *vs.* positive)	0.254 (0.034–1.915)	0.184
Postoperative Gleason score (6 *vs.* 7)	1.078 (0.400–2.907)	0.882
Surgical margin (negative *vs.* positive)	4.838 (1.674–13.983)	0.004
Pathologic stage (T2 *vs.* T3)	1.232 (0.409–3.705)	0.711

In multivariate analysis only positive surgical margin was significantly associated with worse RFS with a PSA cut off point ≥ 0.05 ng/ml, while positive nuclear NF-κB p65 expression, postoperative Gleason score 7 and pathologic stage of the disease were not significantly associated with RFS (Table 7). When PSA cut off point was set to ≥ 0.2 ng/ml, none of the prognostic factors was significantly associated with RFS in multivariate analysis. Figure 3 shows difference in positive cytoplasmic and nuclear staining in patient with GS 6 and GS 7.

Discussion

Increase in incidence of PCa since 1990s mostly starts with PSA testing, either in the form of all types of screening or on the basis of a suspicious digital rectal examination. Nevertheless, the most important part of diagnostic procedure is accurate histopathologic diagnosis, particularly in low-risk PCa where AS could be an option.[15] Despite the fact that in our study biopsy samples were evaluated by two experienced uropathologists, we recorded the postoperative upgrade of GS 6 to GS 7 in 44 patients (3 + 4 in 37 and 4 + 3 in 7), so biopsy undergrading was present in 35.8%. This is in concordance with literature reports where GS from needle biopsies underestimates the GS of the radical prostatectomy specimen in 28% to 57%.[16] Postoperative pathological stage 3 was noticed in 27 (22%), positive surgical margins were detected in 13 (10.6%)

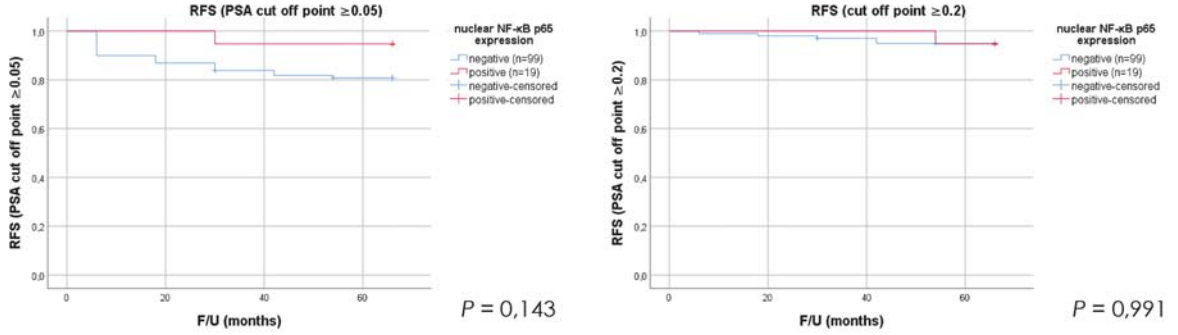

FIGURE 2. Recurrence-free survival (RFS) in patients with positive and negative nuclear factor-kappa beta (NF-κB) p65 expression status in nucleus (N = 118).

and clinically significant biochemical progression (PSA ≥ 0.2 ng/ml) in 6 (5.1%) patients.

Molecular biomarkers offer the possibility to further stratify patients with similar clinicopathological parameters. Domingo-Domenech *et al.*[9] and Ross *et al.*[10] reported that tumors with nuclear NF-κB expression and no additional risk factors (i.e. low GS and low preoperative PSA) had the lowest rate of biochemical recurrence in the nuclear NF-κB positive group. In addition to nuclear staining, we included also the NF-κB cytoplasmic staining and contrary to reported results found that only the cytoplasmic NF-κB variable was associated with worse RFS. This association was statistically significant when PSA cut-off point for recurrence was set to ≥ 0.2 ng/ml (p = 0.013) and borderline significant when PSA cut-off point was set to ≥ 0.05 (p = 0.057). In multivariate analysis positive cytoplasmic NF-κB p65 expression remained negatively associated with RFS (PSA cut-off point ≥ 0.05) with borderline statistical significance (p = 0.078).

The p65 subunit of NF-κB was expressed in the cytoplasm of 173 (56.9%) biopsy cores with GS 6. Only 57 (18.7%) biopsy samples also showed a nuclear staining of NF-κB p65, suggesting a constitutive activation of NF-κB in these tissues. Our results showed a positive correlation between NF-κB cytoplasmic staining and biochemical progression. The main differences with other studies relate to tissue sample type and biochemical progression definition. Unlike Domingo-Domenech *et al.*[9] and Ross *et al.*[10] the studies that used tissue samples from radical prostatectomy, our analysis is preoperative and is based on diagnostic biopsies and their predictive significance. Also, we used more stringent parameters for the determination of biochemical progression, which in previous works was only determined as a value of 0.4 ng/ml in two consecutive measurements. In the present study, NF-κB expression and its subcellular localization were highly variable among different specimens. In another study, nuclear NF-κB was found in 40% of PCa.[8-13] As in the current study, nuclear NF-κB did not significantly correlate with GS. The functional relevance of this immunoreactivity on NF-κB activation is not known. This limitation is based on the fact that p65/NF-κB nuclear translocation is necessary but not sufficient for NF-κB induced transcriptional activity, since both recruitment of NF-κB to target genes and NF-κB-induced transcriptional events after recruitment are needed for this to occur. Furthermore, the minimum percentage of tumor cells with nuclear p65 staining required to potentially result in detectable NF-κB-induced transcriptional activity remains uncharacterized. An important limitation of our study is a significant reduction in the size of diagnostic biopsies during microscopic reevaluation and diagnosis of PCa with GS 6.[13,14]

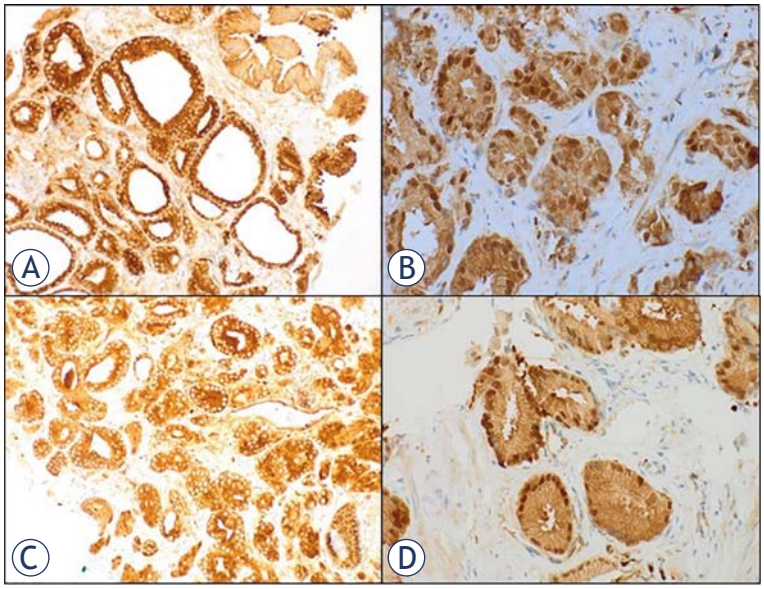

FIGURE 3. Immunohistochemistry of nuclear factor-kappa beta (NF-κB) p65. **(A)** Positive cytoplasmic staining (GS 6). **(B)** Positive nuclear staining. **(C)** Positive cytoplasmic staining (GS 7). **(D)** Positive nuclear staining.

In our group of 20 patients who developed the biochemical progression with PSA cutoff point ≥ 0.05 ng/ml cytoplasmic NF-κB staining was detected in 14 (70%) and nuclear NF-κB staining in only 1 (5%), while among those 6 patients who had the biochemical progression with PSA cutoff point ≥ 0.2 ng/ml cytoplasmic NF-κB staining was noticed in all 6 (100%) and nuclear NF-κB staining in 1 (16.7%). Among several available selection criteria for AS worldwide, at our institution the EAU AS guidelines were used.[17] According to them all patients in our cohort had initial PSA below 10 ng/ml, biopsy GS 6, estimated clinical stage T1c-T2 and 82 of them (66.7%) had ≤ 2 positive cores on biopsy. From clinical point of view the biochemical progression of PCa after radical prostatectomy is defined with PSA ≥ 0.2 ng/ml.[18] In our group of 6 patients with biochemical progression at PSA cut-off point ≥ 0.2 ng/ml, positive cytoplasmic NF-κB staining was present in all 6 and all AS criteria were met in 5 (83.3%) patients. There was no positive nuclear NF-κB staining in any of these 5 patients. As a control group we used 60 patients with biopsy GS 7 and positive cytoplasmic NF-κB staining was present in 57 (95%) of them. Since patients with bi-

opsy GS 7 are not candidates for AS according to EAU AS guidelines there is no need for additional prognostic factor (i.e. positive cytoplasmic NF-κB staining). However, in patients with biopsy GS 6, an additional prognostic factor is needed in order to stratify these patients to a group where only AS is enough. According to our results, positive cytoplasmic NF-κB staining could be a negative predictive factor for the GS 6 PCa indolence and these patients are candidates for primary curative therapy.

There are several limitations of our study. Most importantly, all patients underwent surgical treatment, so the significance of NF-κB activation on prostate needle biopsy samples for disease progression was found only indirectly, based on biochemical progression and is most probably underestimated. Another important limitation is a small number of patients and single institution results.

Conclusions

Cytoplasmic expression of NF-κB is associated with worse RFS, while it is not significantly associated with standard prognostic factors and remains an independent prognostic factor for RFS in multivariate analysis with borderline statistical significance. However, further studies, including larger patient cohorts are needed to confirm these initial results.

References

1. Ferlay J, Colombet M, Soerjomataram I, Dyba T, Randi G, Bettio M, et al. Cancer incidence and mortality patterns in Europe: Estimates for 40 countries and 25 major cancers in 2018. *Eur J Cancer* 2018; **103:** 356-87. doi: 10.1016/j.ejca.2018.07.005.
2. Luengo-Fernandez R, Leal J, Gray A, Sullivan R. Economic burden of cancer across the European Union: a population-based cost analysis. *Lancet Oncol* 2013; **14:** 1165-74. doi: 10.1016/S1470-2045(13)70442-X.
3. Cooperberg MR, Broering JM, Litwin MS, Lubeck DP, Mehta SS, Henning JM, et al. The contemporary management of prostate cancer in the United States: lessons from the cancer of the prostate strategic urologic research endeavor (CapSURE), a national disease registry. *J Urol* 2004; **171:** 1393-401. doi: 10.1097/01.ju.0000107247.81471.06
4. Albertsen PC, Hanley JA, Fine J. 20-year outcomes following conservative management of clinically localized prostate cancer. *JAMA* 2005; **293:** 2095-101. doi: 10.1001/jama.293.17.2095
5. Bangma CH, Roobol MJ. Defining and predicting indolent and low risk prostate cancer. *Crit Rev Oncol Hematol* 2012; **83:** 235-41. doi: 10.1016/j.critrevonc.2011.10.003
6. Karin M, Lin A. NF-κB at the crossroads of life and death. *Nat. Immunol* 2002; **3:** 221-7. doi: 10.1038/ni0302-221
7. May MJ, Ghosh S. Rel/NF-kappa B and I kappa B proteins: an overview. *Semin Cancer Biol* 1997; **8:** 63-73. doi: 10.1006/scbi.1997.0057
8. Lessard L, Karakiewicz PI, Bellon-Gagnon P, Alam-Fahmy M, Ismail HA, Mes-Masson AM, et al. Nuclear localization of nuclear factor-kappaB p65 in primary prostate tumors is highly predictive of pelvic lymph node metastases. *Clin Cancer Res* 2006; **12:** 5741-5. doi: 10.1158/1078-0432.CCR-06-0330
9. Domingo-Domenech J, Mellado B, Ferrer B, Truan D, Codony-Servat J, Sauleda S, et al. Activation of nuclear factor-kappaB in human prostate carcinogenesis and association to biochemical relapse. *Br J Cancer* 2005; **93:** 1285-94. doi: 10.1038/sj.bjc.6602851
10. Ross JS, Kallakury BV, Sheehan CE, Fisher HA, Kaufman RP Jr, Kaur P, et al. Expression of nuclear factor-kappa B and I kappa B alpha proteins in prostatic adenocarcinomas: correlation of nuclear factor-kappa B immunoreactivity with disease recurrence. *Clin Cancer Res* 2004; **10:** 2466-72. doi: 10.1158/1078-0432.ccr-0543-3
11. Setlur SR, Royce TE, Sboner A, Mosquera JM, Demichelis F, Hofer MD, et al. Integrative microarray analysis of pathways dysregulated in metastatic prostate cancer. *Cancer Res* 2007; **67:** 10296-303. doi: 10.1158/1078-0432.ccr-0543-3
12. Park MH, Hong JT. Roles of NF-κB in cancer and inflammatory diseases and their therapeutic approaches. *Cells* 2016; **5:** E15. doi: 10.3390/cells5020015.
13. Lessard L, Begin LR, Gleave ME, Mes-Masson AM, Saad F. Nuclear localisation of nuclear factor-kappaB transcription factors in prostate cancer: an immunohistochemical study. *Br J Cancer* 2005; **93:** 1019-23. doi: 10.1038/sj.bjc.6602796
14. Gannon PO, Lessard L, Stevens LM, Forest V, Bégin LR, Minner S, et al. Large-scale independent validation of the nuclear factor-kappa B p65 prognostic biomarker in prostate cancer. *Eur J Cancer* 2013; **49:** 2441-8. doi: 10.1016/j.ejca.2013.02.026
15. Ganz PA, Barry JM, Burke W, Col NF, Corso PS, Dodson E, et al. NIH State-of-the-Science Conference Statement: role of active surveillance in the management of men with localized prostate cancer. *NIH Consens State Sci Statements* 2011; **28:** 1-27. PMID: 23392076
16. Lucia MS, Bostwick DG, Somerville MC, Fowler IL, Rittmaster RS. Comparison of classic and international society of urological pathology 2005 modified Gleason grading using needle biopsies from the reduction by dutasteride of prostate cancer events (REDUCE) trial. *Arch Pathol Lab Med* 2013; **137:** 1740-6. doi: 10.5858/arpa.2012-0447-OA
17. Komisarenko M, Martin LJ, Finelli A. Active surveillance review: contemporary selection criteria, follow-up, compliance and outcomes. *Transl Androl Urol* 2018; **7:** 243-55. doi: 10.21037/tau.2018.03.02
18. McCormick BZ, Mahmoud AM, Williams SB, Davis JW. Biochemical recurrence after radical prostatectomy: Current status of its use as a treatment endpoint and early management strategies. *Indian J Urol* 2019; **35:** 6-17. doi: 10.4103/iju.IJU_355_18

research article

Evaluation of the training program for p16/Ki-67 dual immunocytochemical staining interpretation for laboratory staff without experience in cervical cytology and immunocytochemistry

Veronika Kloboves Prevodnik[1,2], Ziva Pohar Marinsek[1], Janja Zalar[1], Hermina Rozina[1], Nika Kotnik[3], Tine Jerman[4], Jerneja Varl[2,5], Urska Ivanus[4,2]

[1] Department of Cytopathology, Institute of Oncology Ljubljana, Ljubljana, Slovenia
[2] Faculty of Medicine, University of Ljubljana, Ljubljana, Slovenia
[3] Department of Experimental Allergology and Immunodermatology Oldenburg, Carl von Ossietzky Universität, Oldenburg, Germany
[4] Epidemiology and Cancer Registry, Institute of Oncology Ljubljana, Ljubljana, Slovenia
[5] Department of Experimental Oncology, Institute of Oncology Ljubljana, Ljubljana, Slovenia

Radiol Oncol 2020; 54(2): 201-208.

Received 22 January 2020
Accepted 4 March 2020

Correspondence to: Assoc. Prof. Veronika Kloboves Prevodnik, M.D. Ph.D., Department of Cytopathology, Institute of Oncology Ljubljana, Zaloška 2, SI-1000 Ljubljana, Slovenia. E-mail: vkloboves@onko-i.si

Disclosure: No potential conflicts of interest were disclosed.

Background. p16/Ki-67 dual immunocytochemical staining (DS) is considered easy to interpret if evaluators are properly trained, however, there is no consensus on what constitutes proper training. In the present study we evaluated a protocol for teaching DS evaluation on students inexperienced in cervical cytology.

Methods. Initial training on 40 DS conventional smears was provided by a senior cytotechnologist experienced in such evaluation. Afterwards, two students evaluated 118 cases. Additional training consisted mainly of discussing discrepant cases from the first evaluation and was followed by evaluation of new 383 cases. Agreement and accuracy of students' results were compared among the participants and to the results of the reference after both evaluations. We also noted time needed for evaluation of one slide as well as intra-observer variability of the teacher's results.

Results. At the end of the study, agreement between students and reference was higher compared to those after initial training (overall percent agreement [OPA] 81.4% for each student, kappa 0.512 and 0.527 vs. OPA 78.3% and 87.2%, kappa 0.556 and 0.713, respectively). However, accuracy results differed between the two students. After initial training sensitivity was 4.3% points and 2.9% points higher, respectively compared to the reference, while specificity was 30.6% points and 24.4% points lower, respectively, compared to the reference. At the end of the study, the sensitivity reached by one student was the same as that of the reference, while it was 2.6% points lower for the other student. There was a statistically significant difference in specificity between one student and the reference and also between students (16.7 and 15.1% points). Towards the end of the study, one student needed 5.2 min for evaluating one slide while the other needed 8.2 min. The intra-observer variability of the senior cytotechnologist was in the range of "very good" in both arms of the study.

Conclusions. In teaching DS evaluation, the students' progress has to be monitored using several criteria like agreement, accuracy and time needed for evaluating one slide. The monitoring process has to continue for a while after students reach satisfactory results in order to assure a continuous good performance. Monitoring of teacher's performance is also advisable.

Key words: training protocol; p16/Ki-67 dual immunocytochemical staining; agreement; accuracy; inter-observer reproducibility

Introduction

p16/Ki-67 dual immunocytochemical staining (DS) is considered easy to interpret if evaluators are properly trained. However, there is no consensus on what constitutes proper training. Authors have used different training approaches in studies investigating inter-observer reproducibility and accuracy of DS.[1-6] Most training protocols described in these studies consisted of initial and additional training. The initial training was provided by the manufacturer, however, it was not exactly the same in all cases except that it was completed by a proficiency test. The information on the initial training is sparse. Three of the above mentioned studies do not describe the initial training.[1,2,4] In two studies, participants were shown 15[5] or 40[6] microscope-projected images, while in the third study participants examined a teaching set of slides.[3] The number of cases in the teaching set is not mentioned. In all three studies the training was completed in one or two-half day sessions.[3,5,6] Four authors described additional training which consisted of evaluating from 80 to 469 slides as well as reviewing and discussing cases with discrepant results.[1-3,6] Agreement in DS interpretation among evaluators improved after additional training in all three studies (kappa range: 0.43–0.73 compared to 0.50–0.87).[1-3,6] In the study of Wentzensen *et al*.[2] agreement was evaluated only at the end of the study.

In our recently published study which assessed reproducibility of the DS test we described a training protocol which was designed to introduce DS in three Slovenian cytopathological laboratories participating in the national organized cervical cancer screening program.[6] At the time we designed the protocol we found only one similar study by Waldstrom *et al*.[1] The results of our study demonstrated that initial training by the manufacturer was not enough for achieving accurate results of DS interpretation. Furthermore, the manufacturer provides training when an institution is ready to implement the test. Later on, when we have the need to teach additional personnel, we have to have our own training protocol which will assure the students receive the necessary expertise.

On the basis of the results of our previous study, we proposed a training protocol for staff inexperienced in DS reading.[6] In the present study, we aimed to test the proposed training protocol for DS interpretation on two students inexperienced in DS reading and to discern how improvement in DS evaluation influences the time needed for DS reading of one slide. An additional end point of the study was also monitoring the performance of the senior cytotechnologist involved in teaching DS interpretation to new personnel.

Material and methods

Study design and setting

We used DS slides on conventional cervical smears taken from 501 women who underwent colposcopy at Celje General Hospital or at University Medical Centre Maribor between April 2014 and December 2015. Samples from 118 women were the same ones we have used in our previous study.[6] These women were invited to colposcopy per screening program guidelines, either due to high-grade (HG) cytology, a human Papillomavirus (HPV)-positive triage test after low-grade pathological changes or due to a positive HPV test during follow-up after treatment of high grade cervical intraepithelial neoplasia (CIN). An additional set of samples came from 383 women, of which 87 were referred to colposcopy from the screening program and 296 were non-responders. All non-responders were invited to colposcopy after they have taken their own cervical sample. 250 were HPV positive and 46 were HPV negative.[7] Sample acquisition, procedures following abnormal colposcopy, reasons for excluding patients from the study and classification of histopathology results were the same as already described in our previous study.[6] In both sets of women the same gynecologists participated in colposcopy examinations and the same criteria were used for performing biopsy for histological examinations. After the initial colposcopy, all women were followed via the Cervical Cancer Screening Registry ZORA that registers all cervical cytology, HPV test results and cervical histology results of all Slovenian women.

Two students, a biologist (S1) and a medical doctor (S2) as well as a senior cytotechnologist (SC) participated in the study. SC was employed at the Department of cytopathology, Institute of Oncology Ljubljana, where the study was conducted. She was trained in DS evaluation during our previous study. The two students had no previous knowledge of cervical cytology or of DS evaluation. Four cytopathologist from the Institute of Oncology Ljubljana reviewed all DS slides. Their consensus results were considered as reference.

Fixation of slides, immunocytochemical staining and the rules for slide interpretation have already been described in our previous paper.[6]

The reading of DS slides was divided into primary reading of 118 slides after initial training and the secondary reading of new 383 slides after additional training. In each reading, students spotted the DS cells and passed slides on to the SC who reviewed all of them. The SC reviewed both sets of slides separately after each student and therefore, each case had four readings. Results of both students and of the SC were evaluated after initial and after secondary reading and compared to the reference results. For both students we also noted the time needed to interpret each of the 501 slides. S1 evaluated 501 slides during the course of four months while S2 evaluated all the slides in five months because none of the students were evaluating slides continuously eight hours per day.

The p16/Ki-67 DS study was nested within the randomized trial of HPV self-sampling among non-attenders of ZORA. It was conducted in compliance with the Helsinki Declaration, and was approved by the institutional review board and the National Medical Ethics Committee at the Slovenian Ministry of Health (consents Nos. 155/03/13 and 136/04/14). All women signed informed consent to participate in the study. This research was financed by the Slovenian Research Agency and the Slovenian Ministry of Health (trial No. L3-5512).

Training design

The initial training program for DS interpretation started by lectures and by demonstration of morphology of normal and atypical cervical cytology and of DS interpretation. Afterwards, the students examined 40 teaching slides and discussed difficult cases with SC at a multi-head microscope. Training was completed in one week. Additional training took place after we evaluated the results of the primary reading. It was also provided by SC and lasted two days. Additional training included a troubleshooting slide review of discordant cases of the primary reading as well as a theoretical repetition of the criteria for DS evaluation.

Study outcomes and statistical analysis

The primary outcomes were: (1) agreement in DS interpretation between all three evaluators (S1, S2, SC), between each evaluator and the reference as well as intra-observer agreement for SC; (2) accuracy prior to and after the additional training. For evaluating agreement and accuracy we used the same statistical methods as already described in our previous article.[6] The secondary outcome was measuring screening time per slide of both students. We assessed the mean screening time with standard deviation (SD) for primary and secondary evaluation and also for the last 100 slides. The screening time trends for positive and negative p16/Ki-67 DS results were characterized in terms of an average percent change per slide estimated by the log-linear joinpoint regression. Sensitivity, specificity, positive (PPV) and negative (NPV) predictive values were calculated for one year histopathological follow-up for both evaluation sets. In addition, sensitivity and specificity were calculated at each of the 501 ratings, taking into account only 100 most recent ratings, and presented on a line plot.

We conducted all our analyses with R v3.5.1[8], using 2-tailed tests and the significance level α = 0.050. Joinpoint Regression program[9] was used for the assessment of the screening time trends.

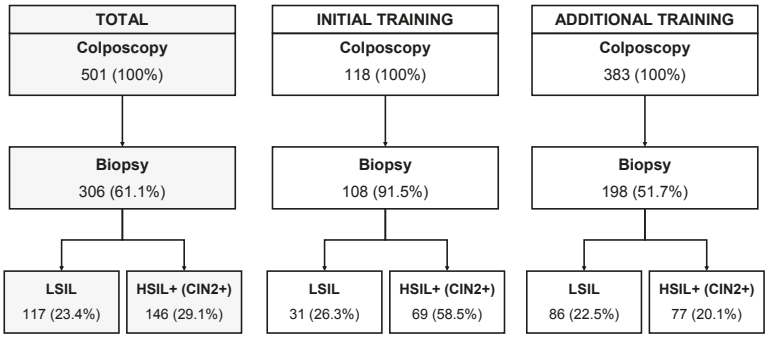

FIGURE 1. Study flow chart with histopathology follow-up results.

Results

Study population

The average age of the 501 women in the study was 44.3 years (SD 11.9). The average age of women whose smears were subject to primary DS evaluation was 36.5 years (SD 11.1) while the average age of women in secondary DS evaluation was 46.7 years (SD 11.2). The study flow chart with histopathology results is shown in Figure 1. Women whose smears were included into the primary DS evaluation had higher prevalence of cervical intraepithelial neoplasia grade 2 or worse (CIN2+) compared to women whose samples were material for the secondary evaluation (58.5 % *vs.* 20.1%) (Figure 1).

TABLE 1. p16/Ki-67 study results and CIN2+ outcome for students, senior cytotechnologist and reference

Reviewer	Categories of p16/Ki67 dual staining result	Initial training (N = 118)		Additional training (N = 383)	
		p16/Ki67 dual staining result N, (%)	CIN2+ outcomes N (PV, %)*	p16/Ki67 dual staining result (N, %)	CIN2+ outcomes N (PV, %)*
S1	positive	91 (77.1)	65 (71.4)	171 (44.6)	65 (38.0)
	suspicious	7 (5.9)	2 (28.6)	7 (1.8)	2 (28.6)
	negative	20 (16.9)	2 (10.0)	205 (53.5)	10 (4.9)
	unsatisfactory	0 (0.0)	0 (0.0)	0 (0.0)	0 (0.0)
S2	positive	92 (78.0)	66 (71.7)	129 (33.7)	64 (49.6)
	suspicious	2 (1.7)	0 (0.0)	1 (0.3)	1 (100.0)
	negative	24 (20.3)	3 (12.5)	253 (66.1)	12 (4.7)
	unsatisfactory	0 (0)	0 (0.0)	0 (0.0)	0 (0.0)
SC (S1)	positive	83 (70.3)	65 (78.3)	143 (37.9)	65 (45.5)
	suspicious	2 (1.7)	2 (100.0)	5 (1.3)	0 (0.0)
	negative	32 (27.1)	2 (6.3)	235 (61.4)	12 (5.1)
	unsatisfactory	1 (0.8)	0 (0.0)	0 (0.0)	0 (0.0)
SC (S2)	positive	83 (70.3)	65 (78.3)	145 (37.9)	64 (44.1)
	suspicious	2 (1.7)	2 (100.0)	4 (1.0)	0 (0.0)
	negative	32 (27.1)	2 (6.3)	234 (61.1)	13 (5.6)
	unsatisfactory	1 (0.8)	0 (0.0)	0 (0.0)	0 (0.0)
Reference	positive	78 (66.1)	64 (82.1)	114 (29.8)	64 (56.1)
	suspicious	2 (1.7)	0 (0)	13 (3.4)	3 (23.1)
	negative	38 (32.2)	5 (13.2)	255 (66.6)	10 (3.9)
	unsatisfactory	0 (0.0)	0 (0.0)	1 (0.3)	0 (0.0)

N = number of cases; Reference = results of four cytopathologists at the Deptment of Cytopathology, Institute of Oncology Ljubljana; S1 = student 1; S2 = student 2; SC (S1) = senior cytotechnologist results obtained during revision of student 1 results; SC (S2) = senior cytotechnologist results obtained during revision of student 2 results; * PV = predictive value (number of CIN2+detected within specific category of p16/Ki-67 dual staining result divided by the number of test results in specific category)

TABLE 2. Individual comparison of p16/Ki-67 agreement and performance between students, senior technologist and reference

Training	Reviewers	OPA	McNemar's test p	κ (cohen) (95% CI)
Initial training (N = 118)	S1/Reference	81.4%	0.000	0.512 (CI: 0.329–0,696)
	S2/Reference	81.4%	0.006	0.527 (CI: 0.349–0,705)
	SC (S1)/ Reference	94.1%	0.131	0.859 (CI: 0.758–0.960)
	SC (S2)/ Reference	94.1%	0.131	0.859 (CI: 0.758–0.960)
	SC (S1)/SC (S2)	100.0%	/	1.000 (CI: /)
Addtional (N = 383)	S1/Reference	78.3%	0.000	0.556 (CI: 0.472–0.641)
	S2/Reference	87.2%	0.775	0.713 (CI: 0.638–0.788)
	SC (S1)/ Reference	86.2%	0.006	0.700 (CI: 0.625–0,775)
	SC (S2)/ Reference	86.4%	0.004	0.707 (CI: 0.632–0.781)
	SC (S1)/SC (S2)	98.7%	1.000	0.973 (CI: 0.949–0.996)

N = number of cases; OPA = overall percent agreement; S1 = student 1; S2 = student 2; SC (S1) = senior cytotechnologist results obtained during revision of student 1 results; SC (S2) = senior cytotechnologist results obtained during revision of student 2 results; SC1/SC2 = intra-observer variability; Reference = results of four cytopathologists at the Deptment of Cytopathology, Institute of Oncology Ljubljana; * Scale for interpretation of κ values = below 0.20 (poor), 0.21-0.40 (fair), 0.41-0.60 (moderate), 0.61-0.80 (good), >0.81 (very good)[10]

p16/Ki-67 dual staining results and agreement

In primary and secondary evaluation both students (S1 and S2) had more positive p16/Ki-67 DS results compared to the reference (Table 1). However, in secondary evaluation, S2 had less positive results (33.7%) compared to the outcome in primary evaluation. Her percentage of positive results was even closer to the reference results (29.8%) than that of SC (37.9%). All evaluators used the suspicious category sparsely, only 0.3–5.9% of results fell into this category.

In primary evaluation, the agreement of DS results between reference and each of the students was moderate, while the agreement between reference and SC was very good. However, S2 reached good agreement in secondary evaluation which even slightly surpassed the agreement result between SC and the reference (Table 2). The agreement between S1 and the reference remained mod-

erate. Intra-observer variability between the two evaluations performed by the SC after each student was very good in primary, as well as in secondary evaluation (Table 2).

Accuracy of p16/Ki-67 results

Reference results showed higher sensitivity and positive predictive value for CIN2+ in primary compared to secondary evaluation (92.8% *vs.* 87.0% and 80.0% *vs.* 52.8%, respectively) (Supplementary Table 1, Figure 2). Specificity and negative predictive value for CIN2+ were lower in primary compared to secondary evaluation (67.3% *vs.* 80.4% and 86.8% *vs.* 96.1%, respectively).

In primary evaluation, the results of both students had slightly higher sensitivity and negative predictive values for CIN2+ but much lower specificity and positive predictive values compared to reference results (Supplementary Table 1, Figure 2, Figure 3). While students preformed similarly in terms of sensitivity and specificity after initial training, after additional training the results of S2 were closer to the results of the reference compared to the results of S1. In secondary evaluation, S2 even reached higher sensitivity and specificity than SC (84.4% *vs.* 83.1% and 78.8% *vs.* 72.2%, respectively). S1 had the highest sensitivity in both evaluations (97.1% and 87.0%) combined with the lowest specificity (36.7% and 63.7%, respectively) among all evaluators. The specificity of S1 was significantly lower than the reference's in both primary and secondary evaluation. Her specificity came close to the specificity of the reference after evaluating approximately 250 slides. However, after this point her performance started to decline (Figure 3).

Screening time

S1 evaluated 501 slides in 96 hours and 40 minutes while S2 needed 95 hours and 56 minutes for evaluating all the slides. In primary evaluation S1 needed less screening time

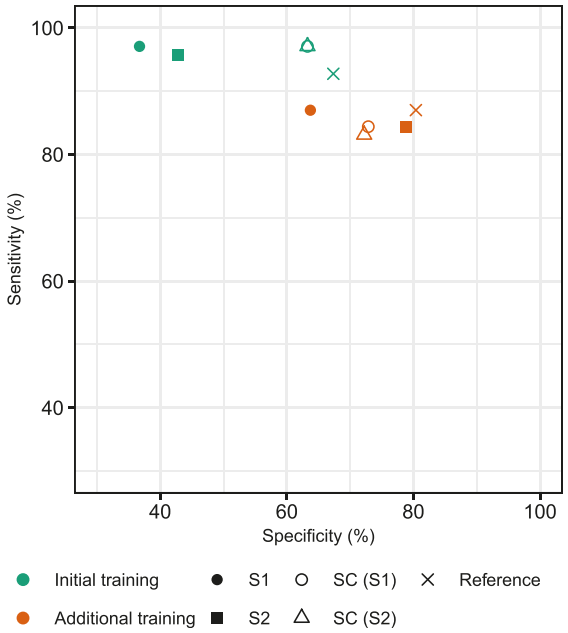

FIGURE 2. Sensitivity and specificity of p16/Ki-67 dual immunocytochemical staining (DS) for detecting CIN2+ for both students and the teacher (senior cytotechnologist).

S1= student 1; S2 = student 2; SC (S1) = senior cytotechnologist – slide review after S1; SC (S2) = senior cytotechnologist – slide review after S2

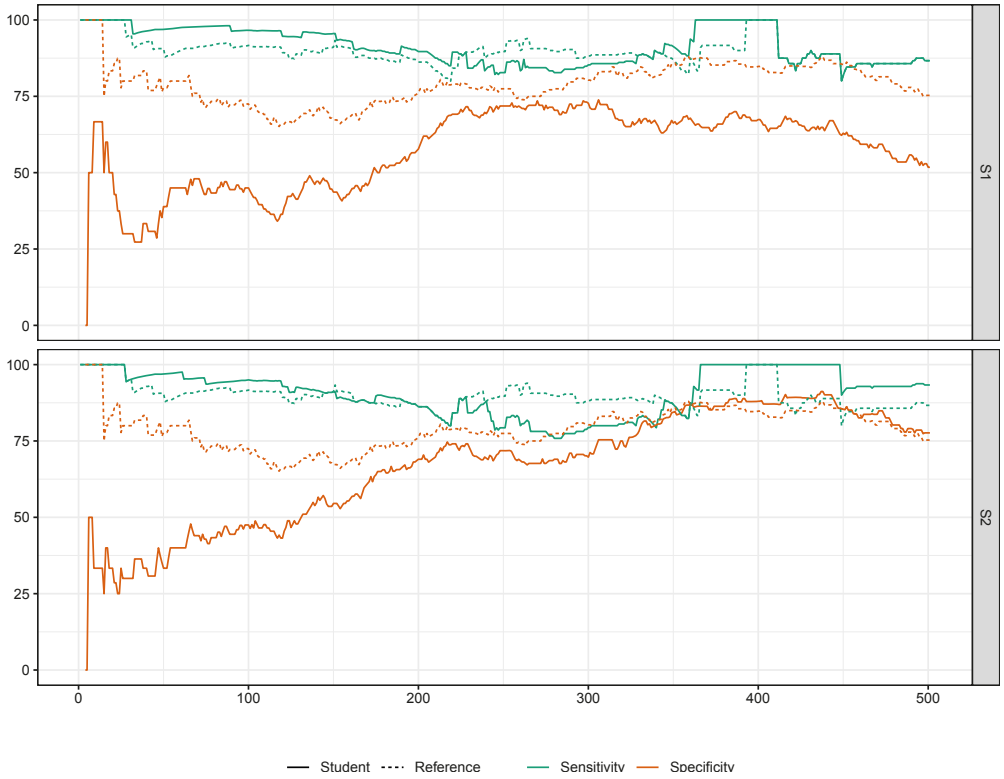

FIGURE 3. Sensitivity and specificity for the results of both students and the reference according to the number of evaluated slides.

S1 = student 1; S2 = student 2

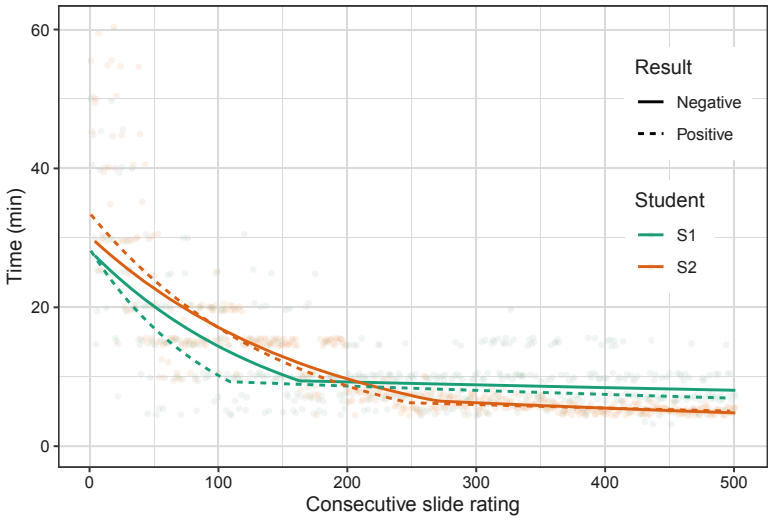

FIGURE 4. Joinpoint regression analysis of students' screening times.

S1 = student 1; S2 = student 2

per slide (18.8 min; SD 10.3) compared to S2 (24.2 min; SD 13.0; $p < 0.001$). In secondary evaluation, the screening times decreased for both students, however, S1 now needed more time (9.3 min; SD 3.9) compared to S2 (7.6 min; SD 3.5; $p < 0.001$). At the end of the training, during the evaluation of the last 100 slides, the average time of two students was 6.7 minutes per slide. However, the difference between them was statistically significant (S1: 8.2 min *vs.* S2: 5.2 min; SD 2.8 and 0.4, respectively; $p < 0.001$).

Joinpoint regression analysis of screening times of S1 showed the joinpoint at 163rd slide for negative slides. There was a 0.7% decrease per each slide ($p < 0.05$) in the first segment and 0.0% decrease in the second segment. The joinpoint for positive slides was at 109th slide with 1.0% decrease per slide ($p < 0.05$) in the first segment and 0.1% decrease ($p < 0.05$) in the second segment (Figure 4). For S2, the joinpoint for negative slides was at 207th slide with 0.6% decrease per slide ($p < 0.05$) in the first segment and 0.1% decrease ($p < 0.05$) in the second segment. The joinpoint for positive slides in case of S2 was at 248th slide with 0.6% decrease ($p < 0.05$) in the first segment and 0.1% decrease ($p < 0.05$) in the second segment.

Discussion

The results of our study confirmed that the training protocol we have used was adequate for teaching the interpretation of p16/Ki-67 DS. At the end of the training one student was competent for independent DS interpretation as evidenced by comparable accuracy results and by good agreement between her results and those of the reference. Towards the end of the training this student needed 5.2 min for evaluating one slide. The training protocol is suitable also for monitoring the performance of the teacher.

We do not have an explanation as to why the results of the other student showed a statistically significant difference in agreement and accuracy when compared to the results of the reference. Since environmental factors were the same for both students, it seems that internal factors played an important role in performance difference. It is well known that interpreting slides is partly a subjective method. Furthermore, in our previous study we demonstrated a number of reasons that contributed significantly to the difficulty of DS interpretation.[6] Weak p16 staining, less preserved cell morphology and strong background staining were important drawbacks of decision making. Similar observations were also made by McMenamin *et al.*[4] and Benevolo *et al.*[5] An additional important information from our previous study was also the fact that 45% of cases which were marked as suspicious for p16/Ki-67 positivity had only one such cell.[6] Therefore, this type of training is not suitable for every person without prior knowledge of DS evaluation. However, by monitoring student's results, we can assess if additional experience to reach the necessary expertise is needed.

Most articles which describe agreement and accuracy of DS interpretation among observers briefly mention the training program they have used. Only the training programs in three studies had some similarities with our own.[1,2,3] However, the initial training provided by the manufacturer is not described in detail in any of them. The secondary training can be compared to ours because it consisted of reviewing a certain number of slides (80, 150 and 469) and of discussing discrepant cases of the first viewing. In the second reading, Allia *et al.*[3] mention evaluation of 350 new slides, while Wentzesen *et al.*[2] used 480 new slides, however, not all reviewers red all of them. In the study of Waldstrom *et al.*[1] they randomly selected 185 slides from set of 469 slides from the first reading. Only the study of Allia *et al.*[3] included three evaluators inexperienced in cervical cytology (two medical students and one biologist) in addition to the four experienced ones.

Unfortunately, we can compare our results to those of Allia *et al.*[3] only to a limited extent due to

differences in methodology. Allia *et al.* compared agreement between results of four evaluators with experience in DS evaluation and between results of three evaluators without experience. Agreement improved after additional training in each group. In our study, the population of 118 women from the first arm of the study had a higher percentage of histologically confirmed CIN2+ compared to the population of 383 women in the second arm (58.5% *vs.* 20.1%). This difference in the prevalence of the disease has to be taken into account when comparing the results of primary and secondary evaluation, especially Kappa values and predictive values of a test. In the Allia's *et al.* paper, the study population contained 14.7% of women with histological diagnoses of CIN2+.[3] Since the populations of women in the two studies were not totally alike, we can compare only the end results indirectly. At the end of Allia's *et al*. study, the specificity of DS for CIN2+ was 66.7% for the experienced evaluators, while the students reached a specificity of 60.5%, a difference of 5.2% points. On the basis of these data Allia *et al*. concluded that DS evaluation "can be performed even by staff not trained in the morphological interpretation of cytology" after a short training phase.[3] At the end of our study the difference in specificity between the reference and the successful student was 1.6% points and 16.7% points for the unsuccessful student. Therefore, we agree with Allia *et al.* that it is possible to perform DS evaluation with personnel not experienced in cervical cytology, however, not after a short training period.

If we translate 97 hours needed for reviewing 501 slides into 12 days with an eight-hour working day, the whole training period in our study would last 19 days. The evaluation of slides after initial training, as well as partly after additional training, has to be considered part of the learning process. This is clearly demonstrated in the graph of continual monitoring of the students' accuracy results. For the successful student the specificity continued rising during the evaluation of the first 118 slides. It continued to rise also for a period after the secondary training until approximately the time when the student evaluated roughly 350 slides altogether. At this point the accuracy results of the student were very similar to the results of the reference (same sensitivity, 87.0%) and slightly lower specificity (84.4 *vs.* 85.7%). The rest of the time used in the evaluation of the last 150 slides was necessary for monitoring the student's performance. The necessity of such action has proven to be correct in the case of the other student. Her accuracy results came close to those of the reference after she evaluated approximately 250 slides, however, her performance started to decline afterwards.

For monitoring the students' progress in DS evaluation it is advisable to use more than one criterion of successfulness. Using only agreement between the students and the reference will be reliable only when positive and negative predictive values of the reference results are high. However, these values depend partly on the percentage of CIN2+ cases within the population of women from which samples for DS evaluation originate. Therefore, comparing accuracy results between students and reference is beneficial because it will demonstrate more exactly where a particular student has difficulties in DS interpretation. For example, high sensitivity and low specificity point to the fact that a student is signing too many cases as positive. An additional measure of a student's successfulness is also the time needed to evaluate one slide.

Since both students were inexperienced in DS evaluation it is reasonable that the time needed to evaluate one slide was progressively decreasing. The decrease was sharper towards the beginning and less pronounced latter on. In addition to the agreement and the accuracy results, time needed for evaluating one slide also showed the difference between the two students. The ultimately unsuccessful student reached faster the point after which her time per slide started to decrease very slowly, compared to the successful student. However, during the evaluation of the last 100 slides, the successful student needed significantly less average time per slide compared to the other student (5.2 min *vs.* 8.2 min). Only McMenamin *et al.* made a quick mention of the time needed per slide evaluation.[4] They reported that their experienced DS evaluators needed less than 1 minute for evaluating a clearly positive slide and 3-4 min for more challenging ones. Their evaluation time per slide is shorter than in our study not only because our students were unexperienced but mainly because we used conventional smears while in the study of Mc Menamin *et al.* ThinPrep specimens were used.[4]

In addition to teaching DS interpretation to students, our training program was designed also to monitor the performance of the cytotechnologist involved in the teaching process. We believe that teacher monitoring is an important element of the training program which helps to assure the students will receive the best training. The intra-observer agreement was within the range of "very good" in both arms of our DS evaluation (OPA 100.0% and 98.7%, kappa 1.000 and 0.937, respec-

tively). This result is even slightly better than the results obtained by McMenamin *et al.*[4] where agreement for three cytotechnologists was 82.8% (0.65), 83.8% (0.67) and 94.9%, (0.91), respectively.

Conclusions

In conclusion we would like to say that teaching p16/Ki-67 interpretation should be a closely monitored process in which students' results have to be compared to the reference results with known accuracy for CIN2+. The students' progress has to be monitored using several criteria like agreement, accuracy and time needed for evaluating one slide. The monitoring process has to continue for a while after students reach satisfactory results in order to assure a continuous good performance. Monitoring of teacher's performance is also advisable.

References

1. Waldstrøm M, Christensen RK, Ørnskov D. Evaluation of p16 INK4a/Ki-67 dual stain in comparison with an mRNA human papillomavirus test on liquid-based cytology samples with low-grade squamous intraepithelial lesion. *Cancer Cytopathol* 2013; **121:** 136-45. doi: 10.1002/cncy.21233

2. Wentzensen N, Fetterman B, Tougawa D, Shiffman M, Castle PE, Wood SN, et al. Interobserver reproducibility and accuracy of p16/Ki67 dual-stain cytology in cervical cancer screening. *Cancer Cytopathol* 2014; **122:** 914-20. doi: 10.1002/cncy.21473

3. Allia E, Ronco G, Coccia A, Luparia P, Macrì L, Fiorito C, et al. Interpretation of p16INK4a/Ki-67 dual immunostaining for the triage of human papillomavirus-positive women by experts and nonexperts in cervical cytology. *Cancer Cytopathol* 2015; **123:** 212-8. doi: 10.1002/cncy.21511

4. McMenamin M, McKenna M, McDowell A, Dawson C, McKenna R. Intra- and inter-observer reproducibility of CINtecR PLUS in ThinPrep cytology preparations. *Cytopathology* 2017; **28:** 284-90. doi: 10.1111/cyt.12426

5. Benevolo M, Allia E, Gustinucci D, Rollo F, Bulletti S, Cesarini E, et al. Interobserver reproducibility of cytologic p16INK4a /Ki-67 dual immunostaining in human papillomavirus-positive women. *Cancer Cytopathol* 2017; **125:** 212-20. doi: 10.1002/cncy.21800

6. Kloboves Prevodnik V, Jerman T, Nolde N, Repše Fokter A, Jezeršek J, Pohar Marinšek Ž, et al. Interobserver variability and accuracy of p16/Ki-67 dual immunocytochemical staining on conventional cervical smears. *Diagn Pathol* 2019; **14:** 1-9. doi: 10.1186/s13000-019-0821-5

7. Ivanus U, Jerman T, Fokter AR, Takac I, Prevodnik VK, Marcec M, et al. Randomised trial of HPV self-sampling among non-attenders in the Slovenian cervical screening programme ZORA: comparing three different screening approaches. *Radiol Oncol* 2018; **52:** 399-412. doi: 10.2478/raon-2018-0036

8. R Core Team. *The R project for statistical computing*. Vienna, Austria: R Foundation for Statistical Computing; 2019. [cited 2019 Dec 15]. Avalable at http://www.R-project.org/

9. National Cancer Institute. *Joinpoint Trend Analysis Software.* Joinpoint Regression Program, Version 4.6.0.0 - April 2018; Statistical Methodology and Applications Branch, Surveillance Research Program.

10. Altman DG. *Practical statistics for medical research*. Boca Raton: Chapman and Hall/CRC; 1991.

research article

Care of patients with non-small-cell lung cancer stage III – the Central European real-world experience

Milada Zemanova[1], Robert Pirker[2], Lubos Petruzelka[1], Zuzana Zbozínkova[3], Dragana Jovanovic[4], Mirjana Rajer[5], Krisztina Bogos[6], Gunta Purkalne[7], Vesna Ceriman[4], Subhash Chaudhary[8], Igor Richter[9], Jirí Kufa[10], Lenka Jakubikova[11], Marius Zemaitis[12], Marketa Cernovska[13], Leona Koubkova[14], Zdenka Vilasova[15], Karin Dieckmann[16], Attila Farkas[17], Jelena Spasic[18], Katerina Fröhlich[3], Andreas Tiefenbacher[2,] Virag Hollosi[6], Juraj Kultan[10], Iveta Kolarová[15], Jiri Votruba[1]

[1] 1st Faculty of Medicine of Charles University in Prague, Czech Republic
[2] Department of Medicine I, Medical University of Vienna, Vienna, Austria
[3] Institute of Biostatistic and Analyses, Faculty of Medicine, Masaryk University, Brno, Czech Republic
[4] Clinic for Pulmonology, Clinical Centre of Serbia, Belgrade, Serbia
[5] Institute of Oncology, Ljubljana, Slovenia
[6] National Koranyi Institute of TB and Pulmonology, Budapest, Hungary
[7] Pauls Stradins Clinical University Hospital, Riga, Latvia
[8] Comprehensive Oncology Center, Nový Jičín, Czech Republic
[9] Comprehensive Oncology Center, Liberec, Czech Republic
[10] Clinic for Pneumology & Tuberculosis, Faculty of Medicine, Palacký University, Olomouc, Czech Republic
[11] Clinic for Pneumology & Tuberculosis, Faculty of Medicine, Masaryk University, Brno, Czech Republic
[12] Hospital of LUHS Kauno Klinikos, Kauno, Lithuania
[13] Thomayer Hospital, Prague, Czech Republic
[14] Department of Pulmonology, University Hospital Motol, Prague, Czech Republic
[15] Comprehensive Oncology Center and Multiscan, Pardubice, Czech Republic
[16] Department of Radiotherapy, Medical University of Vienna, Vienna, Austria
[17] Department of Thoracic Surgery, Semmelweis University, Budapest, Hungary
[18] Institute for Oncology and Radiology of Serbia, Belgrade, Serbia

Radiol Oncol 2020; 54(2): 209-220.

Received 9 January 2020
Accepted 14 April 2020

Correspondence to: Milada Zemanová, Oncology VFN, U Nemocnice 2, 128 08, Prague, Czech Republic. E-mail: milada.zemanova@vfn.cz

Disclosure: No potential conflicts of interest were disclosed.

Background. Management of non-small-cell lung cancer (NSCLC) is affected by regional specificities. The present study aimed at determining diagnostic and therapeutic procedures including outcome of patients with NSCLC stage III in the real-world setting in Central European countries to define areas for improvements.

Patients and methods. This multicentre, prospective and non-interventional study collected data of patients with NSCLC stage III in a web-based registry and analysed them centrally.

Results. Between March 2014 and March 2017, patients (n=583) with the following characteristics were entered: 32% females, 7% never-smokers; ECOG performance status (PS) 0, 1, 2 and 3 in 25%, 58%, 12% and 5%, respectively; 21% prior weight loss; 53% squamous carcinoma, 38% adenocarcinoma; 10% EGFR mutations. Staging procedures included chest X-ray (97% of patients), chest CT (96%), PET-CT (27%), brain imaging (20%), bronchoscopy (89%), endobronchial ultrasound (EBUS) (13%) and CT-guided biopsy (9%). Stages IIIA/IIIB were diagnosed in 55%/45% of patients, respectively. N2/N3 nodes were diagnosed in 60%/23% and pathologically confirmed in 29% of patients. Most patients (56%) were treated by combined modalities. Surgery plus chemotherapy was administered to 20%, definitive chemoradiotherapy to 34%, chemotherapy only to 26%, radiotherapy only to 12% and best supportive care (BSC) to 5% of patients. Median survival and progression-free survival times were 16.8 (15.3;18.5) and 11.2 (10.2;12.2) months, respectively. Stage IIIA, female gender, no weight loss, pathological mediastinal lymph node verification, surgery and combined modality therapy were associated with longer survival.

Conclusions. The real-world study demonstrated a broad heterogeneity in the management of stage III NSCLC in Central European countries and suggested to increase the rates of PET-CT imaging, brain imaging and invasive mediastinal staging.

Key words: diagnostic procedures; multimodality treatment; non-small-cell lung cancer; stage III

Introduction

Management of locally advanced (stage III) non-small cell lung carcinoma (NSCLC) includes a broad spectrum of diagnostic procedures and therapeutic modalities. Diagnosis is primarily based on computer tomography (CT) scan of chest plus upper abdomen and brain, bronchoscopy and CT-guided biopsies. For more precise exclusion of distant metastases, the evaluation with PET-CT is useful. Detailed locoregional staging is done by means of PET-CT[1], endobronchial or endoscopic ultrasound (EBUS/EUS), mediastinoscopy, thoracoscopy, mediastinotomy or other biopsies of suspected nodal lesions in order to distinguish early stages (stages I and II) from stage IIIA/IIIB.[2]

Treatment of NSCLC stage III requires multidisciplinary co-operation in order to deliver appropriate local and systemic therapies for the various subgroups. Occurrence of distant metastases with and without local progression is frequent, thereby leading to 5-year survival rates often less than 20%.[3] According to the 7th edition of the TNM classification[3] stage III was subdivided into stage IIIA and IIIB. The 5-year survival rates were 36% and 19%, respectively.[4] According to the 8th edition, stage III is divided into IIIA, IIIB and IIIC. The 5-year survival rates are 36%, 26% and 13%, respectively.[4] In operable stage IIIA, induction or adjuvant chemotherapy improve overall survival[5,6] and are established as standard treatments. Important prognostic factors associated with prolonged survival are pathological down-staging of mediastinal lymph nodes and/or primary tumors, and complete tumour resection.[7-10] Some trials assessing induction therapy followed by surgery have also included patients with stage IIIB disease and suggested that patients with operable stage IIIB NSCLC have outcomes similar to those with stage IIIAN2 disease.[11] For patients with inoperable stage IIIA or stage IIIB and good performance status (PS), definitive chemoradiotherapy is the treatment of choice.[2] Concurrent chemoradiotherapy is associated with longer survival at increased toxicity compared to the sequential approach.[12] Radiotherapy dose escalation has no clear benefit.[13] Sequential chemoradiotherapy or radiotherapy alone remain options for selected patients.[2] Consolidation therapy with durvalumab after concurrent chemoradiotherapy has recently been shown to improve survival of patients[14] and has been established as standard treatment.

There is evidence that management of NSCLC stage III varies between countries, geographical regions, cancer centres and even treating physicians. Reasons for these variations include differences in regional standards, access to diagnostic procedures as well as therapeutic modalities, and resources. The aim of the present study was to determine diagnostic and therapeutic procedures as well as clinical outcome including survival of patients with NSCLC stage III in the real-world setting in Central European countries and to define areas for future improvements in routine management of these patients.

Patients and methods

Patients

The present study was prospective, observational, non-interventional, multicentric, multinational and registry based. The study had been approved by ethics committees of participating centres and was performed in accordance with the Declaration of Helsinki. Study entry criteria were patients of any age, histological and/or cytological diagnosis of NSCLC stage III according to 7th edition of the TNM classification[3] and signed written informed consent. The study allowed enrolling patients who have been treated between March 2014 and March 2017. Follow-up of patients continued until February 2018.

Data collection

Registration of all data was fully anonymous and performed in an electronic case report form (CRF [eCRF]) by qualified personnel. Patient identification was in the responsibility of each investigator. The following data were collected: age, gender, race, smoking status, PS, weight loss, date of NSCLC diagnosis, histology and mutational status of tumors, staging procedures, method of mediastinal lymph-node examination, TNM and tumor stage. Data collected on therapeutic procedures were primary therapy, surgical procedures (date, extent, completeness of resection, information on repeated resections), thoracic radiotherapy (date, dose, fractions, technique, energy), prophylactic cranial irradiation, and chemotherapy (dates of start and end, number of cycles, cytotoxic drugs). Combined modality therapy was assessed according to investigator statement and/or dates of overlapping therapies. Type of best treatment response, date of recurrence or progression, and dates of death were collected.

TABLE 1. Patient characteristics

Characteristic	IIIA (N = 321)	IIIB (N = 262)	IIIA + IIIB (N = 583)	P *
	N (%)	N (%)	N (%)	
Age				
< 65 years	155 (48.3)	117 (44.7)	272 (46.7)	
≥ 65 years	166 (51.7)	145 (55.3)	311 (53.3)	
Mean ± SD (years)	64.8 ± 10.5	65.1 ± 10.1	64.9 ± 10.3	0.429
Median (years)	65.4	66.0	65.6	
Gender				
Female	92 (28.7)	96 (37.0)	188 (32.2)	
Male	229 (71.3)	166 (63.6)	395 (67.8)	0.050
Smoking status				
Current smoker	161 (50.2)	147 (56.3)	308 (52.8)	
Former smoker	127 (39.6)	92 (35.2)	219 (37.6)	
Never smoker	26 (8.1)	16 (6.1)	42 (7.2)	
Unknown	7 (2.2)	7 (2.7)	14 (2.4)	0.446
Weight loss ≥10% within prior three months				
No	243 (75.7)	163 (62.5)	406 (69.6)	
Yes	50 (15.6)	70 (26.8)	120 (20.6)	
Unknown	28 (8.7)	29 (11.0)	57 (9.8)	<0.001
WHO performance status				
0	86 (26.8)	60 (23.0)	146 (25.0)	
1	194 (60.4)	144 (54.9)	338 (58.0)	
2	31 (9.7)	41 (15.7)	72 (12.3)	
3	10 (3.1)	17 (6.5)	27 (4.6)	0.025
Histology				
Squamous cell carcinoma	176 (54.8)	133 (51.0)	309 (53.0)	
Adenocarcinoma	115 (35.8)	105 (40.0)	220 (37.7)	
NSCLC NOS	18 (5.6)	18 (6.9)	36 (6.2)	
Other	12 (3.7)	6 (2.3)	18 (3.1)	0.477

* = Chi-square test for IIIA *vs.* IIIB; NOS = not otherwise specified; NSCLC = non-small-cell lung cancer; SD = standard deviation

Statistical analyses

Descriptive statistics and frequency tables were used to characterize the sample data set. Statistical significances of differences for categorical and continuous parameters were assessed by means of Fisher's exact test and Mann-Whitney test, respectively. Overall survival (OS) was defined as the time from treatment initiation until death of any cause. Progression-free survival (PFS) was defined as the time from treatment initiation until first documented progression and/or death of any cause. Patients without an event were censored at the time of last follow-up visit. Patients lost to follow-up were counted as interval-censored observations. The assumption was made that patients were lost to follow-up due to their treatment failure and that, therefore, no information is available about them. Interval set (interval between visits) was 6 months.[15] PFS and OS were estimated by Kaplan-Meier analysis and 95% confidence intervals (95% CI) were provided for all point estimates. Statistical significance of differences in survival between the subgroups was assessed by means of the log-rank test. The multivariable Cox proportional hazard model was used to evaluate the effects of potential prognostic factors on survival measures. Hazard ratios (HR) were complemented with 95% confidence intervals and supported with significance levels. Overall response rate (ORR) was defined as the sum of complete response rate (CR) and partial response rate (PR) and disease control rate as ORR plus stable disease rate (SD). All statistical tests were performed at the significance level of P = 0.05.

Results

Patients

A total of 617 patients were enrolled but 34 patients were excluded due to various violations of the study protocol. Thus the study population comprises 583 patients from 16 centres of seven Central European countries: eight centres from Czech Republic (269 patients), two centres from Serbia (109 patients), two centres from Hungary (48 patients) and one centre each from Slovenia (53 patients), Latvia (43 patients), Lithuania (38 patients) and Austria (23 patients). The date for final analysis was February 19, 2018. Minimum follow-up since initial diagnosis was 11 months. Patient characteristics are shown in Table 1: 53.3% aged ≥

TABLE 2. Diagnostic procedures

Procedure	Patients (N = 583)	
	N (%)	range of % in centres
Chest CT scan	567 (97)	67 – 100
Chest X-ray	559 (96)	79 – 100
Bronchoscopy	521 (89)	65 – 100
Upper abdominal CT scan	389 (67)	0 – 100
Upper abdominal US	160 (27)	2 – 87
PET-CT or PET scan	163 (28)	0 – 78
Brain CT or MRI	117 (20)	0 – 91
Bone scan	88 (15)	0 – 79
EBUS or EUS	80 (14)	0 – 71
CT-guided biopsy	54 (9)	0 – 31
VATS	19 (3)	0 – 35
Mediastinoscopy	13 (2)	0 – 13
Others	47 (8)	0 – 30

EBUS = endobronchial ultrasound; EUS = endoscopic ultrasound; VATS = video-assisted thoracoscopic surgery

TABLE 3. TNM subgroups (*Union for International Cancer Control* [UICC] 7)

TNM	Total patient population	Patients undergoing surgery		
	N (%)	N	% of total population	% in stage subgroup
IIIA+IIIB	**583 (100)**	**135**	**32.2**	**NA**
IIIA	**321 (55.1)**	**119**	**20.4**	**37.1**
T4N0	33 (5.7)	10	1.7	30.3
T3N1	39 (6.7)	16	2.7	41.0
T4N1	26 (4.5)	7	1.2	26.9
T1N2	25 (4.3)	14	2.4	56.0
T2N2	98 (16.8)	45	7.7	45.9
T3N2	100 (17.2)	27	4.6	27.0
IIIB	**262 (44.9)**	**16**	**2.8**	**6.1**
T4N2	129 (22.2)	15	2.6	11.6
T1N3	17 (2.9)	0	0	0
T2N3	32 (5.5)	1	0.2	3.1
T3N3	29 (5.0)	0	0	0
T4N3	55 (9.4)	0	0	0
T stage				
T1	42 (7.2)	14	2.4	33.3
T2	130 (22.3)	46	7.9	35.4
T3	168 (28.8)	43	7.4	25.6
T4	243 (41.7)	32	5.5	13.1
N stage				
N0	33 (5.7)	10	1.7	30.3
N1	65 (11.1)	23	3.9	35.4
N2	352 (60.4)	101	17.3	28.7
N3	133 (22.8)	1	0.2	0.8

NA = not applicable

65 years, 32.2% females, 7.2% never-smokers, 20.6% weight loss (≥ 10% within prior three months), 83% PS WHO 0–1. Stages IIIA and IIIB were diagnosed in 321 (55.1%) and 262 (44.9%) patients, respectively. Females, patients with weight loss and patients with poor PS were slightly more frequent among patients with stage IIIB. Squamous cell carcinomas were diagnosed in 309 (53.0%) patients, adenocarcinomas in 220 (37.7%) patients, NSCLC not otherwise specified in 36 (6.2%) patients, and other types (e.g. adeno-squamous, large cell) in 18 (3.1%) patients. Results of molecular analyses were documented for 150 (25.7%) patients (data not shown). EGFR mutations were detected in 14/142 (9.9%) patients, KRAS mutations in 11/31 (35.5%) patients and ALK aberrations in 2/88 (2.3%) patients (data not shown).

Staging procedures

Diagnostic and staging procedures are summarized in Table 2. Widely used procedures were chest x-ray (96%), chest CT scan (97%), bronchoscopy (89%) and upper abdominal CT scan (67%). PET-CT or PET were performed in 28% of patients. Brain imaging by means of CT or MRI was done in 20% of patients. EBUS or EUS were performed in 14% of patients, CT-guided biopsy in 9%, video-assisted thoracoscopic surgery (VATS) in 3%, and mediastinoscopy in 2%. Other procedures included diagnostic thoracotomy in 5%, radical thoracic surgery with gain of histology in 1%, ultrasonography (other than abdominal) (1%) and extracranial MRI examinations. The frequencies of the procedures showed great variations between centres with particularly great variations for PET or PET-CT (0–78%), brain imaging (0–91%) and EBUS/EUS (0–71%) (Table 2).

Stage IIIA and stage IIIB were diagnosed in 55.1% and 44.9% of patients, respectively (Table 1). Subgroups based on T and N descriptors are shown in Table 3. Stages T1–T3 were found in 340 patients (58.3%) mostly having N2 or N3 nodal stage in 301 (51.6%) patients. T4N0, T4N1 and T4N2 tumours were found in 33 (5.7%), 26 (4.5%) and 129 (22.2%) patients, respectively. T3N3 and T4N3 tumours were diagnosed in 29 (5%) and 55 (9.4%) patients, respectively. T3–4N3 tumours (stage IIIC according to 8th TNM classification) were diagnosed in 84 (14.4%) patients. N2 or N3 lymph nodes were found in 485 (83.2%) patients. Histopathological involvement of mediastinal lymph nodes was confirmed in 172 (29.5%) patients by surgery (96 patients), transbronchial biopsy (58 patients), medias-

tinoscopy (11 patients) or other types of biopsy (10 patients) (data not shown).

Treatment

Therapeutic modalities are shown in overview for the total study population in Figure 1, for patients with stage IIIA and those with IIIB in detail in Table 4. Time from diagnosis to treatment initiation ranged from 0 to 369 (median 23) days. Combined therapies of any type were delivered to 326 (55.9%) patients. With regard to a single treatment modality only, surgery was delivered to 1.5% thoracic radiotherapy to 11.8%, chemotherapy to 25.7% and best supportive care (BSC) to 5.0% of patients of the total study population. Prophylactic cranial irradiation was not delivered to any patient.

Surgery was performed in 135 (23.2%) patients (119 IIIA, 16 IIIB) and resulted in radical tumour resection in 121 patients and explorative surgery or non-radical resections in 14 patients (Table 4 and Figure 1). The types of surgery included lobectomy (77 patients), bi-lobectomies (6 patients), pneumonectomy (32 patients) and atypical radical resections (6 patients) (Table 4). Surgery was delivered as single modality (nine patients), in combination with chemotherapy (77 patients) or radiotherapy (eight patients) or as trimodality therapy (41 patients). Adjuvant chemotherapy was about twice as frequent as pre-operative chemotherapy among patients undergoing surgery.

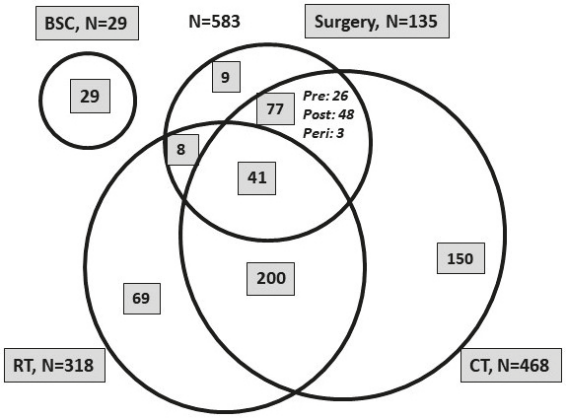

BSC = best supportive care; CT = chemotherapy; pre = preoperative; post = postoperative; peri = perioperative; RT = radiotherapy

FIGURE 1. Treatment modalities and combinations.

TABLE 4. Therapeutic modalities and combinations

Therapeutic modalities	IIIA (N=321)	IIIB (N=262) N (%)	IIIA+IIIB (N=583)
Any combination	**207 (64.5)**	**119 (45.4)**	**326 (55.9)**
Surgery	**119 (37.1)**	**16 (6.1)**	**135 (23.2)**
Surgery alone	9 (2.8)	0	9 (1.5)
Surgery plus radiotherapy	7 (2.2)	1 (0.4)	8 (1.4)
Surgery plus chemotherapy	70 (21.8)	7 (2.7)	77 (13.2)
Preoperative chemotherapy	22 (6.9)	4 (1.5)	26 (4.4)
Perioperative chemotherapy	3 (0.9)	0	3 (0.5)
Adjuvant chemotherapy	45 (14.0)	3 (1.1)	48 (8.2)
Surgery plus RT plus CT (trimodality)	33 (10.3)	8 (3.1)	41 (7.0)
Sequential preoperative RT plus CT	2 (0.6)	0	2 (0.3)
Concurrent preoperative RT plus CT	3 (0.9)	1 (0.4)	4 (0.7)
Sequential postoperative RT plus CT	23 (7.2)	3 (1.1)	26 (4.5)
Concurrent postoperative RT plus CT	5 (1.6)	4 (1.5)	9 (1.5)
Thoracic RT (including other modalities)	**174 (54.2)**	**144 (55.0)**	**318 (54.6)**
Radiotherapy alone	37 (11.5)	32 (12.2)	69 (11.8)
Chemoradiotherapy	**97 (30.2)**	**103 (39.3)**	**200 (34.3)**
Sequential	74 (23.1)	72 (27.5)	146 (25.0)
Concurrent	23 (7.2)	31 (11.8)	54 (9.3)
Chemotherapy (including other modalities)	**256 (79.7)**	**212 (80.9)**	**468 (80.3)**
Chemotherapy alone	58 (18.1)	92 (35.1)	150 (25.7)
Best supportive care alone	**9 (2.8)**	**20 (7.6)**	**29 (5.0)**
Type of surgery	**IIIA (N = 119)**	**IIIB (N = 16)**	**IIIA+IIIB (N = 135)**
Lobectomy	74 (62.3)	3 (18.7)	77 (57.0)
Bi-lobectomy	6 (5.0)	0	6 (4.5)
Pneumonectomy	28 (23.5)	4 (25.0)	32 (23.7)
Atypical radical resection	5 (4.2)	1 (6.2)	6 (4.5)
Non-radical surgery*	6 (5.0)	8 (50.0)	14 (10.4)

* = Non-radical surgery (n = 14) as biopsy (n = 4, all IIIB), exploration (n = 7, IIIA = 5, IIIB = 2) or palliative resection (n = 3, IIIA = 1, IIIB = 2); CT = chemotherapy; RT = radiotherapy

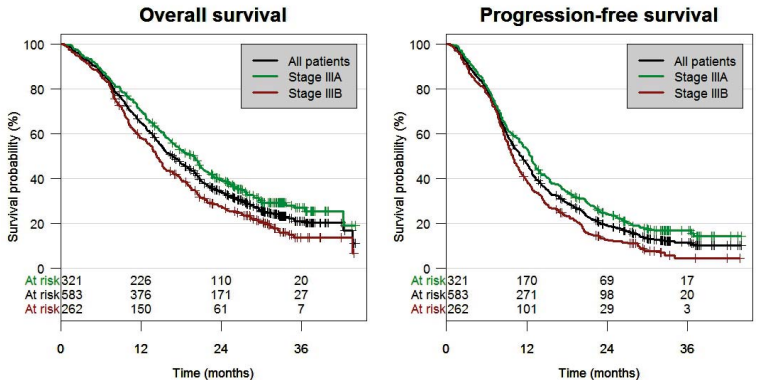

FIGURE 2. Overall survival and progression-free survival.

Thoracic radiotherapy was delivered to 318 (54.6%) patients with similar proportions among stage IIIA and stage IIIB (Table 4). Thoracic radiotherapy was delivered as single modality (69 patients), as definitive chemoradiotherapy (200 patients) and as trimodality therapy (41 patients). Among patients undergoing definitive chemoradiotherapy, the sequential administration was much more frequent than the concurrent one (146 *versus* 54 patients). Among patients undergoing trimodality therapy, concurrent chemoradiotherapy was delivered in 13 patients (Table 4).

Chemotherapy as the most frequent treatment modality was delivered to 468 (80.3%) patients with similar percentages among IIIA and IIIB (Table 4). Chemotherapy was the only treatment modality in 150 patients. Carboplatin was used in 43.6% and cisplatin in 37.4% of patients (data not shown). Platins were combined with vinorelbine (33%), gemcitabine (22%), etoposide (11%) or paclitaxel (11%). Pemetrexed was used in 7.7% of patients in stage IIIB and 2.5% in stage IIIA. Other drugs including docetaxel, vinblastine and bevacizumab were each used in less than 2% of patients. No relevant differences in chemotherapy protocols between stage IIIA and IIIB patients were seen (data not shown).

Treatment outcome

At a median follow-up time of 30 months, 154 (26.4%) patients were alive, 295 (50.6%) patients were dead and 134 (23%) patients were lost to follow-up. Among 334 patients evaluable for overall best response, complete remission, partial remis-

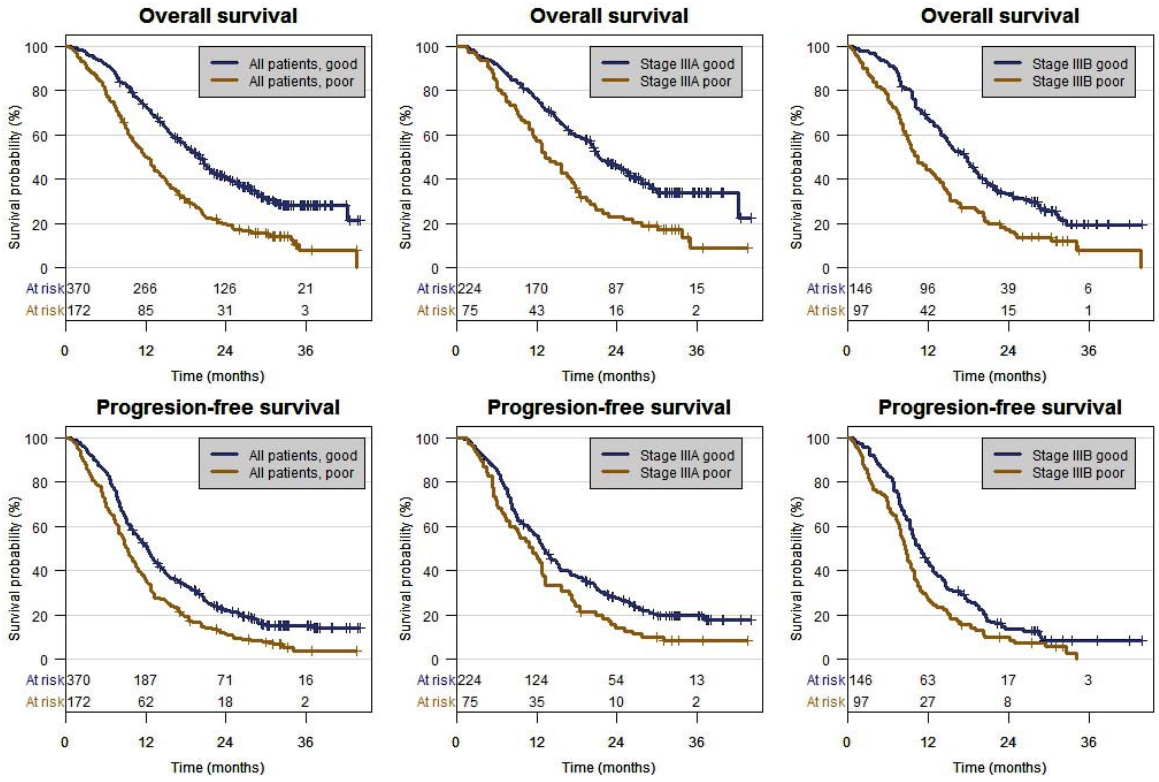

Good = PS 0/1 and no weight loss; poor = PS 2/3 and/or weight loss ≥10% within prior three months

FIGURE 3. Overall survival and progression-free survival by performance status and weight loss in all patients, stage IIIA and stage IIIB.

TABLE 5. Overall survival according to stage and treatment modalities

Characteristic	N	Median	1-year	2-year	3-year
		Months (95% CI)		% (95% CI)	
IIIA					
Total*	321	20.0 (17.1; 21.4)	70.7 (65.9; 75.9)	39.4 (34.3; 45.2)	27.0 (21.8; 33.3)
Good	223	21.4 (20.1; 25.8)	76.3 (70.9; 82.1)	45.6 (39.4; 52.8)	33.8 (27.7; 41.3)
Poor	75	13.3 (11.4; 17.7)	57.3 (47.2; 69.7	23.2 (15.2; 35.2)	9.1 (3.2; 26.0)
IIIB					
Total*	262	14.4 (13.0; 15.9)	58.2 (52.3; 64.5)	27.5 (22.5; 33.7)	13.5 (9.0; 20.2)
Good	146	17.8 (14.8; 19.6)	67.0 (59.8; 75.1)	33.1 (26.1; 42.0)	19.6 (13.2; 29.1)
Poor	97	10.4 (8.8; 19.6)	44.1 (35.2; 55.2)	17.3 (11.1; 27.0)	8.1 (3.0; 21.6)
T3N3 and T4N3**	84	11.6 (9.8; 15.9)	48.5 (38.8; 60.5)	22.6 (15.2; 33.8)	9.4 (3.9; 22.7)
IIIA+IIIB					
Total*	583	16.8 (15.3; 18.5)	65.1 (61.3; 69.1)	34.1 (30.4; 38.2)	21.0 (17.3; 25.4)
Good	369	20.1 (18.0; 21.5)	72.6 (68.2; 77.3)	40.7 (35.9; 46.2)	28.3 (23.6; 34.0)
Poor	172	11.8 (10.2; 14.2)	50.0 (42.9; 57.9)	19.9 (14.6; 27.0)	8.0 (3.6; 17.8)
Surgery					
All surgeries	135	29.0 (27.1; NA)	82.2 (76.0; 88.9)	60.6 (52.8; 69.6)	43.9 (35.2; 54.8)
Alone	9	13.9 (3.2; NA)	55.6 (31.0; 99.7)	22.2 (6.6; 75.4)	22.2 (6.6; 75.4)
Surgery plus CT or RT	85	27.8 (23.6; NA)	80.0 (71.9; 89.0)	57.2 (47.5; 68.9)	37.0 (26.7; 51.3)
Surgery plus adjuvant CT	77	28.3 (24.7; NA)	81.8 (73.6; 90.9)	60.6 (50.6; 72.7)	38.9 (28.0; 54.0)
Trimodality therapy	41	Not reached	92.7 (85.0; 100)	76.9 (64.7; 91.5)	64.8 (49.9; 84.2)
Non-surgical therapy					
All non-surgical	448	14.6 (13.7; 15.9)	59.9 (55.5; 64.7)	26.0 (22.1; 30.5)	13.8 (10.2; 18.8)
CT alone	150	12.7 (11.3; 13.9)	56.5 (49.1; 65.0)	19.1 (13.7; 26.8)	6.2 (2.7; 14.4)
RT alone	69	12.7 (9.6; 18.4)	52.2 (41.6; 65.4)	18.8 (11.6; 30.7)	11.8 (5.9; 23.5)
CRT all	200	19.6 (17.5; 21.6)	72.9 (67.0; 79.3)	36.9 (30.7; 44.5)	22.6 (16.1; 31.6)
CRT sequential	146	20.5 (17.2; 22.8)	75.2 (68.5; 82.5)	38.8 (31.5; 47.9)	23.5 (16.2; 34.0)
CRT concurrent	54	17.9 (14.6; 22.2)	66.7 (55.2; 80.5)	32.0 (21.6; 47.6)	22.5 (12.7; 39.9)
			HR (95% CI)	p-value	
IIIA *vs.* IIIB			0.70 (0.58; 0.85)	< 0.001	
IIIA Good *vs.* IIIA Poor			0.54 (0.40; 0.73)	< 0.001	
IIIB Good *vs.* IIIB Poor			0.57 (0.43; 0.76)	< 0.001	
IIIA *vs.* IIIB Good			0.86 (0.68; 1.09)	0.212	
Tri-modality *vs.* Surgery plus adjuvant CT			0.47 (0.25; 0.89)	0.021	
CRT sequential *vs.* concurrent			0.83 (0.57; 1.20)	0.326	

Good = performance status 0–1 and no weight loss; Poor = performance status 2–3 and/or weight loss ≥ 10%; CRT = chemoradiotherapy; CT = chemotherapy; RT = radiotherapy
* = Total is not sum of Good and Poor, as some patients had no data about weight loss;
** = Stage IIIC in *Union for International Cancer Control* [UICC] 8

sion, stable disease and progressive disease were seen in 27.5%, 35.9%, 24.9% and 11.7% patients, respectively. Information on progression during follow-up was available for 338 patients, while no information was available for the other patients due to death (171 patients) or loss to follow-up (74 patients). Eighty-two (24.3%) patients were without progression and 256 (75.7%) patients had progression, either local (40.2%), distant (26.6%) or both (8.9%). Progression after end of treatment was more frequent among patients with stage IIIB than those with stage IIIA (91.2% *versus* 81.6%).

Survival analyses

OS and PFS are shown in Table 5, Table 6 and Figure 2. Median OS was 16.8 months and the 3-year OS rate was 21%. Median PFS was 11.2 months and the 3-year PFS rate was 11.5%. OS and PFS were longer among patients with IIIA than among those with IIIB and the corresponding hazard ratios were 0.70 (95% CI 0.58–0.85; $p < 0.001$) and 0.71 (95% CI 0.59–0.85; $p < 0.001$), respectively (Table 5; Table 6). Among patients with stage IIIA, median OS was 20 months and the 3-year OS rate was 27%. The corresponding values for patients with stage IIIB were 14.4 months and 13.5%, respectively. Among patients with T3–4/N3 tumours who are classified as stage IIIC based on the 8th edition of the TNM classification, survival outcome (median OS 11.6 months; 3-year OS rate 9.4%) was worse than the outcome of patients with stage IIIB based on the 7th TNM classification.

OS and PFS were longer among patients with PS 0–1 and no weight loss (good prognostic group) than among those with PS 2–3 and/or weight loss ≥ 10% (poor prognostic group) (Table 5; Table 6; Figure 3). These differences were observed in the

TABLE 6. Progression free survival according to stage and risk groups

Characteristic	N	Progression-free survival			
		Median	1-year	2-year	3-year
		Months (95% CI)		% (95% CI)	
IIIA					
Total*	321	12.5 (11.3; 13.6)	52.9 (47.7; 58.7)	24.1 (19.8; 29.3)	16.8 (13.0; 21.7)
Good	223	12.9 (12; 15.2)	55.8 (49.6; 62.7)	27.6 (22.3; 34.3)	19.6 (14.8; 26.0)
Poor	75	11.4 (7.9; 13.2)	45.3 (35.4; 58.1)	14.2 (8.1; 25.0)	8.3 (3.8; 18.1)
IIIB					
Total*	262	9.9 (9.2; 10.8)	38.5 (33.1; 44.9)	12.8 (9.3; 17.7)	4.3 (1.8; 9.9)
Good	146	10.7 (9.6; 12.6)	43.8 (36.5; 52.6)	13.6 (9.0; 20.8)	8.6 (4.7; 15.5)
Poor	97	8.6 (7.8; 9.9)	26.8 (19.3; 37.2)	9.9 (5.4; 18.2)	0
T3N3 and T4N3**	84	9.4 (7.9; 11.3)	34.5 (25.7; 46.3)	10.7 (5.8; 20.0)	2.5 (0.4; 15.1)
IIIA+IIIB					
Total*	583	11.2 (10.2; 12.2)	46.5 (42.6; 50.7)	19.0 (16.0; 22.6)	11.5 (8.9; 14.9)
Good	369	12.2 (11.0; 13.3)	51.0 (46.2; 56.4)	22.1 (18.2; 26.9)	15.4 (11.9; 19.9)
Poor	172	9.2 (8.3; 10.5)	34.9 (28.4; 42.8)	11.7 (7.7; 17.7)	3.7 (1.3; 10.8)
		HR (95% CI)	**p-value**		
IIIA vs IIIB		0.71 (0.59; 0.85)	< 0.001		
IIIA Good vs IIIA Poor		0.69 (0.52; 0.92)	0.011		
IIIB Good vs IIIB Poor		0.69 (0.53; 0.90)	0.006		
IIIA vs IIIB Good		0.80 (0.65; 0.99)	0.037		

Good = performance status 0–1 and no weight loss; Poor = performance status 2–3 and/or weight loss ≥ 10%;
* = Total is not sum of Good and Poor, as some patients had no data about weight loss;
**** =** Stage IIIC in *Union for International Cancer Control* [UICC] 8

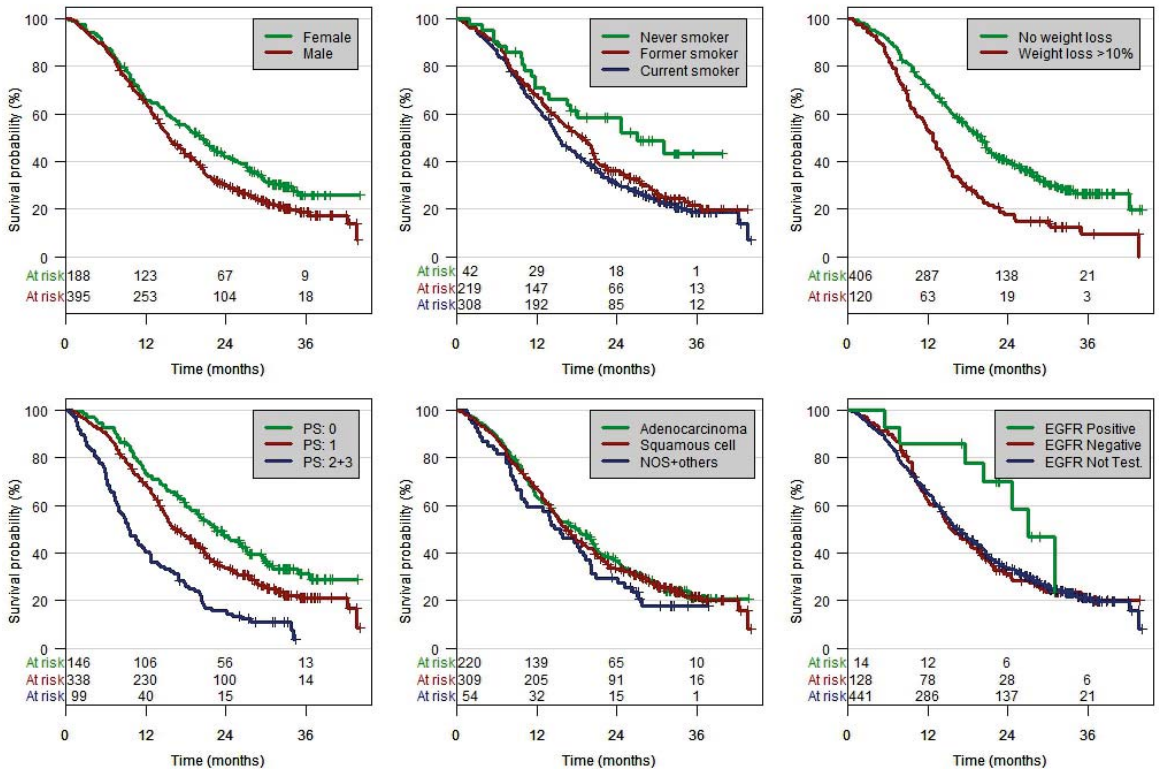

PS = performance status

FIGURE 4. Overall survival by variables.

TABLE 7. Overall survival according to diagnostic variables

Variable		N	Survival				
			Median	Univariate analysis	P-value	Multivariate analysis	P-value
			months (95% CI)	HR (95% Wald CI)		HR (95% Wald CI)	
Stage	IIIA	321	20.0 (17.1; 21.4)		**IIIA *vs.* IIIB:**		
	IIIB	262	14.4 (13.0; 15.9)	0.70 (0.58; 0.85)	< 0.001	0.77 (0.62;0.95)	0.017
Gender	Female	188	20.4 (16.8; 23.8)		**Female *vs.* male:**		
	Male	395	15.4 (14.3; 17.6)	0.76 (0.62; 0.94)	0.010	0.78 (0.64;0.96)	0.044
Smoking status	Current smoker	308	15.3 (14.2; 17.7)		**Never-smokers**	**vs:**	
	Former smoker	219	18.9 (15.9; 20.6)	Current: 0.54 (0.34; 0.84)	0.007	Current: 0.71 (0.42;0.22)	0.218
	Never smoker	42	27.1 (17.0; NA)	Former: 0.61 (0.39; 0.97)	0.036	Former: 0.75 (0.44;1.30)	0.308
Weight loss ≥ 10%	No	406	20.0 (17.9; 21.1)		**No *vs.* yes:**		
	Yes	120	12.7 (10.8; 14.8)	0.54 (0.43; 0.68)	< 0.001	0.68 (0.53;0.88)	0.003
PS	0	146	22.4 (17.7; 26.1)	0 *vs.* ≥ 2: 0.37 (0.28; 0.50)	< 0.001	0.62 (0.43;0.88)	0.007
	1	338	15.4 (13.9; 17.2)	1 *vs.* ≥ 2: 0.52 (0.41; 0.66)	< 0.001	0.69 (0.52;0.91)	0.009
	≥2	99	11.6 (8.8; 14.7)	0 *vs.* 1: 0.72 (0.57; 0.92)	0.007	0.90 (0.68;1.17)	0.422
Histology	Squamous	309	16.3 (15.0; 19.0)		**Adeno *vs.*:**		
	Adenoca	220	18.1 (14.7; 20.6)	Squam: 0.96 (0.79; 1.18)	0.726	Squam: 0.93(0.68;1.26)	0.630
	NOS/others	54	15 (10.1; 20.1)	NOS/oth: 0.79 (0.57; 1.11)	0.18	NOS/oth:0.96(0.63;1.48)	0.857
EGFR mutation positivity	Positive	14	27.1 (20.3; NA)		**Positive *vs*:**		
	Negative	128	15.8 (13.9; 19.7)	Negative: 0.51 (0.24; 1.10)	0.087	Negative:0.57(0.25;1.28)	0.176
	Not tested	441	16.5 (15.0; 18.9)	Not tested: 0.52 (0.25; 1.10)	0.087	Not tested:0.83(0.36;1.89)	0.651
Nodes confirmed	No	411	14.4 (13.3;15.9)		**Yes *vs.* no:**		
	Yes	172	24.7 (21.0; 28.8)	0.56 (0.45; 0.70)	< 0.001	0.67 (0.52;0.87)	0.002
PET-CT or PET scan	Yes	163	19.6 (17.8; 22.8)		**Yes *vs.* no:**		
	No	420	15.4 (14.1; 17.6)	0.73 (0.58–0.91)	0.005	0.84 (0.66;1.07)	0.160

NOS = not otherwise specified; oth = others; nodes confirmed = mediastinal lymph-nodes histologically confirmed; PS = performance status

total study population, in IIIA patients and in IIIB patients. Among the good prognostic group of IIIB patients, the survival outcome was similar to the survival outcome of IIIA patients.

Additional outcome data are summarized in Tables 5, 6 and 7 and Figures 3 and 4. Univariate analysis demonstrated longer OS for females, never-smokers, good PS, stage IIIA, mediastinal node verification, and for those with PET/CT or PET staging exam. In contrast, OS was not different between patients with adenocarcinomas and those with squamous cell carcinomas. Including these variables into the multivariate survival proportional hazard model, the differences in OS remained significant for females *versus* males, no weight loss *versus* weight loss, PS 0–1 *versus* 2–3, stage IIIA *versus* IIIB, and pathological verification of mediastinal nodes *versus* no verification. EGFR mutation status was not significant in the multivariate analysis but trend for better survival was found in the univariate model (Table 7). OS was also assessed in various treatment subgroups. Significant survival benefits were seen in patients undergoing surgery compared to patients without surgery (HR = 0.43; 95% CI 0.33–0.56; p-value < 0.001) and in patients receiving combined treatment modalities compared to patients with a single treatment modality (Table 5, hazard ratios not shown). The best OS outcome was shown for patients receiving trimodality therapy (Table 5). A significant OS difference between concurrent and sequential chemoradiotherapy could not be demonstrated. Time from diagnosis to initiation of treatment start had no impact on outcome (analysis by quartiles, p = 0.585).

Discussion

Our observational study demonstrated a large heterogeneity in both diagnostic procedures and treatment modalities among patients with locally advanced NSCLC in the real-world setting in Central European countries. The results were based on 583 patients from 16 cancer centres of seven countries. The patient characteristics of our study were slightly different from those of recent phase 3 trials[14,16], and these differences might be explained, at least partly, by higher smoking rates in Central European countries compared to other countries and the real-world nature of our study. In our study, two thirds were male, about half of the patients were older than 65 years and 7% were never-smokers. These rates are lower in terms of females and never-smokers than in the PROCLAIM trial[16], but similar to those of the PACIFIC trial.[14] The ma-

jority of our patients (53%) had squamous cell carcinomas and this frequency is slightly higher than the one (47%) of the PACIFIC trial.[14] The low rate (6%) of NSCLC not otherwise specified confirms that accurate pathological examination is well established in Central European countries. Most patients (83%) had good (WHO 0–1) PS and 70% had no weight loss prior to diagnosis. Tumour stages IIIA and IIIB were diagnosed in 55% and 45% of patients, respectively, and these percentages are similar to those of the PACIFIC trial.[14] Although not mandatory for patients with stage III NSCLC, molecular analyses were performed in selected patients. The EGFR mutation rate of 10% is consistent with the previously reported rate of 13.8% among patients with advanced NSCLC.[17] The percentage of patients with ALK translocations (2%) was in the lower range of stage IV patients[18,19], but similar to another study.[20] PD-L1 testing was not yet standard for patients with NSCLC stage at the time of our study.

Our real-world data can also be compared with those from other recent real-world studies.[20-23] All studies were similar in terms of median age (around 65 years), good PS (75–86%), never-smokers (4–9%) and percentage of adenocarcinomas (around 40%). In comparison to our study, the proportion of females were slightly higher in the American study (44.8%) and the Canadian study (46%).[20,22] The percentages of stage IIIA patients were similar between our and the American study but higher (77%) in the Canadian study.[20,22]

A major goal of our study was to determine the diagnostic and staging procedures (Table 2). Computer tomography of the chest, supplemented by CT or ultrasonography of the upper abdomen, was performed in most patients. PET-CT (or PET) and brain imaging were performed in only 28% and 20% of patients, respectively. These percentages, however, greatly varied between centres and reached almost 100% in some centres (Table 2). In the Canadian real-world study, 58% of patients received a PET scan as part of staging and 74% had baseline brain imaging.[22] Bronchoscopy was performed in 89% of patients, thereby being the most frequent intervention for obtaining tumour material for histopathological diagnosis. Only 13.5% of patients had histopathological mediastinal nodal staging prior to therapy. The American and Canadian real-world studies did not provide data on histopathological assessment of mediastinal lymph nodes prior to treatment.[20,22] In a retrospective analysis of 106 patients who had been treated with definitive radiotherapy (plus chemotherapy in most patients), 48.1% of patients had pathological confirmation of nodal disease.[24]

Treatment of our patients involved surgery, radiotherapy and chemotherapy (Table 4). Surgery with and without any other treatment was performed in 23% of all patients, 37.1% and 6.1% of patients with stage IIIA and IIIB, respectively. This percentage is similar to the Canadian study in which 21% of patients underwent surgery, either alone or as part of combined modality therapy. This similarity is somewhat surprising based on the fact that the percentage of our stage IIIB patients was higher than the Canadian one (45% *versus* 33%). Lobectomy and pneumonectomy were performed in 57% and 24% of patients, respectively. The rates of pneumonectomies were similar between our and the Canadian study (23% *versus* 18%). Like in the Canadian study[22], most of our surgical patients (87%) received chemotherapy, more frequently as adjuvant than induction chemotherapy.

Chemoradiotherapy was delivered to 34.3% of our patients (Table 4). The concurrent approach was chosen only in 27% of these patients. This low frequency compared to other studies[21,22] may be explained by patients unfit for the concurrent approach, limitations in the infrastructure of several centres including long waiting lists, and a stricter definition of concurrent *versus* sequential chemoradiotherapy than in other studies.

Overall, 80.3% of patients received systemic chemotherapy, either alone or combined with other treatment modalities. Radiotherapy alone and BSC alone were given to 11.8% and 5% of patients, respectively (Table 4). These percentages are in agreement with the percentage of patients with poor (WHO ≥2) performance status. Although the proportion of patients with BSC was small and most likely caused by patient selection, it was similar to another study in which radiotherapy and BSC alone were delivered to 11% and 21% of patients, respectively.[24]

Our study confirmed tumour stage (IIIA versus IIIB), PS, prior weight loss and gender as prognostic factors. OS of patients with adenocarcinomas did not differ from the one of patients with squamous cell NSCLC. Patients undergoing surgery had better survival than those without surgery (Table 5). The combination of surgery with chemotherapy and/or radiotherapy was also associated with improved survival outcome. The lack of a survival benefit for our patients undergoing concurrent chemoradiotherapy compared to those undergoing sequential chemoradiotherapy in our real-world study (Table 5) might be explained by

the multicentre nature of our study, low number of patients, and the heterogeneity of stage III NSCLC. The survival outcomes were similar between our study and the American real-world study.[20] Median OS times were 20.0 and 22.3 months for stage IIIA patients, respectively, and 14.4 and 14.7 months for stage IIIB patients, respectively. The longer median OS of 27.3 months in the Canadian study can, at least partly, be explained by the higher percentage of stage IIIA patients. The best OS in our study with 64% of patients being alive at three years was seen among patients undergoing trimodality therapy and was consistent with the Canadian study.[22] It remains unclear, however, whether this survival benefit is due to treatment or just selection of patients with good prognostic features. In a randomized trial, the addition of surgery to chemoradiotherapy failed to improve overall survival.[25]

Our observational study has several limitations. Firstly, the findings were based on major academic cancer centres and, therefore, might not be representative for smaller centres. Secondly, there was no even distribution of patients between centres and an abundance of Czech patients was seen. Finally, other patient selection biases including patients lost to follow-up might have also played some role.

Our real-world findings also define areas for future improvements in the management of patients with locally advanced NSCLC in Central Europe. Firstly, the rates of staging by means of PET-CT must be increased, mainly through improving access to these procedures. Secondly, brain imaging should be implemented prior to treatment in all patients who are planned for aggressive treatments such as surgery or chemoradiotherapy. Thirdly, invasive staging of mediastinal lymph nodes prior to treatment should be performed more frequently. In order to achieve these goals, awareness among doctors has to be raised, opportunities for education as well as training of doctors must be increased, and the infrastructure of some centres has yet to be improved.

Conclusions

The present real-world study confirmed known prognostic factors and the broad heterogeneity in diagnostic and therapeutic strategies among patients with stage III NSCLC in Central European countries. Rates of PET-CT staging, invasive staging of mediastinal nodes, and brain imaging prior to combined treatments should be increased in the future.

Acknowledgements

We would like to thank the heads of the all participating centres for permission to use data of patients from their respective regional networks and for the support of this project. We are also indebted to all physicians who provided data for the registry.

This work was supported by the Czech Lung Cancer Cooperative Group (Kooperativní skupina pro léčbu plicní rakoviny, spolek).

References

1. Nappi A, Gallicchio R, Simeon V, Nardelli A, Pelagalli A, Zupa A, et al. [F-18] FDG-PET/CT parameters as predictors of outcome in inoperable NSCLC patients. *Radiol Oncol* 2015; **49:** 320-6. doi: 10.1515/raon-2015-0043
2. Eberhardt WE, De Ruysscher D, Weder W, Le Péchoux C, De Leyn P, Hoffmann H, et al. Panel members. 2nd ESMO consensus conference in lung cancer: locally advanced stage III non-small-cell lung cancer. *Ann Oncol* 2015; **26:** 1573-88. doi: 10.1093/annonc/mdv187
3. Goldstraw P, Crowley J, Chansky K, Giroux DJ, Groome PA, Rami-Porta R, et al. The IASLC Lung Cancer Staging Project: proposals for the revision of the TNM stage groupings in the forthcoming (seventh) edition of the TNM classification of malignant tumours. *J Thorac Oncol* 2007; **2:** 706-14. doi: 10.1097/JTO.0b013e31812f3c1a
4. Goldstraw P, Chansky K, Crowley J, Rami-Porta R, Asamura H, Eberhardt WE, et al. International Association for the Study of Lung Cancer Staging and Prognostic Factors Committee, Advisory Boards, and Participating Institutions. The IASLC Lung Cancer Staging Project: proposals for the revision of the TNM stage groupings in the forthcoming (eighth) edition of the TNM classification for lung cancer. *J Thorac Oncol* 2016; **11:** 39-51. doi: 10.1016/j.jtho.2015.09.009.
5. Pignon JP, Tribodet H, Scagliotti GV, Douillard JY, Shepherd FA, Stephens RJ, et al. Lung adjuvant cisplatin evaluation: a pooled analysis by the LACE collaborative group. *J Clin Oncol* 2008; **26:** 3552-9. doi: 10.1200/JCO.2007.13.9030
6. NSCLC Meta-analysis Collaborative Group. Preoperative chemotherapy for non-small-cell lung cancer: a systematic review and meta-analysis of individual participant data. *Lancet* 2014; **383:** 1561-71. doi: 10.1016/S0140-6736(13)62159-5
7. Betticher DC, Hsu Schmitz SF, Totsch M, Hansen E, Joss C, von Briel C, et al. Prognostic factors affecting long-term outcomes in patients with resected stage IIIA pN2 non-small-cell lung cancer: 5-year follow-up of a phase II study. *Br J Cancer* 2006; **94:** 1099-106.
8. Sher DJ, Fidler MJ, Liptay MJ, Koshy M. Comparative effectiveness of neoadjuvant chemoradiotherapy versus chemotherapy alone followed by surgery for patients with stage IIIA non-small cell lung cancer. *Lung Cancer* 2015; **88:** 267-74. doi: 10.1016/j.lungcan.2015.03.015
9. Thomas M, Rube C, Hoffknecht P, Macha HN, Freitag L, Linder A, et al. Effect of preoperative chemoradiation in addition to preoperative chemotherapy: a randomised trial in stage III non-small-cell lung cancer. *Lancet Oncol* 2008; **9:** 636-48. doi: 10.1016/S1470-2045(08)70156-6
10. Garrido P, Gonzalez-Larriba JL, Insa A, Provencio M, Torres A, Isla D, et al. Long-term survival associated with complete resection after induction chemotherapy in stage IIIA (N2) and IIIB (T4N0-1) non-small-cell lung cancer patients: the Spanish Lung Cancer Group Trial 9901. *J Clin Oncol* 2007; **25:** 4736-42.

11. Barlési F, Doddoli C, Torre JP, Giudicelli R, Fuentes P, Thomas P, et al. Comparative prognostic features of stage IIIAN2 and IIIB non-small-cell lung cancer patients treated with surgery after induction therapy. *Eur J Cardiothorac Surg* 2005; **28:** 629-34. doi: 10.1016/j.ejcts.2005.06.018

12. Auperin A, Le Pechoux C, Rolland E, Curran WJ, Furuse K, Fournel P, et al. Meta-analysis of concomitant versus sequential radiochemotherapy in locally advanced non-small-cell lung cancer. *J Clin Oncol 2010*; **28:** 2181-90. doi: 10.1200/JCO.2009.26.2543

13. Ma L, Men Y, Feng L, Kang J, Sun X, Yuan M, et al. A current review of dose-escalated radiotherapy in locally advanced non-small cell lung cancer. *Radiol Oncol* 2019; **53:** 6-14. doi: 10.2478/raon-2019-0006

14. Antonia SJ, Villegas A, Daniel D, Vicente D, Murakami S, Hui R, et al. PACIFIC Investigators. Durvalumab after chemoradiotherapy in stage III non-small-cell lung cancer. *N Engl J Med* 2017; **377:** 1919-29. doi: 10.1056/NEJMoa1709937

15. Zhang Z, Sun J. Interval censoring. *Stat Methods Med Res* 2010; **19:** 53-70. doi: 10.1177/0962280209105023

16. Senan S, Brade A, Wang LH, Vansteenkiste J, Dakhil S, Biesma B, et al. PROCLAIM: Randomized phase III trial of pemetrexed-cisplatin or etoposide-cisplatin plus thoracic radiation therapy followed by consolidation chemotherapy in locally advanced nonsquamous non-small-cell lung cancer. *J Clin Oncol* 2016; **34:** 953-62. doi: 10.1200/JCO.2015.64.8824

17. Ramlau R, Cufer T, Berzinec P, Dziadziuszko R, Olszewski W, Popper H, et al. INSIGHT study team. Epidermal growth factor receptor mutation-positive non-small-cell lung cancer in the real-world setting in Central Europe: The INSIGHT Study. 10: 1370-4. *J Thorac Oncol* 2015; **10:** 1370-4. doi: 10.1097/JTO.0000000000000621

18. Barlesi F, Mazieres J, Merlio JP, Debieuvre D, Mosser J, Lena H, et al. Biomarkers France contributors. Routine molecular profiling of patients with advanced non-small-cell lung cancer: results of a 1-year nationwide programme of the French Cooperative Thoracic Intergroup (IFCT). *Lancet* 2016; **387:** 1415-26. doi: 10.1016/S0140-6736(16)00004-0

19. Hofman P. ALK in Non-Small Cell Lung Cancer (NSCLC): pathobiology, epidemiology, detection from tumor tissue and algorithm diagnosis in a daily practice. *Cancers* 2017; **9:** pii: E107. doi: 10.3390/cancers9080107

20. Ryan KJ, Skinner KE, Fernandes AW, Punekar RS, Pavilack M, Walker MS, et al. Real-world outcomes in patients with unresected stage III non-small cell lung cancer. *Med Oncol* 2019; **36:** 24. doi: 10.1007/s12032-019-1249-1

21. Ryan KJ, Skinner KE, Fernandes AW, Punekar RS, Pavilack M, Walker MS, et al. Real-world treatment patterns among patients with unresected stage III non-small-cell lung cancer. *Future Oncol* 2019; **15:** 2943-53. doi: 10.2217/fon-2018-0939

22. Moore S, Leung B, Wu J, Ho C. Real-world treatment of stage III NSCLC: the role of trimodality treatment in the era of immunotherapy. *J Thorac Oncol* 2019; **14:** 1430-9. doi: 10.1016/j.jtho.2019.04.005

23. Fernandes AT, Mitra N, Xanthopoulos E, Evans T, Stevenson J, Langer C, et al. The impact of extent and location of mediastinal lymph node involvement on survival in stage III non-small cell lung cancer patients treated with definitive radiotherapy. *Int J Radiat Oncol Biol Phys* 2012; **83:** 340-7. doi: 10.1016/j.ijrobp.2011.05.070

24. Van der Meer FS, Schramel FM, Van Vulpen M, El Sharouni SY. Feasibility of concomitant chemoradiotherapy in daily practice for patients with NSCLC stage III. *Anticancer Res* 2016; **36:** 4673-6. doi: 10.21873/anticanres.11019

25. Albain KS, Swann RS, Rusch VW, Turrisi AT 3rd, Shepherd FA, Smith C, et al. Radiotherapy plus chemotherapy with or without surgical resection for stage III non-small-cell lung cancer: a phase III randomised controlled trial. *Lancet* 2009; **374:** 379-86. doi: 10.1016/S0140-6736(09)60737-6

research article

Diagnostic accuracy of (1→3)-ß-D-glucan to predict Pneumocystis jirovecii pneumonia in non-HIV-infected patients

Petra Rogina[1], Miha Skvarc[2]

[1] Infectious Disease Department, General Hospital Novo mesto, Novo mesto, Slovenia
[2] Infection Control and Microbiology Unit, General Hospital Jesenice, Jesenice, Slovenia

Radiol Oncol 2020; 54(2): 221-226.

Received 31 December 2019
Accepted 14 April 2020

Correspondence to: Assist. Prof. Miha Skvarč, M.D., Ph.D., General Hospital Jesenice, Cesta maršala Tita 112, Jesenice, Slovenia.
E-mail: mihaskvarc@hotmail.com

Disclosure: No potential conflicts of interest were disclosed.

Background. *Pneumocystis jirovecii* pneumonia (PCP) is a common and potentially fatal opportunistic infection in immunocompromised non-HIV individuals. There are problems with clinical and diagnostic protocols for PCP that lack sensitivity and specificity. We designed a retrospective study to compared several methods that were used in diagnostics of PCP.

Patients and methods. One hundred and eight immunocompromised individuals with typical clinical picture for PCP and suspicious radiological findings were included in the study. Serum samples were taken to measure the values of (1→3)-β-D-glucan (Fungitell, Associates of Cape Cod, USA). Lower respiratory tract samples were obtained to perform direct immunofluorescence (DIF, MERIFLUOR® Pneumocystis, Meridian, USA) stain and real-time PCR (qPCR).

Results. Fifty-four (50%) of the 108 patients in our study had (1→3)-β-D-glucan > 500 pg/ml. Patients that had (1→3)-β-D-glucan concentrations < 400 pg/ml in serum, had mean threshold cycles (Ct) 35.43 ± 3.32 *versus* those that had (1→3)-β-D-glucan concentrations >400 pg/mL and mean Ct of 28.97 ± 5.27 (P < 0.001). If we detected *P. jirovecii* with DIF and qPCR than PCP was proven. If the concentration of (1→3)-β-D-glucan was higher than 400 pg/ml and Ct of qPCR was below 28.97 ± 5.27 than we have been able be certain that *P. jirovecii* caused pneumonia (odds ratio [OR] 2.31, 95% confidence interval [CI] 1.62–3.27, P < 0.001).

Conclusions. Measurement of (1→3)-β-D-glucan or qPCR alone could not be used to diagnose PCP. Diagnostic cut-off value for (1→3)-β-D-glucan > 400pg/ml and qPCR below 30 Ct, allow us to conclude that patient has PCP. If the values of (1→3)-β-D-glucan are < 400 pg/ml and qPCR is above 35 Ct than colonization with *P. jirovecii* is more possible than PCP.

Key words: *Pneumocystis jirovecii* pneumonia; (1→3)-β-D-glucan; DIF; real-time PCR; colonization with *P. jirovecii*; non-HIV-infected patients

Introduction

Pneumocystis jirovecii is a cause of *Pneumocystis* pneumonia (PCP) in immunocompromised patients. PCP most often occurs in human immunodeficiency virus (HIV) infected patients associated with high pathogen burdens but also in non-HIV immunocompromised patients.[1-3] The diagnosis is mainly based on clinical and radiographic examinations, which are in majority of cases inconclusive, so microscopic or molecular detection of *P. jirovecii* in lower respiratory tract samples are necessary.[2,3] The mechanism by which *Pneumocystis* organisms induce lung inflammation remains incompletely understood, but studies imply that *Pneumocystis* spp. cell wall constituent (1→3)-β-D-glucans are released and contribute to the development of extensive lung inflammatory reaction.[4-10] Various studies have reported high serum (1→3)-β-D-glucan levels in patients with PCP.[7-15] The (1→3)-β-D-glucan has

high sensitivity for PCP but, it is a not species-specific marker for *P. jirovecii*.[2,11,13,15]

Detection of *P. jiroveci* DNA in respiratory tract specimens without signs and symptoms of PCP is defined as colonization. Molecular diagnostic techniques like quantitative PCR (qPCR) are more sensitive than staining methods like direct immunofluorescence method (DIF). However, qPCR can give sometimes false signal that patient has PCP, although patient is just colonized with fungi.[16-21] Studies have reported prevalence of colonization in susceptible adults from 10.0% to 43.8%.[17-23] Real-time qPCR assays have been shown as most accurate for discrimination of true PCP from colonization with *P. jirovecii*. Flori *et al*. compared the performance of standard staining, standard PCR, and qPCR using 173 BAL specimens from 150 patients. Real-time qPCR gave the best results.[24]

A systematic review, that evaluated PCR kits to confirm PCP, revealed that positive PCR results do not always confirm PCP. Low amounts of DNA can be expected in patients with *P. jirovecii* colonization of and no clinical signs of PCP.[25]

(1→3)-β-D-glucan can be helpful to distinguish PCP from *P. jirovecii* colonization. However, not as standalone test. (1→3)-β-D-glucan is positive in colonization of gastrointestinal tract with candida. It is positive when patients are colonized with *P. jirovecii*.[13,16] Combining best tests is a advisable in immunocompromised cancer patients to be able to treat patients with the right therapy.

We designed a retrospective multicentric study that included patients from 3 tertiary care hospitals and 2 secondary care hospitals. The objective of our study was to distinguish true PCP from colonization with *P. jirovecii* with diagnostic algorithm that includes measurement of (1→3)-β-D-glucan and real-time PCR (qPCR).

Patients and methods

Patients

We included 108 consecutive non-HIV patients on immunosuppression therapy from 2006 to end of 2014 with clinical diagnosis of possible PCP. Possible PCP diagnosis was given to patients at admission to hospital or during diagnostic process that had typical suggestive symptoms and signs and radiological findings for PCP (fever, dry cough, dyspnoea on exertion and bilateral interstitial pneumonia on chest X-ray, and/or ground glass look on thorax CT scan). Patients receiving antifungal therapy or therapy that works against *P. jirovecii* were excluded from the study. Patients with excessive colonization with *Candida spp.* on mucosal barriers were also excluded from the study.

Methods

Microbiological diagnosis was based on the detection of *P. jirovecii* with DIF (MERIFLUOR® Pneumocystis, Meridian, USA) and on in-house developed qPCR from lower respiratory tract sample (induced sputum, aspiration of trachea or bronchoalveolar lavage – BAL). DNA was extracted from lower respiratory tract samples using QIAamp DNA mini kit (Qiagen, Germany). In-house qPCR developed after article of Alanio *et al*.[16] was performed using a reaction mix Platinum® Quantitative PCR SuperMix-UDG with ROX (Invitrogen, USA) and PCR primers to detect *Pneumocystis* PjFI and PjRI with hybridization probe PjSL (TIB MolBiol, Germany). The qPCR assay developed for this study amplifies a 121-bp fragment of the *P. jirovecii* mitochondrial large-subunit rRNA gene. The primers PjF1 (5′-CTGTTTCCCTTTCGAC TATCTACCTT-3′) and PjR1 (5′-CACTGAATATCTCGAGG GAGTATGAA-3′) and the TaqMan-MGB probe PjSL (5′-TCGCACATAGTCTGATTAT-3′) were designed by using Primer Express software (Applied Biosystems, Foster City, CA, USA). DNA sample volume was 5 μL. PCR reaction with a final volume of 25 μL was carried out with following conditions: 50ºC for 2 min, 95ºC for 2 min, followed by 45 cycles consisting of 15 sec at 95ºC, 60 sec at 60ºC. The results are presented as threshold cycles (Ct). We used Quality Control for Molecular Diagnostics (QCMD, UK) samples from *Pneumocystis jirovecii* pneumonia (PCP) DNA scheme to evaluate our qPCR (sensitivity 97%, specificity 100%). Serum samples were collected to measure the values of (1→3)-β-D-glucan (Fungitell, Associates of Cape Cod, USA).

In all patients 2 sets of blood cultures were collected. Lower respiratory tract samples were collected to detect potential bacterial cause of deteriorating health.

Institutional review board approved of General Hospital Jesenice approved the study under condition that patients' data were anonymized. The results of the study did not influence the course of the treatment.

Statistical analysis

Microbiologically proven PCP was defined as positive DIF and positive qPCR. Colonization was suspected when DIF was negative and if any amount

of DNA with qPCR was found. (1→3)-β-D-glucan in patients with possible colonization with *P. jirovecii* had to be positive (above 80 pg/ml).

Mean values for (1→3)-β-D-glucan and Ct values between different patients' groups and (1→3)-β-D-glucan ranges were compared using an independent T-test. Receiver operating curve (ROC) analysis with area under the curve (AUC) and confidence interval (CI) were performed to calculate diagnostic accuracy. Univariate logistic regression was performed to explore the association of laboratory parameters with the disease. The statistical significance level was set at 0.05 (two-tailed). All analyses were conducted with SPSS version 23.0 statistical software.

Results

One hundred and eight immunosuppressed patients (mean age 53 ± 15 years) with possible PCP were included into final analysis. Majority of patients were in some way immunocompromised. They received immunosuppressive therapy because of transplanted solid organ (53 patients, 49%) with mean (1→3)-β-D-glucan value of 330.01 ± 191 pg/mL. The rest of patients had autoimmune diseases or malignant disease (Table 1).

Patient's data were divided into 6 groups according to (1→3)-β-D-glucan values. In the first group were patients with (1→3)-β-D-glucan value < 100 pg/mL, followed by group of patients with (1→3)-β-D-glucan value from 100 pg/mL till 200 pg/mL and so on till the last group with (1→3)-β-D-glucan values > 500 pg/mL. The largest group of patients (50% of all patients) were in the range of (1→3)-β-D-glucan > 500 pg/mL. Twenty-four patients with possible PCP had (1→3)-β-D-glucan < 100 pg/mL, with mean value of 81.14 ± 3.41 pg/mL (Table 2).

Results for patients in different (1→3)-β-D-glucan ranges and mean qPCR Ct values are presented in Table 3. Patients in the last 2 ranges ((1→3)-β-D-glucan 400-500pg/m and > 500pg/ml) had significantly more *P. jirovecii* DNA detected in lower respiratory tract ((1→3)-β-D-glucan 400-500 pg/mL, mean Ct 29.41 ± 6.25; (1→3)-β-D-glucan > 500 pg/ml, mean Ct 28.90 ± 5.18, P < 0.001) in comparison to other groups of patients. Statistically significant difference in Ct values was noticed when (1→3)-β-D-glucan concentrations exceeded 400pg/ml ((1→3)-β-D-glucan < 400 pg/mL, mean Ct 35.43 ± 3.32 *versus* (1→3)-β-D-glucan > 400 pg/mL, mean Ct 28.97 ± 5.27, P < 0.001). Moreover, analysis showed that majority of patients (57%) had (1→3)-β-D-glucan > 400 pg/ml and had the greatest chance to have PCP ((1→3)-β-D-glucan > 400 pg/mL: OR 2.31 (95% CI 1.62–3.27), p < 0.001).

We compared (1→3)-β-D-glucan values and qPCR Ct of 42 patients with microbiologically confirmed PCP (DIF positive, qPCR positive) to those 66 patients that had possible PCP at initial presentation to predict true PCP (Table 4). Forty-two patients had statistically significant higher concentrations of (1→3)-β-D-glucan and *P. jirovecii* DNA (P < 0.001). Subgroup of 26 patients, that had DIF positive and qPCR Ct < 30, had slightly higher

TABLE 1. Average (1→3)-β-D-glucan values for each group of immunocompromised patients

Diagnosis	N = 108 patients	(1→3)-β-D-glucan (pg/mL) ± SD
Malignant disease	20 (18%)	240.34 ± 162.45
Transplantation	53 (49%)	330.01 ± 191.26
Autoimmune disease	35 (33%)	427.73 ± 152.23

TABLE 2. Average (1→3)-β-D-glucan values for each (1→3)-β-D-glucan range

(1→3)-β-D-glucan group	N = 108 patients	(1→3)-β-D-glucan (pg/mL) ± SD
< 100 pg/mL	24	81.14 ± 3.41
100–200 pg/mL	11	124.4 ± 22.37
200–300 pg/mL	4	238,75 ± 16,55
300–400 pg/mL	7	336.75 ± 20.18
400–500 pg/mL	8	454.13 ± 31.3
> 500 pg/mL*	54	> 500 pg/mL

* Mean could not be calculated since samples dilutions to measure real (1→3)-β-D-glucan concentrations were not performed.

TABLE 3. Average Ct values for each (1→3)-β-D-glucan range

(1→3)-β-D-glucan group	N = 108 patients	Mean Ct ± SD
Group 1 < 100 pg/mL	24	35.43 ± 3.51
Group 2 100–200 pg/mL	11	34.82 ± 3.65
Group 3 200–300 pg/mL	4	37.33 ± 2.36
Group 4 300–400 pg/mL	7	35.27 ± 2.75
Group 5 400–500 pg/mL	8	29.41 ± 6.25*
Group 6 > 500 pg/mL	54	28.90 ± 5.18*

Ct = threshold cycle; SD = standard deviation

* Statistically significant difference seen when Ct from group 1 to 4 are compared to group 5 and 6 combined, P < 0.001. Odds ratio (OR) is the greatest to predict PCP if (1→3)-β-D-glucan > 400 pg/mL, OR 2.31 (95%CI 1.62-3.27), p < 0.001).

TABLE 4. (1→3)-β-D-glucan values for patients with microbiologically confirmed PCP and possible PCP

PCP	108 patients	(1→3)-β-D-glucan (pg/mL) ± SD	qPCR Ct ± SD
Possible PCP	66 (61%)	**256.06 ± 183.48**	**35.01 ± 3.8**
Microbiologically confirmed PCP (DIF and qPCR positive)	42 (39%)	**467.5 ± 95.5**	**27.2 ± 4.6**
Subgroup definite PCP (DIF positive and qPCR Ct < 30 and response to treatment)	26 (24%)	494.81 ± 17.73*	
P value		**< 0.001**	**< 0.001**

Ct = threshold cycle; DIF = direct immunofluorescence; PCP = pneumocystis pneumonia; qPCR = real time PCR; SD = standard deviation

* Area under the curve (AUC) to predict PCP (positive DIF and qPCR) with measurement of (1→3)-β-D-glucan: AUC = 0.817, 95% CI: 0.736–0.898, sensitivity = 83.3%, specificity = 64.6%, cut off 496.45 pg/mL, p < 0.001

(1→3)-β-D-glucan mean values than the group of microbiologically confirmed PCP. The subgroup cut-off for (1→3)-β-D-glucan was set to 496.45 pg/mL, and determined PCP with greatest AUC and statistically significance (AUC = 0.817, 95% CI: 0.736–0.898, sensitivity = 83.3%, specificity = 64.6%, p < 0.001).

Discussion

Our experience with (1→3)-β-D-glucan and qPCR indicated that cut-off of > 400 pg/mL for (1→3)-β-D-glucan could be used to predict microbiologically confirmed PCP with greatest statistical significance. Results of the analysis indicated that colonization is possible when levels of (1→3)-β-D-glucan are moderate, in our case < 400 pg/mL, and low concentrations of *P. jirovecii* DNA with qPCR are detected, in our case > 35 cycles.

Fifty percent of the patients in our study had (1→3)-β-D-glucan > 500 pg/mL and mean qPCR Ct 28.9 ± 5.18. The second largest group of patients (24 patients) with possible PCP were those with (1→3)-β-D-glucan < 100 pg/mL, and mean qPCR Ct 35.43 ± 3.51. Patients with microbiologically confirmed PCP had mean (1→3)-β-D-glucan of 467.5 ± 95.5 and mean qPCr Ct 27.2 ± 4.6. Even more, true PCP where patients with it, had response to therapy, can be predicted when cut-off for (1→3)-β-D-glucan is set to 496.45 pg/ml. At this cut-off, AUC to predict PCP was 0.817.

Similar results were produced in recent studies.[26,27] In an older study cut-off value of 340 copies/mL was used to discriminate probable PCP from colonization. At this qPCR cut-off, (1→3)-β-D-glucan levels were significantly higher in patients with both definite PCP and probable PCP than in colonized patients.[26] It was recently shown that serum (1→3)-β-D-glucan levels of 143 pg/mL can be used to distinguish PCP from colonisation with *P. jirovecii*.[28] To diagnose and treat PCP you have to have a lot of experience.[29] Our results were not concordant with latter studies because we measured much higher (1→3)-β-D-glucan levels in the patients with true PCP. The clinicians in majority of included institutions seldomly get the chance to treat PCP and are not experienced enough.

When PCR was introduced, it remarkably increased sensitivity to diagnose PCP, resulting in an increase in the number of documented PCP cases.[30-34] On the other hand multiple evidences indicate that *P. jirovecii* can colonize the mucosal epithelium of both healthy individuals and those with compromised immunity.[34-36] Results of qPCR in the area where differentiation between PCP and colonization is demanding, if we look at them separately from (1→3)-β-D-glucan. It was suggested that every (1→3)-β-D-glucan values should be interpreted with qPCR and vice versa in patients with possible PCP.[16,26,29]

Montesinos *et al*. also showed with their in-house PCR test cut-off value Ct = 34 to discriminate definite PCP from unlikely PCP with 65% sensitivity and 85% specificity.[37] Other studies have suggested applying two qPCR cut-off values to increase sensitivity and specificity of qPCR. There is a grey zone of unclear clinical significance between these two cut-off values where the differential diagnosis of PCP *versus* colonization cannot be determined.[16,24,38-40] In recent literature two cut-offs were proposed to predict definite PCP. The two cut-offs for qPCR provide 100% sensitivity and 100% specificity to diagnosis definite PCP. The higher cut-off value represents the value below which the diagnosis of PCP is unlikely. The authors suggested that the range between these two cut-off values represents an indeterminate zone.[16,39,41-42]

According to our study, *P. jirovecii* DNA copy number above the cut-off value Ct ≥35 would support a diagnosis of colonization, and a copy number below the cut-off value would support a diagnosis of PCP. However, good sensitivity of qPCR can be misleading, since qPCR detects very low fungal load that can lead to over-diagnosis of PCP due to misinterpretation of findings.[33,42] Our cut-off was determined with the help of (1→3)-β-D-glucan, which is a good indicator for PCP if the values are high and we detect a lot of *P. jirovecii* DNA in lower respiratory tract.

Our study had some limitations. We could not gather the information that treatment with antimicrobials helped patients which would confirm that patients really had PCP for all included individuals. The influence of different samples from lower respiratory tract on qPCR was not assessed. Although our qPCR displayed high accuracy for discriminating colonization from PCP, the cut-off values used in our study should be standardized to copies/ml and compared to other qPCRs. The cut-off values for (1→3)-β-D-glucan was not always measured the same day as qPCR was done which could influence on the concentration of (1→3)-β-D-glucan. For future studies, patients that have their clinical picture and response to therapy consistent with possible PCP, and are randomized according to the analysed samples, should be included to resolve the discrepancy seen in our study.

Conclusions

The protocol we presented here could better support clinicians in their decisions whether patient in front of them has PCP. Our diagnostic cut-off values allow identification of true PCP *versus* colonization with *P. jirovecii* with better diagnostic accuracy. However, according to our results qPCR cannot be used alone to confirm PCP. PCP has to be confirmed with qPCR and with (1→3)-β-D-glucan.

Acknowledgment

We thank Institute of Microbiology and Immunology, Faculty of Medicine, University of Ljubljana for their routine diagnostic support when needed.

References

1. Tamburrini E, Mencarini P, Visconti E, Zolfo M, De Luca A, Siracusano A, et al. Detection of Pneumocystis carinii DNA in blood by PCR is not of value for diagnosis of P. carinii pneumonia. *J Clin Microbiol* 1996; **34:** 1586-8. PMID: 8735128
2. Maschmeyer G, Helweg-Larsen J, Pagano L, Robin C, Cordonnier C, Schellongowski P, et al. ECIL guidelines for treatment of Pneumocystis jirovecii pneumonia in non-HIV-infected haematology patients. *J Antimicrob Chemother* 2016; **71:** 2405-13. doi: 10.1093/jac/dkw158
3. Maertens J, Cesaro S, Maschmeyer G, Einsele H, Donnelly JP, Alanio A, et al. ECIL guidelines for preventing Pneumocystis jirovecii pneumonia in patients with haematological malignancies and stem cell transplant recipients. *J Antimicrob Chemother* 2016; **71:** 2397-404. doi: 10.1093/jac/dkw157.
4. Wang J, Gigliotti F, Maggirwar S, Johnston C, Finkelstein JN, Wright TW. Pneumocystis carinii activates the NF-kappaB signaling pathway in alveolar epithelial cells. *Infect Immun* 2005; **73:** 2766-77. doi: 10.1128/IAI.73.5.2766-2777.2005
5. Vassallo R, Standing JE, Limper AH. Isolated Pneumocystis carinii cell wall glucan provokes lower respiratory tract inflammatory responses. *J Immunol* 2000; **164:** 3755-63. doi: 10.4049/jimmunol.164.7.3755
6. Tasaka S, Hasegawa N, Kobayashi S, Yamada W, Nishimura T, Takeuchi T, et al. Serum indicators for the diagnosis of *Pneumocystis* pneumonia. *Chest* 2007; **131:** 1173-80. doi: 10.1378/chest.06-1467
7. Cuetara MS, Alhambra A, Chaves F, Moragues MD, Ponton J, del Palacio A. Use of a serum (1→3)-β-D-glucan assay for diagnosis and follow-up of *Pneumocystis jiroveci* pneumonia. *Clin Infect Dis* 2008; **47:** 1364-6. doi: 10.1086/592753
8. Persat F, Ranque S, Derouin F, Michel-Nguyen A, Picot S, Sulahian A. Contribution of the (1→3)-β-D-glucan assay for diagnosis of invasive fungal infections. *J Clin Microbiol* 2008; **46:** 1009-13. doi: 10.1128/JCM.02091-07
9. Pisculli ML, Sax PE. Use of a serum β-glucan assay for diagnosis of HIV-related *Pneumocystis jiroveci* pneumonia in patients with negative microscopic examination results. *Clin Infect Dis* 2008; **46:** 1928-30. doi: 10.1086/588564
10. Desmet S, Van Wijngaerden E, Maertens J, Verhaegen J, Verbeken E, De Munter P, et al. Serum (1–3)-β-D-glucan as a tool for diagnosis of *Pneumocystis jirovecii* pneumonia in patients with human immunodeficiency virus infection or hematological malignancy. *J Clin Microbiol* 2009; **47:** 3871-4. doi: 10.1128/JCM.01756-09
11. Held J, Koch M, Reischl U, Danner T, Serr A. Serum (1→3)-β-D-glucan measurement as early indicator for *Pneumocystis jirovecii* pneumonia and evaluation of its prognostic value. *Clin Microbiol Infect* 2011; **17:** 595-602. doi: 10.1111/j.1469-0691.2010.03318.x
12. Finkelman MA. *Pneumocystis jirovecii* infection: cell wall (1→3)-β-D-glucan biology and diagnostic utility. *Crit Rev Microbiol* 2010; **36:** 271-81. doi: 10.3109/1040841X.2010.484001
13. Karageorgopoulos DE, Qu JM, Korbila IP, Zhu YG, Vasileiou VA, Falagas ME. Accuracy of β-D-glucan for the diagnosis of *Pneumocystis jirovecii* pneumonia: a meta-analysis. *Clin Microbiol Infect* 2013; **19:** 39-49. doi: 10.1111/j.1469-0691.2011.03760.x
14. Wood BR, Komarow L, Zolopa AR, Finkelman MA, Powderly WG, Sax PE. Test performance of blood beta-glucan for *Pneumocystis jirovecii* pneumonia in patients with AIDS and respiratory symptoms. *AIDS* 2013; **27:** 967-72. doi: 10.1097/QAD.0b013e32835cb646
15. Sax PE, Komarow L, Finkelman MA, Grant PM, Andersen J, Scully E, et al. Blood (1→3)-β-D-glucan as a diagnostic test for HIV-related *Pneumocystis jirovecii* pneumonia. *Clin Infect Dis* 2011; **53:** 197-202. doi: 10.1093/cid/cir335
16. Alanio A, Desoubeaux G, Sarfati C, Hamane S, Bergeron A, Azoulay E, et al. Real-time PCR assay-based strategy for differentiation between active Pneumocystis jirovecii pneumonia and colonization in immunocompromised patients. *Clin Microbiol Infect* 2011; **17:** 1531-7. doi: 10.1111/j.1469-0691.2010.03400.x
17. Morris A, Wei K, Afshar K, Huang L. Epidemiology and clinical significance of pneumocystis colonization. *J Infect Dis* 2008; **197:** 10-7. doi: 10.1086/523814

18. Can H, Caner A, Döşkaya M, Değirmenci A, Karaçalı S, Polat C**,** et al**.** Detection of Pneumocystis in the nasal swabs of immune-suppressed rats by use of PCR and microbiology. *Med Sci Monit Basic Res* 2013; **19:** 62-7. doi: 10.12659/MSMBR.883777.

19. Spencer L, Ukwu M, Alexander T, Valadez K, Liu L, Frederick T, et al. Epidemiology of Pneumocystis colonization in families. *Clin Infect Dis* 2008; **46:** 1237-40. doi: 10.1086/533449

20. Turner D, Schwarz Y, Yust I. Induced sputum for diagnosing Pneumocystis carinii pneumonia in HIV patients: new data, new issues. *Eur Respir J* 2003; **21:** 204-8. doi: 10.1183/09031936.03.00035303

21. Damiani C, Le Gal S, Da Costa C, Virmaux M, Nevez G, Totet A. Combined quantification of pulmonary *Pneumocystis jirovecii* DNA and serum (1->3)-β-D-glucan for differential diagnosis of pneumocystis pneumonia and *Pneumocystis* colonization. *J Clin Microbiol* 2013; **51:** 3380-8. doi: 10.1128/JCM.01554-13

22. Nevez G, Totet A, Pautard JC, Raccurt C. *Pneumocystis carinii* detection using nested-PCR in nasopharyngeal aspirates of immunocompetent infants with bronchiolitis. *J Eukaryot Microbiol* 2001; **48(1 Suppl):** 122S-3S. doi: 10.1111/j.1550-7408.2001.tb00479.x

23. Totet A, Meliani L, Lacube P, Pautard JC, Raccurt C, Roux P, et al. Immunocompetent infants as a human reservoir for *Pneumocystis jirovecii*: rapid screening by non-invasive sampling and real-time PCR at the mitochondrial large subunit rRNA gene. *J Eukaryot Microbiol* 2003; **50(Suppl):** 668-9. doi: 10.1111/j.1550-7408.2003.tb00678.x

24. Flori P, Bellete B, Durand F, Raberin H, Cazorla C, Hafid J, et al. Comparison between real-time PCR, conventional PCR and different staining techniques for diagnosing *Pneumocystis jiroveci* pneumonia from bronchoalveolar lavage specimens. *J Med Microbiol* 2004; **53:** 603-7. doi: 10.1099/jmm.0.45528-0

25. Fan LC, Lu HW, Cheng KB, Li HP, Xu JF. Evaluation of PCR in bronchoalveolar lavage fluid for diagnosis of *Pneumocystis jiroveciii* pneumonia: a bivariate meta-analysis and systematic review. *PloS one* 2013; **8:** e73099. doi: 10.1371/journal.pone.0073099

26. Matsumura Y, Ito Y, Iinuma Y, Yasuma K, Yamamoto M, Matsushima A, et al. Quantitative real-time PCR and the (1→3)-β-D-glucan assay for differentiation between *Pneumocystis jirovecii* pneumonia and colonization. *Clin Microbiol Infect* 2012; **18:** 591-7. doi: 10.1111/j.1469-0691.2011.03605.x

27. Damiani C, Le Gal S, Lejeune D, Brahimi N, Virmaux M, Nevez G, et al. Serum (1→3)-β-D-glucan levels in primary infection and pulmonary colonization with *Pneumocystis jirovecii*. *J Clin Microbiol* 2011; **49:** 2000-2. doi: 10.1128/JCM.00249-11

28. Desoubeaux G, Chesnay A, Mercier V, Bras-Cachinho J, Moshiri P, Eymieux S, et al. Combination of β-(1, 3)-D-glucan testing in serum and qPCR in nasopharyngeal aspirate for facilitated diagnosis of Pneumocystis jirovecii pneumonia. *Mycoses* 2019; **62:** 1015-22. doi: 10.1111/myc.12997

29. Corsi-Vasquez G, Ostrosky-Zeichner L, Pilkington EF 3rd, Sax PE. Point-counterpoint: should serum β-d-Glucan testing be used for the diagnosis of Pneumocystis jirovecii pneumonia? *J Clin Microbiol* 2019; **58:** pii: e01340-19. doi: 10.1128/JCM.01340-19

30. Azoulay E, Bergeron A, Chevret S, Bele N, Schlemmer B, Menotti J. Polymerase chain reaction for diagnosing pneumocystis pneumonia in non-HIV immunocompromised patients with pulmonary infiltrates. *Chest* 2009; **135:** 655-61. doi: 10.1378/chest.08-1309

31. Jarboui MA, Sellami A, Sellami H, Cheikhrouhou F, Makni F, Ben Arab N, et al. Molecular diagnosis of Pneumocystis jirovecii pneumonia in immunocompromised patients. *Mycoses* 2010; **53:** 329-33. doi: 10.1111/j.1439-0507.2009.01715.x

32. Carmona EM, Limper AH. Update on the diagnosis and treatment of *Pneumocystis* pneumonia. *Ther Adv Respir Dis* 2011; **5:** 41-59. doi: 10.1177/1753465810380102

33. Nevez G, Raccurt C, Jounieaux V, Dei-Cas E, Mazars E. Pneumocystosis versus pulmonary Pneumocystis carinii colonization in HIV-negative and HIV-positive patients. *AIDS* 1999; **13:** 535-6. doi: 10.1097/00002030-199903110-00020

34. Huang L, Crothers K, Morris A, Groner G, Fox M, Turner JR, et al. Pneumocystis colonization in HIV-infected patients. *J Eukaryot Microbiol* 2003; **50(Suppl):** 616-7. doi: 10.1111/j.1550-7408.2003.tb00651.x

35. Vargas SL, Pizarro P, Lopez-Vieyra M, Neira-Avile´s P, Bustamante R, Ponce CA. Pneumocystis colonization in older adults and diagnostic yield of single versus paired noninvasive respiratory sampling. *Clin Infect Dis* 2010; **50:** e19-e21. doi: 10.1086/649869

36. Montesinos I, Brancart F, Schepers K, Jacobs F, Denis O, Delforge ML. Comparison of 2 real-time PCR assays for diagnosis of *Pneumocystis jirovecii* pneumonia in human immunodeficiency virus (HIV) and non-HIV immunocompromised patients. *Diagn Microbiol Infect Dis* 2015; **82:** 143-7. doi: 10.1016/j.diagmicrobio.2015.03.006

37. Fauchier T, Hasseine L, Gari-Toussaint M, Casanova V, Marty PM, Pomares C. Detection of *Pneumocystis jirovecii* by quantitative PCR to differentiate colonization and pneumonia in Immunocompromised HIV-positive and HIV-negative patients. *J Clin Microbiol* 2016; **54:** 1487-95. doi: 10.1128/JCM.03174-15

38. Mühlethaler K, Bögli-Stuber K, Wasmer S, von Garnier C, Dumont P, Rauch A, et al. Quantitative PCR to diagnose *Pneumocystis* pneumonia in immunocompromised non-HIV patients. *Eur Respir J* 2012; **39:** 971-8. doi: 10.1183/09031936.00095811

39. Robert-Gangneux F, Belaz S, Revest M, Tattevin P, Jouneau S, Decaux O, et al. Diagnosis of Pneumocystis jirovecii pneumonia in immunocompromised patients by real-time PCR: a 4-year prospective study. *J Clin Microbiol* 2014; **52:** 3370-6. doi: 10.1128/JCM.01480-14.

40. Botterel F, Cabaret O, Foulet F, Cordonnier C, Costa JM, Bretagne S. Clinical significance of quantifying *Pneumocystis jirovecii* DNA by using real-time PCR in bronchoalveolar lavage fluid from immunocompromised patients. *J Clin Microbiol* 2012; **50:** 227-31. doi: 10.1128/JCM.06036-11

41. Larsen HH, Huang L, Kovacs JA, Crothers K, Silcott VA, Morris A, et al. A prospective, blinded study of quantitative touch-down polymerase chain reaction using oralwash samples for diagnosis of *Pneumocystis* pneumonia in HIV-infected patients. *J Infect Dis* 2004; **189:** 1679-83. doi: 10.1086/383322

42. Huggett JF, Taylor MS, Kocjan G, Evans HE, Morris-Jones S, Gant V, et al. Development and evaluation of a real-time PCR assay for detection of *Pneumocystis jirovecii* DNA in bronchoalveolar lavage fluid of HIV-infected patients. *Thorax* 2008; **63:** 154-9. doi: 10.1136/thx.2007.081687

research article

Stereotactic body radiation therapy (SBRT) for the treatment of primary lung cancer in recipients of lung transplant

Assaf Moore[1,3], Mordechai R. Kramer[2,3], Dror Rosengarten[2,3], Osnat Shtraichman[2,3], Alona Zer[1,3], Elizabeth Dudnik[1,3], Yasmin Korzets[1], Aaron M. Allen[1,3]

[1] Institute of Oncology, Davidoff Cancer Center, Rabin Medical Center, Petach Tiqva, Israel
[2] The Institute of Pulmonary Medicine, Rabin Medical Center, Petach Tiqva, Israel
[3] Sackler Faculty of Medicine, Tel Aviv University, Tel Aviv, Israel

Radiol Oncol 2020; 54(2): 227-232.

Received 21 December 2019
Accepted 29 February 2020

Correspondence to: Aaron M. Allen, Radiotherapy Department, Davidoff Center, 39 Jabotinski St., Petach Tikvah, Israel.
E-mail: ahron.alon@gmail.com

Disclosure: No potential conflicts of interest were disclosed.

Background. Lung transplantation is a life-saving treatment for patients with end stage lung disease. There may be a higher incidence of lung cancer in lung transplant recipients, and these cancers tend to be diagnosed at a more advanced stage. There is very little data on the safety and efficacy of stereotactic body radiation therapy (SBRT) for lesions in the native lung in lung-transplant recipients.

Patients and methods. A retrospective chart review of all patients who have undergone lung transplantation and were treated with SBRT for lung cancer in the native lung in the Davidoff Cancer Center was performed.

Results. Four patients who were treated with SBRT to a total of 5 lesions were included. Two patients were treated without histological confirmation of malignancy. All cases were discussed in a multidisciplinary tumor board before being referred for radiotherapy. Standard SBRT dosing was used. Responses were assessed by imaging. Three lesions exhibited a complete response and two lesions had a partial response. The patients who had partial responses developed distant metastases and died shortly. No patient developed measurable toxicity.

Conclusions. SBRT is effective and safe for the management of lung cancer in lung-transplant patients. Standard dose and fractionation can be used.

Key words: Stereotactic Body Radiation Therapy (SBRT); lung transplantation; lung cancer; radiotherapy

Introduction

Lung transplant is a life-saving last resort treatment for patients with end stage lung disease. The most common indications are chronic obstructive pulmonary disease (COPD) and idiopathic pulmonary fibrosis (IPF).[1] This risk for lung cancer thus arises mainly from the native lung.[1] There is a higher incidence of lung cancer in lung transplant recipients compared with the general population.[2–6] This finding might be related to smoking, immunosuppression and/or underlying lung disease.[4,5] Due to the improved life expectancy of transplanted patients and these predisposing factors, the incidence of lung cancer in lung transplant recipients is expected to increase.[1] These cancers are often diagnosed in a more advanced stage and with a worse prognosis.[3,4] For patients diagnosed with a potentially curable disease, curative treatment options include surgery and radiotherapy. We hereby present our experience with SBRT for the definitive treatment of four patients who underwent single lung transplantation and were diagnosed with lung cancer in the native lung.

Patients and methods

Patients

The study includes all consecutive patients located in the registry of the Institute of Pulmonary Medicine who underwent lung transplantation and were treated with SBRT for lung cancer in the native lung at the Davidoff Cancer Center (DCC) at Rabin Medical Center (RMC) between June 2011 and June 2015.

Data collection and outcomes

This retrospective study was approved by the medical center's institutional Helsinki review board. No informed consent was required. Data were collected from medical records and included demographics, medical comorbidities, location and extent of disease, imaging findings, radiation treatment details, imaging and clinical follow-up, performance status, response to treatment, survival, and cause of death.

Treatment planning

Patients were immobilized for simulation using a customized vacuum cushion for CT simulation. Patients were simulated using a multiphase 4-dimentional CT simulation to monitor breathing-related tumor motion. Images were reconstructed on the Advantage Workstation (GE Healthcare, Chicago, IL). An expansion in the cranio-caudal and axial dimensions for the internal target volumes (ITVs) was created based on tumor motion and location in 10 phases of breathing. The planning treatment volume (PTV) was defined as a 3-mm margin around the ITV. The PTV was reduced in case of proximity to vital normal tissue. Patients were treated with IMRT using dynamic sliding window multileaf collimator (MLC) or volumetric modulated arc therapy VMAT). Image guidance with cone beam CT preceded each fraction. Specification of the dose-volume histogram (DVH) constraints is available in Table 1. Dose calculations were performed using the Eclipse™ treatment planning system (Varian, Palo Alto, CA), AAA algorithm version 8. Treatment was prescribed to the 95% isodose line with PTV tolerance of ± 5%. Quality assurance verification plans were performed with the ArcCHECK™ dosimeter (Sun Nuclear Corporation, Melbourne, FL). Before each treatment, image guided radiotherapy was used based on cone beam CT (CBCT) to position the patients.

TABLE 1. Dose-volume histogram constraints for organs at risk

Organ	Constraints
Total Lung Dose (both lungs)	V20 < 10%
Spinal Cord	Max dose < 18 Gy
Esophagus	Dose to 1cc < 27 Gy
Heart	Dose to 1cc < 30 Gy

Gy = Gray; V20 = proportion of the lung receiving 20Gy

Post RT evaluation

The treated tumors were assessed by CT or PET-CT eight weeks from completion of SBRT. Further imaging studies were scheduled at the treating physician's discretion.

Results

Four consecutive cases of lung transplant recipients who underwent SBRT for a lung lesion are included. All cases were discussed in a multidisciplinary team including pulmonologists, thoracic surgeons, radiation oncologists, medical oncologists and radiologists before being referred for radiotherapy. All patients were asymptomatic at diagnosis. Radiotherapy treatment parameters are summarized in Table 2.

Case 1

A 72-year-old man with a history of heavy smoking, COPD, hypertension, diabetes mellitus type 2, chronic renal failure, peripheral vascular disease and fatty liver disease. The patient underwent left lung transplant in 2006 due to severe emphysema, and was treated with tacrolimus and azathioprine to prevent rejection. In November 2011, an 8 mm nodule was detected in the right lower lobe. The lesion increased in size to 26 mm in May 2015. A biopsy yielded moderately differentiated squamous cell carcinoma. A positron emission tomography–computed tomography (PET-CT) demonstrated high fluorodeoxyglucose (FDG) uptake in the nodule with no evidence of disease outside the lung. The patient was treated in June 2015 with a dose of 54 Gray (Gy) in three 18 Gy fractions. Treatment was well tolerated with no adverse events or measurable toxicity. Follow-up imaging demonstrated a complete response (CR). In February 2017, a new nodule appeared in the right lower lobe that in-

TABLE 2. SBRT treatment parameters

	Case 1 1st course	Case 1 2nd course	Case 2	Case 3	Case 4
Prescribed dose (Gy), number of fractions	54 Gy, 3	54 Gy, 3	60 Gy, 5	54 Gy, 3	60 Gy, 5
MLD – both lungs (Gy)	3.3	3.6	4.4	2.5	6
V5 – both lungs, (%)	15.6	21.5	18.9	10.2	27.1
V20 – both lungs, (%)	4.9	3.2	5.7	2.9	8
MLD – transplanted lung (Gy)	4.5	0.8	2.2	0.6	1.8
V5 – transplanted lung, (%)	20.4	1.4	9.6	0.1	6.1
V20 – transplanted lung, (%)	7	0	2.3	0	0

Gy = Gray; MLD = mean lung dose, V5 = the % of a structure's volume that receives 5 Gy; V20 = the % of a structure's volume that receives 20 Gy

creased in size on follow-up imaging. A PET-CT in April 2017 demonstrated high FDG uptake in the nodule with no evidence of disease outside the lung. The patient was treated in July 2017 to a dose of 54 Gy in three 18 Gy fractions. The post SBRT PET-CT demonstrated shrinkage of the treated nodule, however, clear metastases in the liver and bone. A liver biopsy yielded adenocarcinoma of lung origin. The patient succumbed to metastatic disease in January 2018.

Case 2

A 76-year-old woman with a history of heavy smoking, COPD, diabetes mellitus type 2, chronic renal failure and atrial fibrillation. The patient underwent left lung transplant in 2002 due to severe emphysema, and was treated with tacrolimus and mycophenolic acid to prevent rejection. In June 2010, a central 0.5 mm nodule was detected in the right lower lobe. The lesion increased in size up to 13 mm in October 2011, and demonstrated high FDG uptake with no evidence of disease outside the lung. The patient was discussed in a multidisciplinary tumor board and it was decided to treat the lesion with SBRT without histological confirmation. The patient was treated in February 2012 to a dose of 60 Gy in five 12 Gy fractions. Treatment was well tolerated with no adverse events or measurable toxicity. Follow-up imaging demonstrated a complete response (Figure 1). The patient passed away in May 2018 secondary to pneumonia and sepsis.

Case 3

A 72-year-old man with a history of hypertension, diabetes mellitus type 2, chronic renal failure and ischemic heart disease. Underwent right lung transplant in 2002 due to IPF, and was treated with tacrolimus and mycophenolic acid to prevent rejection. In 2013 a nodule was detected in the left lower lobe and increased in size to 15 mm in October 2013. There was no FDG uptake in the nodule. The patient was discussed in a multidisciplinary tumor board and it was decided to treat the lesion

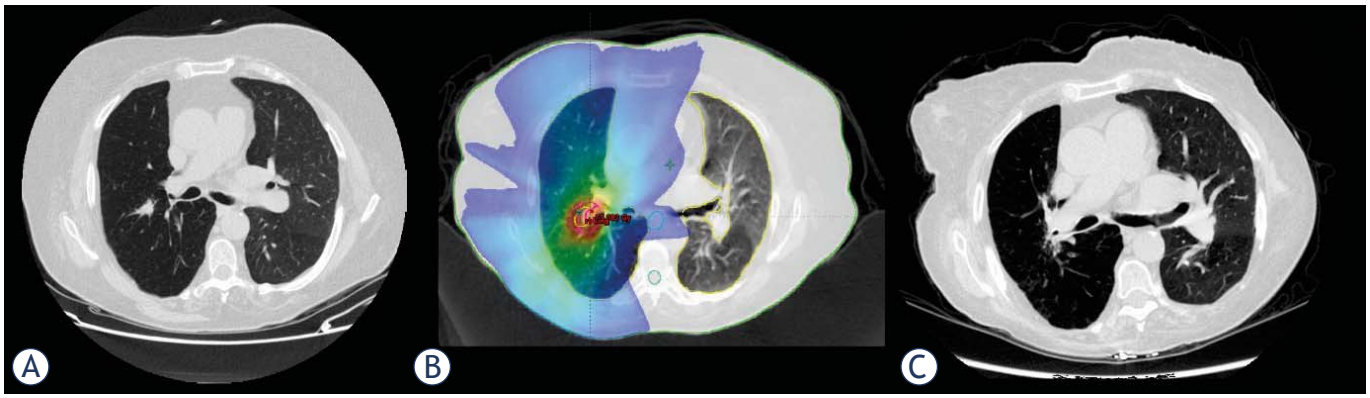

FIGURE 1. (A) Pretreatment CT demonstrating a central nodule in the right lower lobe **(B)** Radiation field arrangement and dose color wash for SBRT **(C)** CT 2 months after treatment completion demonstrating a complete disappearance of the target nodule.

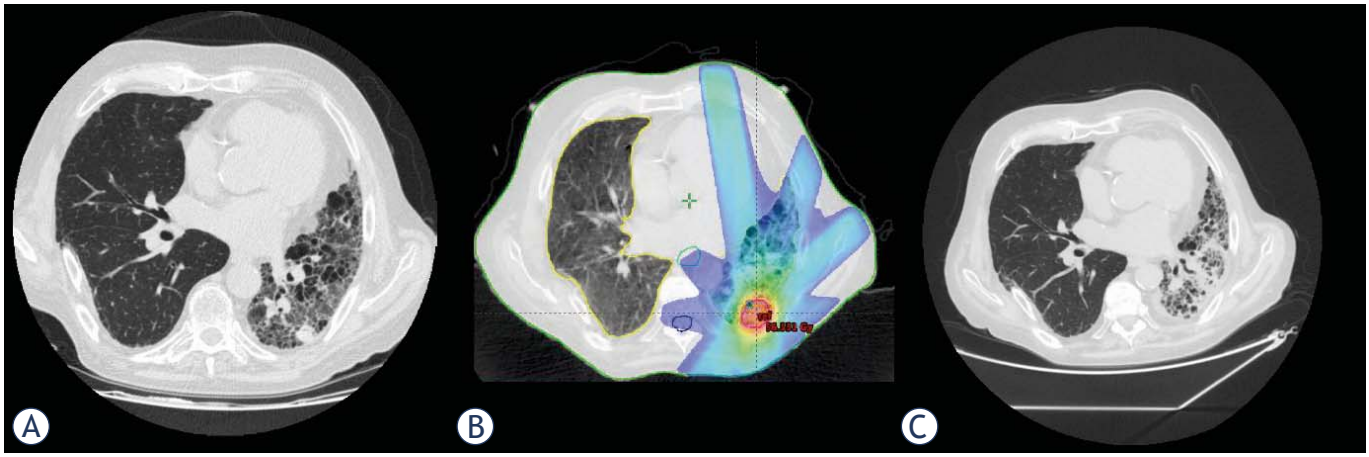

FIGURE 2. (A) Pretreatment CT demonstrating a nodule was detected in the left lower lobe **(B)** Radiation field arrangement and dose color wash for SBRT **(C)** CT 2 months after treatment completion demonstrating a complete disappearance of the target nodule.

with SBRT without histological confirmation. The patient was treated in February 2012 to a dose of 54 Gy in three 18 Gy fractions. Treatment was well tolerated with no adverse events or measurable toxicity. The post SBRT, CT scans yielded a disappearance of the treated nodule (Figure 2). The patient passed away in October 2015 secondary to bacteremia and sepsis.

Case 4

A 65-year-old man with a history of hypertension and diabetes mellitus type 2. Underwent left lung transplant in 2009 due to severe IPF, and was treated with tacrolimus and mycophenolic acid to prevent rejection. In 2011, a mass was detected in the anterior right mediastinum with involvement of the pleura and right upper lobe. A PET-CT demonstrated high FDG uptake in the mass that increased in size to 3.8 cm with no evidence of disease outside the lung. A biopsy yielded moderately differentiated small cell lung cancer (SCLC). The patient was discussed in a multidisciplinary tumor board, and determined to be a poor surgical candidate, was referred for SBRT and then planned for "adjuvant" chemotherapy. The patient was treated in June 2011 to a dose of 60 Gy in five 12 Gy fractions. Treatment was well tolerated with no adverse events or measurable toxicity. The post SBRT, CT scans yielded a partial response (PR) of the treated nodule (Figure 3), however, appearance of metastases in the liver and nodes above and below the diaphragm. The patient succumbed to a rapid progression of metastatic disease in August 2011.

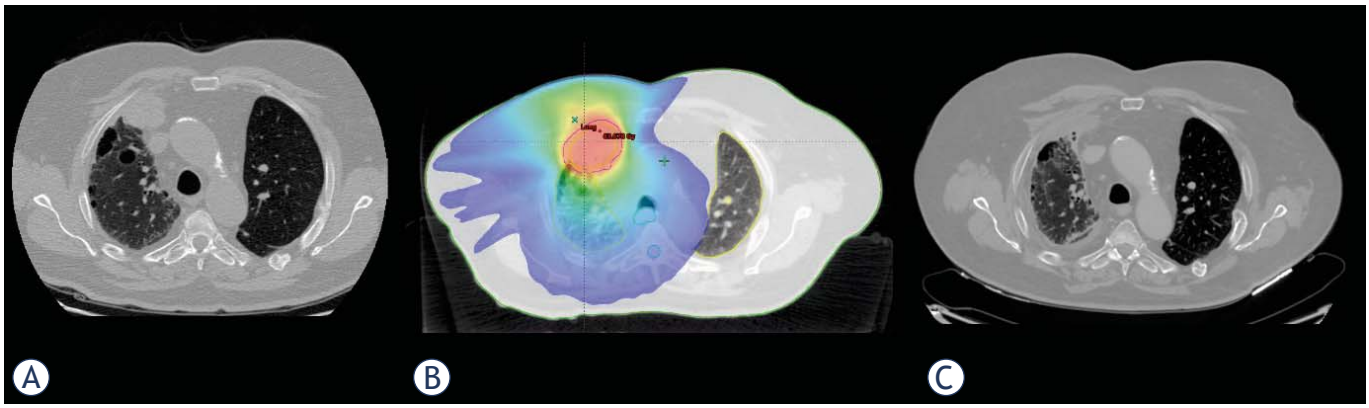

FIGURE 3. (A) Pretreatment CT demonstrating a mass in the anterior right mediastinum with involvement of the pleura and right upper lobe **(B)** Radiation field arrangement and dose color wash for SBRT **(C)** CT 2 months after treatment completion demonstrating regression of the target nodule.

Discussion

Lung cancer in lung transplant recipients is a unique clinical scenario, in which patients suffer from at least two major life-threatening conditions. Treatment options for these patients may be limited due to the underlying condition, other comorbidities and their immunosuppressed state. Treating these patients requires a multi-disciplinary effort. Characterizing this group of patients is beyond the scope of this report.

We present a series of 4 consecutive patients who were treated with SBRT to a total of 5 lesions in the native lungs. One patient had proven squamous cell carcinoma and then adenocarcinoma, one had small cell carcinoma, and two were treated without histological confirmation of malignancy.

Surgery remains the standard-of-care treatment for medically-operable early stage non-small cell lung cancer. Radiotherapy for the definitive treatment of early lung cancer was traditionally indicated for the medically-inoperable or those refusing surgery.[7] Lung resection is challenging in patients with a major pulmonary disease, and especially when these patients have undergone lung transplantation and are immunosuppressed. Specific concerns include Impaired wound healing and anastomotic complications.[8] Data on the safety of these procedures is scarce. In one series that included both malignant and benign/infectious causes for pulmonary resection of the native or allograft, of the 11 patients included, 3 patients died of post-procedural infectious complications, 2 died of acute respiratory distress syndrome and organ failure and 1 died as a result of bronchiolitis obliterans organizing pneumonia.[8]

Radiotherapy is an integral modality in the treatment of early lung cancer. SBRT has been studied extensively in medically inoperable patients, and may in fact achieve better control than standard radiotherapy.[7,9,10] SBRT has also been proven effective for medically operable patients, even compared with surgery.[11,12] While it is unknown whether radiotherapy and SBRT specifically can be safely and effectively used in lung transplant recipients, toxicity in clinical trials has been low with no treatment-related mortality.[7,9,10] Data on the interaction between immunosuppression and advanced oncologic treatments is scarce. This applies to systemic therapy such as tyrosine kinase inhibitors, but even more concerning - with immunotherapeutic agents facing a risk for organ rejection.[13] The immune system's role in mediating response to radiotherapy is being studied, however the exact implications of immunosuppression during radiotherapy are poorly understood.[14] In this series, all lesions achieved excellent response by imaging – 3 lesions exhibited a complete response and two lesions partial responses. The patients who had partial responses developed distant metastases and died shortly, thus; the maximal response may not have been achieved during the short follow-up. None of the lesions who exhibited a complete response recurred locally. Based on this small series, even in immunosuppressed patients, SBRT to lung lesions is effective at achieving local control.

There have been several reports of SBRT in the treatment of patients with lung cancer who had previously undergone solid organ transplant. In a series of 15 patients (9 of which underwent lung transplant), no patients experienced grade 3 or 4 toxicity, however, one patient with a history of single lung transplant died of radiation pneumonitis 7 months after SBRT to a lesion within the transplanted lung. The cumulative incidence of local failure was 7% and 13% at 1 and 2 year and the incidence of distant failure was 40% at 1 year.[15] In another series, two patients were treated with SBRT-range dosing sequentially with chemotherapy. One achieved a durable complete response, while another progressed shortly.[4] One case ineligible for surgical management of stage IB adenocarcinoma arising from a donor lung post-double lung transplantation, was safely and effectively treated to a dose of 60 Gy in 8 fractions.[16]

The doses and organs at risk constraints we have used did not differ from our institutional policy towards non-transplanted patients and seemed to be effective and safe. However, whether an optimal dose and fractionation exists or whether tighter constraints are required, has not been determined and no clear recommendation can be made.

While there were no cases of grade 2 or higher pneumonitis in our patients, organ transplanted patients, and specifically lung transplanted patients could prove a diagnostic challenge for this type of toxicity, as the differential diagnosis for clinical deterioration is broad and might not be distinguishable by imaging.

The main limitations of this study relate to its retrospective design and lack of a control arm, which are generally associated with methodological biases and difficulties in results interpretation. The most concerning bias in our study is clearly associated with patient selection, as patients who have undergone transplantation usually have other comorbidities and their cancers may have a more aggressive course.

It is clear that SBRT is a safe and efficient modality for the treatment of recipients of lung transplant and could offer long-term control and potentially a definitive solution. There are no randomized comparative reports comparing it with invasive procedures. Physicians must consider the potential early and late toxicities of thoracic radiation, including pneumonitis, esophagitis and vascular toxicity. These may be avoided by minimizing volumes and strictly maintaining dose constraints. SBRT could serve to achieve these objectives.

Conclusions

SBRT for the management of lung cancer in the native lung in lung-transplanted patients is effective and safe and can offer long-term control. Standard dose and fractionation can be used. It should be considered in clinical situations where surgical procedures are not feasible. These results should encourage clinicians to investigate its role further, potentially in place of invasive procedures.

References

1. Mathew J, Kratzke RA. Lung cancer and lung transplantation: a review. *J Thorac Oncol* 2009; **4:** 753-60. doi: 10.1097/JTO.0b013e31819afdd9
2. Choi YH, Leung AN, Miro S, Poirier C, Hunt S, Theodore J. Primary bronchogenic carcinoma after heart or lung transplantation: radiologic and clinical findings. *J Thorac Imaging* 2000; **15:** 36-40. doi: 10.1097/00005382-200001000-00008
3. Raviv Y, Shitrit D, Amital A, Fox B, Rosengarten D, Fruchter O, et al. Lung cancer in lung transplant recipients: experience of a tertiary hospital and literature review. *Lung Cancer* 2011; **74:** 280-3. doi: 10.1016/j.lungcan.2011.02.012
4. Du L, Pennell NA, Elson P, Hashemi-Sadraei N. Lung cancer treatment outcomes in recipients of lung transplant. *Transl Lung Cancer Res* 2015; **4:** 784-91. doi: 10.3978/j.issn.2218-6751.2015.12.08
5. Collins J, Kazerooni EA, Lacomis J, McAdams HP, Leung AN, Shiau M, et al. Bronchogenic carcinoma after lung transplantation: frequency, clinical characteristics, and imaging findings. *Radiology* 2002; **224:** 131-8. doi: 10.1148/radiol.2241011189
6. Dickson RP, Davis RD, Rea JB, Palmer SM. High frequency of bronchogenic carcinoma after single-lung transplantation. *J Heart Lung Transplant* 2006; **25:** 1297-301. doi: 10.1016/j.healun.2006.09.009
7. Timmerman RD, Hu C, Michalski J, Straube W, Galvin J, Johnstone D, et al. Long-term results of RTOG 0236: a phase II trial of stereotactic body radiation therapy (SBRT) in the treatment of patients with medically inoperable stage I non-small cell lung cancer. *Int J Radiat Oncol Biol Phys* 2014; **90:** S30. doi: 10.1016/j.ijrobp.2014.05.135
8. Fitton TP, Bethea BT, Borja MC, Yuh DD, Yang SC, Orens JB, et al. Pulmonary resection following lung transplantation. *Ann Thorac Surg* 2003; **76:** 1680-6. doi: 10.1016/s0003-4975(03)00975-5
9. Nyman J, Hallqvist A, Lund J-A, Brustugun OT, Bergman B, Bergström P, et al. SPACE - A randomized study of SBRT vs conventional fractionated radiotherapy in medically inoperable stage I NSCLC. *Radiother Oncol* 2016; **121:** 1-8. doi: 10.1016/j.radonc.2016.08.015
10. Ball D, Mai GT, Vinod S, Babington S4, Ruben J5, Kron T, et al. Stereotactic ablative radiotherapy versus standard radiotherapy in stage 1 non-small-cell lung cancer (TROG 09.02 CHISEL): a phase 3, open-label, randomised controlled trial. *Lancet Oncol* 2019; **20:** 494-503. doi: 10.1016/S1470-2045(18)30896-9
11. Chang JY, Senan S, Paul MA, Mehran RJ, Louie AV, Balter P, et al. Stereotactic ablative radiotherapy versus lobectomy for operable stage I non-small-cell lung cancer: a pooled analysis of two randomised trials. *Lancet Oncol* 2015; **16:** 630-7. doi: 10.1016/S1470-2045(15)70168-3
12. Zheng X, Schipper M, Kidwell K, Lin J, Reddy R, Ren Y, et al. Survival outcome after stereotactic body radiation therapy and surgery for stage I non-small cell lung cancer: a meta-analysis. *Int J Radiat Oncol Biol Phys* 2014; **90:** 603-11. doi: 10.1016/j.ijrobp.2014.05.055
13. Ros J, Matos I, Martin-Liberal J. Immunotherapy in organ-transplanted cancer patients: efficacy and risk of organ rejection. *Ann Oncol* 2019; **30:** 1173-7. doi: 10.1093/annonc/mdz129
14. Walle T, Martinez Monge R, Cerwenka A, Ajona D, Melero I, Lecanda F. Radiation effects on antitumor immune responses: current perspectives and challenges. *Ther Adv Med Oncol* 2018; **10:** 1758834017742575. doi: 10.1177/1758834017742575
15. Fleming CW, Stephans KL, Broughman JR, Rybicki L, Budev M, Ahmad U, et al. Outcomes after SBRT for inoperable early stage lung cancers arising in organ transplant patients. *Int J Radiat Oncol Biol Phys* 2019; **105:** E486. doi: 10.1016/j.ijrobp.2019.06.1382
16. Chen H, Tikkanen J, Boldt RG, Louie A V. Stereotactic ablative radiotherapy for early-stage lung cancer following double lung transplantation. *Radiat Oncol* 2018; **13:** 142. doi: 10.1186/s13014-018-1089-8

research article

Sorafenib for the treatment of hepatocellular carcinoma: a single-centre real-world study

Jurij Hanzel[1], Tajda Kosir Bozic[1], Borut Stabuc[1,2], Rado Jansa[1,2]

[1] Department of Gastroenterology, University Medical Centre Ljubljana, Ljubljana, Slovenia
[2] Faculty of Medicine, University of Ljubljana, Ljubljana, Slovenia

Radiol Oncol 2020; 54(2): 233-236.

Received 18 November 2019
Accepted 1 December 2019

Correspondence to: Rado Janša, Ph.D., M.D., Department of Gastroenterology, University Medical Centre Ljubljana, Japljeva ulica 2, SI-1000 Ljubljana, Slovenia. E-mail: rado.jansa@kclj.si

Disclosure: No potential conflicts of interest were disclosed.

Background. Sorafenib is an oral multi-kinase inhibitor used for the treatment of hepatocellular carcinoma. Its efficacy in randomised controlled trials was demonstrated in patients with well-preserved liver function and good functional status. In the real-world setting, treatment is often offered to patients outside these criteria. We therefore performed a single-centre real-world cohort study on the efficacy of sorafenib in patients with hepatocellular carcinoma.

Patients and methods. We identified all patients with hepatocellular carcinoma initiating treatment with sorafenib between January 2015 and January 2018. The primary endpoint was overall survival (OS) since starting sorafenib. Clinical and demographic variables associated with survival were studied.

Results. The median OS was 13.4 months (95% CI 8.2–18.6). Multivariable Cox's regression identified worse ECOG performance status (HR 2.21; 95% CI 1.56–3.16; $P < 0.0001$), Child-Pugh class C (HR 52.4; 95% CI 3.20–859; $P = 0.005$) and absence of prior locoregional treatment (HR 2.30; 95% CI 1.37–3.86; $P = 0.002$) to be associated with increased mortality.

Conclusions. Careful selection of patients for treatment with sorafenib is of paramount importance to optimize outcomes.

Key words: survival; multivariable analysis; real-world cohort study

Introduction

Sorafenib is an oral multi-kinase inhibitor, which inhibits tumours angiogenesis through inhibition of vascular endothelial growth factor (VEGF) and platelet-derived growth factor (PDGF) signalling pathways. It has demonstrated a significant prolongation in overall survival of patients with advanced-stage hepatocellular carcinoma (HCC) up to 2.8 months.[1,2] The two landmark trials included mainly patients with compensated liver cirrhosis of viral aetiology and an excellent baseline functional status. Consequently, sorafenib is formally indicated only in patients with well-preserved liver function (Child-Pugh A) and advanced tumours (Barcelona Clinic Liver Cancer [BCLC] C) or intermediate stage tumours (BCLC B) progressing after locoregional therapy.[3]

Nevertheless, sorafenib is often used outside these criteria in the real-world setting, mainly due to the absence of alternative treatment options. As these patient subgroups were not studied in registrational trials, only large observational non-randomized cohort studies can help inform practice.[4-6]

We therefore a retrospective real-world cohort study of patients treated with sorafenib for advanced HCC, investigating its efficacy and variables associated with OS.

Patients and methods

Patients and study design

We performed a retrospective cohort study of all patients with HCC initiating treatment with sorafenib between January 2015 and January 2018,

who were followed until October 2018 at a single tertiary centre. Data collection was approved by the institutional ethics committee, while treatment did not differ from the standard of care and thus did not require additional approval.

We included all consecutive patients aged at least 18 years with a histologically or radiologically confirmed diagnosis of HCC, who were treated with sorafenib. The decision for initiation of the drug was made based on the consensus of the Liver Multidisciplinary Team. Patient records were retrospectively reviewed for demographic and clinical information. The date of death was extracted from the national health insurance database.

The primary outcome was OS from initiation of sorafenib. We explored the relationship of clinical characteristics with OS.

Statistical analysis

Continuous variables are given as medians with interquartile ranges (IQR). Univariable association analyses with survival were performed using the Kaplan-Meier method with log-rank testing. Multivariable analysis was performed using a Cox-proportional hazards model with stepwise backward selection where variables were removed if they did not achieve statistical significance at $P < 0.05$. All analyses were performed on an intention-to-treat basis. Analyses were performed using SPSS, Version 25 (IBM, Chicago, USA).

TABLE 1. Patient characteristics at initiation of sorafenib (n = 115)

Variable	
Male gender, n (%)	96 (84)
Age, years, median (IQR)	67 (60–72)
ECOG performance status	
0	31 (27)
1	47 (40.9)
2	36 (31.3)
3	1 (0.9)
Aetiology of underlying liver disease, n (%)	
Alcoholic liver disease	56 (49)
Hepatitis B	11 (9.6)
Hepatitis C	7 (6.1)
Non-alcoholic steatohepatitis	18 (15.7)
Cryptogenic	10 (8.7)
Wilson's disease	1 (0.9)
Primary biliary cholangitis	1 (0.9)
HCC in non-cirrhotic liver	11 (9.6)
Child-Pugh class, n (%)	
A	77 (66.9)
B	37 (32.2)
C	1 (0.9)
BCLC stage, n (%)	
A	3 (2.6)
B	42 (36.5)
C	70 (60.9)
Prior treatment, n (%)	45 (39.1)
Resection	10 (8.7)
RFA	2 (1.8)
Transplant	3 (2.6)
TACE	29 (25.2)
Radioembolization	5 (4.3)
AFP, kU/L, median (IQR)	6–1518)

AFP = alpha-fetoprotein; BCLC = Barcelona Clinic Liver Cancer; ECOG = Eastern Cooperative Oncology Group; HCC = hepatocellular carcinoma; IQR = interquartile range; RFA = radiofrequency ablation; TACE = transarterial chemoembolization

Results

Patient characteristics

We included 115 patients, who were predominantly male with Child-Pugh class A alcoholic cirrhosis with good performance status (Table 1).

Survival outcomes

A total of 83 patients (72%) died during the study period. The median OS since initiation of sorafenib was 13.4 months (95% CI 8.2–18.6).

In univariable analysis, reduced OS was associated with worse ECOG performance status ($P < 0.0001$), higher Child-Pugh class ($P < 0.0001$), higher baseline AFP ($P = 0.003$) and absence of prior locoregional treatment ($P < 0.0001$) (Table 2). The associations of liver disease aetiology ($P = 0.192$), BCLC stage ($P = 0.539$), gender ($P = 0.944$) and age at treatment initiation ($P = 0.201$) with OS were not statistically significant.

Multivariable analysis demonstrated significant associations between mortality and ECOG performance status (HR 2.21; 95% CI 1.56–3.16; $P < 0.0001$), Child-Pugh class C (HR 52.4; 95% CI 3.20–859; $P = 0.005$) and absence of prior locoregional treatment (HR 2.30; 95% CI 1.37–3.86; $P = 0.002$), but not baseline AFP (HR 1.00; 95% CI 0.8–1.2; $P = 0.278$) (Table 2, Figure 1).

Discussion

HCC is among the leading causes of cancer-related deaths. It primarily develops from cirrhosis, and many patients are infected with hepatitis C virus (HCV) or hepatitis B virus (HBV). Treatment with the multikinase inhibitor sorafenib is a systemic therapy option for patients with advanced HCC since 2008.

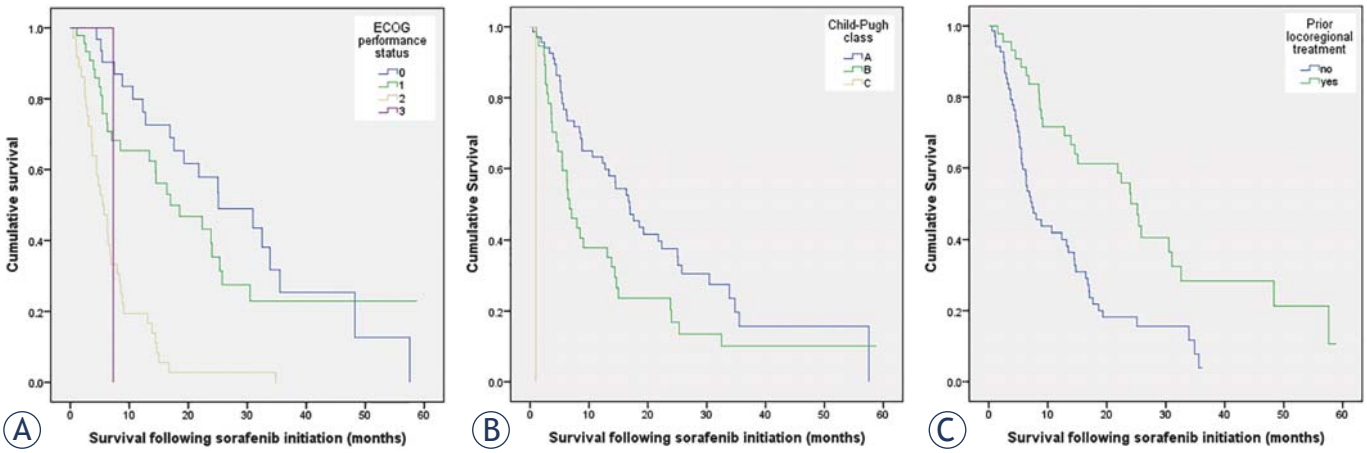

FIGURE 1. Kaplan-Meier plots of overall survival (OS) after initiating sorafenib stratified by **(A)** ECOG performance status, **(B)** Child-Pugh class, and **(C)** prior locoregional treatment.

Systemic therapy has helped prolong survival after disease progression. Clinical management of patients should target improvement of patient OS. Sorafenib therapy is recommended in guidelines as the first-line option in patients who cannot benefit from resection, transplantation, ablation or TACE, and still have preserved liver function and significantly prolonged OS and TTP.

Sorafenib monotherapy remains the standard of care in unresectable HCC. Sorafenib has demonstrated survival benefit in patients with unresectable HCC in two (2) randomized, placebo-con-

TABLE 2. Factors associated with overall survival (OS) after initiation of sorafenib

	Univariable analysis		Multivariable analysis	
	Median survival in months (95% CI)	Log rank *P* value	Hazard ratio (95% CI)	Cox's regression *P* value
ECOG performance status				
0	25.1 (12.8–37.4)	<0.0001	2.21 (1.56–3.16)	<0.0001
1	17.0 (7.0–26.9)			
2	5.5 (3.7–7.3)			
3	7.3 (/)			
Child-Pugh class				
A	16.9 (12.8–21.0)	<0.0001	1.00	
B	6.7 (4.7–8.7)		1.34 (0.80–2.26)	0.271
C	1.0 (/)		52.4 (3.20–859)	0.005
Baseline AFP				
< 200	17.0 (9.3–24.6)	0.003	1.00 (0.8–1.2)	0.278
≥ 200	6.7 (5.6–7.8)			
Prior locoregional treatment				
Yes	24.0 (20.1–27.9)	<0.0001	1.00	
No	7.3 (5.0–9.5)		2.30 (1.37–3.86)	0.002
Liver disease aetiology				
Alcoholic	8.6 (3.80–13.3)	0.192		
Other	16.7 (13.5–19.9)			
BCLC stage				
A	22.4 (7.0–37.7)	0.539		
B	14.5 (5.1–23.9)			
C	13.4 (7.1–19.7)			
Gender				
Female	8.8 (7.0–10.7)	0.944		
Male	13.8 (10.1–17.6)			
Age				
< 70 years	15.0 (11.2–18.8)	0.201		
≥ 70 years	8.4 (6.0–10.8)			

AFP = alpha-fetoprotein; BCLC = Barcelona Clinic Liver Cancer; ECOG = Eastern Cooperative Oncology Group; IQR = interquartile range

trolled, double-blind, phase III trials: SHARP and AP. The use of sorafenib significantly increased OS: 10.7 months *vs*. 7.9 months (SHARP study) and radiologic progression was significantly lower in the sorafenib group of patients.[8]

The use of Sorafenib also significantly increased OS in Asian-Pacific study. However, the results compared with SHARP study were worst especially because of different demographic characteristics of patients, more extrahepatic spread, greater number of hepatic tumor lesions and poorer ECOG performance status.

In GIDEON, real life analysis of the sorafenib group of patients median OS was 8.6 month *vs*. 10.4 in SHARP study. Clinical outcomes of advanced HCC patients treated with sorafenib in real-life practice are better compared to the other studies conducted in the Asia-Pacific region in terms of survival and tolerability. Extrahepatic spread and combination with other therapies are of predictive value for OS of advanced HCC. Further studies are required to maximize the effect of sorafenib in combination with other modalities.[7,8]

In our retrospective study, we collected and analyzed the clinical outcomes of advanced HCC patients who underwent treatment with sorafenib in real-life clinical setting. We found that HCC patients with Child-Pugh A exhibited a significantly higher median survival. In the present study, factors that are predictive of OS in HCC patient treated with sorafenib include gender, extrahepatic spread, and combined other therapies.[7,8]

In the Slovenian study, HCC patients treated with sorafenib had median OS of 13.4 months, which is longer than that reported in SHARP (10.5 months) and GIDEON (Global Investigation of Therapeutic Decisions in HCC and of its treatment with sorafenib) (10.8 months).

Multivariable analysis of the Slovenian group of patients demonstrated significant associations between mortality and ECOG performance status, Child-Pugh class C and absence of prior locoregional treatment, but not baseline AFP.

There are several limitations in this retrospective designed analysis. Being a retrospective study, it is difficult to ascertain the actual cause of death in our cohort. The population size examined in our study is relatively small, which may limit the statistical power. Small population size may have influences on subgroup analysis. Other limitations include the reduced initial dose of sorafenib based on clinical decision made by individual physicians and adjustment of dosages during treatment due to intolerance.

However, our results are comparable with results of other worldwide studies.

In conclusions, careful selection of patients for sorafenib treatment is important. Treatment of HCC patients should be performed in experienced centers, where the decision of treatment of each patients should be made after previous presentation of patients at multidisciplinary board of experts.

References

1 Llovet JM, Hilgard P, de Oliveira AC, Hilgard P, Gane E, Blanc JF, et al. Sorafenib in Advanced Hepatocellular Carcinoma. *N Engl J Med* 2008; **13:** 378-90. doi: 10.1056/NEJMoa0708857

2 Cheng AL, Kang YK, Chen Z, Tsao CJ, Qin S, Kim JS, et al. Efficacy and safety of sorafenib in patients in the Asia-Pacific region with advanced hepatocellular carcinoma: a phase III randomised, double-blind, placebo-controlled trial. *Lancet Oncol* 2009; **10:** 25-34. doi: 10.1016/S1470-2045(08)70285-7

3 Vogel A, Cervantes A, Chau I, Daniele B, Llovet JM, Meyer T, et al. Hepatocellular carcinoma: ESMO Clinical Practice Guidelines for diagnosis, treatment and follow-up. *Ann Oncol* 2018; **29(Suppl 4):** iv238-55. doi: 10.1093/annonc/mdy308

4 Marrero JA, Kudo M, Venook AP, Ye SL, Bronowicki JP, Chen XP, et al. Observational registry of sorafenib use in clinical practice across Child-Pugh subgroups: The GIDEON study. *J Hepatol* 2016; **65:** 1140-7. doi: 10.1016/j.jhep.2016.07.020

5 Lee S, Kim BK, Kim SU, Park SY, Kim JK, Lee HW, et al. Clinical outcomes and prognostic factors of patients with advanced hepatocellular carcinoma treated with sorafenib as first-line therapy: a Korean multicenter study: Sorafenib as a first-line therapy. *J Gastroenterol Hepatol* 2014; **29:** 1463-9. doi: 10.1111/jgh.12542

6 Doyle A, Marsh P, Gill R, Rodov M, Mohsen W, Varma P, et al. Sorafenib in the treatment of hepatocellular carcinoma: a multicentre real-world study. *Scand J Gastroenterol* 2016; **51:** 979-85. doi: 10.3109/00365521.2016.1166518

7 Llovet LM, Bruix J. Management of HCC. *Hepathology* 2008; **48:** 1312-27. doi: 10.1002/hep.22506.

8 Forner A, Llovet LM, Bruix J. Hepatocellular carcinoma. *Lancet* 2012; **379:** 1245-55. doi: 10.1016/S0140-6736(11)61347-0

research article

Sarcopenia and myosteatosis at presentation adversely affect survival after esophagectomy for esophageal cancer

Matevz Srpcic[1,2], Taja Jordan[3], Karteek Popuri[4], Mihael Sok[1,2]

[1] Department of thoracic surgery, Surgical clinic, University Medical Centre Ljubljana, Slovenia
[2] Faculty of Medicine, University of Ljubljana, Slovenia
[3] Institute of radiology, University Medical Centre Ljubljana, Slovenia
[4] Simon Fraser University, Burnaby, Canada

Radiol Oncol 2020; 54(2): 237-246.

Received 7 January 2020
Accepted 3 March 2020

Correspondence to: Matevž Srpčič, M.D., Department of Thoracic Surgery, Surgical Clinic, University Medical Centre Ljubljana, Zaloška 7, SI-1000 Ljubljana, Slovenia. Phone: +386 1 522 3813; fax +386 1 522 2485; E-mail: matevz.srpcic@kclj.si

Disclosure: MSr, TJ and MSo declare that they have no competing interests. KP is a co-founder of and actively directs Voronoi Health Analytics Incorporated, a Canadian corporation that sells commercial licenses for the ABACS (Automated Body Composition Analyzer using Computed tomography image Segmentation) software.

Background. Esophageal cancer remains a disease with poor survival and many complications. Measuring muscle mass and quality can identify patients with diminished muscle mass (sarcopenia) and muscle fat infiltration (myosteatosis). We studied the impact of sarcopenia and myosteatosis in resectable esophageal cancer on overall survival and complications.

Patients and methods. 139 patients received a radical esophagectomy. Skeletal muscle area (SMA) and muscle attenuation (MA) in CT images at L3 level were recorded and groups with and without sarcopenia and myosteatosis were compared for overall survival (OS), perioperative mortality, conduit complications, pleuropulmonary complications, respiratory failure requiring mechanical ventilation and other significant complications.

Results. Prevalence of sarcopenia and myosteatosis at presentation was 16.5% and 51.8%, respectively. Both were associated with decreased OS. Median survival was 18.3 months (CI 5.4–31.1) *vs.* 31.0 months (CI 7.4–54.6) for sarcopenia/no sarcopenia (log rank p = 0.042) and 19.0 months (CI 13.3–24.7) *vs.* 57.1 months (CI 15.2–99.0) for myosteatosis (log rank p = 0.044), respectively. A relationship between sarcopenia and myosteatosis and other negative outcomes after esophagectomy could not be established.

Conclusions. Sarcopenia and myosteatosis before esophagectomy are associated with decreased overall survival but not with more frequent perioperative complications. Identification of patients at risk can guide therapeutic decisions and interventions aimed at replenishing muscle reserves.

Key words: sarcopenia; myosteatosis; esophagectomy; survival; esophageal cancer; muscle depletion

Introduction

Constant gradual improvements of operative techniques and perioperative care have reduced the dangers of esophagectomy, the cornerstone of radical treatment of resectable esophageal cancer, but it remains a major procedure burdened with high morbidity and mortality.[1] Overall 5-year survival in resectable esophageal cancer has improved in recent years by about 2–3 fold.[2] This improvement was attributed to centralization of surgical treatment and introduction of neoadjuvant chemoradiotherapy.[3] Advances were also made in perioperative care and better understanding and prevention of the detrimental effects of muscle depletion so typical of esophageal malignancies.[4]

Further improvement in outcomes can be achieved by tailoring the treatment to patients' ability to withstand the trauma of surgery and to return to a functional life after treatment. Adequate

fitness for treatment has traditionally been assessed from various performance scores, risk scores as well as more basic patients' characteristics like age and body mass index.[5] Body mass index (BMI) at presentation has proven to be an inaccurate predictor of outcomes since it does not correspond to body composition well.[6,7] Better methods to assess the most important parameter of body composition, the skeletal muscle content, have been introduced. They include functional tests like muscle strength measurements and measurements of muscle mass with dual energy x-ray imaging (DEXA), bioimpedance analysis or cross-sectional imaging (CT or MRI).[8] Cross-sectional imaging (or planimetry) has the advantage of being readily available in cancer patients for staging purposes. This has encouraged many studies to examine the relationship between overall muscle mass, its quality and their effect on outcomes. A reliable relationship between planimetrically determined muscle mass and quality and its function, determined by other methods available, has been established. Muscle area at the level of 3rd lumbal vertebra, normalized for height (skeletal muscle index (SMI)) is highly correlated with total body skeletal muscle mass.[9]

Estimating survival chances for a patient presenting with resectable esophageal cancer is important in planning appropriate treatment strategies and interventions aimed at improving survival and quality of life. Pronounced weight loss is a hallmark of malignant disease, especially pronounced in digestive tract tumors, among them in esophageal and pancreatic cancers in particular.[10] In their seminal work, the team from University of Alberta have shown that skeletal muscle depletion (sarcopenia and low muscle attenuation) is the real negative predictor of survival regardless of overall body weight in cancer patients.[6]

Sarcopenia is defined by the European Working Group on Sarcopenia in Older people as the presence of low muscle mass (under the 5th percentile) and low muscle function (strength or performance)[11] typically presenting in advanced age but also in cancer and other diseases. It is a well established predictor of poor survival and treatment outcomes in cancer patients.[6] Myosteatosis is defined as abnormal fat infiltration in skeletal muscle. It is negatively associated with muscle strength and quality and is brought on by aging[12], diabetes[13], obesity[14] and malignant disease.[6,15,16] Radiodensity of human muscle on CT scan (or muscle attenuation, MA) correlates well with its triglyceride content.[14] Measuring the attenuation values of muscle tissue corresponds well to the extent of myosteatosis, which is a sign of muscle wasting and again a predictor of poor outcome.[17]

By assessing muscle mass and quality before treatment an individualized risk assessment for overall survival and complications during treatment can be improved, patients at risk identified and appropriate interventions (mainly directed towards maintaining and gaining muscle mass) undertaken.[18] Our aim was to study the impact of muscle depletion (sarcopenia and myosteatosis) on outcomes (overall survival [OS], perioperative mortality and rate of complications) in resectable esophageal cancer.

Patients and methods

Study population

All patients who received an esophagectomy with curative intent for esophageal or esophago-gastric junction cancer at Clinical Department of Thoracic Surgery at University Medical Centre Ljubljana were eligible for inclusion in the study. Patients received either upfront surgery or neoadjuvant chemoradiotherapy followed by esophagectomy according to national guidelines. All patients received individualized nutritional support and counselling according to ESPEN best practice guidelines[19] and in all patients a catheter feeding jejunostomy was placed during esophagectomy. Clinical parameters were recorded prospectively in a database since 2003. Out of the 162 patients operated on consecutively between 2008 and 2018 CT images suitable for analysis of muscle mass and quality were available for 139 patients which were included in the study. Requirements for adequate images were the inclusion of L3 level and availability of non-contrast images for attenuation analysis. Only images recorded at presentation before the initiation of any treatment were considered.

Our study design was approved and the need for obtaining informed consent from participants waived by the Slovenian National medical ethics committee (approval number 0120–301/2016–2).

Definitions

We grouped complications into following groups. *Conduit complications* included clinically silent fistulae seen on esophagograms and/or CT scans, clinically important leaks that required interventions and frank gastric necroses. *Respiratory complications* included respiratory failure requiring mechanical ventilation and pneumonia, defined as the

presence of new infiltrates on chest radiography and a positive culture result from bronchoalveolar lavage or sputum requiring antibiotics. *Respiratory failure* requiring mechanical ventilation was recorded separately as well.

Other complications were defined as other serious complications (Dindo Clavien 2 or greater)[20] requiring intervention (*i.e.* early reoperation, cardioversion, endoscopic intervention) or directoscopically proven laryngeal nerve paralysis.[21]

OS was defined as the time interval between esophagectomy and death of any cause. Patients alive on 1.10.2018 as reported by Cancer registry of Slovenia were censored at that date.

BMI was calculated as patient weight [kg]/height [m]^2, recorded at admission one day before surgery.

CT body composition analysis (planimetry)

Pre-operative abdominal CT or whole body PET-CT scans were obtained. In each patient a single slice at the level of the 3rd lumbar vertebra (L3) was selected for automatic segmentation. CT scans were analyzed using the "Automated Body Composition Analyzer using Computed tomography image Segmentation" (ABACS) software[22,23], which uses a priori information about the skeletal muscle shape in the L3 region and predefined Hounsfield units (HU) values to recognize different tissues. HU values used to assess the total cross-sectional area for muscular tissue (SMA – skeletal muscle area) were −29 to +150 HU. Muscle attenuation (MA) was assessed by averaging HU of skeletal muscle. Additionally, SMI was calculated using the following formula: (SMA [cm2])/(patient height [m2]). All abdominal CT and PET-CT scans were analyzed by one blinded independent radiologist.

The following planimetry data were reported: number of days between CT and esophagectomy, SMA (skeletal muscle area) reported in cm^2, SMI (skeletal muscle index) is SMA corrected for height (*i.e.* divided by height squared) and expressed in cm^2/m^2. MA (muscle attenuation) was reported in Hounsfield units.

Previously defined muscle index cut-off values for sarcopenia in a healthy non-elderly Caucasian population were used to define limits for SMI in men at less than 43.1 cm^2/m^{2}and less than 32.7 cm^2/m^2 in women. Cutoff values for myosteatosis from the same study were used with myosteatosis defined as MA of less than 30.9 HU in men and 24.8 HU in women.[24]

Outcomes and statistical analysis

Standard descriptive statistics of demographic and clinical characteristics for patients with and without sarcopenia and myosteatosis were summarized. Differences in demographic and clinical characteristics between groups (sarcopenia/no sarcopenia and myosteatosis/no myosteatosis) were evaluated with Pearson's Chi-square tests for categorical and t-tests for parametric variables.

Primary outcome studied was overall survival. It was reported in each group with the Kaplan-Meier curve and the survival of groups with/without sarcopenia and with/without myosteatosis was compared using the log rank Mantel Cox test.

Secondary outcomes of interest were the incidences of complications in groups with/without sarcopenia and with/without myosteatosis. They were compared with Pearson's Chi-square test. P value of < 0.05 was considered significant. All statistical analyses were performed using Statistical Package for the Social Sciences (SPSS, version 22.0, Armonk NY).

Results

Patient characterictics

One hundred and thirty-nine patients underwent esophagectomy with primary reconstruction with curative intent. Overall demographic, clinical and complication characterictics are summarized in Table 1. Mean BMI was 26.3 ± 4.8 with only 7 (5.0%) having a BMI less than 18.5. As many as 46 (33.1%) patients reported having lost 10% or more of their normal body weight prior to esophagectomy. Average time between CT and esophagectomy was 76.9 ± 52.3 days with a much shorter time in those receiving primary resection compared to those with neoadjuvant treatment. Sarcopenia was present in 23 (16.5%) patients and myosteatosis in 72 (51.8%).

Surgery and pathology

Eighty-seven (62.6%) patients received an open esophagectomy and 52 (37.4%) had a hybrid or completely minimally invasive procedure. Type of procedure data, radicality rates, numbers of lymph nodes harvested and histology and staging data are given in Table 1.

Complications and survival

9 patients died after esophagectomy during the initial hospitalization (in hospital mortality of 6.5%).

TABLE 1. Demographic, preoperative, procedure and outcome data in all patients (N = 139)

Demographic and preoperative data	
Age at Surgery (mean ± SD) [years]	63.9 ± 9.5
min-max	30–83
Gender (N, % female)	22 (15.8%)
BMI (mean ± SD) [kg/ m^2]	26.3 ± 4.8
Weight loss > 10% (N, %)	46 (33.1%)
Neoadjuvant therapy (N, %)	74 (53.2 %)
Planimetry data	
Days between CT and esophagectomy	
all (mean ± SD)	76.9 ± 52.3
min-max	6–192
median	84
Neoadjuvant (mean ± SD)	115.2 ± 36.0
min-max	14–192
median	125
No neoadjuvant (mean ± SD)	33.5 ± 28.5
min-max	6–141
median	23
SMA [cm^2] (mean ± SD)	
male	157.6 ± 28.0
female	103.9 ± 16.3
SMI [cm^2/m^2] (mean ± SD)	
male	52.1 ± 9.5
female	39.8 ± 6.8
Muscle attenuation [HU] (mean ± SD)	
male	31.2 ± 8.3
female	27.8 ± 8.7
sarcopenia (N, %)	23 (16.5%)
myosteatosis (N, %)	72 (51.8%)

Procedure data	
Surgical approach (N, %)	
open	87 (62.6%)
MIE	52 (37.4%)
Type of esophagectomy (N, %)	
Ivor-Lewis	109 (78.4%)
McKeown	26 (18.7%)
Transhiatal	4 (2.9%)
Radicality (N, %)	
R0	130 (93.5%)
R1	5 (3.6%)
R2	4 (2.9%)
Lymph nodes (mean ± SD) (N, %)	23.4 ± 12.3
min-max	0–76
median	21
Cancer type (N, %)	
Adenocarcinoma	74 (53.2%)
Squamous cell carcinoma	64 (46.0%)
GIST	1 (0.7%)
Pathological Stage (AJCC 2017) (N, %)	
I	51 (36.7%)
II	27 (19.4%)
III	36 (25.9%)
IVA	23 (16.5%)
IVB	2 (1.4%)
Complications (N, %)	
In hospital mortality	9 (6.5%)
Any complication	65 (46.8%)
Conduit complications	21 (15.1%)
Pleuropulmonary complications	37 (26.6%)
Respiratory failure	26 (18.7%)
Any other complications	42 (30.2%)
Median survival [months]	**26.8 (95% CI 8.1–45,7)**
1 year survival	73.7%
3 year survival	45.1%
5 year survival	40.3%

AJCC = American joint committee on cancer; BMI = body mass index; CI = confidence interval; CT = computed tomography; GIST = gastrointestinal stromal tumor; HU = Hounsfield units; MIE = minimally invasive esophagectomy; SD = standard deviation; SMA = skeletal muscle area; SMI = skeletal muscle index

Almost half or 65 patients (46.8%) experienced a complication of Dindo-Clavien grade 2 severity or greater[20] after the procedure. Rates of other complications and survival rates are shown in Table 1. Survival is shown as a Kaplan-Meier curve in Figure 1. Median follow up was 18.1 months (range 0–115). 72 patients (51.8%) died during the observation period and 67 (48.1%) were censored.

Sarcopenia and myosteatosis subgroups

Demographic and clinical data was compared between patients with and without sarcopenia and with and without myosteatosis (Table 2). Patients with myosteatosis were significantly older than patients without it whereas in patients with or without sarcopenia age difference didn't reach statistical significance. BMI was significantly lower in sarcopenic patients but significantly higher in patients with myosteatosis.

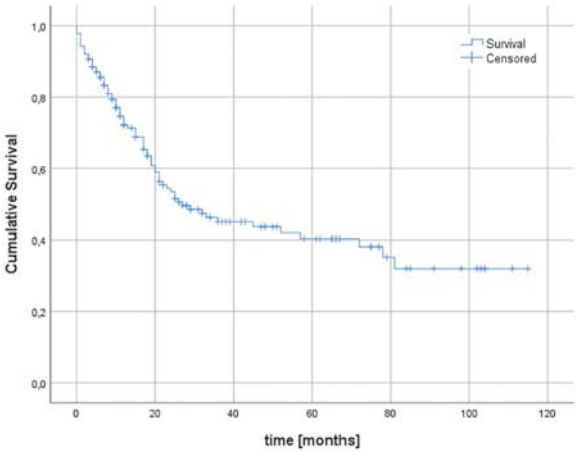

FIGURE 1. Cumulative survival Kaplan-Meier curve.

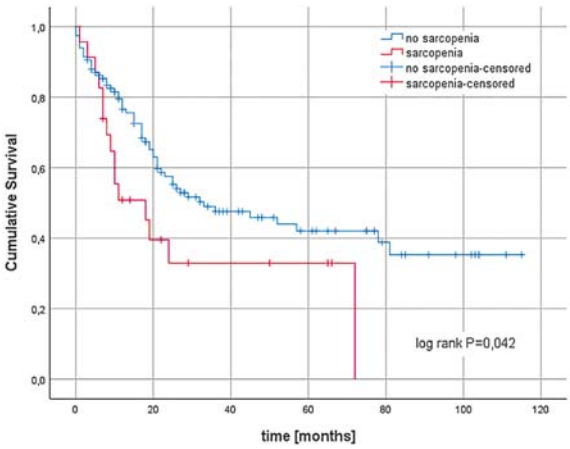

FIGURE 2. Kaplan-Meier survival curves for sarcopenia.

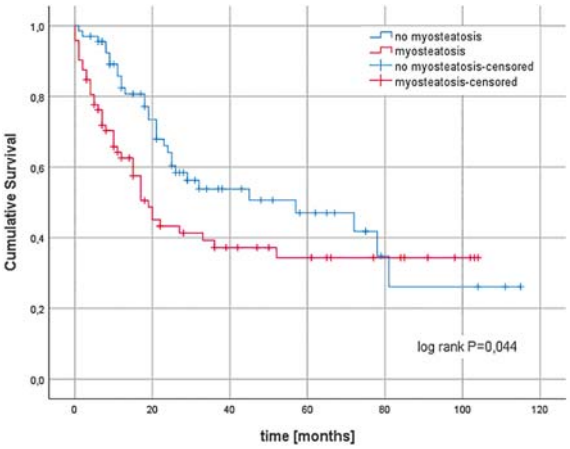

FIGURE 3. Kaplan-Meier survival curves for myosteatosis.

There was no statistically significant difference in sex distribution, days between CT and esophagectomy, weight loss, neoadjuvant therapy, cancer type, pathological stage, lymph nodes harvested or surgical approach between sarcopenia/no sarcopenia and myosteatosis/no myosteatosis groups.

Complications and survival were compared between sarcopenia/no sarcopenia and myosteatosis/no myosteatosis groups as shown in Table 3 and Figure 2 and 3.

No statistically significant difference in in hospital mortality, any complications, pleuropulmonary complications, respiratory failure or any other complications was found between sarcopenia/no sarcopenia and myosteatosis/no myosteatosis groups. Conduit complications were however significantly less common in the myosteatosis group (5/72 (6.9%) *vs.* 16/67 (23.9%) in patients without myosteatosis (OR 0.238 (0.082–0.692), p = 0.005).

Survival for sarcopenia/no sarcopenia and myosteatosis/no myosteatosis is given in two Kaplan Meier plots in Figures 2 and 3. Survival curves were compared with the log rank Mantel Cox test and differences in survival between each pair were statistically significant (p = 0.042 for sarcopenia/no sarcopenia and p = 0.044 for myosteatosis/no myosteatosis).

Discussion

Our prospective cohort study shows that diminished muscle reserves, measured as sarcopenia (loss of muscle mass) and myosteatosis (infiltration of muscle with fat), are associated with decreased overall survival in patients receiving esophagectomy as part of radical esophageal cancer treatment. A relationship between sarcopenia and myosteatosis and other negative outcomes after esophagectomy (perioperative mortality and incidence of complications) could not be established.

Effects of muscle mass loss have been studied in numerous other malignancies as well as non malignant diseases[25-27] but studies reporting myosteatosis as well as sarcopenia are still rare.[28] Prevalence of sarcopenia in studies on correlation between muscle area and survival in esophageal cancer can range widely from 16%–80%.[29-31] Choosing the right cutoff values for defining sarcopenia and myosteatosis can be challenging. In keeping with the definition of sarcopenia as absolute muscle mass below the 5th percentile of the population[32] we chose recently published cutoff values for a population closely resembling ours. Van der Werf *et al.* have published sex specific percentiles for SMI and MA for a healthy Caucasian population.[24] They

TABLE 2. Demographic, preoperative, pathological and procedure data compared between sarcopenia/no sarcopenia and myosteatosis/no myosteatosis groups

	Sarcopenia (N = 23 (16.5%))	No Sarcopenia (N = 116 (83.5%))	p	Myosteatosis (N = 72 (51.8%))	No Myosteatosis (N = 67 (48.2%))	p
Age at Surgery (mean ± SD)	67.1 ± 7.8	63.3 ± 9.7	0.076	67.1 ± 7.7	60.5 ± 10.0	*< 0.001*
Female sex (n (%))	3 (13.0%)	19 (16.4%)	0.689	10 (13.9%)	12 (17.9%)	0.516
BMI (mean ± SD)	23.8 ± 5.9	26.7 ± 4.4	*0.006*	27.3 ± 4.9	25.2 ± 4.4	*0.006*
Days between CT and esophagectomy (mean ± SD)	81.4 ± 57.6	76.1 ± 51.4	0.654	78.8 ± 52.8	75.0 ± 52.1	0.666
Weight loss > 10% (n (%))	11 (47.8%)	35 (30.2%)	0.100	25 (34.7%)	21 (31.3%)	0.672
Neoadjuvant Therapy (n (%))	14 (60.9%)	60 (51.7%)	0.422	34 (47.2%)	40 (59.7%)	0.141
Cancer Type (n (%))			0.864			0.500
Adenocarcinoma	13 (56.6%)	61 (52.6%)		37 (51.4%)	37 (55.2%)	
Squamous cell carcinoma	10 (43.4%)	54 (46.6%)		35 (48.6%)	29 (43.3%)	
GIST		1 (0.8%)			1 (1.5%)	
Pathological Stage (AJCC 2017) (n (%))			0.650			0.546
I	8 (34.8%)	43 (37.1%)		26 (36.1%)	25 (37.3%)	
II	6 (26.1%)	21 (18.1%)		11 (15.3%)	16 (23.9%)	
III	4 (17.4%)	32 (27.6%)		21 (29.2%)	15 (22.4%)	
IVA	4 (17.4%)	19 (16.4%)		12 (16.7%)	11 (16.4%)	
IVB	1 (4.3%)	1 (0.8%)		2 (2.8%)	0	
Lymph nodes (mean ± SD)	28.8 ± 10.5	23.9 ± 12.6	0.266	24.4 ± 11.1	22.4 ± 13.5	0.337
Surgical approach			0.258			0.167
open	12 (52.2%)	75 (64.7%)		49 (68.1%)	38 (56.7%)	
MIE	11 (47.8%)	41 (35.3%)		23 (31.9%)	29 (43.3%)	

AJCC = American joint committee on cancer; BMI = body mass index; CT = computed tomography; GIST-gastrointestinal stromal tumor; HU = Hounsfield units; MIE = minimally invasive esophagectomy; SD = standard deviation; SMA = skeletal muscle area; SMI = skeletal muscle index

proposed using the 5th percentile for cutoff values for SMI and MA in non-elderly (age 20–60) to avoid age related muscle loss. These values (SMI 43.1 cm^2/m^2 for men and 32.7 cm^2/m^2 for women) are markedly lower then ones used in most previous studies. Consequently, the prevalence of sarcopenia in our study (16.5%) is also lower than 26–75% reported in other studies in resectable esophageal cancer. Mean SMA and SMI was 157.6 ± 28.0 cm^2 and 52.1 ± 9.5 cm^2/m^2 in males and 103.9 ± 16.3 cm^2 and 39.8 ± 6.8 cm^2/m^2 in females (both significantly different between sexes with $p < 0.001$) which correlates well with studies in similar populations. We believe that choosing the right population with which patients are compared is crucial in determining the real prevalence of sarcopenia (*e.g.*, the study by Nishigori *et al.* in Japanese esophageal cancer patients[33] used the cutoff points obtained in Canadian obese patients[34] and reported sarcopenia in 75% of patients).

Defining myosteatosis is even more difficult, since the term is not used much yet and reports are scarcer. We chose cutoffs according to the same principle, *i.e.* at the 5th percentile of a healthy population. We did not find a statistically significant difference in muscle attenuation between males and females (31.2 ± 8.3 HU *vs.* 27.8 ± 8.7 HU, p = 0.082), but with small numbers in our groups and the availability of sex-specific cutoff values for attenuation we opted for those. Myosteatosis was present in 51.8% of our patients and there was no significant relationship between sarcopenia and myosteatosis (OR 1.256 (CI 0.510–3.093, p = 0.620)). This is in contrast with the study by Stretch *et al.* where the proportions of patients with sarcopenia and myosteatosis were inverse (40.7% *vs.* 25.2%) but they similarly reported no correlation between muscle mass and muscle radiodensity. A possible reason for this are the higher cutoffs they used for sarcopenia (40th percentile of their patients or 47.7 cm^2/m^2 and 36.5 cm^2/m^2).[28]

On univariate analysis sarcopenia and myosteatosis were associated with lower overall survival in our study group (Kaplan Meier log rank p = 0.042

TABLE 3. Complication and survival data compared between sarcopenia/no sarcopenia and myosteatosis/no myosteatosis groups

	Sarcopenia (N = 23 (16.5%))	No Sarcopenia (N = 116 (83.5%))	Odds Ratio (OR. 95% CI)	p
Complications (n (%))				
In hospital mortality	1 (4.3%)	8 (6.9%)	0.614 (0.073–5.158)	0.650
Any complication	11 (47.8%)	54 (46.6%)	1.052 (0.430–2.578)	0.911
Conduit complications	4 (17.4%)	17 (14.7%)	1.226 (0.371–4.049)	0.738
Pleuropulmonary complications	8 (34.8%)	29 (25.0%)	1.600 (0.615–4.160)	0.332
Respiratory failure	5 (21.7%)	21 (18.1%)	1.230 (0.410–3.689)	0.711
Any other complications	4 (17.4%)	38 (32.8%)	0.432 (0.137–1.359)	0.143
Median survival [months]	18.3 (CI 5.4–31.1)	31.0 (CI 7.4–54.6)		*0.042*
1 year survival	50.8%	78.5%		
3 year survival	32.9%	47.7%		
5 year survival	32.9%	42.2%		

	myosteatosis (N = 72 (51.8%))	no myosteatosis (N = 67 (48.2%))	odds ratio (OR. 95% CI)	p
Complications (n (%))				
In hospital mortality	7 (9.7%)	2 (3.0%)	3.500 (0.701–17.486)	0.107
Any complication	32 (44.4%)	33 (49.3%)	0.824 (0.423–1.607)	0.570
Conduit complications	5 (6.9%)	16 (23.9%)	0.238 (0.082–0.692)	*0.005*
Pleuropulmonary complications	17 (23.6%)	20 (30.0%)	0.726 (0.341–1.545)	0.406
Respiratory failure	14 (19.4%)	12 (17.9%)	1.066 (0.453–2.510)	0.884
Any other complications	24 (33.3%)	18 (26.9%)	1.361 (0.656–2.822)	0.407
Median survival [months]	19.0 (CI 13.3–24.7)	57.1 (CI 15.2–99.0)		*0.044*
1 year survival	64.2%	84.0%		
3 year survival	36.9%	53.7%		
5 year survival	33.9%	46.9%		

CI = confidence interval; OR = odds ratio

and p = 0.044, respectively). For sarcopenia this is in accordance with previously published data and for myosteatosis this is one of the first published reports. Dijksterhuis *et al.* have published a report on body composition, survival and toxicity in advanced esophagogastric cancer patients receiving palliative chemotherapy where they used BMI-specific cutoff values to define myosteatosis (< 41 HU in non obese (BMI < 25) and < 33 HU in overweight patients). Prevalence of myosteatosis in their group was 50% and they found a lower risk of grade III and IV toxicity in patients with higher muscular density but no association between sarcopenia or myosteatosis and survival was found.[35] Tamandl *et al.* published a study with 200 patients receiving an esophagectomy. They stratified patients in low- and high-muscle attenuation groups with a cutoff of 40HU in a population similar to ours. Average MA was 36 HU (31–41) and patients with MA < 40 HU had significantly poorer overall survival.[36] The percentage of patients with MA over and under 40 HU is not given, so we cannot compare the prevalence to our results but this definition of reduced muscle attenuation uses a cutoff considerably higher than ours.

On the other hand, a study by Gabiatti *et al.* in patients with locally advanced esophageal cancer receiving definitive chemoradiotherapy demonstrated favorable progression free survival and overall survival in a subgroup of patients with myosteatosis but without systemic inflammation.[37]

Sarcopenia has been studied extensively as a predictive factor in esophageal cancer. A recently published meta-analysis by Boshier *et al.* reviewed

29 studies with 3193 patients (38% sarcopenic) in which various methods were used to diagnose sarcopenia.[38] Sarcopenic patients had more pulmonary complications and lower overall survival. A similar meta-analysis by Deng *et al.* reviewed 11 cohort studies including 1520 patients (52.3% sarcopenic). Patients with sarcopenia had lower 3-year and 5-year survival after resection.[39]

Complications and perioperative mortality were compared in our study between sarcopenia/no sarcopenia and myosteatosis/no myosteatosis groups and no statistically significant negative effect of muscle depletion was found. This is in concordance with most other studies who failed to show a connection even in studies who showed differences in long term survival.[29,40] Insufficient statistical power in most studies including ours to detect a potential difference in complication rates is no doubt a strong factor. For conduit complications however, the incidence in our cohort was significantly lower in the myosteatosis group (5/72 (6.9%) *vs.* 16/67 (23.9%) in patients without myosteatosis, (OR 0.238 (0.082–0.692), p = 0.005). It is difficult to explain the reason for this observation. A higher BMI in patients with myosteatosis could indicate a better nutritional status at presentation. Despite the lower incidence of this dangerous complication perioperative mortality in patients with myosteatosis was not different than in patients without it.

General clinical data in our cohort does not differ significantly from similar published series in resectable esophageal cancer. Patients with myosteatosis were significantly older than patients without it (67.1 ± 7.7 *vs.* 60.5 ± 10.0 (p < 0.001)) whereas in patients with or without sarcopenia age difference didn't reach statistical significance (67.1 ± 7.8 *vs.* 63.3 ± 9.7 (p = 0.076)). BMI was significantly lower in sarcopenic patients (23.8 ± 5.9 *vs.* 26.7 ± 4.4 (p = 0.006)) but significantly higher in patients with myosteatosis (27.3 ± 4.9 *vs.* 25.2 ± 4.4 (p = 0.006)). 13 patients (9.4%) had both sarcopenia and myosteatosis, their BMI was 25.5 ± 6.1 (range 18.1–37.1). 33.1% of our patients lost 10% or more of their body weight but this did not confer a greater risk of having sarcopenia (OR 2.12 (CI 0.855–5.266), p = 0.100) or myosteatosis (OR 1.165 (CI 0.574–2.366), p = 0.672). As suggested elsewhere[28] sarcopenia and myosteatosis are probably two separate entities with different causes and effects reflecting different disturbances in metabolic processes.

Underlying causes of sarcopenia and myosteatosis are most likely overlapping to some extent. Possible mechanisms, through which they negatively affect survival, are various. Diminished food intake due to dysphagia and loss of appetite as well as a chronic inflammation state in esophageal cancer lead to sarcopenia. This in turn causes diminished mobility and rehabilitation after surgery[41], respiratory complications[33], inferior wound healing[42] and diminished tolerance of chemo and radiotherapy.[35] Skeletal muscle has been described as an endocrine organ[43] and it is the derangement of this function that is also a possible cause of inferior survival. Carefully designed studies are needed to corroborate this hypothesis.

The inclusion of myosteatosis assessment is in our opinion a strength of our study. We see that myosteatosis is more prevalent than sarcopenia and is a more sensitive marker of muscle degradation which precedes muscle mass and overall body mass loss. It is nevertheless at least as detrimental to prognosis as sarcopenia. Our study also uses recently published cut-off values that in our opinion assess the incidence of sarcopenia better than previous studies. However, this hinders the comparability of our results with others. It is not without weaknesses either. All CT images were recorded at staging with approximately half the patients going straight to resection and the other half receiving neoadjuvant treatment first. No repeat CT images were taken after neoadjuvant treatment if there were no clinical signs of progression according to our group's guidelines. The distribution of intervals from CT to esophagectomy is therefore bimodal and the planimetric data reflects patients' muscle reserves at beginning of any treatment and not necessarily at esophagectomy. This is a shortcoming when assessing the impact on perioperative mortality and complications since muscle mass loss is a well known process during neoadjuvant therapy.[44-47] The large variation in times between CT and esophagectomy should in our opinion however not be regarded as a weakness when assessing the impact on overall survival of radical esophageal cancer treatment. Our study also lacks statistical power to detect a potential difference in mortality and complications, an issue that has fraught all previous studies as well. With growing numbers of cases in which CT images are available for analysis and with potential pooling of data these statistical issues can be overcome in the future.

Lastly, due to the univariate nature of our analysis no causal effect between survival and muscle depletion markers can be established, but the association shown can serve as an incentive for further research.

Conclusions

In a prospective cohort study from a dedicated database on esophagectomies we studied the association of sarcopenia and myosteatosis with outcomes after curative esophagectomies with or without neoadjuvant chemoradiotherapy. Prevalence of sarcopenia and myosteatosis at presentation was 16.5% and 51.8%, respectively. Both sarcopenia and myosteatosis were associated with decreased overall survival. For sarcopenia this is in accordance with previously published data and for myosteatosis this is one of the first published reports. Identifying novel predictors of outcomes can be beneficial for tailoring treatment options in patients with esophageal cancer as well as for planning intervention strategies targeted at improving functional body reserves.

Authors' contributions

MSr and MSo designed the study. MSr collected, analyzed and interpreted the data and was the major contributor in writing the manuscript. TJ collected the imaging data and was a minor contributor in writing the manuscript. TJ and KP analyzed and interpreted the imaging data. MSo designed the data collecting database. All authors read and approved the final manuscript.

Acknowledgements

The authors would like to sincerely thank Professor Vickie Baracos, Ph.D., for her invaluable advice and guidance in designing this study. Funding was provided by University Medical Centre Ljubljana, Slovenia. The funding body had no immediate role in the design of the study and collection, analysis, and interpretation of data and in writing the manuscript.

References

1. Low DE, Alderson D, Cecconello I, Chang AC, Darling GE, D'Journo XB, et al. International consensus on standardization of data collection for complications associated with esophagectomy: esophagectomy complications consensus group (ECCG). *Ann Surg* 2015; **262:** 286-94. doi: 10.1097/SLA.0000000000001098
2. Miller KD, Siegel RL, Lin CC, Mariotto AB, Kramer JL, Rowland JH, et al. Cancer treatment and survivorship statistics, 2016. *CA Cancer J Clin* 2016; **66:** 271-89. doi: 10.3322/caac.21349
3. van Putten M, de Vos-Geelen J, Nieuwenhuijzen G, Siersema PD, Lemmens VEPP, Rosman C, et al. Long-term survival improvement in oesophageal cancer in the Netherlands. *Eur J Cancer* 2018; **94:** 138-47. doi: 10.1016/j.ejca.2018.02.025
4. Soma D, Kawamura YI, Yamashita S, Wake H, Nohara K, Yamada K, et al. Sarcopenia, the depletion of muscle mass, an independent predictor of respiratory complications after oncological esophagectomy. *Dis Esophagus* 2019; **32.** pii: doy092. doi: 10.1093/dote/doy092
5. Markar SR, Low DE. Physiology, not chronology, dictates outcomes after esophagectomy for esophageal cancer: outcomes in patients 80 years and older. *Ann Surg Oncol* 2013; **20:** 1020-6. doi: 10.1245/s10434-012-2703-x
6. Martin L, Birdsell L, MacDonald N, Reiman T, Clandinin MT, McCargar LJ, et al. Cancer cachexia in the age of obesity: skeletal muscle depletion is a powerful prognostic factor, independent of body mass index. *J Clin Oncol* 2013; **31:** 1539-47. doi: 10.1200/JCO.2012.45.2722
7. Gonzalez MC, Correia MITD, Heymsfield SB. A requiem for BMI in the clinical setting. *Curr Opin Clin Nutr Metab Care* 2017; **20:** 314-21. doi: 10.1097/MCO.0000000000000395
8. Di Sebastiano KM, Mourtzakis M. A critical evaluation of body composition modalities used to assess adipose and skeletal muscle tissue in cancer. *Appl Physiol Nutr Metab* 2012; **37:** 811-21. doi: 10.1139/h2012-079
9. Shen W, Punyanitya M, Wang Z, Gallagher D, St-Onge M-P, Albu J, et al. Total body skeletal muscle and adipose tissue volumes: estimation from a single abdominal cross-sectional image. *J Appl Physiol Bethesda Md (1985)* 2004; **97:** 2333-8. doi: 10.1152/japplphysiol.00744.2004
10. Muscaritoli M, Lucia S, Farcomeni A, Lorusso V, Saracino V, Barone C, et al. Prevalence of malnutrition in patients at first medical oncology visit: the PreMiO study. *Oncotarget* 2017; **8:** 79884-96. doi: 10.18632/oncotarget.20168
11. Cruz-Jentoft AJ, Baeyens JP, Bauer JM, Boirie Y, Cederholm T, Landi F, et al. Sarcopenia: European consensus on definition and diagnosis. *Age Ageing* 2010; **39:** 412-23. doi: 10.1093/ageing/afq034
12. Delmonico MJ, Harris TB, Visser M, Park SW, Conroy MB, Velasquez-Mieyer P, et al. Longitudinal study of muscle strength, quality, and adipose tissue infiltration. *Am J Clin Nutr* 2009; **90:** 1579-85. doi: 10.3945/ajcn.2009.28047
13. Miljkovic I, Kuipers AL, Cvejkus R, Bunker CH, Patrick AL, Gordon CL, et al. Myosteatosis increases with aging and is associated with incident diabetes in African ancestry men. *Obes Silver Spring Md* 2016; **24:** 476-82. doi: 10.1002/oby.21328
14. Goodpaster BH, Theriault R, Watkins SC, Kelley DE. Intramuscular lipid content is increased in obesity and decreased by weight loss. *Metabolism* 2000; **49:** 467-72. doi: 10.1016/s0026-0495(00)80010-4
15. Sabel MS, Lee J, Cai S, Englesbe MJ, Holcombe S, Wang S. Sarcopenia as a prognostic factor among patients with stage III melanoma. *Ann Surg Oncol* 2011; **18:** 3579-85. doi: 10.1245/s10434-011-1976-9
16. Antoun S, Lanoy E, Iacovelli R, Albiges-Sauvin L, Loriot Y, Merad-Taoufik M, et al. Skeletal muscle density predicts prognosis in patients with metastatic renal cell carcinoma treated with targeted therapies. *Cancer* 2013; **119:** 3377-84. doi: 10.1002/cncr.28218
17. Aubrey J, Esfandiari N, Baracos VE, Buteau FA, Frenette J, Putman CT, et al. Measurement of skeletal muscle radiation attenuation and basis of its biological variation. *Acta Physiol Oxf Engl* 2014; **210:** 489-97. doi: 10.1111/apha.12224
18. Jordan T, Mastnak DM, Palamar N, Kozjek NR. Nutritional therapy for patients with esophageal cancer. *Nutr Cancer* 2018; **70:** 23-9. doi: 10.1080/01635581.2017.1374417
19. Arends J, Baracos V, Bertz H, Bozzetti F, Calder PC, Deutz NEP, et al. ESPEN expert group recommendations for action against cancer-related malnutrition. *Clin Nutr Edinb Scotl* 2017; **36:** 1187-96. doi: 10.1016/j.clnu.2017.06.017
20. Dindo D, Demartines N, Clavien P-A. Classification of surgical complications. *Ann Surg* 2004; **240:** 205-13. doi: 10.1097/01.sla.0000133083.54934.ae
21. Seder CW, Raymond DP, Wright CD, Gaissert HA, Chang AC, Clinton S, et al. The Society of Thoracic Surgeons General Thoracic Surgery Database 2017 update on outcomes and quality. *Ann Thorac Surg* 2017; **103:** 1378-83. doi: 10.1016/j.athoracsur.2017.02.073

22. Popuri K, Cobzas D, Esfandiari N, Baracos V, Jägersand M. Body composition assessment in axial CT images using FEM-based automatic segmentation of skeletal muscle. *IEEE Trans Med Imaging* 2016; **35:** 512-20. doi: 10.1109/TMI.2015.2479252

23. Chung H, Cobzas D, Birdsell L, Lieffers J, Baracos V. Automated segmentation of muscle and adipose tissue on CT images for human body composition analysis. *Med Imaging* 2009; **7261:** 72610K. doi: 10.1117/12.812412

24. van der Werf A, Langius JAE, de van der Schueren MAE, Nurmohamed SA, van der Pant KAMI, Blauwhoff-Buskermolen S, et al. Percentiles for skeletal muscle index, area and radiation attenuation based on computed tomography imaging in a healthy Caucasian population. *Eur J Clin Nutr* 2018; **72:** 288-96. doi: 10.1038/s41430-017-0034-5

25. Deng H-Y, Hou L, Zha P, Huang K-L, Peng L. Sarcopenia is an independent unfavorable prognostic factor of non-small cell lung cancer after surgical resection: a comprehensive systematic review and meta-analysis. *Eur J Surg Oncol* 2019; **45:** 728-35. doi: 10.1016/j.ejso.2018.09.026

26. Levolger S, van Vugt JLA, de Bruin RWF, IJzermans JNM. Systematic review of sarcopenia in patients operated on for gastrointestinal and hepatopancreatobiliary malignancies. *Br J Surg* 2015; **102:** 1448-58. doi: 10.1002/bjs.9893

27. Waduud MA, Wood B, Keleabetswe P, Manning J, Linton E, Drozd M, et al. Influence of psoas muscle area on mortality following elective abdominal aortic aneurysm repair. *Br J Surg* 2019; **106:** 367-74. doi: 10.1002/bjs.11074

28. Stretch C, Aubin J-M, Mickiewicz B, Leugner D, Al-Manasra T, Tobola E, et al. Sarcopenia and myosteatosis are accompanied by distinct biological profiles in patients with pancreatic and periampullary adenocarcinomas. *PloS One* 2018; **13:** e0196235. doi: 10.1371/journal.pone.0196235

29. Paireder M, Asari R, Kristo I, Rieder E, Tamandl D, Ba-Ssalamah A, et al. Impact of sarcopenia on outcome in patients with esophageal resection following neoadjuvant chemotherapy for esophageal cancer. *Eur J Surg Oncol* 2017; **43:** 478-84. doi: 10.1016/j.ejso.2016.11.015

30. Elliott JA, Doyle SL, Murphy CF, King S, Guinan EM, Beddy P, et al. Sarcopenia: prevalence, and impact on operative and oncologic outcomes in the multimodal management of locally advanced esophageal cancer. *Ann Surg* 2017; **266:** 822-30. doi: 10.1097/SLA.0000000000002398

31. Järvinen T, Ilonen I, Kauppi J, Salo J, Räsänen J. Loss of skeletal muscle mass during neoadjuvant treatments correlates with worse prognosis in esophageal cancer: a retrospective cohort study. *World J Surg Oncol* 2018; **16:** 27. doi: 10.1186/s12957-018-1327-4

32. Fearon K, Strasser F, Anker SD, Bosaeus I, Bruera E, Fainsinger RL, et al. Definition and classification of cancer cachexia: an international consensus. *Lancet Oncol* 2011; **12:** 489-95. doi: 10.1016/S1470-2045(10)70218-7

33. Nishigori T, Okabe H, Tanaka E, Tsunoda S, Hisamori S, Sakai Y. Sarcopenia as a predictor of pulmonary complications after esophagectomy for thoracic esophageal cancer. *J Surg Oncol* 2016; **113:** 678-84. doi: 10.1002/jso.24214

34. Prado CMM, Lieffers JR, McCargar LJ, Reiman T, Sawyer MB, Martin L, et al. Prevalence and clinical implications of sarcopenic obesity in patients with solid tumours of the respiratory and gastrointestinal tracts: a population-based study. *Lancet Oncol* 2008; **9:** 629-35. doi: 10.1016/S1470-2045(08)70153-0

35. Dijksterhuis WPM, Pruijt MJ, van der Woude SO, Klaassen R, Kurk SA, van Oijen MGH, et al. Association between body composition, survival, and toxicity in advanced esophagogastric cancer patients receiving palliative chemotherapy. *J Cachexia Sarcopenia Muscle* 2019; **10:** 199-206. doi: 10.1002/jcsm.12371

36. Tamandl D, Paireder M, Asari R, Baltzer PA, Schoppmann SF, Ba-Ssalamah A. Markers of sarcopenia quantified by computed tomography predict adverse long-term outcome in patients with resected oesophageal or gastro-oesophageal junction cancer. *Eur Radiol* 2016; **26:** 1359-67. doi: 10.1007/s00330-015-3963-1

37. Gabiatti CTB, Martins MCL, Miyazaki DL, Silva LP, Lascala F, Macedo LT, et al. Myosteatosis in a systemic inflammation-dependent manner predicts favorable survival outcomes in locally advanced esophageal cancer. *Cancer Med* 2019; **8:** 6967-76. doi: 10.1002/cam4.2593

38. Boshier PR, Heneghan R, Markar SR, Baracos VE, Low DE. Assessment of body composition and sarcopenia in patients with esophageal cancer: a systematic review and meta-analysis. *Dis Esophagus* 2018; **31.** doi: 10.1093/dote/doy047

39. Deng H-Y, Zha P, Peng L, Hou L, Huang K-L, Li X-Y. Preoperative sarcopenia is a predictor of poor prognosis of esophageal cancer after esophagectomy: a comprehensive systematic review and meta-analysis. *Dis Esophagus* 2019; **32.** doi: 10.1093/dote/doy115

40. Tsukioka T, Nishiyama N, Izumi N, Mizuguchi S, Komatsu H, Okada S, et al. Sarcopenia is a novel poor prognostic factor in male patients with pathological Stage I non-small cell lung cancer. *Jpn J Clin Oncol* 2017; **47:** 363-8. doi: 10.1093/jjco/hyx009

41. JR, Bathe OF, Fassbender K, Winget M, Baracos VE. Sarcopenia is associated with postoperative infection and delayed recovery from colorectal cancer resection surgery. *Br J Cancer* 2012; **107:** 931-6. doi: 10.1038/bjc.2012.350

42. Achim V, Bash J, Mowery A, Guimaraes AR, Li R, Schindler J, et al. Prognostic indication of sarcopenia for wound complication after total laryngectomy. *JAMA Otolaryngol Head Neck Surg* 2017; **143:** 1159-65. doi: 10.1001/jamaoto.2017.0547

43. Pedersen BK, Febbraio MA. Muscles, exercise and obesity: skeletal muscle as a secretory organ. *Nat Rev Endocrinol* 2012; **8:** 457-65. doi: 10.1038/nrendo.2012.49

44. Guinan EM, Doyle SL, Bennett AE, O'Neill L, Gannon J, Elliott JA, et al. Sarcopenia during neoadjuvant therapy for oesophageal cancer: characterising the impact on muscle strength and physical performance. *Support Care Cancer* 2018; **26:** 1569-76. doi: 10.1007/s00520-017-3993-0

45. Reisinger KW, Bosmans JWAM, Uittenbogaart M, Alsoumali A, Poeze M, Sosef MN, et al. Loss of skeletal muscle mass during neoadjuvant chemoradiotherapy predicts postoperative mortality in esophageal cancer surgery. *Ann Surg Oncol* 2015; **22:** 4445-52. doi: 10.1245/s10434-015-4558-4

46. Yip C, Goh V, Davies A, Gossage J, Mitchell-Hay R, Hynes O, et al. Assessment of sarcopenia and changes in body composition after neoadjuvant chemotherapy and associations with clinical outcomes in oesophageal cancer. *Eur Radiol* 2014; **24:** 998-1005. doi: 10.1007/s00330-014-3110-4

47. Awad S, Tan BH, Cui H, Bhalla A, Fearon KCH, Parsons SL, et al. Marked changes in body composition following neoadjuvant chemotherapy for oesophagogastric cancer. *Clin Nutr Edinb Scotl* 2012; **31:** 74-7. doi: 10.1016/j.clnu.2011.08.008

research article

The influence of shielding reinforcement in a vault with limited dimensions on the neutron dose equivalent in vicinity of medical electron linear accelerator

Ana Ivkovic[1,2], Dario Faj[1,3], Mladen Kasabasic[1,2], Marina Poje Sovilj[4], Ivana Krpan[1,3], Marina Grabar Branilovic[5], Hrvoje Brkic[1,3]

[1] Faculty of Medicine, J. J. Strossmayer University of Osijek, Osijek, Croatia
[2] University Hospital Osijek, Osijek, Croatia
[3] Faculty of Dental Medicine and Health, J. J. Strossmayer University of Osijek, Osijek, Croatia
[4] Department of Physics, J. J. Strossmayer University of Osijek, Osijek, Croatia
[5] Department of Organic Chemistry and Biochemistry, Rudjer Bošković Institute, Zagreb, Croatia

Radiol Oncol 2020; 54(2): 247-252.

Received 2 February 2020
Accepted 11 March 2020

Correspondence to: Hrvoje Brkić, Faculty of Medicine in Osijek, J. Huttlera 4, 31000 Osijek, Croatia. E-mail: hbrkic@mefos.hr

Disclosure: No potential conflicts of interest were disclosed.

Background. High energy electron linear accelerators (LINACs) producing photon beams with energies higher than 10 MeV are widely used in radiation therapy. In these beams, fast neutrons are generated, which results in undesired contamination of the therapeutic beam. In this study, measurements and Monte Carlo (MC) simulations were used to obtain neutron spectra and dose equivalents in vicinity of linear accelerator.

Materials and methods. LINAC Siemens Oncor Expression in Osijek University Hospital is placed in vault that was previously used for ^{60}Co machine. Then, the shielding of the vault was enhanced using lead and steel plates. Measurements of neutron dose equivalent around LINAC and the vault were done using CR-39 solid state nuclear track detectors. To compensate energy dependence of detectors, neutron energy spectra was calculated in measuring positions using MC simulations.

Results. The vault is a source of photoneutrons, but a vast majority of neutrons originates from accelerator head. Neutron spectra obtained from MC simulations show significant changes between the measuring positions. Annual neutron dose equivalent per year was estimated to be less than 324 μSv in the measuring points outside of the vault.

Conclusions. Since detectors used in this paper are very dependent on neutron energy, it is extremely important to know the neutron spectra in measuring points. Though, patient dosimetry should include neutrons, estimated annual neutron doses outside the vault were far below exposure limit of ionizing radiation for workers.

Key words: vault reconstruction; ^{60}Co decommission; Monte Carlo simulations; CR-39; neutron dose equivalent

Introduction

High energy electron linear accelerators (LINACs) producing photon beams with energies higher than 10 MeV are widely used in radiation therapy (RT). In these beams, fast neutrons are generated, which results in undesired contamination of the therapeutic beam.[1-6] Neutron contamination in high-energy RT implies an increase of secondary radiation-induced cancer risk.[7] It is also well known that an essential requirement for successful radiation therapy is that the discrepancies between dose distributions calculated at the treatment planning stage and those delivered to the patient are minimized.[8] All modern RT modalities aim to be highly conformal, which is achieved by using

many small fields and requires longer beam-on times. The additional dose from photoneutrons is proportional to the beam-on time[9], causing higher photoneutron doses then expected in modern RT techniques, so it is important to determine the full radiation field correctly in order to evaluate the exposure of patients and medical personnel.

The head of the LINAC is the primary source of photoneutrons in vicinity of linear accelerators since it consists mainly of high-Z materials such as tungsten and steel.[1,10] Also, the vault in which the machine is placed can be the source of photoneutrons.[11] In Croatia, three linear accelerators were placed in vaults that were previously used for ^{60}Co machines.[5] Because of the difference in photon energies between the devices, shielding of the vault had to be enhanced. Also, ^{60}Co and LINAC machines and their auxiliary systems differ in size. ^{60}Co vaults are smaller than the vaults designed for high energy photon LINACs and during the reconstruction of ^{60}Co vaults for LINACs, the main limitation was the space. The vault walls had to be enhanced for photon shielding, but there was no space for adding more concrete to the walls. Therefore, lead and steel panels were added into the walls instead.

LINAC Siemens Oncor Expression 18 MV placed in Osijek University Hospital is one of the LINAC's placed in the reconstructed vaults. Measurements of the neutron flux and dose equivalent that were done in Osijek University Hospital are already published.[2] Measurements were done during all stages of installation, namely before and after lead shielding was added to the walls. It was done using solid state nuclear track detector (SSNTD) LR115.[5] Back then, the neutron spectra at the positions of measurements were unknown and the results had a large uncertainty due to the energy dependence of detectors. In this paper the measurements were repeated with SSNTD CR-39, but energy dependence was taken into consideration using Monte Carlo (MC) simulations. Neutron dose equivalents for patients and staff were assessed and compared to the results presented before.[2]

Additionally, we investigated the origin of the photoneutrons to show if the steel panels added to the vault walls could be significant sources of photoneutrons. The MC simulations were done for different orientations of the gantry and different points around the accelerator and vault in order to show whether these panels increase total radiation dose to patients and staff.

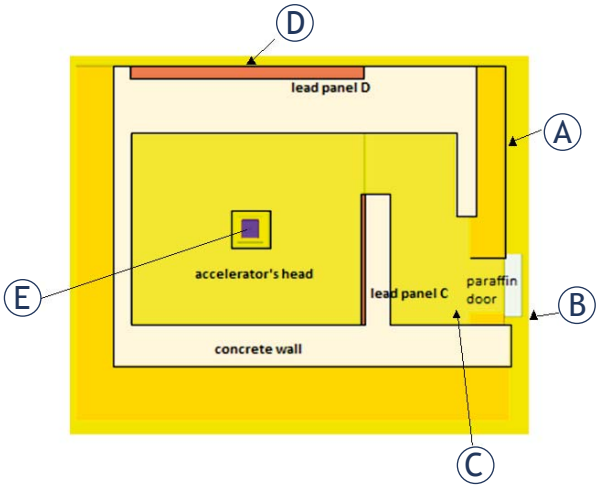

FIGURE 1. Top view (down) of the vault where Siemens Oncor Expression accelerator at Osijek University Hospital is placed with marked positions of measurements. **(A)**, **(B)** and **(D)** are positions outside the vault, **(C)** and E are inside the vault. Position E is in isocenter.

Materials and methods

The model of dual photon beam (6MV and 18 MV) medical LINAC Siemens ONCOR Expression at Osijek University Hospital was built using MCNP611® beta code.[12] Due to negligible cross sections for neutron productions in a low energy photon beam (6 MV), only the high energy photon beam (18 MV) was modeled. Data used for accelerator's geometry building and materials of which accelerator's head consists were provided by manufacturer. Model of the accelerator head was built as it was described in our previous publications.[1,10,13] For the purpose of this study the accelerator vault was also constructed using MCNP Code (Figure 1). The model of the vault was built using macrobodies, such as boxes and cylinders. The materials for the model were taken from Compendium of Material Composition Data for radiation transport modeling.[14] The majority of vault walls is made of concrete and bricks. As seen in the Figure 1, lead panels were placed in the vault wall (D) and the wall that defines the maze (C). The door at the maze entrance is made of lead and filled with paraffin. All the data used in construction of the vault were obtained from the technical service of Osijek University Hospital.

Each simulation had at least $5{\cdot}10^8$ initial events (electrons incident on target). The criteria for acceptance of the simulations were that R value (relative error) falls below 0.1 and that all 10 statistical checks are met.[12] The energy cut-off for both electrons and photons was 1 keV, and for neutrons it remained 0 MeV. The continuous energy neutron cross sections

library ENDF/B-VII (Evaluated Nuclear data file B-VII) was used for neutron transport.[15]

In Figure 1, measuring positions (A, B, C and D) used previously are presented.[5] In this research, the measurements were done using SSNTD CR-39 in the same measuring positions as before, with additional measuring position E in isocenter. Therefore, F4 tallies for detecting neutrons in positions A, B, C, D and E were modeled. Tallies in positions A, B, C and D were modeled as boxes with dimensions 20x20x20 cm^3 while the tally at the isocenter was modeled as a box with dimensions 1x1x1 cm^3. The efficiency of the calculations is very low because only a few percent of all the electrons impinging on target produce photons in the beam, and only a few of those photons with high energies produce photoneutrons. To improve efficiency of MC simulations, *i.e.* particle sampling in the detector region, DXTRAN spheres were setup around all neutron detectors. Neutron spectra were collected in energy bins ranging from $1 \cdot 10^{-9}$ to 18 MeV in logarithmic scale that corresponds to energy bins for the NCRP flux to dose conversion factors.[16] Each detector had all the model cells flagged, in order to determine the place of origin of neutrons. 18 MV photon beam with field size 10x10 cm^2 was modeled. Simulations were run with accelerator head pointing down (gantry angle 0°) and in the direction of point D (gantry angle 270°).

As seen in the Figure 1, the measurements were performed in five positions: at the operator's console (A), on both sides of the vault door approximately 150 cm above the floor (B –outside the vault, C – inside the vault), on the outside wall of the accelerator vault at the central axis of the beam (D) (5) and isocenter (E). Position E is important for radiation protection of a patient while positions A, B, C and D are important for the staff working in the area around the vault. In our previous measurements with SSNTD LR 115 and boron converter, the dose was calculated without known neutron spectra for the aforementioned positions.[5] In this research, spectra for measuring positions are obtained and taken into account when calculating neutron dose.

The neutron detector consisted of CR-39 solid state nuclear track detector with dimensions 2x3 cm^2 and boron foil BN-1 (ALGADE Laboratoire DOSIRAD, France) that is a ^{10}B converter for reaction (n,α). Detectors that contain a ^{10}B converter are very sensitive to low energy neutrons and less sensitive to fast neutrons.

After the irradiation, CR-39 detectors were separated from boron foils and etched in 30% KOH aqueous solution at 70°C for 6 hours. After etching, detectors were rinsed in distilled water and dried. The detectors were scanned with built-in microscope camera (Zeiss Axiovert 200) using 10x16 magnification. 100 images were taken on average for each film. The number of images depended on the number of tracks registered on the film. In order to get a less than 10% error, the measured area had to be large enough, so that the number of counted tracks is over 100 (N>100).[17]

Tracks were counted using ImageJ/Fiji 1.46 software. First, the tracks were counted manually, *i.e.* track by track. Manual track counting was used as a reference. Tracks were counted so that each track in the image was marked. Marked tracks were added to a tally sheet. Manual counting is time consuming and impractical, especially if there are many images to process. Therefore, counting was automated. Images were converted to grayscale and a grayscale threshold was applied along with other criteria (track size, shape). Tracks in processed images were counted automatically by the software. Track density is a quantity obtained by division of counted tracks and total area of film used for counting.

As in previous measurements CR-39 detectors were placed in positions A, B, C, D and E approximately 150 cm above the floor as in.[5] Measurements for gantry angles 0° and 270° with collimator opening 10cm x 10cm were done for all 5 measuring points.

Since track densities in measuring positions A, B and D are comparable to background measurements, we investigated the total neutron fluence in these positions and how many neutrons reaching these positions are going to produce alpha particles that will eventually form track in SSNTD CR-39. Total neutron fluencies, number of alpha particles and the spectra for positions A, B, C, D and E, for gantry angles 0° and 270°, are obtained from MCNP simulations. The spectra for 0° and 270° are convoluted with cross section of neutron on boron for reaction ^{10}B (n, α) ^{7}Li. Cross section data is taken from ENDF/B-VII (Evaluated Nuclear Data File B-VII).[15] Therefore, the probability of alpha particles production per 1 atom of boron is obtained. The number of tracks on CR-39 is proportional to the number of alpha particles originating from boron foil. The quantity used in experimental part is track density in units track/mm^2 (mm^2 is approximately the size of the field of view that was used for detector scanning on microscope). In order to compare experimental data with simulation, the number of alpha particles per mm^2 of boron has to be calculated and normalized to 2500 MU. Using the data obtained from the manufacturer, the num-

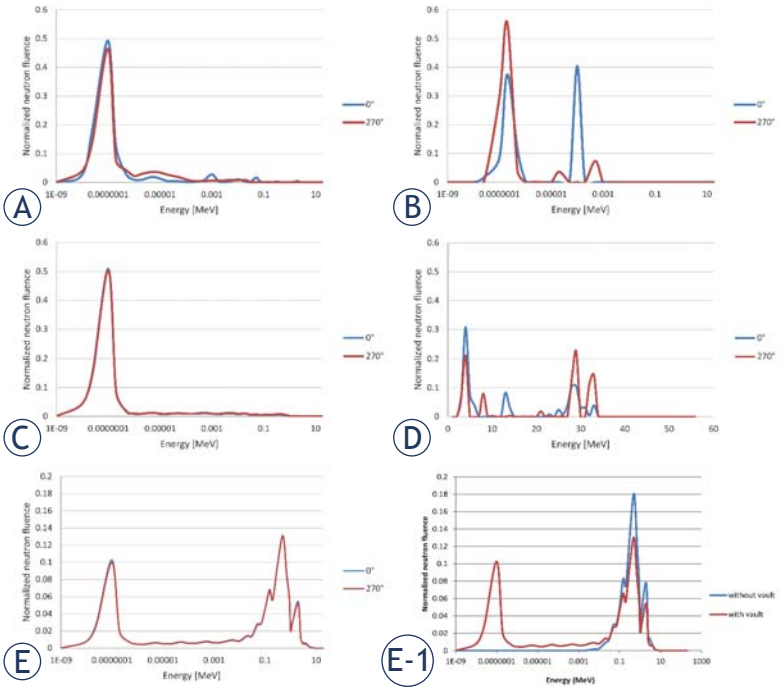

FIGURE 2. Neutron spectra in measuring positions **(A)**, **(B)**, **(C)**, **(D)** and **(E)** for photon field size 10 x 10 cm² and gantry angles 0° and 270°. **(E - 1)** is normalized neutron spectrum in measuring position E for simulations with and without vault.

ber of alpha particles produced in (n,α) reaction on 1 mm² of boron foil was calculated.

Statistical analysis

Relative error of MC simulations is below 10% which is in agreement with statistical checks performed by code itself.[12] All measurements using SSNTD were repeated at least 6 times and relative error did not exceed 8.7%. Relative error in experimental measurements was estimated the maximum deviation from mean.

Results

Calculated normalized neutron fluence spectra for 10x10 cm² field and gantry angles 0º and 270º in measuring points A,B,C, D and E are presented in Figure 2 as well as neutron spectrum in isocenter (measuring position E) calculated in simulations with and without vault (Figure 2, E–1).

Total MC calculated neutron fluence per electron impinging on target in measuring positions A, B, C, D and E for gantry angles 0° and 270° is presented in Table 1.

Normalized neutron fluence obtained from MC calculations according to the place of origin is presented in Figure 3. Data is given for all measuring positions and gantry angles 0° and 270°.

Track density caused by background irradiation was 0.47 tracks per mm² with its standard deviation 0.09 tracks per mm². Track density caused by background radiation is subtracted from measured track density. In measuring positions A, B and D measured track density is slightly larger than background. Mean value of detector sensitivities for all measuring position is 0.0002.

Neutron dose equivalents for all measuring positions for gantry angles 0° and 270° together with already published data[2] are presented in Table 2.

TABLE 1. Total MC calculated neutron fluence in measuring positions A, B, C, D and E for gantry angles 0° and 270°. Neutron fluence is in number of neutrons per cm² per electron impinging on target. Results are normalized to source particle

	Measuring position				
Gantry angle	A	B	C	D	E
0°	$5.6 \cdot 10^{-13}$	$5.3 \cdot 10^{-14}$	$3.6 \cdot 10^{-10}$	$8.4 \cdot 10^{-24}$	$1.5 \cdot 10^{-8}$
270°	$6.6 \cdot 10^{-13}$	$3.4 \cdot 10^{-14}$	$4.2 \cdot 10^{-10}$	$1.6 \cdot 10^{-22}$	$1.5 \cdot 10^{-8}$

Discussion

Neutron spectra obtained from MC simulations show significant changes between the measuring positions (Figure 2). There are also changes in spectra (Figure 2) when gantry angle changes from 0° to 270°. Since detectors used in this paper are very dependent on neutron energy, it is extremely important to know the neutron energy in measuring points. Simulations with and without LINAC vault have shown that surrounding structures also influence the neutron fluence and energy spectrum (Figure 2, E-1). Therefore, it is important to simulate not only the accelerator, but all surrounding structures as well.

Furthermore, neutron spectrum with vault has a significant neutron component in lower energy part of spectrum, around 0.1 eV. Simulations that include the vault have 38% larger neutron fluence than simulations without vault. The reason for that is because the vault serves as a box that does not allow neutrons to escape so they are bouncing back and forth in the vault. Therefore, more neutrons are detected on the tally in isocenter (E). When simulation doesn't include the vault, neutrons are dispersed and it is easy for them to escape. Furthermore, the vault itself is a source of photoneutrons with small energies, but only 1% of all neutrons detected in isocenter originate from

the vault walls (Figure 3, position E). Therefore, the small energy peak mainly comes from the wall attenuation of neutrons originating from accelerator head. It means that a part of the neutron fluence will move from high to low energy part of the spectrum which can be observed in Figure 2, E-1.

According to Table 1, the change of the gantry angle did not have significant influence on total neutron fluence in measuring positions A, B, C and E, but in position D total neutron fluence is 20 times larger for gantry angle 270° than for angle 0°. This was an expected result since the photon beam is directly pointed to the position D when gantry is rotated to 270°. Position D is on the outer side of the wall which contains a lead panel used for high energy photon shielding purposes. At the same time, the lead panel has become a source of photoneutrons (Figure 3).

According to MC simulations in measuring positions C and E there is a great number of alpha particles that can produce track in detector and consequently in these positions, track densities are significantly larger than track density caused by background radiation. However, in positions A, B and D (especially D) number of alpha particles is 1 or several orders of magnitude smaller. Mean value of detector sensitivities for all measuring position is 0.0002, *i.e.* every 5000th neutron reaching detector will make track in the detector.

According to Table 2 our previous measurements[5] overestimated neutron dose equivalent, especially for measuring position D. The underlying reason for overestimation was the unknown neutron spectra in measuring positions. Measuring position E (isocenter) was added to this research, since the neutron dose to patients was one of the interests of this study. Neutron dose equivalent in isocenter is 3.3 mSv per Gy photon dose in isocenter. If we take a radiotherapy treatment of prostate for example, with prescribed dose of 74 Gy and all rectangular fields 10x10 cm^2 4 field box technique, 250 MU daily, then the equivalent neutron dose is 0.3 Sv. The neutron dose is comparable to

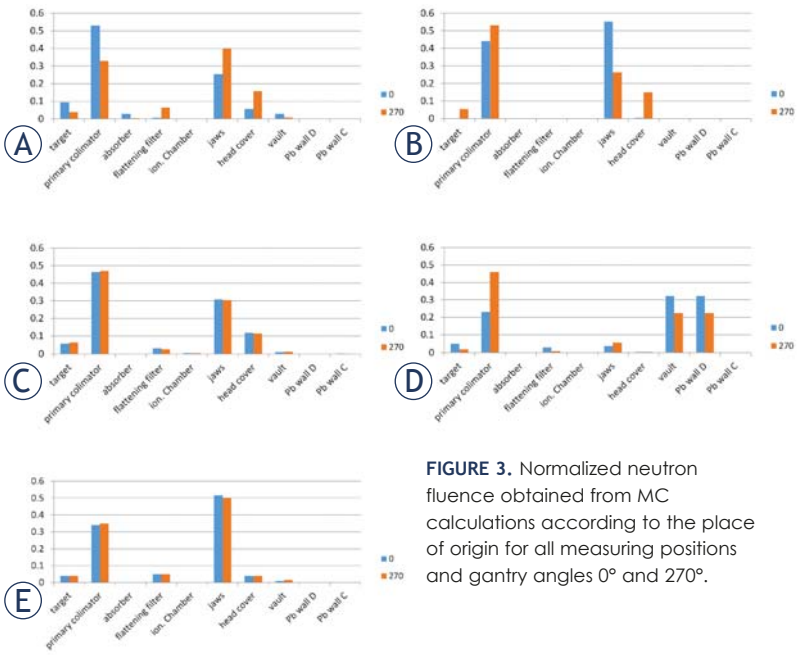

FIGURE 3. Normalized neutron fluence obtained from MC calculations according to the place of origin for all measuring positions and gantry angles 0° and 270°.

the published results.[18] Measurements with neutron dosimeters that consist of SSNTD CR-39 and boron foil BN-1 showed that neutron dose rate in isocenter is large enough that these detectors can be used in in vivo patient dosimetry. Neutron dose to the patient can be calculated from track density and calibration coefficients listed in Table 3.

Outside the vault, in positions A, B and D, it is difficult to measure the neutron dose because the track density on detectors is of the same order of magnitude as track density caused by the background radiation. Therefore, application of neutron dosimeters described in this study in personal dosimetry is questionable. According to the MC simulations, mean neutron dose per year in is 324 μSv, 83 μSv and $2.7 \cdot 10^{-5}$ μSv in positions A, B and D respectively. Calculated neutron doses are far below exposure limit of ionizing radiation for workers which is 20 mSv per year.[19] Therefore, neutron personal dosimetry is not necessary. In our previ-

TABLE 2. Neutron dose equivalents in μSv per Gy photon dose in isocenter for all measuring positions and gantry angles 0° and 270°

		Gantry 0°					Gantry 270°				
		A (μSv/Gy)	B (μSv/Gy)	C (μSv/Gy)	D (μSv/Gy)	E (μSv/Gy)	A (μSv/Gy)	B (μSv/Gy)	C (μSv/Gy)	D (μSv/Gy)	E (μSv/Gy)
Poje *et al.*[5]	LR 115	0.04	0.08	10	0.04		0.1	0.17	20	0.13	
	Active detector	0.052	0.1	14.3	0.052						
Our results	CR-39	0.008 (0.0006)	0.0006 (0.00004)	8.2 (0.6)	$1.3 \cdot 10^{-12}$ ($7 \cdot 10^{-14}$)	3297 (264)	0.01 (0.008)	0.004 (0.0002)	10.3 (0.5)	$4.21 \cdot 10^{-11}$ ($2 \cdot 10^{-12}$)	3333 (202)

Data from Table 2 are obtained by using calibration coefficients for neutron detector CR-39. In Table 3 calibration coefficients for measuring positions C and E are presented.

TABLE 3. Calibration coefficients for neutron detector CR-39 for measuring positions C and E for gantry angles 0° and 270°

Position	G 0°	G 270°
	μSv/(track/mm²)	μSv/(track/mm²)
C	6,52	11,20
E	151,61	194,97

ously published data[5], estimated dose for workers was 2 mSv per year which is higher than the doses estimated in this study.

Conclusions

Problem of placing high energy linear accelerators in small vaults that are not originally built for linear accelerators is still very present in Southern European countries. Since the space is limited, photon shielding problems are often solved by inserting lead or iron plates in vault walls. High Z elements are new sources of photoneutrons which complicate assessment of neutron spectra and dose in vicinity of linear accelerators. In this study, MC simulations of linear accelerator Siemens Oncor Expression in Osijek University Hospital were done and neutron spectra and dose equivalents in vicinity of linear accelerator were obtained. It is important to include the vault in MC model when assessing neutron dose to patients, otherwise the dose can be overestimated. Simulations showed that lead panels inserted as photon shielding in vault walls are the source of photoneutrons and they contribute to patient and staff dose. However, neutron dose to staff working in vicinity of accelerator vaults is small and there is no need for personal neutron dosimetry. In experimental part of this study, SSNTD CR-39 was used to measure neutron doses in positions inside and outside the vault. Neutron dose rate outside the vault was of the same order of magnitude as the background radiation and their use in personal dosimetry is questionable. In isocenter, neutron detectors are calibrated against spectra obtained from MC simulations and can be used in *in vivo* dosimetry to estimate neutron dose to patients.

Acknowledgments

The study was financed by J. J Strossmayer University project ZUP2018

References

1. Brkić H, Ivković A, Kasabašić M, Poje Sovilj M, Jurković S, Štimac D, et al. The influence of field size and off-axis distance on photoneutron spectra of the 18 MV Siemens Oncor linear accelerator beam. *Radiat Meas* 2016; **93:** 28-34. doi: 10.1016/j.radmeas.2016.07.002
2. Vukovic B, Faj D, Poje M, Varga M, Radolic V, Miklavcic I, et al. A neutron track etch detector for electron linear accelerators in radiotherapy. *Radiol Oncol* 2010; **44:** 62-6. doi: 10.2478/v10019-010-0003-2
3. Vanhavere F, Huyskens D, Struelens L. Peripheral neutron and gamma doses in radiotherapy with an 18 MV linear accelerator. *Radiat Prot Dosimetry* 2004; **110:** 607-12. doi: 10.1093/rpd/nch135
4. Domingo C, García-Fusté MJ, Morales E, Amgarou K, Terrón JA, Rosello J, et al. Neutron spectrometry and determination of neutron ambient dose equivalents in different LINAC radiotherapy rooms. *Radiat Meas* 2010; **45:** 1391-7. doi: 10.1016/j.radmeas.2010.05.023
5. Poje M, Ivković A, Jurković S, Žauhar G, Vuković B, Radolić V, Miklavčić I, et al. The neutron dose equivalent around high energy medical electron linear accelerators. *Nucl Technol Radiat Prot* 2014; **29:** 171-8. doi:10.2298/NTRP1403207P
6. Tóth ÁÁ, Petrović B, Jovančević N, Krmar M, Rutonjski L, Čudić O. The evaluation of the neutron dose equivalent in the two-bend maze. *Phys Medica* 2017; **36:** 119-25. doi: 10.1016/j.ejmp.2017.03.017
7. Irazola L, Terrón JA, Sánchez-Nieto B, Roberto B, Sánchez-Doblado F. Peripheral equivalent neutron dose model implementation for radiotherapy patients. *Phys Medica* 2017; **42:** 345-52. doi: 10.1016/j.ejmp.2017.03.018
8. Puchalska M, Sihver L. PHITS simulations of absorbed dose out-of-field and neutron energy spectra for ELEKTA SL25 medical linear accelerator. *Phys Med Biol* 2015; **60:** N261. doi: 10.1088/0031-9155/60/12/N261
9. Howell RM, Ferenci MS, Hertel NE, Fullerton GD. Investigation of secondary neutron dose for 18MV dynamic MLC IMRT delivery. *Med Physics-New York-Institute Phys* 2005; **32:** 786-93. doi: 10.1118/1.1861162
10. Brkić H, Kasabašić M, Ivković A, Agić D, Krpan I, Faj D. Influence of head cover on the neutron dose equivalent in monte carlo simulations of high energy medical linear accelerator. *Nucl Technol Radiat Prot* 2019; **33:** 217-22. doi: 10.2298/NTRP1802217B
11. Karimi AH, Brkić H, Shahbazi-Gahrouei D, Haghighi SB, Jabbari I. Essential considerations for accurate evaluation of photoneutron contamination in radiotherapy. *Appl Radiat Isot* 2018; **145:** 24-31. doi: 10.1016/j.apradiso.2018.12.007
12. Cox LJ, Casswell L. MCNP (TM) Release 6.1. 1 beta: Creating and testing the code distribution 2014. [cited 2020 Jan 15]. Available at: https://permalink.lanl.gov/object/tr?what=info:lanl-repo/lareport/LA-UR-14-24330
13. Ivković A, Faj D, Galić S, Karimi AH, Kasabašić M, Brkić H. Accuracy of empirical formulas in evaluation of neutron dose equivalent inside the 60Co vaults reconstructed for medical linear accelerators. *Int J Radiat Res* 2020; **18:** 99-107. doi: 10.18869/acadpub.ijrr.18.1.99
14. McConn RJ, Gesh CJ, Pagh RT, Rucker RA, Williams III R. *Compendium of material composition data for radiation transport modeling.* Richland, WA (US): Pacific Northwest National Laboratory (PNNL); 2011.
15. Chadwick MB, Obložinský P, Herman M, Greene NM, McKnight RD, Smith DL, et al. ENDF/B-VII. 0: next generation evaluated nuclear data library for nuclear science and technology. *Nucl Data Sheets* 2006; **107:** 2931-3060. doi: 10.1016/j.nds.2006.11.001
16. NCRP60 60, Bethesda USA MD. Neutron Contamination from Medical Electron Accelerators: Recommendations of the National Council on Radiation Protection and Measurements 1984. [cited 2020 Jan 15]. Available from: https://ncrponline.org/publications/reports/ncrp-reports-60-79/
17. Jönsson G. Statistics and error considerations at the application of SSNTD-technique in radon measurement. *Nucl Tracks Radiat Meas* 1993; **22:** 347-9. doi: 10.1016/0969-8078(93)90083-G
18. Howell RM, Ferenci MS, Hertel NE, Fullerton GD, Fox T, Davis LW. Measurements of secondary neutron dose from 15 MV and 18 MV IMRT. *Radiat Prot Dosimetry* 2005; **115:** 508-12. doi: 10.1093/rpd/nci041
19. Protection IC on R. ICRP Publication 75: *General Principles for the Radiation Protection of Workers*. Vol. 21. Elsevier Health Sciences; 1997.

Radiol Oncol 2020; 54(2): 135-143.
doi: 10.2478/raon-2020-0025

Sodobni in inovativni pristopi k zdravljenju mišično neinvazivnega raka sečnega mehurja. Vloga transuretralne resekcije tumorja mehurja in organoidi

Taskovska M, Kreft ME, Smrkolj T

Izhodišča. Rak sečnega mehurja je sedmi najpogostejši rak pri moških. Približno 75 % vseh rak sečnega mehurja je mišično neinvazivnih. Zlati standard za dokončno diagnostiko in prva linija zdravljenja mišično neinvazivnega raka sečnega mehurja je transuretralna resekcija tumorja mehurja (TURM). V preteklosti so za TURM uporabljali monopolarni resektoskop, danes večina urologov uporablja bipolarnega. Po TURM je glede na gradus tumorja indicirano dodatno zdravljenje z intravezikalno aplikacijo kemo- in/ali imunoterapevtika. Cilj intravezikalne aplikacije kemo- in/ali imunoterapevtika je preprečiti ponovitev tumorja in potrebo po ponovnem kirurškem zdravljenju. Razvoj tehnologije, molekularne in celične biologije, omogoča raziskovalcem gojenje organoidov - sistemov humanih celic, ki jih gojijo v laboratoriju in imajo lastnosti tkiv, iz katerih izhajajo. Čeprav se organoidi že uporabljajo za preučevanje različnih bolezni na področju urološke onkologije, pa je podatkov za uporabo organoidov raka sečnega mehurja v literaturi zelo malo.

Zaključki. Monopolarni in bipolarni tok resektoskopa imata različen vpliv na urotelij, posledično na onkološki učinek ter patohistološko interpretacijo preparata. Vzorci tumorja sečnega mehurja so uporabni za pripravo organoidov in preučevanje onkogeneze. Organoidi sečnega mehurja so osnova za personalizirano medicino in so uporabni za testiranje učinkovitosti kemo-/imunoterapije pri bolnikih z rakom sečnega mehurja.

Radiol Oncol 2020; 54(2): 144-148.
doi: 10.2478/raon-2020-0017

Mahansko odstranjevanje strdka pri nenadni obojestranski zapori možganske arterije

Jeromel M, Milošević ZV, Pretnar Oblak J

Izhodišča. Nenadna zapora obeh notranjih karotidnih in/ali srednjih možganskih arterij je zelo redka in povezana s slabim kliničnim izhodom. V literaturi je le nekaj tovrstnih primerov bolnikov, ki so bili zdravljeni z znotrajžilnim mehanskim odstranjevanjem strdka. Strategija znotrajžilnega pristopa in klinični izhod zato nista jasna.

Metode. Sistematični pregled literature smo izvedli preko več elektronskih baz podatkov, pri čemer smo uporabljali naslednje iskalne zahteve: nenadna obojestranska kap, mehanska ponovna vzpostavitev pretoka, odstranitev strdka.

Rezultati. V literaturi smo našli pet poročil o šestih bolnikih z obojestransko nenadno zaporo notranje karotidne in/ali srednje možganske arterije, ki so jih zdravili z mehansko odstranitvijo strdka. Dodajamo tudi primer bolnika, ki je po našem vedenju prvi primer obojestranske zapore velike možganske arterije, nastale med intravenskim trombolitičnim zdravljenjem, kjer je bil klinični izhod po mehanski odstranitvi strdka popolnoma odvisen od kolateralnih možganskih pretokov in ne od časa, ki je minil od začetka nastanka zapore.

Zaključki. Nenadna zapora obeh notranjih karotidnih in/ali srednjih možganskih arterij vodi v hudo nevrološko stanje (komo) z nepredvidljivim izhodom bolezni tudi v času, ko imamo na voljo metode za mehansko odstranitev strdka. Videti je, da je prisotnost kolateralnih pretokov bolj pomembna kot pa čas do ponovne vzpostavitve pretoka, zato sočasna odstranitev strdka sama po sebi verjetno ne izboljša kliničnega izhoda bolnika.

Radiol Oncol 2020; 54(2): 149-158.
doi: 10.2478/raon-2020-0029

Glavne in dodatne značilnosti kriterijev LI-RADS za oceno kombiniranega hepatocelularnega-holangiokarcinoma

Granata V, Fusco R, Setola SV, Sandomenico F, Barretta ML, Belli A, Palaia R, Tatangelo F, Grassi R, Izzo F, Petrillo A

Izhodišča. Namen raziskave je bil določiti, katere značilnosti kriterijev LI-RADS verzije 2018 (v2018) omogočajo natančno karakterizacijo kombiniranega hepatocelularnega-holangiokarcinoma (cHCC-CCA).

Bolnikii in metode. V retrospektivno raziskavo smo zajeli 62 bolnikov (srednja starost 63 let; razpon 38–80 let) z operabilnimi HCC-ji, ki so bili pred operacijo potrjeni z biopsijo. Pri vseh bolnikih smo naredili računalniško tomografijo (CT), pri 23 bolnikih tudi magnetnoresonančna preiskavo (MR). HCC smo v radioloških izvidih opisali s pomočjo glavnih in dodatnih značilnosti glede na kriterije LI-RADS v2018.

Rezultati. Dokončna histološka diagnoza je pokazala, da je imelo 51 bolnikov HCC in 11 bolnikov cHCC-CAA. Srednja velikost vseh lezij je bila 46,0 mm (razpon 10–190 mm), srednja velikost cHCC-CCA je bila 33,5 mm (razpon 20–80 mm) in srednja velikost HCC 47,5 mm (razpon 10–190 mm). Glede na kategorije LI-RADS je bilo 54 (87,1 %) lezij opredeljenih kot LR-5, 1 (1,6 %) lezija kot LR-3 in 7 (11,3 %) kot LR-M. 39 (63 %) lezij je bilo hipervaskularnih v arterijski fazi preiskave; med njimi so tako značilnost kazali 4 cHCC-CCA (36,4 % izmed vseh cHCC-CCC) in 35 pravih HCC (68,6 % izmed vseh HCC). 43 (69,3 %) lezij je izplavljalo kontrastno sredstvo; izplavljanje je bilo vidno pri 6 cHCC-CCAs (54,5 % izmed vseh cHCC--CCA) in 37 pravih HCC (72,5 % izmed vseh HCC). Pri samo dveh bolnikih s cHCC-CCA (18,2 % izmed vseh cHCC-CCA) je bila vidna kapsula. Pet cHCC-CCA (71,4 % izmed vseh cHCC-CCA) je bilo hiperintenzivnih na T2 poudarjenih sekvencah (T2-w), dve leziji (28,6 %) sta bili heterogenega signala na T2-w. Pri vseh cHCC-CCA je bila vidna restrikcija difuzije. Pri sedmih bolnikih s cHCC-CCA je bilo vidno progresivno obarvanje in satelitni noduli.

Zaključki. Značilnosti, ki nakazujejo možnost cHCC-CCA so prisotnost satelitnih nodulov, hiperintenziven signal na T2-w, restrikcija difuzije, odsotnost kapsule in progresivno obarvanje po kontrastnem sredstvu.

Radiol Oncol 2020; 54(2): 159-167.
doi: 10.2478/raon-2020-0021

Povezava hondromalacije pogačice z anatomskimi parametri proksimalne tibije, ocenjenimi z magnetno resonanco

Tabary M, Esfahani A, Nouraie M, Babaei MR, Khoshdel AR, Araghi F, Shahrezaee M

Izhodišča. Magnetna resonance (MR) je neinvazivna visoko občutljiva preiskava za oceno zgodnje hondromalacije pogačice. Morfologijo pogačice in sosednje femuralne trohlee je ocenjevalo več razsikav. Namen naše študije je ocena povezave hondromalacijo pogačice s tibialnimi, patelarnimi in femoralnimi anatomskimi indeksi s pomočjo MR.

Bolniki in metode. Med letoma 2017 in 2019 smo v raziskavo vključili 100 preiskav MR kolena pri bolnikih s hondromalacijo pogačice in 100 preiskav MR pri bolnikih brez hondromalacije ob ustrezni starosti. Preiskave MR smo opravili po standardnem protokolu. Hondromalacijo pogačice smo ocenili po modificirani Outerbridgeovi klasifikaciji (stopnje 1–4). V kolenskem sklepu ter okolnih strukturah smo izmerili 25 parametrov in jih primerjali s stopnjo hondromalacije pogačice.

Rezultati. Hondromalacija pogačice je bila omembno povezana z nagibom tibialnega platoja, globino trohlee femurja, nagibom lateralne fasete trohlee femurja ter lateralnim nagibom pogačice. Povečan nagib lateralne fasete trohlee femurja (Razmerje obetov [OR] 1,15, 1,03–1,30 pri 95 % intervalu zaupanja), povečan lateralni nagib pogačice (OR 1,13, 1,02–1,26 pri 95 % intervalu zaupanja), povečan medialni nagib tibialnega platoja (OR 0,85, 0,73 in 0,98 pri 95 % intervalu zaupanja) ter povečana globina trohlee (0,06, 0,02 in 0,17 pri 95 % intervalu zaupanja) so bili povezani z zvišano možnostjo za hondromalacijo pogačice. Model za oceno stopnje hondromalacije v odvisnosti od višine pogačice je pokazal OR 75,9.

Zaključki. Rezultati raziskave so pokazali novo povezavo anatomskih parametrov proksimalne tibije s hondromalacijo pogačice. Pokazali so tudi na povezavo višine pogačice s stopnjo hondromalacije.

Radiol Oncol 2020; 54(2): 168-179.
doi: 10.2478/raon-2020-0015

Odziv na pulzno obsevanje z nizko hitrostjo doze v izogenih celičnih linijah pri ploščatoceličnih rakih glave in vratu z različno radiosenzitivnostjo

Todorović V, Prevc A, Nikšić Žakelj M, Savarin M, Buček S, Grošelj B, Strojan P, Čemažar M, Serša G

Izhodišča. Zdravljenje lokoregionalnih ponavljajočih ploščatoceličnih rakov glave in vratu predstavlja izziv zaradi razvoja radiorezistence. Pulzno obsevanje z nizko hitrostjo doze temelji na pojavu povečane radiosenzitivnosti na nizke doze sevanja ter učinku hitrosti doze sevanja. Namen te raziskave je bil ovrednotiti pojav povečane radiosenzitivnosti na nizke doze sevanja in učinek pulznega obsevanja z nizko hitrostjo doze na modelu izogenih celic ploščatoceličnih rakov glave in vratu z različno radiosenzitivnostjo.

Materiali in metode. Preživetje izogenih starševskih celic FaDu in radiorezistentnih celic FaDu-RR po obsevanju z različnimi protokoli smo določili s testom klonogenosti. S pretočno citometrijo smo preučili učinek obsevanja na razporeditev celic v celičnem ciklu. Z obratno transkripcijo in kvantitativno verižno reakcijo s polimerazo smo določili izražanje genov, ki so vključeni v signaliziranje poškodb DNA.

Rezultati. V radiorezistentnih celicah FaDu-RR smo pokazali pojav povečane radiosenzitivnosti na nizke doze sevanja ter povečano občutljivost na pulzno obsevanje z nizko hitrostjo doze v primerjavi s starševskimi celicami FaDu. Pri obeh celičnih linijah smo zaustavili celični cikel v fazi G_2/M pet ur po obsevanju. Normalen celični cikel se je ponovno vzpostavil 24 ur po obsevanju v starševskih, ne pa v radiorezistentnih celicah, ki so zastale v fazi G_1. Izražanje genov, ki so vključeni v signaliziranje poškodb DNA, je v radiorezistentnih celicah zmanjšano v primerjavi s starševskimi celicami. Obsevanje je povečalo izražanje teh genov v radiorezistentnih celicah, medtem ko se je v starševskih celicah zmanjšalo izražanje le nekaj genov.

Zaključki. Pokazali smo prisotnost pojava povečane radiosenzitivnosti na nizke doze sevanja v izogenih radiorezistentnih celicah, ne pa v starševskih celicah. Preživetje celic, kjer smo ugotovili povečano radiosenzitivnost na nizke doze sevanja, a so bile sicer radiorezistentne, se je po pulznem obsevanju z nizko hitrostjo doze značilno zmanjšalo. Manjše preživetje celic po obsevanju z nizko hitrostjo doze je povezano s spremembami v izražanju genov, ki so vključeni v signaliziranje poškodb DNA, najverjetneje preko spremenjene regulacije kontrolnih točk celičnega cikla.

Radiol Oncol 2020; 54(2): 180-186.
doi: 10.2478/raon-2020-0020

Prevalenca okultnega raka jajčnikov pri 155 preventivnih operacijah visoko ogroženih asimptomatskih bolnicah. Slovenska populacijska raziskava

Gornjec A, Merlo S, Novaković S, Stegel V, Gazić B, Perhavec A, Blatnik A, Krajc M

Izhodišča. Določali smo prevalenco, lokalizacijo, patohistološke značilnosti in napoved izhoda bolezni pri bolnicah z okultnim rakom jajčnikov. Jajčnike in/ali jajcevode smo preventivno odstraniili pri asimptomatskih nosilkah *BRCA* patogenih in verjetno patogenih različic ter visoko ogroženih *BRCA* negativnih ženskah.

Bolnice in metode. Retrospektivno smo analizirali vse ginekološke preventivne operacije od januarja 2009 do decembra 2015. Bolnice smo spremljali do januarja 2019. Vse vključene bolnice so imele pred posegom opravljeno genetsko svetovanje in *BRCA* testiranje. Zbrali in analizirali smo podatke o kliničnih lastnostih bolnic, dodatnem zdravljenju in spremljanju po končanem zdravljenju.

Rezultati. Odstranili smo 155 jajčnikov in jajcevodov pri 110 nosilkah patogenih in verjetno patogenih različic na *BRCA1*, 35 na *BRCA2* in 10 visoko ogroženih *BRCA* negativnih ženskah. Povprečna starost bolnic je bila 48,3 let. Odkrili smo devet okultnih rakov jajčnikov in jajcevodov (5,8 % vseh operiranih); osem pri nosilkah *BRCA1* in en pri visoko rizični *BRCA* negativni bolnici. Od devetih so bili štirje serozni tubarni intraepitelni karcinomi (trije pri *BRCA1* nosilkah in enega pri visoko rizični *BRCA* negativni bolnici), pet je bilo invazivnih tubo-ovarijskih seroznih karcinomov (vsi pri *BRCA1* nosilkah). Le ena izmed devetih bolnic (11,1 %) z okultnim rakom je imela predoperativno blago povišano vrednost tumorskega označevalca CA-125.

Zaključki. Prevalenca okultnih seroznih karcinomov po preventivni ginekološki operaciji pri visoko rizičnih asimptomatskih bolnicah je bila 5,8 %. Starost ob preventivnih ginekoloških operacijah mora biti skrbno načrtovana po smernicah za določen tip mutacije, oziraje se na končano rodno obdobje. Pri nosilkah *BRCA* patogenih in verjetno patogenih različic in visoko rizičnih *BRCA* negativnih bolnicah bi morala biti operacija opravljena po 35. letu starosti in pri *BRCA1* nosilkah pred 40. letom starosti. Ugotavljamo, da je smiselno ponuditi preventivno ginekološko operacijo tudi visoko rizičnim *BRCA* negativnim bolnicam. Rezultati analize potrjujejo tubarno hipotezo nastanka seroznega raka jajčnikov/jajcevodov. Citološka preiskava izpirka peritonealne votline je pomembno vplivala na odločitev o vrsti dodatnega zdravljenja in bi naj bila narejena ob vsaki preventivni ginekološki operaciji. Merjenje vrednosti tumorskega označevalca CA-125 se pri naših preiskovankah ni izkazalo za učinkovito presejanje za zgodnje odkrivanje raka jajčnikov.

Radiol Oncol 2020; 54(2): 187-193.
doi: 10.2478/raon-2020-0023

Prehranski vnos joda, zdravljenje z radiojodom in anaplastični rak ščitnice

Bešić N, Gazić B

Izhodišča. Anaplastični rak ščitnice je eden najbolj agresivnih tumorjev. Namen raziskave je bil ugotoviti, ali obstaja povezava med večjim prehranskim vnosom joda, pogostostjo anaplastičnega raka ščitnice in značilnostmi tega raka ter ugotoviti, kako pogosto smo bolnike z anaplastičnim rakom ščitnice v preteklosti zdravili z radiojodom.

Bolniki in metode. V retrospektivno raziskavo smo vključili 220 bolnikov (152 žensk, 68 moških; povprečna starost 68 let) z anaplastičnim rakom ščitnice, ki so se na Onkološkem inštitutu Ljubljana zdravili od leta 1972 do 2017. Sol je bila jodirana z 10 mg kalijevega jodida / kg pred letom 1999 in s 25 mg kalijevega jodida / kg po letu 1999. Bolnike smo razvrstili v 15-letna obdobja: 1972–1986, 1987–2001 in 2002–2017.

Rezultati. Incidenca anaplastičnega raka ščitnice se je zmanjšala po večjem jodiranju soli ($p = 0,04$). Bolniki so sedaj starejši ($p = 0,013$) in imajo redkeje zasevke v bezgavkah ($p = 0,012$) kot v preteklosti. Pogostost oddaljenih zasevkov se sčasoma ni spreminjala. Srednje preživetje bolnikov v prvem, drugem in tretjem obdobju je bilo tri, štiri in tri mesece ($p < 0,05$). Predhodno smo z radiojodom zdravili 7,7 % bolnikov.

Zaključki. Število bolnikov z anamnezo zdravljenja z radiojodom se sčasoma ni spreminjalo. Incidenca anaplastičnega raka ščitnice v Sloveniji se je verjetno zmanjšala zaradi uporabe bolj jodirane soli kot v preteklosti.

Radiol Oncol 2020; 54(2): 194-200.
doi: 10.2478/raon-2020-0019

Pomen aktivacije nuklearnega faktorja kappa beta na vzorcih igelne biopsije pri ugotavljanju indolentnosti raka prostate, ki smo ga po Gleasonu ocenili 6

Zupančič M, Pospihalj B, Cerović S, Gazić B, Drev P, Hočevar M, Perhavec A

Izhodišča. Namen raziskave je bil ugotoviti, ali je imunohistokemično izražanje nuklearnega faktorja kappa beta (NF-κB) na vzorcih igelnih biopsije negativni napovedni dejavnik za indolentnost raka prostate z oceno po Gleasonu 3 + 3 = 6 (GS 6).

Bolniki in metode. Raziskavo smo zasnovali na retrospektivni analizi podatkov pri 123 bolnikih z rakom prostate, ki so imeli začetno celokupno vrednost prostatičnega specifičnega antigena (PSA) ≤ 10 ng/ml, število vzorcev igelne biopsije prostate ≥ 8, GS 6 pri biopsiji in ocenjen klinični stadij T1/T2. Vsem smo naredili laparoskopsko radikalno prostatektomijo in njihova arhivirana, s formalinom fiksirana tkiva v parafinskih blokih uporabili za dodatno imunohistokemično barvanje na NF-κB p65. Citoplazemsko in jedrno izražanje NF-κB p65 v vzorcih igelne biopsije prostate s prisotnim rakom prostate smo ločeno primerjali s pooperativnim patološkim stadijem, pozitivnimi kirurškimi robovi, GS in biokemičnim napredovanjem bolezni.

Rezultati. Po 66 mesecih spremljanja je do biokemičnega napredovanja bolezni (PSA ≥ 0,2 ng/ml) prišlo pri 6 (5,1 %) bolnikih, pri 3 (50 %) s pooperativnim GS 6 in pri 3 (50 %) s pooperativnim GS 7. Tako citoplazemsko kot tudi jedrno izražanje NF-κB p65 nista bili statistično povezani s patološkim stadijem, pozitivnim kirurškim robom in pooperativnim GS. Pri bolniki s pozitivno citoplazemsko NF-κB reakcijo smo ugotovili biokemična napredovanja bolezni z mejno vrednostjo PSA 0,2 ng/ml značilno več (p = 0,015) kot pri bolnikih z negativno reakcijo, medtem ko je bil pri mejni vrednosti PSA 0,05 ng/ml nakazan le trend večjega števila biokemičnih napredovanj bolezni (p = 0,068).

Zaključki. Citoplazemsko izražanje NF-κB je povezano z večjim številom biokemičnih napredovanj bolezni in bi lahko bilo neodvisen napovedni dejavnik za preživetje brez ponovitve bolezni. Za potrditev teh začetnih rezultatov pa bo potrebna analiza na večjem številu bolnikov.

Radiol Oncol 2020; 54(2): 201-208.
doi: 10.2478/raon-2020-0018

Testiranje programa usposabljanja laboratorijskega osebja brez znanja cervikalne citologije in imunocitokemije za ocenjevanje dvojnega imunocitokemičnega barvanja p16/Ki-67

Kloboves Prevodnik V, Pohar Marinšek Ž, Zalar J, Rozina H, Kotnik N, Jerman T, Varl J, Ivanuš U

Izhodišča. Ustrezno usposobljeni laboratorijski delavci naj ne bi imeli težav pri ocenjevanju p16/Ki-67 dvojnega imunocitokemičnega barvanja (DB), vendar trenutno še ni soglasja, kakšno usposabljanje je najbolj primerno. V raziskavi smo na dveh študentih brez znanja cervikalne citologije testirali program učenja ocenjevanja DB.

Metode. Začetno usposabljanje, ki ga je vodil starejši presejalec, je potekalo na 40 konvencionalnih brisih materničnega vratu pobarvanih z DB. Po začetnem usposabljanju sta dva študenta brez znanja cervikalne citologije in imunocitokemije ocenila 118 preparatov z DB. Sledilo je dodatno usposabljanje, ki je zajemalo predvsem pregled preparatov DB z neskladnimi ocenami iz prvega ocenjevanja na večglavem diskusijskem mikroskopu. Nato sta študenta ocenila dodatnih 383 preparatov. Ujemanje in zanesljivost ocen DB za odkrivanje CIN2+ obeh študentov smo po obeh ocenjevanjih primerjali med seboj in z referenčnimi rezultati. Pozorni smo bili tudi na čas potreben za oceno enega preparata in na variabilnost rezultatov učitelja.

Rezultati. Ujemanje rezultatov med študentoma in referenco je bilo po zaključku raziskave večje v primerjavi s tistim po začetnem usposabljanju. Po začetnem usposabljanju je bil odstotek ujemanja za vsakega študenta 81,4 % ter *kapa* 0,512 in 0,527, po dodatnem usposabljanju pa je bil odstotek ujemanja 78,3 % in 87,2 % ter *kapa* 0,556 in 0,713. Zanesljivost ocen testa za odkrivanje CIN2+ se je na koncu raziskave med študentoma razlikovala. Po začetnem usposabljanju je bila občutljivost ocen obeh študentov za 4,3 % in 2,9 % točk višja v primerjavi z referenco, nasprotno pa je bila specifičnost nižja za 30,6 % in 24,4 % točk. Ob koncu raziskave je bila občutljivost ocen testa enega študenta enaka kot pri referenci, medtem ko je bila pri drugem študentu za 2,6 % točk nižja. Med enim študentom in referenco ter med obema študentoma je prišlo do statistično pomembne razlike v specifičnosti (16,7 in 15,1 % točk). Proti koncu raziskave je en študent za oceno enega preparata potreboval 5,2 min, drugi pa 8,2 min. V obeh rokah raziskave je bila notranja variabilnost ocen starejšega presejalca v območju „zelo dobro".

Zaključki. Med usposabljanjem za ocenjevanje DB je napredek študentov potrebno spremljati z več različnimi merili, kot so ujemanje in zanesljivost rezultatov za odkrivanje CIN2+ ter čas, potreben za ocenjevanje enega preparata. Spremljanje napredka je potrebno izvajati še nekaj časa po tem, ko študenti že dosežejo zadovoljive rezultate. Le tako lahko zagotovimo nadaljnje dobro delo. Priporočljivo je tudi spremljanje rezultatov učitelja.

Radiol Oncol 2020; 54(2): 209-220.
doi: 10.2478/raon-2020-0026

Obravnava bolnikov z nedrobnoceličnim pljučnim rakom stadija III. Srednjeevropska izkušnja v klinični praksi

Zemanová M, Pirker R, Petruželka L, Zbožínková Z, Jovanović D, Rajer M, Bogos K, Purkalne G, Ceriman V, Chaudhary S, Richter I, Kufa I, Jakubíková L, Zemaitis M, Černovská M, Koubková L, Vilasová Z, Dieckmann K, Farkas A, Spasić J, Fröhlich K, Tiefenbacher A, Hollósi V, Kultan J, Kolářová I, Votruba J

Izhodišča. Na obravnavo nedrobnoceličnega raka pljuč vplivajo regionalne posebnosti. Cilj raziskave je bil določiti diagnostične in terapevtske postopke, vključno z izidi zdravljenja bolnikov z nedrobnoceličnim rakom pljuč stadija III v vsakodnevni klinični praksi v srednjeevropskih državah, z namenom opredelite področja, kjer bi lahko dosegli izboljšave.

Bolniki in metode. V multicentrični, prospektivni in neintervencijski raziskavi smo v spletnem registru zbrali podatke bolnikov z nedrobnoceličnim rakom pljuč stadija III in jih centralno analizirali.

Rezultati. Med marcem 2014 in marcem 2017 smo vključili 583 bolnikov z nedrobnoceličnim rakom pljuč stadija III z naslednjimi značilnostmi: 32 % je bilo žensk; 7 % bolnikov ni nikoli kadilo; splošno stanje zmogljivosti po ECOG 0, 1, 2 in 3 je bilo 25 %, 58 %, 12 % in 5 %; 21 % bolnikov je predhodno izgubljalo težo; 53 % bolnikov je imelo ploščatocelični rak, 38 % žlezni rak; 10 % bolnikov je imelo mutacijo EGFR. Stadij smo določili s pomočjo rentgenskega slikanje prsnega koša (97 % bolnikov), CT-jem prsnega koša (96 %), PET-CT-jem (27 %), slikovno preiskavo možgan (20 %), bronhoskopijo (89 %), endobronhialnim ultrazvokom (13 %) in CT-vodeno biopsijo (9 %). Stadij IIIA / IIIB smo diagnosticirali pri 55 % oz. 45 % bolnikih, N2 / N3 pa pri 60 % / 23 % in patološko potrdili pri 29 % bolnikih. Večino bolnikov (56%) smo zdravili kombinirano. Operativno in s kemoterapij smo zdravili 20 % bolnikov, s kemoradioterapijo 34 %, samo s kemoterapijo 26 %, samo z radioterapijo 12 % in samo z najboljšo podporno terapijo 5 % bolnikov. Srednji čas preživetja je bil 16,8 (15,3–18,5) mesecev, čas preživetja brez napredovanja bolezni pa 11,2 (10,2–12,2) mesecev. Stadij IIIA, ženski spol, odsotnost hujšanja, preverjanje patoloških mediastinalnih bezgavk, operacija in kombinirana terapija so bili povezani z daljšim preživetjem.

Zaključki. Raziskava vsakodnevne klinične prakse je pokazala široko heterogenost pri obravnavi bolnikov z nedrobnoceličnim rakom pljuč stadija III v srednjeevropskih državah. Pomembno bi bilo povečati število preiskav s pomočjo PET-CT-ja, slikovne preiskave možgan in invazivno mediastinalno diagnostiko.

Radiol Oncol 2020; 54(2): 221-226.
doi: 10.2478/raon-2020-0028

Natančnost diagnosticiranja pljučnice povzročene s *Pneumocystis jirovecii* s testom (1→3)-β-D-glucan pri bolnikih, ki niso okuženi s HIV

Rogina P, Skvarč M

Izhodišča. Pljučnica *Pneumocystis jirovecii* (*P. jirovecii*) je potencialno usodna oportunistična okužba pri imunsko ogroženih posameznikih, ki niso okuženi s HIV. Običajni diagnostični in klinični protokoli so premalo občutljivi in specifični, da bi zaznali to pljučnico. Naredili smo retrospektivno raziskavo in proučili več metod, ki smo jih uporabili v diagnostiki pljučnice povzročene s *Pneumocystis jirovecii (PCP)*.

Bolniki in metode. V raziskavo smo vključili 108 bolnikov z oslabljenim imunskim sistemom, s tipično klinično sliko pljučnice *P. jirovecii* in s sumljivimi radiološkimi izvidi. Vzorce seruma smo odvzeli za merjenje vrednosti (1→3)-β-D-glukana (Fungitell, Associates of Cape Cod, ZDA). Vzorce iz spodnjih dihal smo pridobili za dokazovanje genoma *P. jirovecii* s pomočjo verižne polimerazne reakcije (qPCR).

Rezultati. V raziskavi je 54 bolnikov (50 %) od 108 imelo (1→3)-β-D-glukan > 500 pg/ml. Bolniki, ki so imeli v serumu koncentracije (1→3)-β-D-glukana < 400 pg/ml, so imeli nižje koncentracije genoma *P. jirovecii* v dihalih. Število cilklov pomnoževanja genoma (ang. *Cycle threshold* [Ct]) je bilo 35,43 ± 3,32 v primerjavi s tistimi, ki so imeli (1→3)-β-D- koncentracije glucan > 400 pg/ml in povprečen Ct 28,97 ± 5,27 (P < 0,001), in s tem večjo verjetnost, da imajo PCP. Če je koncentracija (1→3)-β-D-glukana bila višja od 400 pg/ml in je bila Ct vrednost qPCR-ja pod 28,97 ± 5,27, smo lahko bili z veliko verjetnostjo prepričani, da je *P. jirovecii* povzročila pljučnico (razmerje obetov [OR] 2,31, 95 % interval zaupanja [CI] 1,62–3,27, P < 0,001).

Zaključki. Izključno merjenje (1→3)-β-D-glukana ali samo rezultat qPCR-ja nista zadostna, da bi potrdili ali izključili pljučnico *P. jirovecii*. Vrednosti (1→3)-β-D-glukana > 400 pg/ml in qPCR pod 30 Ct nam omogočata, da z veliko gotovostjo sodimo, da ima bolnik PCP. Če je vrednosti (1→3)-β-D-glukana < 400 pg/ml in je qPCR nad 35 Ct, je bolj verjetna kolonizacija dihal s *P. jirovecii* kot pa PCP.

Radiol Oncol 2020; 54(2): 227-232.
doi: 10.2478/raon-2020-0022

Stereotaktično obsevanje (SBRT) za zdravljenje primarnega pljučnega raka pri prejemnikih presajenih pljuč

Moore A, Kramer MR, Rosengarten D, Shtraichman O, Zer A, Dudnik E, Korzets Y, Allen AM

Izhodišča. Presaditev pljuč je reševalno zdravljenje za bolnike s pljučno boleznijo v terminalni fazi. Incidenca pljučnega raka pri prejemnikih presaditve pljuč bi lahko bila večja. Ti raki se po navadi odkrijejo v napredovalem stadiju. Podatkov o varnosti in učinkovitosti stereotaktičnega obsevanja (SBRT) za lezije preostalih lastnih pljuč pri prejemnikih presajenih pljuč je zelo malo.

Bolniki in metode. Naredili smo retrospektivni pregled vseh bolnikov v Centru Davidoff Cancer, ki so bili predhodno zdravljeni s transplantacijo pljuč in so razvili rak v lastnih pljučih ter smo jih zdravili s tehniko SBRT.

Rezultati. V analizo smo vključili štiri bolnike, ki smo jih zdravili s SBRT na skupno 5 lezij. Dva bolnika nista imela histološke potrditve malignosti. Vse primere smo pred napotitvijo na obsevanje obravnavali na multidisciplinarnem konziliju. Uporabili smo standardno zdravljenje SBRT. Odgovor smo ocenili s slikovno diagnostiko. Tri lezije so pokazale popoln odziv, dve leziji pa delen. Bolniki, ki so imeli delen odziv, so razvili oddaljene metastaze in so kmalu umrli. Pri nobenem bolniku nismo zabeležili toksičnosti.

Zaključki. Tehnika SBRT je učinkovita in varna za zdravljenje pljučnega raka pri bolnikih s presajenimi pljuči. Uporabljamo lahko standardno dozo in frakcionacijo.

Radiol Oncol 2020; 54(2): 233-236.
doi: 10.2478/raon-2020-0027

Uporaba sorafeniba pri zdravljenju hepatoceličnega raka. Retrospektivna monocentrična analiza

Hanžel J, Košir Božič T, Štabuc B, Janša R

Izhodišča. Sorafenib je peroralni zaviralec multikinaze, ki ga uporabljamo pri zdravljenje hepatoceličnega raka. Njegovo učinkovitost smo preizkušali v naključnih kontroliranih preizkusih pri bolnikih z dobro ohranjenim delovanjem jeter in dobrim funkcionalnim statusom. V praksi je bolnikom pogosto na voljo zdravljenje tudi zunaj teh meril. Zato smo izvedli kohortno raziskavo o učinkovitosti sorafeniba pri bolnikih s hepatocelularnim rakom.

Bolniki in metode. V raziskavo smo vključili vse bolnike s hepatocelularnim rakom, ki so pričeli zdravljenje s sorafenibom med januarjem 2015 in januarjem 2018 na Kliničnem oddelku za gastroenterologijo UKC Ljubljana. Primarni cilj raziskave je bil ugotoviti celokupno preživetje od začetka uporabe sorafeniba. Preučevali smo klinične in demografske spremenljivke, povezane s preživetjem.

Rezultati. Srednje celokupno preživetje je bilo 13,4 meseca (95 % interval zaupanja [CI] 8,2–18,6). Pri multivariatni Cox regresiji so bili neugodni napovedni dejavniki slabo stanje telesne zmogljivosti (ECOG PS) (razmerje ogroženosti [HR] 2,21; 95 % CI 1,56–3,16; P < 0,0001), razred Child-Pugh C (HR 52,4; 95% CI 3,20–859; P = 0,005) in odsotnost predhodnega locoregionalnega zdravljenja (HR 2,30; 95% IZ 1,37–3,86; P = 0,002) ter so bili povezani s povečano smrtnostjo.

Zaključki. Za optimizacijo zdravljenja oziroma boljše preživetje je potrebna skrbna izbira bolnikov za zdravljenje s sorafenibom.

Radiol Oncol 2020; 54(2): 237-246.
doi: 10.2478/raon-2020-0016

Sarkopenija in miosteatoza ob začetku zdravljenja negativno vplivata na preživetje po ezofagektomiji zaradi raka požiralnika

Srpčič M, Jordan T, Popuri K, Sok M

Izhodišča. Rak požiralnika ostaja bolezen s slabim preživetjem in številnimi zapleti. Merjenje mišične mase in in njene kakovosti lahko prepozna bolnike z zmanjšano mišično maso (sarkopenijo) in infiltracijo mišic z maščevjem (miosteatozo). Preučevali smo vpliv sarkopenije in miosteatoze pri bolnikih z resektabilnim rakom požiralnika na celokupno preživetje in zaplete.

Bolniki in metode. Pri 139 bolnikih smo napravili radikalno ezofagektomijo. Izmerili smo površino skeletne mišičnine in mišično atenuacijo na posnetkih CT v višini vretenca L3 in primerjali celokupno preživetje, perioperativno smrtnost, zaplete na presadku, plevropulmonalne zaplete, dihalno odpoved in druge značilne zaplete med skupinami z in brez sarkopenije in miosteatoze.

Rezultati. Prevalenci sarkopenije in miosteatoze ob začetku zdravljenja sta bili 16,5 % in 51,8 %. Obe sta bili povezani z zmanjšanim celokupnim preživetjem. Mediano preživetje je bilo 18,3 mesecev (interval zaupanja [CI] 5,4–31,1) proti 31,0 mesecev (CI 7,4–54,6) za sarkopenijo/brez sarkopenije (*log rank* p = 0,042) in 19,0 mesecev (CI 13,3–24,7) proti 57,1 mesecev (CI 15,2–99,0) za miosteatozo (log rank p=0,044). Povezave med sarkopenijo in miosteatozo ter drugimi negativnimi izidi po ezofagektomiji nismo uspeli odkriti.

Zaključki. Sarkopenija in miosteatoza ob diagnozi pred ezofagektomijo sta povezani s slabšim celokupnim preživetjem, ne pa z bolj pogostimi perioperativnimi zapleti. Prepoznava bolnikov s povečanim tveganjem lahko pomaga pri odločitvah o zdravljenju in ukrepih, ki naj povrnejo mišične zaloge.

Radiol Oncol 2020; 54(2): 247-252.
doi: 10.2478/raon-2020-0024

Vpliv povečanja ščitenja v majhnem obsevalnem prostoru na ekvivalentno nevtronsko dozo v bližini linearnega pospeševalnika

Ivković A, Faj D, Kasabašić M, Poje Sovilj M, Krpan I, Grabar Branilović M, Brkić H

Izhodišča. Visoko energijske linearne pospeševalnike (LINAC), ki proizvajajo fotonske žarke z energijami višjimi od 10 MeV, pogosto uporabljamo v radioterapiji. Pri teh energijah nastajajo hitri nevtroni, ki neželeno kontaminirajo terapevtske žarke. V raziskavi smo želeli določiti nevtronski spekter in dozne ekvivalente v okolici linearnega pospeševalnika z dvema metodama, z meritvami in s simulacijo Monte Carlo (MC).

Materiali in metode. Linearni pospeševalnik Siemens Oncor Expression univerzitetne bolnišnice v Osijeku smo postavili v obsevalni prostor, v katerem je bil predhodno obsevalni aparat z virom ^{60}Co. Zaščito v prostoru smo povečali z vgradnjo svinčenih in jeklenih plošč. Meritve nevtronske doze smo izvedli z detektorji CR-39. Energijsko odvisnost detektorjev smo kompenzirali z izračuni energijskega spektra nevtronov z uporabo simulacij Monte Carlo.

Rezultati. Večina nevtronov ima izvor v glavi linearnega pospeševalnika. Simulacije Monte Carlo so pokazale pomembne razlike v nevtronskem spektru v odvisnosti od mesta meritev. Letna ekvivalentna nevtronska doza na mestih izven obsevalne sobe je bila ocenjena na manj kot 324 μSv.

Zaključki. Odziv detektorjev, ki smo jih uporabili v raziskavi je bil močno odvisen od energije nevtronov, zato je zelo pomembno, da poznamo nevtronski spekter na mestih, kjer smo izvajali meritve. Čeprav bi nevtronsko dozo načeloma morali upoštevati pri klinični dozimetriji, smo v razsikavi pokazali, da je ocenjena letna nevtronska doza precej nižja od mejnih doz ionizirajočega sevanja, ki so predpisane za izpostavljene delavce.

Fundacija "Docent dr. J. Cholewa"
je neprofitno, neinstitucionalno in nestrankarsko
združenje posameznikov, ustanov in organizacij, ki želijo
materialno spodbujati in poglabljati raziskovalno
dejavnost v onkologiji.

Dunajska 106
1000 Ljubljana

IBAN: SI56 0203 3001 7879 431

Activity of "Dr. J. Cholewa" Foundation for Cancer Research and Education – a report for the second quarter of 2020

Doc. Dr. Josip Cholewa Foundation for cancer research and education continues with its planned activities in the second quarter of 2020. Its primary focus remains the provision of grants and scholarships and other forms of financial assistance for basic, clinical and public health research in the field of oncology. In parallel, it also makes efforts to provide financial and other support for the organisation of congresses, symposia and other forms of meetings to spread the knowledge about prevention and treatment of cancer, and finally about rehabilitation for cancer patients. In Foundation's strategy, the spread of knowledge should not be restricted only to the professionals that treat cancer patients, but also to the patients themselves and to the general public.

The Foundation continues to provide support for »Radiology and Oncology«, a quarterly scientific magazine with a respectable impact factor that publishes research and review articles about all aspects of cancer. The magazine is edited and published in Ljubljana, Slovenia. »Radiology and Oncology« is an open access journal available to everyone free of charge. Its long tradition represents a guarantee for the continuity of international exchange of ideas and research results in the field of oncology for all in Slovenia that are interested and involved in helping people affected by many different aspects of cancer.

The Foundation will continue with its activities in the future, especially since the problems associated with cancer affect more and more people in Slovenia and elsewhere. Ever more treatment that is successful reflects in results with longer survival in many patients with previously incurable cancer conditions. Thus adding many new dimensions in life of cancer survivors and their families.

Viljem Kovač, M.D., Ph.D.
Borut Štabuc, M.D., Ph.D.
Tomaž Benulič, M.D.
Andrej Plesničar, M.D., M.Sc.

TANTUM VERDE®

benzidaminijev klorid

Za lajšanje bolečine in oteklin v ustni votlini in žrelu, ki so posledica radiomukozitisa

Bistvene informacije iz Povzetka glavnih značilnosti zdravila

Tantum Verde 1,5 mg/ml oralno pršilo, raztopina
Tantum Verde 3 mg/ml oralno pršilo, raztopina
Sestava 1,5 mg/ml: 1 ml raztopine vsebuje 1,5 mg benzidaminijevega klorida, kar ustreza 1,34 mg benzidamina. V enem razpršku je 0,17 ml raztopine. En razpršek vsebuje 0,255 mg benzidaminijevega klorida, kar ustreza 0,2278 mg benzidamina. **Sestava 3 mg/ml:** 1 ml raztopine vsebuje 3 mg benzidaminijevega klorida, kar ustreza 2,68 mg benzidamina. V enem razpršku je 0,17 ml raztopine. En razpršek vsebuje 0,51 mg benzidaminijevega klorida, kar ustreza 0,4556 mg benzidamina. **Terapevtske indikacije:** Samozdravljenje: Lajšanje bolečine in oteklin pri vnetju v ustni votlini in žrelu, ki so lahko posledica okužb in stanj po operaciji. Po nasvetu in navodilu zdravnika: Lajšanje bolečine in oteklin v ustni votlini in žrelu, ki so posledica radiomukozitisa. **Odmerjanje in način uporabe:** Odmerjanje 1,5 mg/ml: Odrasli: 4 do 8 razpršk 2- do 6-krat na dan (vsake 1,5 do 3 ure). Pediatrična populacija: Mladostniki, stari od 12 do 18 let: 4-8 razpršk 2- do 6-krat na dan. Otroci od 6 do 12 let: 4 razprški 2- do 6-krat na dan. Otroci, mlajši od 6 let: 1 razpršek na 4 kg telesne mase; do največ 4 razprške 2- do 6-krat na dan. Odmerjanje 3 mg/ml: Uporaba 2- do 6-krat na dan (vsake 1,5 do 3 ure). Odrasli: 2 do 4 razprški 2- do 6-krat na dan. Pediatrična populacija: Mladostniki, stari od 12 do 18 let: 2 do 4 razprški 2- do 6-krat na dan. Otroci od 6 do 12 let: 2 razprška 2- do 6-krat na dan. Otroci, mlajši od 6 let: 1 razpršek na 8 kg telesne mase; do največ 2 razprška 2- do 6-krat na dan. Starejši bolniki, bolniki z jetrno okvaro in bolniki z ledvično okvaro: Uporabo oralnega pršila z benzidaminijevim kloridom se svetuje pod nadzorom zdravnika. Način uporabe: Za orofaringealno uporabo. Zdravilo se razprši v usta in žrelo. **Kontraindikacije:** Preobčutljivost na učinkovino ali katero koli pomožno snov. **Posebna opozorila in previdnostni ukrepi:** Če se simptomi v treh dneh ne izboljšajo, se mora bolnik posvetovati z zdravnikom ali zobozdravnikom, kot je primerno. Benzidamin ni priporočljiv za bolnike s preobčutljivostjo nasalicilno kislino ali druga nesteroidna protivnetna zdravila. Pri bolnikih, ki imajo ali so imeli bronhialno astmo, lahko pride do bronhospazma, zato je potrebna previdnost. To zdravilo vsebuje majhne količine etanola (alkohola), in sicer manj kot 100 mg na odmerek. To zdravilo vsebuje metilparahidroksibenzoat (E218). Lahko povzroči alergijske reakcije (lahko zapoznele). Zdravilo z jakostjo 3 mg/ml vsebuje makrogolglicerol hidroksistearat 40. Lahko povzroči želodčne težave in drisko. **Medsebojno delovanje z drugimi zdravili in druge oblike interakcij:** Študij medsebojnega delovanja niso izvedli. **Nosečnost in dojenje:** O uporabi benzidamina pri nosečnicah in doječih ženskah ni zadostnih podatkov. Uporaba zdravila med nosečnostjo in dojenjem ni priporočljiva. **Vpliv na sposobnost vožnje in upravljanja strojev:** Zdravilo v priporočenem odmerku nima vpliva na sposobnost vožnje in upravljanja strojev. **Neželeni učinki:** Neznana pogostnost (ni mogoče oceniti iz razpoložljivih podatkov): anafilaktične reakcije, preobčutljivostne reakcije, odrevenelost, laringospazem, suha usta, navzea in bruhanje, angioedem, fotosenzitivnost, pekoč občutek v ustih. Neposredno po uporabi se lahko pojavi občutek odrevenelosti v ustih in v žrelu. Ta učinek se pojavi zaradi načina delovanja zdravila in po kratkem času izgine. **Način in režim izdaje zdravila:** BRp-Izdaja zdravila je brez recepta v lekarnah in specializiranih prodajalnah.

Imetnik dovoljenja za promet: Aziende Chimiche Riunite Angelini Francesco – A.C.R.A.F. S.p.A., Viale Amelia 70, 00181 Rim, Italija **Datum zadnje revizije besedila:** 14. 10. 2019

Pred svetovanjem ali izdajo preberite celoten Povzetek glavnih značilnosti zdravila.

Samo za strokovno javnost.

Datum priprave informacije: november 2019

Odgovoren za trženje: Bonifar d.o.o.

ANGELINI

PR/BSI/BEN/2019/012

vsak dan

Verzenios®

abemaciklib

dvakrat na dan

EDINI

zaviralec CDK4 & 6, ki se jemlje NEPREKINJENO VSAK DAN, 2x NA DAN[1, 2, 3]

SKRAJŠAN POVZETEK GLAVNIH ZNAČILNOSTI ZDRAVILA

▼Za to zdravilo se izvaja dodatno spremljanje varnosti. Tako bodo hitreje na voljo nove informacije o njegovi varnosti. Zdravstvene delavce naprošamo, da poročajo o katerem koli domnevnem neželenem učinku zdravila. Glejte poglavje 4.8, kako poročati o neželenih učinkih.
IME ZDRAVILA: Verzenios 50 mg/100 mg/150 mg filmsko obložene tablete **KAKOVOSTNA IN KOLIČINSKA SESTAVA:** Ena filmsko obložena tableta vsebuje 50 mg/100 mg/150 mg abemaciklib. Ena filmsko obložena tableta vsebuje 14 mg/28 mg/42 mg laktoze (v obliki monohidrata). **Terapevtske indikacije:** Zdravilo Verzenios je indicirano za zdravljenje žensk z lokalno napredovalim ali metastatskim, na hormonske receptorje (HR – *Hormone Receptor*) pozitivnim in na receptorje humanega epidermalnega rastnega faktorja 2 (HER2 – *Human Epidermal Growth Factor Receptor 2*) negativnim rakom dojk v kombinaciji z zaviralcem aromataze ali s fulvestrantom kot začetnim endokrinim zdravljenjem ali pri ženskah, ki so prejele predhodno endokrino zdravljenje. Pri ženskah v pred- in perimenopavzi je treba endokrino zdravljenje kombinirati z agonistom gonadoliberina (LHRH – *Luteinizing Hormone–Releasing Hormone*). **Odmerjanje in način uporabe:** Zdravljenje z zdravilom Verzenios mora uvesti in nadzorovati zdravnik, ki ima izkušnje z uporabo zdravil za zdravljenje rakavih bolezni. *Zdravilo Verzenios v kombinaciji z endokrinim zdravljenjem:* Priporočeni odmerek abemaciklib je 150 mg dvakrat na dan, kadar se uporablja v kombinaciji z endokrinim zdravljenjem. Zdravilo Verzenios je treba jemati, dokler ima bolnica od zdravljenja klinično korist ali do pojava nesprejemljive toksičnosti. Če bolnica bruha ali izpusti odmerek zdravila Verzenios, ji je treba naročiti, da naj naslednji odmerek vzame ob predvidenem času; dodatnega odmerka ne sme vzeti. Obvladovanje nekaterih neželenih učinkov lahko zahteva prekinitev in/ali zmanjšanje odmerka. Zdravljenje z abemaciklibom prekinite v primeru povišanja vrednosti AST in/ali ALT >3 x ZMN SKUPAJ s celokupnim bilirubinom > 2,0 x ZMN v odsotnosti holestaze ter pri bolnicah z intersticijsko pljučno boleznijo (ILD)/pnevmonitis stopnje 3 ali 4. Sočasni uporabi močnih zaviralcev CYP3A4 se je treba izogibati. Če se uporabi močnih zaviralcev CYP3A4 ni mogoče izogniti, je treba odmerek abemaciklib znižati na 100 mg dvakrat na dan. Pri bolnicah, pri katerih je bil odmerek znižan na 100 mg abemaciklib dvakrat na dan in pri katerih se sočasnemu dajanju močnega zaviralca CYP3A4 ni mogoče izogniti, je treba odmerek abemaciklib dodatno znižati na 50 mg dvakrat na dan. Pri bolnicah, pri katerih je bil odmerek znižan na 50 mg abemaciklib dvakrat na dan in pri katerih se sočasnemu dajanju močnega zaviralca CYP3A4 ni mogoče izogniti, je mogoče z odmerkom abemaciklib nadaljevati ob natančnem spremljanju znakov toksičnosti. Alternativno je mogoče odmerek abemaciklib znižati na 50 mg enkrat na dan ali prekiniti dajanje abemaciklib. Če je uporaba zaviralca CYP3A4 prekinjena, je treba odmerek abemaciklib povečati na odmerek, kakršen je bil pred uvedbo zaviralca CYP3A4 (po 3–5 razpolovnih časih zaviralca CYP3A4). Prilagajanje odmerka glede na starost in pri bolnicah z blago ali zmerno ledvično okvaro ter z blago (Child Pugh A) ali zmerno (Child Pugh B) jetrno okvaro ni potrebno. Pri dajanju abemaciklib bolnicam s hudo ledvično okvaro sta potrebna previdnost in skrbno spremljanje glede znakov toksičnosti. Način uporabe: Zdravilo Verzenios je namenjeno za peroralno uporabo. Odmerek se lahko vzame s hrano ali brez nje. Zdravilo se ne sme jemati z grenivko ali grenivkinim sokom. Bolnice naj odmerke vzamejo vsak dan ob približno istem času. Tableto je treba zaužiti celo (bolnice je pred zaužitjem ne smejo gristi, drobiti ali deliti). **Kontraindikacije:** Preobčutljivost na učinkovino ali katero koli pomožno snov. **Posebna opozorila in previdnostni ukrepi:** Pri bolnicah, ki so prejemale abemaciklib, so poročali o nevtropeniji, o večji pogostnosti okužb kot pri bolnicah, zdravljenih s placebom in endokrinim zdravljenjem, o povečanih vrednostih ALT in AST. Pri bolnicah, pri katerih se pojavi nevtropenija stopnje 3 ali 4, je priporočljivo prilagoditi odmerek. Bolnice je treba spremljati za znake in simptome globoke venske tromboze in pljučne embolije ter jih zdraviti, kot je medicinsko utemeljeno. Glede na povečanje vrednosti ALT ali AST je mogoče potrebna prilagoditev odmerka. Driska je najpogostejši neželeni učinek. Bolnice je treba ob prvem znaku tekočega blata začeti zdraviti z antidiaroiki, kot je loperamid, povečati vnos peroralnih tekočin in obvestiti zdravnika. Sočasni uporabi induktorjev CYP3A4 se je treba izogibati zaradi tveganja za zmanjšano učinkovitost abemaciklib. Bolnice z redkimi dednimi motnjami, kot so intoleranca za galaktozo, popolno pomanjkanje laktaze ali malapsorpcija glukoze/galaktoze, tega zdravila ne smejo jemati. Bolnice spremljajte glede pljučnih simptomov, ki kažejo na ILD/pnevmonitis, in jih ustrezno zdravite. Glede na stopnjo ILD/pnevmonitisa je morda potrebno prilagajanje odmerka abemaciklib. **Medsebojno delovanje z drugimi zdravili in druge oblike interakcij:** Abemaciklib se primarno presnavlja s CYP3A4. Sočasna uporaba abemaciklib in zaviralcev CYP3A4 lahko poveča plazemsko koncentracijo abemaciklib. Uporabi močnih zaviralcev CYP3A4 sočasno z abemaciklibom se je treba izogibati. Če je močne zaviralce CYP3A4 treba dajati sočasno, je treba odmerek abemaciklib zmanjšati, nato pa bolnico skrbno spremljati glede toksičnosti. Pri bolnicah, zdravljenih z zmernimi ali šibkimi zaviralci CYP3A4, ni potrebno prilagajanje odmerka, vendar jih je treba skrbno spremljati za znake toksičnosti. Sočasni uporabi močnih induktorjev CYP3A4 (vključno, vendar ne omejeno na: karbamazepin, fenitoin, rifampicin in šentjanževko) se je treba izogibati zaradi tveganja za zmanjšano učinkovitost abemaciklib. Abemaciklib in njegovi glavni aktivni presnovki zavirajo prenašalce v ledvicah, in sicer kationski organski prenašalec 2 (OCT2) ter prenašalca MATE1. *In vivo* lahko pride do medsebojnega delovanja abemaciklib in klinično pomembnih substratov teh prenašalcev, kot je dofelitid ali kreatinin. Trenutno ni znano, ali lahko abemaciklib zmanjša učinkovitost sistemskih hormonskih kontraceptivov, zato se ženskam, ki uporabljajo sistemske hormonske kontraceptive, svetuje, da hkrati uporabljajo tudi mehansko metodo. **Neželeni učinki:** Najpogostejši neželeni učinki so driska, okužbe, nevtropenija, anemija, utrujenost, navzea, bruhanje in zmanjšanje apetita. *Zelo pogosti:* okužbe, nevtropenija, levkopenija, anemija, trombocitopenija, driska, bruhanje, navzea, zmanjšanje apetita, disgevzija, omotica, alopecija, pruritus, izpuščaj, utrujenost, pireksija, povečana vrednost alanin-aminotransferaze, povečana vrednost aspartat-aminotransferaze *Pogosti:* limfopenija, povečano solzenje, venska trombembolija, intersticijska pljučna bolezen (ILD)/pnevmonitis, suha koža, mišična šibkost *Občasni:* febrilna nevtropenija **Rok uporabnosti:** 3 leta **Posebna navodila za shranjevanje:** Za shranjevanje zdravila niso potrebna posebna navodila. **Imetnik dovoljenja za promet z zdravilom**: Eli Lilly Nederland B.V., Papendorpseweg 83, 3528BJ, Utrecht, Nizozemska. Datum prve odobritve dovoljenja za promet: 27. september 2018 **Datum zadnje revizije besedila**: 16.1.2020 **Režim izdaje:** Rp/Spec - Predpisovanje in izdaja zdravila je le na recept zdravnika specialista ustreznega področja medicine ali od njega pooblaščenega zdravnika.

Reference:
1. Povzetek glavnih značilnosti zdravila Verzenios. Datum zadnje revizije besedila: 16.1.2020. **2.** Povzetek glavnih značilnosti zdravila Ibrance. Dostop preverjen 10.4.2020.
3. Povzetek glavnih značilnosti zdravila Kisqali. Dostop preverjen 10.4.2020.

Pomembno: Predpisovanje in izdaja zdravila je le na recept zdravnika specialista ustreznega področja medicine ali od njega pooblaščenega zdravnika. Pred predpisovanjem zdravila Verzenios si preberite zadnji veljavni Povzetek glavnih značilnosti zdravil. Podrobne informacije o zdravilu so objavljene na spletni strani Evropske agencije za zdravila http://www.ema.europa.eu

Eli Lilly farmacevtska družba, d.o.o., Dunajska cesta 167, 1000 Ljubljana, telefon 01 / 580 00 10, faks 01 / 569 17 05
PP-AL-SI-0059, 20.04.2020, Samo za strokovno javnost.

Lilly

KEYTRUDA®
(pembrolizumab, MSD)

Pomaga spreminjati pričakovanja o preživetju

- pri metastatskem NSCLC *,1,2
- in napredovalem melanomu[3]

*NSCLC – non-small cell lung cancer

Reference: 1. Gandhi L, Rodríguez-Abreu D, Gadgeel S, et. al.; for the KEYNOTE-189 investigators. Pembrolizumab plus chemotherapy in metastatic non–small-cell lung cancer. N Engl J Med. 2018;378(22):2078–2092. **2.** Keytruda EU SmPC **3.** Hamid O, Robert C, Daud A, et. al. 5-year survival outcomes for patients with advanced melanoma treated with pembrolizumab in KEYNOTE-001. Annals of Oncology 2019; 30: 582-588.

SKRAJŠAN POVZETEK GLAVNIH ZNAČILNOSTI ZDRAVILA
Pred predpisovanjem, prosimo, preberite celoten Povzetek glavnih značilnosti zdravila!
Ime zdravila: KEYTRUDA 25 mg/ml koncentrat za raztopino za infundiranje vsebuje pembrolizumab. **Terapevtske indikacije:** Zdravilo KEYTRUDA je kot samostojno zdravljenje indicirano za zdravljenje: napredovalega (neoperabilnega ali metastatskega) melanoma pri odraslih; za adjuvantno zdravljenje odraslih z melanomom v stadiju III, ki se je razširil na bezgavke, po popolni kirurški odstranitvi; metastatskega nedrobnoceličnega pljučnega raka (NSCLC) v prvi liniji zdravljenja pri odraslih, ki imajo tumorje z ≥ 50 % izraženostjo PD-L1 (TPS) in brez pozitivnih tumorskih mutacij EGFR ali ALK; lokalno napredovalega ali metastatskega NSCLC pri odraslih, ki imajo tumorje z ≥ 1 % izraženostjo PD-L1 (TPS) in so bili predhodno zdravljeni z vsaj eno shemo kemoterapije, bolniki s pozitivnimi tumorskimi mutacijami EGFR ali ALK so pred prejemom zdravila KEYTRUDA morali prejeti tudi tarčno zdravljenje; odraslih bolnikov s ponovljenim ali neodzivnim klasičnim Hodgkinovim limfomom (cHL), pri katerih avtologna presaditev matičnih celic (ASCT) in zdravljenje z brentuksimabom vedotinom (BV) nista bila uspešna, in odraslih bolnikov, ki za presaditev niso primerni, zdravljenje z BV pa pri njih ni bilo uspešno; lokalno napredovalega ali metastatskega urotelijskega raka pri odraslih, predhodno zdravljenih s kemoterapijo, ki je vključevala platino; lokalno napredovalega ali metastatskega urotelijskega raka pri odraslih, ki niso primerni za zdravljenje s kemoterapijo, ki vsebuje cisplatin in imajo tumorje z izraženostjo PD-L1 ≥ 10, ocenjeno s kombinirano pozitivno oceno (CPS); ponovljenega ali metastatskega ploščatoceličnega raka glave in vratu (HNSCC) pri odraslih, ki imajo tumorje z ≥ 50 % izraženostjo PD-L1 (TPS), in pri katerih je bolezen napredovala med zdravljenjem ali po zdravljenju s kemoterapijo, ki je vključevala platino. Zdravilo KEYTRUDA je kot samostojno zdravljenje ali v kombinaciji s kemoterapijo s platino in 5-fluorouracilom (5-FU) indicirano za prvo linijo zdravljenja metastatskega ali neoperabilnega ponovljenega ploščatoceličnega raka glave in vratu pri odraslih, ki imajo tumorje z izraženostjo PD-L1 s CPS ≥ 1. Zdravilo KEYTRUDA je v kombinaciji s pemetreksedom in kemoterapijo na osnovi platine indicirano za prvo linijo zdravljenja metastatskega neploščatoceličnega NSCLC pri odraslih, pri katerih tumorji nimajo pozitivnih mutacij EGFR ali ALK; v kombinaciji s karboplatinom in bodisi paklitakselom bodisi nab-paklitakselom je indicirano za prvo linijo zdravljenja metastatskega ploščatoceličnega NSCLC pri odraslih; v kombinaciji z aksitinibom je indicirano za prvo linijo zdravljenja napredovalega raka ledvičnih celic (RCC) pri odraslih. **Odmerjanje in način uporabe:** Testiranje PD-L1 pri bolnikih z NSCLC, urotelijskim rakom ali HNSCC: Za samostojno zdravljenje z zdravilom KEYTRUDA je priporočljivo opraviti testiranje izraženosti PD-L1 tumorja z validirano preiskavo, da izberemo bolnike z NSCLC ali predhodno nezdravljenim urotelijskim rakom. Bolnike s HNSCC je treba za samostojno zdravljenje z zdravilom KEYTRUDA ali v kombinaciji s kemoterapijo s platino in 5-fluorouracilom (5-FU) izbrati na podlagi izraženosti PD-L1, potrjene z validirano preiskavo. Odmerjanje: Priporočeni odmerek zdravila KEYTRUDA za samostojno zdravljenje je bodisi 200 mg na 3 tedne ali 400 mg na 6 tednov, apliciran z intravensko infuzijo v 30 minutah. Priporočeni odmerek za kombinirano zdravljenje je 200 mg na 3 tedne, apliciran z intravensko infuzijo v 30 minutah. Za uporabo v kombinaciji glejte povzetke glavnih značilnosti sočasno uporabljenih zdravil. Če se uporablja kot del kombiniranega zdravljenja skupaj z intravensko kemoterapijo, je treba zdravilo KEYTRUDA aplicirati prvo. Bolnike je treba zdraviti do napredovanja bolezni ali nesprejemljivih toksičnih učinkov. Pri adjuvantnem zdravljenju melanoma je treba zdravilo uporabljati do ponovitve bolezni, pojava nesprejemljivih toksičnih učinkov oziroma mora zdravljenje trajati do enega leta. Če je aksitinib uporabljen v kombinaciji s pembrolizumabom, se lahko razmisli o povečanju odmerka aksitiniba nad začetnih 5 mg v presledkih šest tednov ali več. Pri bolnikih starih ≥ 65 let, bolnikih z blago do zmerno okvaro ledvic, bolnikih z blago okvaro jeter prilagoditev odmerka ni potrebna. Odložitev odmerka ali ukinitev zdravljenja: Zmanjšanje odmerka zdravila KEYTRUDA ni priporočljivo. Za obvladovanje neželenih učinkov je treba uporabo zdravila KEYTRUDA zadržati ali ukiniti, prosimo, glejte celoten Povzetek glavnih značilnosti zdravila. Kontraindikacije: Preobčutljivost na učinkovino ali katero koli pomožno snov. **Povzetek posebnih opozoril, previdnostnih ukrepov, interakcij in neželenih učinkov:** Imunsko pogojeni neželeni učinki (pnevmonitis, kolitis, hepatitis, nefritis, endokrinopatije, neželeni učinki na kožo in drugi): Pri bolnikih, ki so prejemali pembrolizumab, so se pojavili imunsko pogojeni neželeni učinki, vključno s hudimi in smrtnimi primeri. Večina imunsko pogojenih neželenih učinkov, ki so se pojavili med zdravljenjem s pembrolizumabom, je bila reverzibilnih in so jih obvladali s prekinitvami uporabe pembrolizumaba, uporabo kortikosteroidov in/ali podporno oskrbo. Pojavijo se lahko tudi po zadnjem odmerku pembrolizumaba in hkrati prizadanejo več organskih sistemov. V primeru suma na imunsko pogojene neželene učinke je treba poskrbeti za ustrezno oceno za potrditev etiologije oziroma izključitev drugih vzrokov. Glede na izrazitost neželenega učinka je treba zadržati uporabo pembrolizumaba in uporabiti kortikosteroide – za natančna navodila, prosimo, glejte Povzetek glavnih značilnosti zdravila Keytruda. Zdravljenje s pembrolizumabom lahko poveča tveganje za zavrnitev pri prejemnikih presadkov čvrstih organov. Pri bolnikih, ki so prejemali pembrolizumab, so poročali o hudih z infuzijo povezanih reakcijah, vključno s preobčutljivostjo in anafilaksijo. Pembrolizumab se iz obtoka odstrani s katabolizmom, zato presnovnih medsebojnih delovanj zdravil ni pričakovati. Uporabi sistemskih kortikosteroidov ali imunosupresivov pred uvedbo pembrolizumaba se je treba izogibati, ker lahko vplivajo na farmakodinamično aktivnost in učinkovitost pembrolizumaba. Vendar pa je kortikosteroide ali druge imunosupresive mogoče uporabiti za zdravljenje imunsko pogojenih neželenih učinkov. Kortikosteroide je mogoče uporabiti tudi kot premedikacijo, če je pembrolizumab uporabljen v kombinaciji s kemoterapijo, kot antiemetično profilakso in/ali za ublažitev neželenih učinkov, povezanih s kemoterapijo. Ženske v rodni dobi morajo med zdravljenjem s pembrolizumabom in vsaj še 4 mesece po zadnjem odmerku pembrolizumaba uporabljati učinkovito kontracepcijo, med nosečnostjo in dojenjem se ga ne sme uporabljati. Varnost pembrolizumaba pri samostojnem zdravljenju so v kliničnih študijah ocenili pri 5.884 bolnikih z napredovalim melanomom, kirurško odstranjenim melanomom v stadiju III (adjuvantno zdravljenje), NSCLC, cHL, urotelijskim rakom ali HNSCC s štirimi odmerki (2 mg/kg na 3 tedne, 200 mg na 3 tedne in 10 mg/kg na 2 ali 3 tedne). V tej populaciji bolnikov je mediani čas opazovanja znašal 7,3 mesece (v razponu od 1 dneva do 31 mesecev), najpogostejši neželeni učinki zdravljenja s pembrolizumabom so bili utrujenost (32 %), navzea (20 %) in diareja (20 %). Večina poročanih neželenih učinkov pri samostojnem zdravljenju je bila po izrazitosti 1. ali 2. stopnje. Najresnejši neželeni učinki so bili imunsko pogojeni neželeni učinki in hude z infuzijo povezane reakcije. Varnost pembrolizumaba pri kombiniranem zdravljenju s kemoterapijo so ocenili pri 1.067 bolnikih NSCLC ali HNSCC, ki so v kliničnih študijah prejemali pembrolizumab v odmerkih 200 mg, 2 mg/kg ali 10 mg/kg na vsake 3 tedne. V tej populaciji bolnikov so bili najpogostejši neželeni učinki naslednji: anemija (50 %), navzea (50 %), utrujenost (37 %), zaprtost (35%), diareja (30 %), nevtropenija (30 %), zmanjšanje apetita (28 %) in bruhanje (25 %). Pri kombiniranem zdravljenju s pembrolizumabom je pri bolnikih z NSCLC pojavnost neželenih učinkov 3. do 5. stopnje znašala 67 %, pri zdravljenju samo s kemoterapijo pa 66 %, pri kombiniranem zdravljenju s pembrolizumabom pri bolnikih s HNSCC 85 % in pri zdravljenju s kemoterapijo v kombinaciji s cetuksimabom 84 %. Varnost pembrolizumaba v kombinaciji z aksitinibom so ocenili v klinični študiji pri 429 bolnikih z napredovalim rakom ledvičnih celic, ki so prejemali 200 mg pembrolizumaba na 3 tedne in 5 mg aksitiniba dvakrat na dan. V tej populaciji bolnikov so bili najpogostejši neželeni učinki diareja (54 %), hipertenzija (45 %), utrujenost (38 %), hipotiroidizem (35 %), zmanjšan apetit (30 %), sindrom palmarno-plantarne eritrodisestezije (28 %), navzea (28 %), zvišanje vrednosti ALT (27 %), zvišanje vrednosti AST (26 %), disfonija (25 %), kašelj (21 %) in zaprtost (21 %). Pojavnost neželenih učinkov 3. do 5. stopnje je bila med kombiniranim zdravljenjem s pembrolizumabom 76 % in pri zdravljenju s sunitinibom samim 71 %. Za celoten seznam neželenih učinkov, prosimo, glejte celoten Povzetek glavnih značilnosti zdravila. **Način in režim izdaje zdravila:** H – Predpisovanje in izdaja zdravila je le na recept, zdravilo se uporablja samo v bolnišnicah. **Imetnik dovoljenja za promet z zdravilom:** Merck Sharp & Dohme B.V., Waarderweg 39, 2031 BN Haarlem, Nizozemska. **Datum zadnje revizije besedila:** 24. marec 2020.

MSD
Merck Sharp & Dohme inovativna zdravila d.o.o.,
Šmartinska cesta 140, 1000 Ljubljana
tel: +386 1/ 520 42 01, fax: +386 1/ 520 43 50

Pripravljeno v Sloveniji, april 2020; SI-KEY-00091 EXP: 04/2022
Samo za strokovno javnost.
H - Predpisovanje in izdaja zdravila je le na recept, zdravilo pa se uporablja samo v bolnišnicah. Pred predpisovanjem, prosimo, preberite celoten Povzetek glavnih značilnosti zdravila Keytruda, ki je na voljo pri naših strokovnih sodelavcih ali na lokalnem sedežu družbe.

Roche

Za bolnike s HER2 pozitivnim zgodnjim rakom dojk z ostankom invazivne bolezni po neoadjuvantnem zdravljenju s taksani in proti HER2 usmerjenim zdravljenjem[1]

PODALJŠAMO PREŽIVETJE* BOLNIKOM Z ZGODNJIM HER2 POZITIVNIM RAKOM DOJK.

Kadcyla®
trastuzumab emtanzin

SKRAJŠAN POVZETEK GLAVNIH ZNAČILNOSTI ZDRAVILA
Kadcyla 100 mg in 160 mg prašek za koncentrat za raztopino za infundiranje

Ime zdravila: Kadcyla 100 mg in 160 mg prašek za koncentrat za raztopino za infundiranje. **Kakovostna in količinska sestava:** Kadcyla 100 mg: Ena viala praška za koncentrat za raztopino za infundiranje vsebuje 100 mg trastuzumaba emtanzina. Po rekonstituciji vsebuje ena viala s 5 ml raztopine 20 mg/ml trastuzumaba emtanzina. Kadcyla 160 mg: Ena viala praška za koncentrat za raztopino za infundiranje vsebuje 160 mg trastuzumaba emtanzina. Po rekonstituciji vsebuje ena viala z 8 ml raztopine 20 mg/ml trastuzumaba emtanzina. Trastuzumab emtanzin je konjugirano zdravilo iz protitelesa trastuzumaba in zaviralca mikrotubulov DM1. **Terapevtske indikacije:** Zgodnji rak dojk: Zdravilo Kadcyla je kot monoterapija indicirano za adjuvantno zdravljenje odraslih bolnikov s HER2-pozitivnim zgodnjim rakom dojk, ki imajo rezidualno invazivno bolezen v dojki in/ali bezgavkah, po neoadjuvantnem zdravljenju na osnovi taksanov in proti HER2 usmerjene terapije. Razsejani rak dojk: Zdravilo Kadcyla je kot monoterapija indicirano za zdravljenje odraslih bolnikov s HER2-pozitivnim, neoperabilnim, lokalno napredovalim ali razsejanim rakom dojk, predhodno zdravljenih s trastuzumabom in taksanom, samostojno ali v kombinaciji. Bolniki so pred tem: prejemali predhodno zdravljenje za lokalno napredovalo ali razsejano bolezen ali se jim je bolezen ponovila med adjuvantnim zdravljenjem ali v šestih mesecih po koncu adjuvantnega zdravljenja. **Odmerjanje in način uporabe:** Zdravilo Kadcyla sme predpisati le zdravnik in se ga sme v obliki intravenske infuzije uporabiti le pod nadzorom zdravnika, ki ima izkušnje z zdravljenjem onkoloških bolnikov. Bolniki, zdravljeni s trastuzumabom emtanzinom, morajo imeti HER2-pozitivni tumor, imunohistokemično opredeljen kot 3+ ali razmerje pri *in situ hibridizaciji* (ISH) ali *fluorescentni in situ hibridizaciji* (FISH) ≥ 2,0, določeno z validiranim testom (z diagnostičnim medicinskim pripomočkom *in vitro* z oznako CE). Če takšnega pripomočka z oznako CE ni na voljo, je treba stanje HER2 oceniti z drugim validiranim testom. Za preprečitev napak pri dajanju zdravila je pomembno preveriti nalepke na vialah in tako zagotoviti, da je pripravljeno in uporabljeno zdravilo res zdravilo Kadcyla (trastuzumab emtanzin) in ne zdravilo Herceptin (trastuzumab). Odmerjanje: Priporočeni odmerek trastuzumaba emtanzina je 3,6 mg/kg telesne mase v intravenski infuziji na 3 tedne. Začetni odmerek je treba dati kot 90-minutno intravensko infuzijo. Bolnike je treba med infundiranjem in vsaj še 90 minut po prvem odmerku opazovati zaradi možnosti zvišanja telesne temperature, pojava mrzlice in drugih z infundiranjem povezanih reakcij. Mesto infundiranja je treba skrbno kontrolirati zaradi možne subkutane infiltracije med dajanjem zdravila. Če je bolnik predhodno infuzijo dobro prenesel, je mogoče poznejše odmerke trastuzumaba emtanzina dati kot 30-minutno infuzijo. Bolnike je treba opazovati med infundiranjem in vsaj še 30 minut po njem. Če se pojavijo z infundiranjem povezani simptomi, je treba hitrost infundiranja trastuzumaba emtanzina upočasniti ali infundiranje prekiniti. Pri življenje ogrožujočih infuzijskih reakcijah je treba trastuzumab emtanzin prenehati uporabljati. Trajanje zdravljenja: *Zgodnji rak dojk (EBC):* Bolniki naj prejmejo 14 ciklov zdravljenja v celoti, razen v primeru ponovitve bolezni ali neobvladljive toksičnosti. *Razsejani rak dojk (MBC):* Bolniki naj prejemajo zdravljenje do napredovanja bolezni ali neobvladljive toksičnosti. *Prilagoditev odmerka:* Obvladovanje simptomatskih neželenih učinkov lahko zahteva začasno prekinitev zdravljenja, zmanjšanje odmerka ali prenehanje zdravljenja trastuzumabom emtanzinom v skladu s smernicami (za podrobnejša navodila glede prilagoditve odmerka prosimo glejte SmPC zdravila). Odmerka trastuzumaba emtanzina se po zmanjšanju ne sme več povečati. *Zapoznel ali izpuščen odmerek:* Če je bolnik načrtovani odmerek izpustil, mu ga je treba dati čim prej brez čakanja do naslednjega načrtovanega cikla. Urnik uporabe je treba prilagoditi tako, da se ohrani 3-tedenski presledek med odmerki. Naslednji odmerek je treba uporabiti v skladu z zgornjimi priporočili za odmerjanje. *Periferna nevropatija:* Uporabo trastuzumaba emtanzina je treba prehodno prekiniti pri bolnikih s periferno nevropatijo 3. ali 4. stopnje, in sicer za toliko časa, da se zmanjša na ≤ 2. stopnjo. *Posebne populacije: Starejši bolniki:* Bolnikom, starim ≥ 65 let, odmerka ni treba prilagoditi. Za ugotovitev varnosti in učinkovitosti pri bolnikih, starih ≥ 75 let, ni dovolj podatkov. *Ledvična okvara:* Bolnikom z blago ali zmerno ledvično okvaro začetnega odmerka ni treba prilagoditi. Bolnike s hudo ledvično okvaro je zato treba natančno kontrolirati. *Jetrna okvara:* Bolnikom z blago ali zmerno jetrno okvaro začetnega odmerka ni treba prilagoditi. Pri bolnikih s hudo jetrno okvaro trastuzumaba emtanzina niso preučevali. Pri zdravljenju bolnikov z jetrno okvaro moramo biti previdni zaradi znane hepatotoksičnosti, opažene pri uporabi trastuzumaba emtanzina. *Pediatrična populacija:* Varnost in učinkovitost pri otrocih in mladostnikih do 18. leta starosti nista ugotovljeni. Za indikacijo rak dojk pri pediatrični populaciji ni relevantne uporabe. Način uporabe: Zdravilo Kadcyla je namenjeno intravenski uporabi. Trastuzumab emtanzin mora pripraviti in razredčiti zdravstveni delavec. Zdravilo je treba dati kot intravensko infuzijo. Ne sme se ga dajati kot hitro intravensko infuzijo ali bolus. **Kontraindikacije:** Preobčutljivost na zdravilno učinkovino ali katero koli pomožno snov. **Posebna opozorila in previdnostni ukrepi:** *Trombocitopenija:* Število trombocitov je priporočljivo kontrolirati pred vsakim odmerkom trastuzumaba emtanzina. Bolnike s trombocitopenijo in bolnike, ki prejemajo antikoagulante, je treba med zdravljenjem s trastuzumabom emtanzinom natančno kontrolirati. *Krvavitve:* V nekaterih od opaženih primerov so imeli bolniki trombocitopenijo ali pa so prejemali tudi antikoagulantno ali antitrombotično zdravljenje, pri drugih pa ni bilo znanih dodatnih dejavnikov tveganja. Pri uporabi teh zdravil je potrebna previdnost in razmisliti je treba o dodatnem nadzoru, kadar je sočasna uporaba klinično potrebna. *Hepatotoksičnost:* Delovanje jeter je treba kontrolirati pred uvedbo zdravljenja in pred vsakim odmerkom. Bolniki z izhodiščnim zvišanjem ALT imajo lahko večje tveganje za poškodbo jeter z večjim tveganjem za jetrne neželene dogodke stopnje 3 do 5 ali zvišanje jetrnih testov. Trastuzumab emtanzin ni bil raziskan pri bolnikih, ki imajo pred uvedbo zdravljenja serumske transaminaze > 2,5 × ZNM ali celokupni bilirubin > 1,5 × ZNM. Pri bolnikih, ki imajo serumske transaminaze > 3 × ZNM in obenem celokupni bilirubin > 2 × ZNM, je treba zdravljenje s trastuzumabom emtanzinom dokončno ukiniti. Pri zdravljenju bolnikov z jetrno okvaro moramo biti previdni. *Nevrotoksični učinki:* Bolnike je treba stalno klinično kontrolirati zaradi možnih znakov ali simptomov nevrotoksičnosti. *Disfunkcija levega prekata:* Bolniki, zdravljeni s trastuzumabom emtanzinom, imajo večje tveganje za pojav disfunkcije levega prekata. Pri bolnikih, zdravljenih s trastuzumabom emtanzinom, so opažali iztisni delež levega prekata (LVEF) < 40 %, zato je možno simptomatsko kongestivno srčno popuščanje. Pred uvedbo zdravljenja in tudi ob rednih intervalih med zdravljenjem je treba opraviti standardno preiskavo delovanja srca. V primerih disfunkcije levega prekata je treba odmerek preložiti ali zdravljenje prenehati, če je to potrebno. *Pljučna toksičnost:* Pri bolnikih z ugotovljeno intersticijsko boleznijo pljuč ali pnevmonitisom je priporočljivo zdravljenje s trastuzumabom emtanzinom dokončno ukiniti, razen v primeru pnevmonitisa zaradi obsevanja med adjuvantnim zdravljenjem, kjer je treba trastuzumab emtanzin dokončno ukiniti pri pnevmonitisu [3] 3. stopnje ali 2. stopnje brez odziva na standardno zdravljenje. Bolniki z dispnejo v mirovanju zaradi zapletov napredovale maligne bolezni, sočasnih bolezni in sočasnega obsevanja pljuč imajo lahko večje tveganje za pljučne neželene dogodke. *Z infundiranjem povezane reakcije:* Trastuzumab emtanzin ni raziskan pri bolnikih, pri katerih so predhodno zdravljenje s trastuzumabom trajno ukinili zaradi reakcij, povezanih z infundiranjem. Zdravljenje takšnih bolnikov s tem zdravilom ni priporočljivo. Pri bolnikih s hudimi reakcijami, povezanimi z infundiranjem, je treba zdravljenje prekiniti, dokler znaki in simptomi ne minejo. O ponovnem zdravljenju je treba presoditi glede na klinično oceno tega, kako huda je bila reakcija. Zdravljenje je treba dokončno ukiniti pri pojavu smrtno nevarnih reakcij, povezanih z infundiranjem. *Preobčutljivostne reakcije:* Trastuzumab emtanzin ni raziskan pri bolnikih, pri katerih so zdravljenje s trastuzumabom dokončno ukinili zaradi preobčutljivosti. Zdravljenje takšnih bolnikov s trastuzumabom emtanzinom ni priporočljivo. Bolnike je treba skrbno opazovati zaradi možnosti pojava preobčutljivostnih/alergijskih reakcij, ki imajo lahko enako klinično sliko kot reakcije, povezane z infundiranjem. V kliničnih študijah s trastuzumabom emtanzinom so zabeležili resne anafilaktične reakcije. Za takojšnjo uporabo morajo biti na voljo zdravila za zdravljenje takšnih reakcij in oprema za nujne primere. Pri dejanski preobčutljivostni reakciji je treba zdravljenje s trastuzumabom emtanzinom dokončno ukiniti. **Medsebojno delovanje z drugimi zdravili in druge oblike interakcij:** Formalnih študij medsebojnega delovanja niso izvedli. Študije presnove *in vitro* v človeških jetrnih mikrosomih kažejo, da se DM1 presnovi v glavnem s CYP3A4 in v manjši meri s CYP3A5. Izogniti se je treba sočasni uporabi močnih zaviralcev CYP3A4 in trastuzumaba emtanzina, ker obstaja možnost večje izpostavljenosti DM1 in toksičnih učinkov. Razmisliti je treba o uporabi drugega zdravila, ki nima potenciala za zavrtje CYP3A4 ali pa je ta majhen. Če je sočasna uporaba močnih zaviralcev CYP3A4 neizogibna, pride v poštev odložitev zdravljenja s trastuzumabom emtanzinom, dokler se močni zaviralec CYP3A4 ne odstrani iz obtoka, če je to mogoče. Če zdravljenja s trastuzumabom emtanzinom med sočasno uporabo močnega zaviralca CYP3A4 ni mogoče odložiti, je treba bolnike natančno kontrolirati zaradi možnih neželenih učinkov. **Neželeni učinki:** Neželeni učinki, ki so se pojavili pri bolnikih, zdravljenih z trastuzumabom emtanzinom: *Zelo pogosti:* okužba sečil, trombocitopenija, anemija, nespečnost, periferna nevropatija, glavobol, krvavitev, epistaksa, kašelj, dispneja, stomatitis, driska, bruhanje, navzea, zaprtost, suhost ust, bolečine v trebuhu, zvišanje transaminaz, mišično-skeletne bolečine, artralgija, mialgija, utrujenost, pireksija inastenija. *Pogosti:* nevtropenija, levkopenija, preobčutljivost na zdravilo, hipokaliemija, omotica, spremenjen okus, okvara spomina, suho oko, konjunktivitis, zamegljen vid, močnejše solzenje, disfunkcija levega prekata, hipertenzija, dispepsija, krvavitev iz dlesni, zvišanje alkalne fosfataze v krvi, zvišanje bilirubina v krvi, izpuščaj, srbenje, alopecija, bolezni nohtov, sindrom palmarno-plantarne eritrodizestezije, urtikarija, periferni edemi, mrzlica, in z infundiranjem povezane reakcije. Poročanje o domnevnih neželenih učinkih: Poročanje o domnevnih neželenih učinkih zdravila po izdaji dovoljenja za promet je pomembno. Omogoča namreč stalno spremljanje razmerja med koristmi in tveganji zdravila. Od zdravstvenih delavcev se zahteva, da poročajo o katerem koli domnevnem neželenem učinku zdravila na: Javna agencija Republike Slovenije za zdravila in medicinske pripomočke, Sektor za farmakovigilanco, Nacionalni center za farmakovigilanco, Slovenčeva ulica 22, SI-1000 Ljubljana, Tel: +386 (0)8 2000 500, Faks: +386 (0)8 2000 510, e-pošta: h-farmakovigilanca@jazmp.si, spletna stran: www.jazmp.si. Za zagotavljanje sledljivosti zdravila je pomembno, da pri izpolnjevanju obrazca o domnevnih neželenih učinkih zdravila navedete številko serije biološkega zdravila. **Režim izdaje zdravila:** H. **Imetnik dovoljenja za promet:** Roche Registration GmbH, Emil-Barell-Strasse 1, 79639 Grenzach-Wyhlen, Nemčija. **Verzija: 3.0/19**.

Vir: 1. Povzetek glavnih značilnosti zdravila Kadcyla, dostopano maja 2020 na: https://www.ema.europa.eu/en/documents/product-information/kadcyla-epar-product-information_sl.pdf.

* preživetje brez invazivne bolezni

SAMO ZA STROKOVNO JAVNOST • M-SI-00000008 • **Informacija pripravljena:** maj 2020
Dodatne informacije so na voljo pri: Roche farmacevtska družba d.o.o., Stegne 13G, 1000 Ljubljana.

Lonsurf®

trifluridin/tipiracil

Več časa za trenutke, ki štejejo

Kolorektalni rak

Zdravilo Lonsurf je indicirano v monoterapiji za zdravljenje odraslih bolnikov z metastatskim kolorektalnim rakom (KRR), ki so bili predhodno že zdravljeni ali niso primerni za zdravljenja, ki so na voljo. Ta vključujejo kemoterapijo na osnovi fluoropirimidina, oksaliplatina in irinotekana, zdravljenje z zaviralci žilnega endotelijskega rastnega dejavnika (VEGF – Vascular Endothelial Growth Factor) in zaviralci receptorjev za epidermalni rastni dejavnik (EGFR – Epidermal Growth Factor Receptor).

Rak želodca

Zdravilo Lonsurf je indicirano v monoterapiji za zdravljenje odraslih bolnikov z metastatskim rakom želodca vključno z adenokarcinomom gastro-ezofagealnega prehoda, ki so bili predhodno že zdravljeni z najmanj dvema sistemskima režimoma zdravljenja za napredovalo bolezen.

Družba Servier ima licenco družbe Taiho za zdravilo Lonsurf®. Pri globalnem razvoju zdravila sodelujeta obe družbi in ga tržita na svojih določenih področjih.

SERVIER

Skrajšan povzetek glavnih značilnosti zdravila: Lonsurf 15 mg/6,14 mg filmsko obložene tablete in Lonsurf 20 mg/8,19 mg filmsko obložene tablete

▼ Za to zdravilo se izvaja dodatno spremljanje varnosti. Tako bodo hitreje na voljo nove informacije o njegovi varnosti. Zdravstvene delavce naprošamo, da poročajo o katerem koli domnevnem neželenem učinku zdravila. **SESTAVA*: Lonsurf 15 mg/6,14 mg:** Ena filmsko obložena tableta vsebuje 15 mg trifluridina in 6,14 mg tipiracila (v obliki klorida). **Lonsurf 20 mg/8,19 mg**: Ena filmsko obložena tableta vsebuje 20 mg trifluridina in 8,19 mg tipiracila (v obliki klorida). **TERAPEVTSKE INDIKACIJE*:** Kolorektalni rak – zdravilo Lonsurf je indicirano v monoterapiji za zdravljenje odraslih bolnikov z metastatskim kolorektalnim rakom, ki so bili predhodno že zdravljeni ali niso primerni za zdravljenja, ki so na voljo. Ta vključujejo kemoterapijo na osnovi fluoropirimidina, oksaliplatina in irinotekana, zdravljenje z zaviralci žilnega endotelijskega rastnega dejavnika (VEGF – Vascular Endothelial Growth Factor) in zaviralci receptorjev za epidermalni rastni dejavnik (EGFR – Epidermal Growth Factor Receptor). Rak želodca – zdravilo Lonsurf je indicirano v monoterapiji za zdravljenje odraslih bolnikov z metastatskim rakom želodca vključno z adenokarcinomom gastro-ezofagealnega prehoda, ki so bili predhodno že zdravljeni z najmanj dvema sistemskima režimoma zdravljenja za napredovalo bolezen. **ODMERJANJE IN NAČIN UPORABE*:** Priporočeni začetni odmerek zdravila Lonsurf pri odraslih je 35 mg/m^2/odmerek peroralno dvakrat dnevno na 1. do 5. dan in 8. do 12. dan vsakega 28-dnevnega cikla zdravljenja, najpozneje 1 uro po zaključku jutranjega in večernega obroka (20 mg/m^2/odmerek dvakrat dnevno pri bolnikih s hudo ledvično okvaro). Odmerjanje, izračunano glede na telesno površino, ne sme preseči 80 mg/odmerek. Možne prilagoditve odmerka glede na varnost in prenašanje zdravila: dovoljena so zmanjšanja odmerka na najmanjši odmerek 20 mg/m^2 dvakrat dnevno (oz. 15 mg/m^2 dvakrat dnevno pri bolnikih s hudo ledvično okvaro). Potem ko je bil odmerek zmanjšan, povečanje ni dovoljeno. **KONTRAINDIKACIJE*:** Preobčutljivost na zdravilni učinkovini ali katero koli pomožno snov. **OPOZORILA IN PREVIDNOSTNI UKREPI*:** Supresija kostnega mozga: Pred uvedbo zdravljenja in po potrebi za spremljanje toksičnosti zdravila, najmanj pred vsakim ciklom zdravljenja, je treba pregledati celotno krvno sliko. Zdravljenja ne smete začeti, če je absolutno število nevtrofilcev < 1,5 x 10^9/l, če je število trombocitov < 75 x 10^9/l ali če se je pri bolniku zaradi predhodnih zdravljenj pojavila klinično pomembna nehematološka toksičnost 3. ali 4. stopnje, ki še traja. Bolnike je treba skrbno spremljati zaradi morebitnih okužb, uvesti je treba ustrezne ukrepe, kot je klinično indicirano. Toksičnost za prebavila: Potrebna je uporaba antiemetikov, antidiaroikov ter drugih ukrepov, kot je klinično indicirano. Če je potrebno, prilagodite odmerke. Ledvična okvara: Zdravilo Lonsurf ni primerno za uporabo pri bolnikih s končno stopnjo ledvične okvare. Bolnike z ledvično okvaro je potrebno med zdravljenjem skrbno spremljati; bolnike z zmerno ali hudo ledvično okvaro je treba zaradi hematološke toksičnosti bolj pogosto spremljati. Jetrna okvara: Uporaba zdravila Lonsurf pri bolnikih z obstoječo zmerno ali hudo jetrno okvaro ni priporočljiva. Proteinurija: Pred začetkom zdravljenja in med njim je priporočljivo spremljanje proteinurije z urinskimi testnimi lističi. Pomožne snovi: Zdravilo vsebuje laktozo. **INTERAKCIJE*:** Zdravila, ki medsebojno delujejo z nukleozidnimi prenašalci CNT1, ENT1 in ENT2, zaviralci OCT2 ali MATE1, substrati humane timidin-kinaze (npr. zidovudinom), hormonskimi kontraceptivi. **PLODNOST*, NOSEČNOST IN DOJENJE*:** Ni priporočljivo. **KONTRACEPCIJA*:** Ženske in moški morajo uporabljati učinkovito metodo kontracepcije med zdravljenjem in do 6 mesecev po zaključku zdravljenja. **VPLIV NA SPOSOBNOST VOŽNJE IN UPRAVLJANJA STROJEV*:** Med zdravljenjem se lahko pojavijo utrujenost, omotica ali splošno slabo počutje. **NEŽELENI UČINKI*:** *Zelo pogosti:* nevtropenija, levkopenija, anemija, trombocitopenija, zmanjšan apetit, diareja, navzea, bruhanje, utrujenost. *Pogosti:* okužba spodnjih dihal, febrilna nevtropenija, limfopenija, hipoalbuminemija, disgevzija, periferna nevropatija, dispneja, bolečina v trebuhu, zaprtje, stomatitis, bolezni ustne votline, hiperbilirubinemija, sindrom palmarne plantarne eritrodisestezije, izpuščaj, alopecija, pruritus, suha koža, proteinurija, pireksija, edem, vnetje sluznice, splošno slabo počutje, zvišanje jetrnih encimov, zvišanje alkalne fosfataze v krvi, zmanjšanje telesne mase. *Občasni:* septični šok, infekcijski enteritis, pljučnica, okužba žolčevoda, gripa, okužba sečil, gingivitis, herpes zoster, tinea pedis, okužba s kandido, bakterijska okužba, okužba, nevtropenična sepsa, okužba zgornjih dihal, konjunktivitis, bolečina zaradi raka, pancitopenija, granulocitopenija, monocitopenija, eritropenija, levkocitoza, monocitoza, dehidracija, hiperglikemija, hiperkaliemija, hipokaliemija, hipofosfatemija, hipernatriemija, hiponatriemija, hipokalciemija, protin, anksioznost, nespečnost, nevrotoksičnost, disestezija, hiperestezija, hipoestezija, sinkopa, parestezija, pekoč občutek, letargija, omotica, glavobol, zmanjšana ostrina vida, zamegljen vid, diplopija, katarakta, suho oko, vrtoglavica, neugodje v ušesu, angina pektoris, aritmija, palpitacije, embolija, hipertenzija, hipotenzija, vročinski oblivi, pljučna embolija, plevralni izliv, izcedek iz nosu, disfonija, orofaringealna bolečina, epistaksa, kašelj, hemoragični enterokolitis, krvavitev v prebavilih, akutni pankreatitis, ascites, ileus, subileus, kolitis, gastritis, refluksni gastritis, ezofagitis, moteno praznjenje želodca, abdominalna distenzija, analno vnetje, razjede v ustih, dispepsija, gastroezofagealna refluksna bolezen, proktalgija, bukalni polip, krvavitev dlesni, glositis, parodontalna bolezen, bolezen zob, siljenje na bruhanje, flatulenca, slab zadah, hepatotoksičnost, razširitev žolčnih vodov, luščenje kože, urtikarija, preobčutljivostne reakcije na svetlobo, eritem, akne, hiperhidroza, žulj, bolezni nohtov, otekanje sklepov, artralgija, bolečina v kosteh, mialgija, mišično-skeletna bolečina, mišična oslabelost, mišični krči, bolečina v okončinah, ledvična odpoved, neinfektivni cistitis, motnje mikcije, hematurija, levkociturija, motnje menstruacije, poslabšanje splošnega zdravstvenega stanja, bolečina, občutek spremembe telesne temperature, kseroza, nelagodje, zvišanje kreatinina v krvi, podaljšanje intervala QT na elektrokardiogramu, povečanje mednarodnega umerjenega razmerja (INR), podaljšanje aktiviranega parcialnega tromboplastinskega časa (aPTČ), zvišanje sečnine v krvi, zvišanje laktatne dehidrogenaze v krvi, znižanje celokupnih proteinov, zvišanje C-reaktivnega proteina, zmanjšan hematokrit. *Post-marketinške izkušnje:* intersticijska bolezen pljuč. **PREVELIKO ODMERJANJE*:** Neželeni učinki, o katerih so poročali v povezavi s prevelikim odmerjanjem, so bili v skladu z uveljavljenim varnostnim profilom. Glavni pričakovani zaplet prevelikega odmerjanja je supresija kostnega mozga. **FARMAKODINAMIČNE LASTNOSTI*:** *Farmakoterapevtska skupina:* zdravila z delovanjem na novotvorbe, antimetaboliti, oznaka ATC: L01BC59. Zdravilo Lonsurf sestavljata antineoplastični timidinski nukleozidni analog, trifluridin, in zaviralec timidin-fosforilaze (TPaze), tipiracilijev klorid. Po privzemu v rakave celice timidin-kinaza fosforilira trifluridin. Ta se v celicah nato presnovi v substrat deoksiribonukleinske kisline (DNA), ki se vgradi neposredno v DNA ter tako preprečuje celično proliferacijo. TPaza hitro razgradi trifluridin in njegova presnova po peroralni uporabi je hitra zaradi učinka prvega prehoda, zato je v zdravilo vključen zaviralec TPaze, tipiracilijev klorid. **PAKIRANJE*:** 20 filmsko obloženih tablet. **NAČIN PREDPISOVANJA IN IZDAJE ZDRAVILA:** Rp/Spec. **Imetnik dovoljenja za promet:** Les Laboratoires Servier, 50, rue Carnot, 92284 Suresnes cedex, Francija. **Številka dovoljenja za promet z zdravilom:** EU/1/16/1096/001 (Lonsurf 15 mg/6,14 mg), EU/1/16/1096/004 (Lonsurf 20 mg/8,19 mg). **Datum zadnje revizije besedila: april 2020.*Pred predpisovanjem preberite celoten povzetek glavnih značilnosti zdravila. Celoten povzetek glavnih značilnosti zdravila in podrobnejše informacije so na voljo pri: Servier Pharma d.o.o., Podmilščakova ulica 24, 1000 Ljubljana, tel: 01 563 48 11, www.servier.si.**

Datum priprave informacije: april 2020.
LNF AD1 C2 19/20 Samo za strokovno javnost.

Instructions for authors

The editorial policy

Radiology and Oncology is a multidisciplinary journal devoted to the publishing original and high quality scientific papers and review articles, pertinent to diagnostic and interventional radiology, computerized tomography, magnetic resonance, ultrasound, nuclear medicine, radiotherapy, clinical and experimental oncology, radiobiology, medical physics and radiation protection. Therefore, the scope of the journal is to cover beside radiology the diagnostic and therapeutic aspects in oncology, which distinguishes it from other journals in the field.

The Editorial Board requires that the paper has not been published or submitted for publication elsewhere; the authors are responsible for all statements in their papers. Accepted articles become the property of the journal and, therefore cannot be published elsewhere without the written permission of the editors.

Submission of the manuscript

The manuscript written in English should be submitted to the journal via online submission system Editorial Manager available for this journal at: **www.radioloncol.com**.

In case of problems, please contact Sašo Trupej at **saso.trupej@computing.si** or the Editor of this journal at **gsersa@onko-i.si**

All articles are subjected to the editorial review and when the articles are appropriated they are reviewed by independent referees. In the cover letter, which must accompany the article, the authors are requested to suggest 3-4 researchers, competent to review their manuscript. However, please note that this will be treated only as a suggestion; the final selection of reviewers is exclusively the Editor's decision. The authors' names are revealed to the referees, but not vice versa.

Manuscripts which do not comply with the technical requirements stated herein will be returned to the authors for the correction before peer-review. The editorial board reserves the right to ask authors to make appropriate changes of the contents as well as grammatical and stylistic corrections when necessary. Page charges will be charged for manuscripts exceeding the recommended length, as well as additional editorial work and requests for printed reprints.

Articles are published printed and on-line as the open access (**https://content.sciendo.com/raon**).

All articles are subject to 900 EUR + VAT publication fee. Exceptionally, waiver of payment may be negotiated with editorial office, upon lack of funds.

Manuscripts submitted under multiple authorship are reviewed on the assumption that all listed authors concur in the submission and are responsible for its content; they must have agreed to its publication and have given the corresponding author the authority to act on their behalf in all matters pertaining to publication. The corresponding author is responsible for informing the coauthors of the manuscript status throughout the submission, review, and production process.

Preparation of manuscripts

Radiology and Oncology will consider manuscripts prepared according to the Uniform Requirements for Manuscripts Submitted to Biomedical Journals by International Committee of Medical Journal Editors (www.icmje.org). The manuscript should be written in grammatically and stylistically correct language. Abbreviations should be avoided. If their use is necessary, they should be explained at the first time mentioned. The technical data should conform to the SI system. The manuscript, excluding the references, tables, figures and figure legends, must not exceed 5000 words, and the number of figures and tables is limited to 8. Organize the text so that it includes: Introduction, Materials and methods, Results and Discussion. Exceptionally, the results and discussion can be combined in a single section. Start each section on a new page, and number each page consecutively with Arabic numerals.

The Title page should include a concise and informative title, followed by the full name(s) of the author(s); the institutional affiliation of each author; the name and address of the corresponding author (including telephone, fax and E-mail), and an abbreviated title (not exceeding 60 characters). This should be followed by the abstract page, summarizing in less than 250 words the reasons for the study, experimental approach, the major findings (with specific data if possible), and the principal conclusions, and providing 3-6 key words for indexing purposes. Structured abstracts are required. Slovene authors are requested to provide title and the abstract in Slovene language in a separate file. The text of the research article should then proceed as follows:

Introduction should summarize the rationale for the study or observation, citing only the essential references and stating the aim of the study.

Materials and methods should provide enough information to enable experiments to be repeated. New methods should be described in details.

Results should be presented clearly and concisely without repeating the data in the figures and tables. Emphasis should be on clear and precise presentation of results and their significance in relation to the aim of the investigation.

Discussion should explain the results rather than simply repeating them and interpret their significance and draw conclusions. It should discuss the results of the study in the light of previously published work.

Charts, Illustrations, Images and Tables

Charts, Illustrations, Images and Tables must be numbered and referred to in the text, with the appropriate location indicated. Charts, Illustrations and Images, provided electronically, should be of appropriate quality for good reproduction. Illustrations and charts must be vector image, created in CMYK color space, preferred font "Century Gothic", and saved as .AI, .EPS or .PDF format. Color charts, illustrations and Images are encouraged, and are published without additional charge. Image size must be 2.000 pixels on the longer side and saved as .JPG (maximum quality) format. In Images, mask the identities of the patients. Tables should be typed double-spaced, with a descriptive title and, if appropriate, units of numerical measurements included in the column heading. The files with the figures and tables can be uploaded as separate files.

References

References must be numbered in the order in which they appear in the text and their corresponding numbers quoted in the text. Authors are responsible for the accuracy of their references. References to the Abstracts and Letters to the Editor must be identified as such. Citation of papers in preparation or submitted for publication, unpublished observations, and personal communications should not be included in the reference list. If essential, such material may be incorporated in the appropriate place in the text. References follow the style of Index Medicus, DOI number (if exists) should be included.

All authors should be listed when their number does not exceed six; when there are seven or more authors, the first six listed are followed by "et al.". The following are some examples of references from articles, books and book chapters:

Dent RAG, Cole P. In vitro maturation of monocytes in squamous carcinoma of the lung. *Br J Cancer* 1981; **43:** 486-95. doi: 10.1038/bjc.1981.71

Chapman S, Nakielny R. *A guide to radiological procedures*. London: Bailliere Tindall; 1986.

Evans R, Alexander P. Mechanisms of extracellular killing of nucleated mammalian cells by macrophages. In: Nelson DS, editor. *Immunobiology of macrophage.* New York: Academic Press; 1976. p. 45-74.

Authorization for the use of human subjects or experimental animals

When reporting experiments on human subjects, authors should state whether the procedures followed the Helsinki Declaration. Patients have the right to privacy; therefore the identifying information (patient's names, hospital unit numbers) should not be published unless it is essential. In such cases the patient's informed consent for publication is needed, and should appear as an appropriate statement in the article. Institutional approval and Clinical Trial registration number is required. Retrospective clinical studies must be approved by the accredited Institutional Review Board/Committee for Medical Ethics or other equivalent body. These statements should appear in the Materials and methods section.

The research using animal subjects should be conducted according to the EU Directive 2010/63/EU and following the Guidelines for the welfare and use of animals in cancer research (Br J Cancer 2010; 102: 1555 – 77). Authors must state the committee approving the experiments, and must confirm that all experiments were performed in accordance with relevant regulations.

These statements should appear in the Materials and methods section (or for contributions without this section, within the main text or in the captions of relevant figures or tables).

Transfer of copyright agreement

For the publication of accepted articles, authors are required to send the License to Publish to the publisher on the address of the editorial office. A properly completed License to Publish, signed by the Corresponding Author on behalf of all the authors, must be provided for each submitted manuscript.

The non-commercial use of each article will be governed by the Creative Commons Attribution-NonCommercial-NoDerivs license.

Conflict of interest

When the manuscript is submitted for publication, the authors are expected to disclose any relationship that might pose real, apparent or potential conflict of interest with respect to the results reported in that manuscript. Potential conflicts of interest include not only financial relationships but also other, non-financial relationships. In the Acknowledgement section the source of funding support should be mentioned. The Editors will make effort to ensure that conflicts of interest will not compromise the evaluation process of the submitted manuscripts; potential editors and reviewers will exempt themselves from review process when such conflict of interest exists. The statement of disclosure must be in the Cover letter accompanying the manuscript or submitted on the form available on **www.icmje.org/coi_disclosure.pdf**

Page proofs

Page proofs will be sent by E-mail to the corresponding author. It is their responsibility to check the proofs carefully and return a list of essential corrections to the editorial office within three days of receipt. Only grammatical corrections are acceptable at that time.

Open access

Papers are published electronically as open access on **https://content.sciendo.com/raon**, also papers accepted for publication as E-ahead of print.

XALKORI® – 1. linija zdravljenja napredovalega, ALK pozitivnega nedrobnoceličnega pljučnega raka[1]

ALK = anaplastična limfomska kinaza

BISTVENI PODATKI IZ POVZETKA GLAVNIH ZNAČILNOSTI ZDRAVILA

XALKORI 200 mg, 250 mg trde kapsule

Sestava in oblika zdravila: Ena kapsula vsebuje 200 mg ali 250 mg krizotiniba. **Indikacije:** Monoterapija za: - prvo linijo zdravljenja odraslih bolnikov z napredovalim nedrobnoceličnim pljučnim rakom (NSCLC – *Non-Small Cell Lung Cancer*), ki je ALK (anaplastična limfomska kinaza) pozitiven; - zdravljenje odraslih bolnikov s predhodno zdravljenim, napredovalim NSCLC, ki je ALK pozitiven; - zdravljenje odraslih bolnikov z napredovalim NSCLC, ki je ROS1 pozitiven. **Odmerjanje in način uporabe:** Zdravljenje mora uvesti in nadzorovati zdravnik z izkušnjami z uporabo zdravil za zdravljenje rakavih bolezni. Preverjanje prisotnosti ALK in ROS1: Pri izbiri bolnikov za zdravljenje je treba pred zdravljenjem opraviti točno in validirano preverjanje prisotnosti ALK ali ROS1. Odmerjanje: Priporočeni odmerek je 250 mg dvakrat na dan (500 mg na dan), bolniki pa morajo zdravilo jemati brez prekinitev. Če bolnik pozabi vzeti odmerek, ga mora vzeti takoj, ko se spomni, razen če do naslednjega odmerka manjka manj kot 6 ur. V tem primeru bolnik pozabljenega odmerka ne sme vzeti. *Prilagajanja odmerkov:* Glede na varnost uporabe zdravila pri posameznem bolniku in kako bolnik zdravljenje prenaša, utegne biti potrebna prekinitev in/ali zmanjšanje odmerka pri bolnikih, ki se zdravijo s krizotinibom 250 mg peroralno dvakrat na dan (za režim zmanjševanja odmerka glejte poglavje 4.2 v povzetku glavnih značilnosti zdravila). Za prilagajanje odmerkov pri *hematološki in nehematološki toksičnosti* (povečanje vrednosti AST, ALT, bilirubina; ILD/pnevmonitis; podaljšanje intervala QTc, bradikardija, bolezni oči) glejte preglednici 1 in 2 v poglavju 4.2 povzetka glavnih značilnosti zdravila. *Okvara jeter:* Pri zdravljenju pri bolnikih z okvaro jeter je potrebna previdnost. Pri blagi okvari jeter prilagajanje začetnega odmerka ni priporočeno, pri zmerni okvari jeter je priporočeni začetni odmerek 200 mg dvakrat na dan, pri hudi okvari jeter pa 250 mg enkrat na dan (za merila glede klasifikacije okvare jeter glejte poglavje 4.2 v povzetku glavnih značilnosti zdravila). *Okvara ledvic:* Pri blagi in zmerni okvari prilagajanje začetnega odmerka ni priporočeno. Pri hudi okvari ledvic (ki ne zahteva peritonealne dialize ali hemodialize) je začetni odmerek 250 mg peroralno enkrat na dan; po vsaj 4 tednih zdravljenja se lahko poveča na 200 mg dvakrat na dan. *Starejši bolniki (≥ 65 let):* Prilagajanje začetnega odmerka ni potrebno. *Pediatrična populacija:* Varnost in učinkovitost nista bili dokazani. Način uporabe: Kapsule je treba pogoltniti cele, z nekaj vode, s hrano ali brez nje. Ne sme se jih zdrobiti, raztopiti ali odpreti. Izogibati se je treba uživanju grenivk, grenivkinega soka ter uporabi šentjanževke. **Kontraindikacije:** Preobčutljivost na krizotinib ali katerokoli pomožno snov. **Posebna opozorila in previdnostni ukrepi:** Določanje statusa ALK in ROS1: Pomembno je izbrati dobro validirano in robustno metodologijo, da se izognemo lažno negativnim ali lažno pozitivnim rezultatom. Hepatotoksičnost: V kliničnih študijah so poročali o hepatotoksičnosti, ki jo je povzročilo zdravilo (vključno s primeri s smrtnim izidom). Delovanje jeter, vključno z ALT, AST in skupnim bilirubinom, je treba preveriti enkrat na teden v prvih 2 mesecih zdravljenja, nato pa enkrat na mesec in kot je klinično indicirano. Ponovitve preverjanj morajo biti pogostejše pri povečanjih vrednosti stopnje 2, 3 ali 4. Intersticijska bolezen pljuč (ILD)/pnevmonitis: Lahko se pojavi huda, življenjsko nevarna ali smrtna ILD/pnevmonitis. Bolnike s simptomi ILD/pnevmonitisa je treba spremljati, zdravljenje pa prekiniti ob sumu na ILD/pnevmonitis. Podaljšanje intervala QT: Opažali so podaljšanje intervala QTc. Pri bolnikih z obstoječo bradikardijo, podaljšanjem intervala QTc v anamnezi ali predispozicijo zanj, pri bolnikih, ki jemljejo antiaritmike ali druga zdravila, ki podaljšujejo interval QT, ter pri bolnikih s pomembno obstoječo srčno boleznijo in/ali motnjami elektrolitov je treba krizotinib uporabljati previdno; potrebno je redno spremljanje EKG, elektrolitov in delovanja ledvic; preiskavi EKG in elektrolitov je treba opraviti čimbližje uporabi prvega odmerka, potem se priporoča redno spremljanje. Če se interval QTc podaljša za 60 ms ali več, je treba zdravljenje s krizotinibom začasno prekiniti in se posvetovati s kardiologom. Bradikardija: Lahko se pojavi simptomatska bradikardija (lahko se razvije več tednov po začetku zdravljenja); izogibati se je treba uporabi krizotiniba v kombinaciji z drugimi zdravili, ki povzročajo bradikardijo; pri simptomatski bradikardiji je treba prilagoditi odmerek. Srčno popuščanje: Poročali so o hudih, življenjsko nevarnih ali smrtnih neželenih učinkih srčnega popuščanja. Bolnike je treba spremljati glede pojavov znakov in simptomov srčnega popuščanja in ob pojavu simptomov zmanjšati odmerjanje ali prekiniti zdravljenje. Nevtropenija in levkopenija: V kliničnih študijah so poročali o nevtropeniji, levkopeniji in febrilni nevtropeniji; spremljati je treba popolno krvno sliko (pogostejše preiskave, če se opazijo abnormalnosti stopnje 3 ali 4 ali če se pojavi povišana telesna temperatura ali okužba). Perforacija v prebavilih: V kliničnih študijah so poročali o perforacijah v prebavilih, v obdobju trženja pa o smrtnih primerih perforacij v prebavilih. Krizotinib je treba pri bolnikih s tveganjem za nastanek perforacije v prebavilih uporabljati previdno; bolniki, pri katerih se razvije perforacija v prebavilih, se morajo prenehati zdraviti s krizotinibom; bolnike je treba poučiti o prvih znakih perforacije in jim svetovati, naj se nemudoma posvetujejo z zdravnikom. Vplivi na ledvice: V kliničnih študijah so opazili zvišanje ravni kreatinina v krvi in zmanjšanje očistka kreatinina. V kliničnih študijah in v obdobju trženja so poročali tudi o odpovedi ledvic, akutni odpovedi ledvic, primerih s smrtnim izidom, primerih, ki so zahtevali hemodializo in hiperkaliemiji stopnje 4. Vplivi na vid: V kliničnih študijah so poročali o izpadu vidnega polja stopnje 4 z izgubo vida. Če se na novo pojavi huda izguba vida, je treba zdravljenje prekiniti in opraviti oftalmološki pregled. Če so motnje vida trdovratne ali se poslabšajo, je priporočljiv oftalmološki pregled. Histološka preiskava, ki ne nakazuje adenokarcinoma: Na voljo so le omejeni podatki pri NSCLC, ki je ALK in ROS1 pozitiven in ima histološke značilnosti, ki ne nakazujejo adenokarcinoma, vključno s ploščatoceličnim karcinomom (SCC). **Medsebojno delovanje z drugimi zdravili in druge oblike interakcij:** Izogibati se je treba sočasni uporabi z močnimi zaviralci CYP3A4, npr. atazanavir, ritonavir, kobicistat, itrakonazol, ketokonazol, posakonazol, vorikonazol, klaritromicin, telitromicin in eritromicin (razen če morebitna korist za bolnika odtehta tveganje, v tem primeru je treba bolnike skrbno spremljati glede neželenih učinkov krizotiniba), ter grenivko in grenivkinim sokom, saj lahko povečajo koncentracije krizotiniba v plazmi. Izogibati se je treba sočasni uporabi z močnimi induktorji CYP3A4, npr. karbamazepin, fenobarbital, fenitoin, rifampicin in šentjanževka, saj lahko zmanjšajo koncentracije krizotiniba v plazmi. Učinek zmernih induktorjev CYP3A4, npr. efavirenz in rifabutin, še ni jasen, zato se je treba sočasni uporabi s krizotinibom izogibati. Zdravila, katerih koncentracije v plazmi lahko krizotinib spremeni (midazolam, alfentanil, cisaprid, ciklosporin, derivati ergot alkaloidov, fentanil, pimozid, kinidin, sirolimus, takrolimus, digoksin, dabigatran, kolhicin, pravastatin: sočasni uporabi s temi zdravili se je treba izogibati oziroma izvajati skrben klinični nadzor; bupropion, efavirenz, peroralni kontraceptivi, raltegravir, irinotekan, morfin, nalokson, metformin, prokainamid). Zdravila, ki podaljšujejo interval QT ali ki lahko povzročijo Torsades de pointes (antiaritmiki skupine IA (kinidin, disopiramid), antiaritmiki skupine III (amiodaron, sotalol, dofetilid, ibutilid), metadon, cisaprid, moksifloksacin, antipsihotiki) – v primeru sočasne uporabe je potreben skrben nadzor intervala QT. Zdravila, ki povzročajo bradikardijo (nedihidropiridinski zaviralci kalcijevih kanalčkov (verapamil, diltiazem), antagonisti adrenergičnih receptorjev beta, klonidin, gvanfacin, digoksin, meflokin, antiholinesteraze, pilokarpin) – krizotinib je treba uporabljati previdno. **Plodnost, nosečnost in dojenje:** Ženske v rodni dobi se morajo izogibati zanositvi. Med zdravljenjem in najmanj 90 dni po njem je treba uporabljati ustrezno kontracepcijo (velja tudi za moške). Zdravilo lahko škoduje plodu in se ga med nosečnostjo ne sme uporabljati, razen če klinično stanje matere ne zahteva takega zdravljenja. Matere naj se med jemanjem zdravila dojenju izogibajo. Zdravilo lahko zmanjša plodnost moških in žensk. **Vpliv na sposobnost vožnje in upravljanja strojev:** Lahko se pojavijo simptomatska bradikardija (npr. sinkopa, omotica, hipotenzija), motnje vida ali utrujenost; potrebna je previdnost. **Neželeni učinki:** Najresnejši neželeni učinki so bili hepatotoksičnost, ILD/pnevmonitis, nevtropenija in podaljšanje intervala QT. Najpogostejši neželeni učinki (≥ 25 %) so bili motnje vida, navzea, diareja, bruhanje, edem, zaprtje, povečane vrednosti transaminaz, utrujenost, pomanjkanje apetita, omotica in nevropatija. Ostali zelo pogosti (≥ 1/10 bolnikov) neželeni učinki so: nevtropenija, anemija, levkopenija, disgevzija, bradikardija, bolečina v trebuhu in izpuščaj. **Način in režim izdaje:** Predpisovanje in izdaja zdravila je le na recept, zdravilo pa se uporablja samo v bolnišnicah. Izjemoma se lahko uporablja pri nadaljevanju zdravljenja na domu ob odpustu iz bolnišnice in nadaljnjem zdravljenju. **Imetnik dovoljenja za promet:** Pfizer Europe MA EEIG, Boulevard de la Plaine 17, 1050 Bruxelles, Belgija. **Datum zadnje revizije besedila:** 31.10.2019.

Pred predpisovanjem se seznanite s celotnim povzetkom glavnih značilnosti zdravila.

XALKORI® KRIZOTINIB

Vir: 1. Povzetek glavnih značilnosti zdravila Xalkori, 31.10.2019

Pfizer Luxembourg SARL, GRAND DUCHY OF LUXEMBOURG, 51, Avenue J.F. Kennedy, L-1855,
Pfizer podružnica Ljubljana, Letališka cesta 29a, 1000 Ljubljana

XAR-01-20 Samo za strokovno javnost

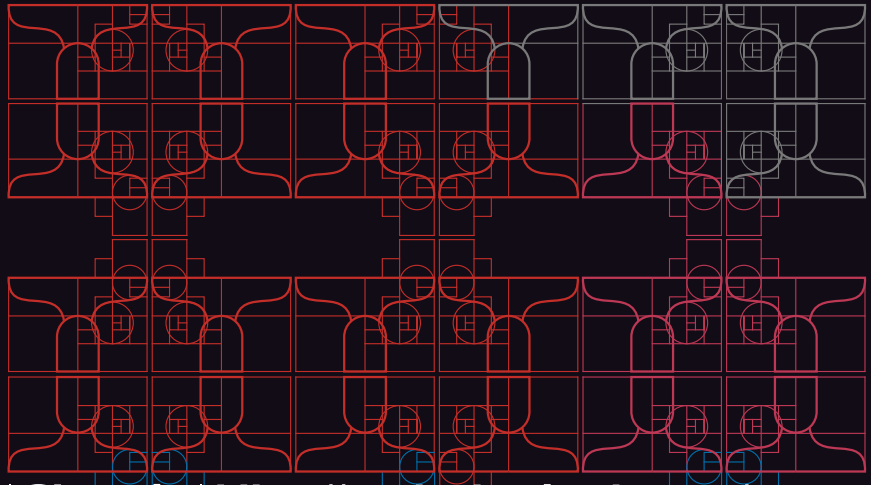

Radiology and Oncology | Ljubljana | Slovenia | https://content.sciendo.com/raon

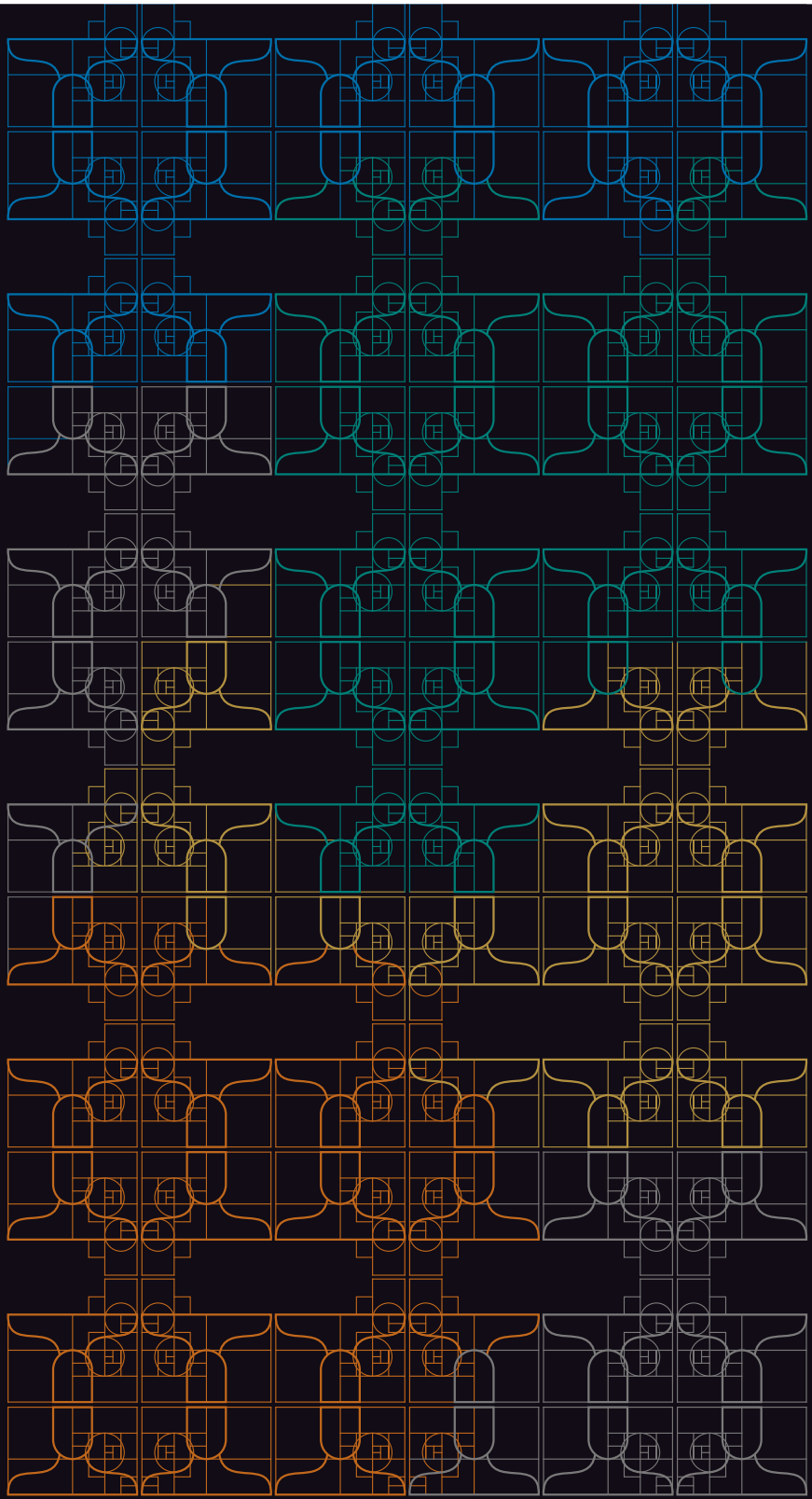

ISSN 1318 - 2099